„Dunărea de Jos" University of Galați
The School for Doctoral Studies in Mechanical and Industrial Engineering

SUMMARY

PHD THESIS

STUDIES CONCERNING THE ANALYSIS OF AN FLOATING DOCK STRUCTURE ON EXTREME LOADS

PhD student,
Eng. Elisabeta C. BURLACU

Scientific leader,
Prof. PhD. Eng. Leonard DOMNIȘORU

Series I6: Mechanical Engineering No. 51

GALAŢI
2019

„Dunărea de Jos" University of Galați
The School for Doctoral Studies in Mechanical and Industrial Engineering

SUMMARY

PHD THESIS

STUDIES CONCERNING THE ANALYSIS OF AN FLOATING DOCK STRUCTURE ON EXTREME LOADS

Translation from the Romanian PhD Thesis Summary

PhD student
Eng. Elisabeta C. BURLACU

Scientific leader, Prof PhD. Eng. Leonard DOMNIȘORU

Scientific references Prof PhD. Eng. D.H.C. Anton HADĂR
Prof PhD. Eng. Ioan Călin ROȘCA
Prof PhD. Eng. Costel Iulian MOCANU

Series I6: Mechanical Engineering No. 51
GALAŢI
2019

The series of doctoral theses publicly supported in UDJG starting with October 1, 2013:

Field of **ENGINEERIG SCIENCES**:

Series I 1**: Biotechnology**
Series I 2**: Computers and information technology**
Series I 3**. Electrical engineering**
Series I 4**: Industrial engineering**
Series I 5: **Materials engineering**
Series I 6**: Mechanical engineering**
Series I 7**: Food engineering**
Series I 8: **System engineering**
Series I 9**: Engineering and management in agriculture and rural development**

Field of **ECONOMIC SCIENCES**

Series E 1: **Economy**
Series E 2: **Management**

Field of **HUMANITIES**

Series U 1: **Philology - English**
Series U 2: **Philology - Romanian**
Series U 3**: History**
Series U 4: **Philology - French**

Field of **MATHEMATICS AND SCIENCE OF NATURE**

Series C: **Chemistry**

TABLE OF CONTENTS

Keywords: *floating dock, 3D-FEM model, seakeeping, transversal stability, operating capabilities, 1D equivalent beam model, loads from quasi – static head – follow and oblique waves, continue upper side tanks, discontinuous upper side tanks, Femap NX/Nastran, extreme random waves.*

INTRODUCTION

Actuality and importance of the theme

To increase shipyards production and repair capacities, including to facilitate the launching operations of floating structures, without additional investment in the yard's land platform, floating docks with various docking capacities are currently widely used. In the current design of floating docks, we consider the standard operation of the docks in calm water conditions, corresponding to the protected water places, including statistical coefficients for increasing the design loads for other operating conditions, according to the norms of the floating docks classification companies [1], [2], [3]. To increase shipyards production and repair capacities, including to facilitate the launching operations of floating structures, without additional investment in the yard's land platform, floating docks with various docking capacities are currently widely used. In the current design of floating docks, we consider the standard operation of the docks in calm water conditions, corresponding to the protected water places, including statistical coefficients for increasing the design loads for other operating conditions, according to the norms of the floating docks classification companies

The objectives of the thesis

The topic of the thesis has as general objective the development of an integrated multicriterial methodology for evaluating the operating capacity of floating docks at extreme loads, in order to carry out a comparative study of the main constructive types and to identify the specific advantages in service.

The comparative study developed in this thesis includes three constructive versions of floating docks, with maximum docking capacity of 828 t (60 m length) and 27000 t (209,2 m length), with continuous upper wing ballast tanks (CWT) or discontinuous upper ballast tanks (NWT), which are docks resulting from new projects or based on the conversion of existing floating structures, such as off – shore barges.

The specific objectives of the scientific research developed in this thesis are the following:

- The current state of the docking techniques of the ships in shipyards presenting the main constructive versions of the floating docks, and the achievement of a synthesis of the methods for the operating capacity analysis of floating docks at extreme loads, with the definition of the safety limit criteria.
- The development of a software package for the preliminary analysis of floating docks with two reference surfaces, outer and inner shell between the upper side wing ballast tanks on the main deck of the pontoon, using equivalent 1D beam models of the hull of the dock, for hydrostatic curves calculations, for equilibrium computation of the dock in still water and equivalent quasi–static waves, with the calculation of the sectional efforts and the deformations of the structure based on non–linear iterative procedures, the calculation of the transversal stability diagrams at large heeling angles, the procedure for calculation of the displacement and trim based on draught survey measurements. These program modules allow the evaluation of the free board limit criterion, preliminary global strength and allowable deformations criteria, including the ultimate bending moment criterion, as well as the intact transverse stability criteria.
- A comparative study for three constructive versions of floating docks of the structural capacity based on local and global strength criteria, allowable stresses referred to yielding stresses material limit, using 3D-FEM models, full extended along the dock's length, in one side or both, considering the extreme loads from quasi–static equivalent head-follow and oblique waves. The development of user functions and procedures directly implemented in the FEM structural analysis program, for the export of the mass distribution and the external - inner shapes of the floating dock from the 3D models to

the equivalent 1D beam models, respectively the import of the dock - waves equilibrium parameters from the 1D models for the calculation functions and application of pressure from quasi-static waves on the immersed surfaces of the 3D models. The analysis should also include the evaluation of preliminary general strength criteria, using equivalent 1D beam structural models. The definition of a set of loading cases that allows the evaluation of the floating docks operating limit cases: full ballasted and docking at maximum capacity.

- A comparative study for three floating docks of the dynamic behaviour in random waves, when relocating on river or coastal routes, with or without docked mass, depending on the constructive particularities, based on the seakeeping criteria formulated on the main components of dock oscillations, in terms of the most probable short–term statistical response. The study will highlight the influence of towing speed and dock – wave heading angle on navigation restrictions when docks are relocated. Concluding the sensitivity analysis and validating the hydrodynamic numerical model used in the analysis of oscillations, based on an experimental model with full shapes at the towing tank, under head, follow and beam regular waves, to which the maximum dynamic response is estimated to occur. Carrying out the seakeeping analysis of a river – costal tug, capable to provide the towing force at the relocation of the studied floating docks and to verify the additional navigation restrictions that would interfere with those determined by the docks' analyses. Connected to the analysis of the component of the roll motion, the general and meteorological (dynamic) transversal stability criteria and the supplementary restrictions for the floating docks are evaluated.
- A multicriterial analysis of the three constructive types of floating docks, based on the studies formulated in the previous objectives makes it possible to have a synthesis of the operating restrictions of the docks and to obtain practical references for the safety exploitation of the floating docks.

Structure of the thesis

The thesis has 10 chapters and annexes, according to the formulated research objectives.

The first chapter briefly presents the related techniques of different launching methods in the shipyards of floating structures, with advantages and disadvantages of each technique. It continues with the presentation of different types of floating docks and a short history, followed by a synthetic presentation of the current state of the analysis methods for evaluating the operation capabilities in safety of the floating docks, based on the norms of the classification societies of shipping.

The second chapter presents the theoretical fundaments for the analysis of operating capacity of floating docks, including: methods for analysis of loads in still water and equivalent quasi–static head, follow and oblique waves on equivalent 1D beam models, the free board limit criteria, preliminary global strength and intact transverse stability for large healing angle; methods for analysing the structural capacity for still water and head - follow equivalent quasi–static waves loads, based on full extended 3D-FEM models along the length and one side, local and global strength criteria, including structural stability; methods for structural analysis in equivalent quasi – static oblique wave, based on full extended 3D-FEM models along length and both sides, with dock equilibrium parameters in oblique wave, based on 1D equivalent beam models, local - global strength and structural stability criteria, methods for analysing the dynamic behaviour of the floating docks in random waves, seakeeping criteria.

The third chapter presents the sensitivity analysis and the validation of the hydrodynamic model and the program code for the study of the dynamic behaviour of a single hull floating structure, based on an experimental model at scale 1:16, of a river – costal research vessel, with dock–like shapes, granted by SDG Ship Design Group Company of Galați, at the towing tank of the Faculty of Naval Architecture, from the "Dunărea de Jos" University of Galați. The analysis concerns the main components of the oscillations of the floating structures, heave, pitch and roll, for the conditions of head, follow and beam waves.

The fourth chapter presents the characteristics of the three types of floating docks selected for the multicriterial comparative study of the operating capabilities, two small docks, with a length of 60 m and a maximum docking capacity of 828 t, with continuous lateral upper

wing tanks (*Dock60_CWT*) and discontinuous lateral upper wing tanks (*Dock60_NWT*), and a large floating dock, with a length of 209,2 m and a maximum capacity of 27000 t (Dock_VARD_Tulcea), resulting from the conversion of an off-shore barge by increasing the width of the pontoon and adding some upper side tanks, discontinuous on the main deck, made available by VARD Tulcea Shipyard. Also, in this chapter the 1D equivalent beam models and full extended 3D-FEM models are presented, developed by Femap NX/Nastran program, for the three types of the floating docks.

Chapter five presents the structural comparative study of the two small floating docks (Dock60_CWT, Dock60_NWT), using 1D equivalent beam models and 3D-FEM models, under still water and equivalent quasi-static head - follow and oblique waves (0 - 90º) loads, based on the global - local strength, sectional efforts, admissible deformations and stresses criteria, as well as the minimum free board criterion, being highlighted the extreme cases of operation. The analysis includes five cases of loading: light, full ballasted, and for the maximum docking capacity of 828 t, having uniform, sagging and hogging mass distribution.

Chapter six presents the comparative study of the dynamic behaviour in random waves of the two small floating docks (Dock60_CWT, Dock60_NWT), in the case of relocation without docked mass on board, for the towing speed range from 0 to 18 km/h and heading angle 0 - 360º, according to the transit scenarios on river and costal routes between the Romanian shipyards from the Danube and Black Sea. Based on the navigation criteria (seakeeping), the restrictions imposed to ensure the operation of relocating the two floating docks in random waves are highlighted. Also, at the end of the chapter, the two floating docks are analysed by the criteria of intact transverse stability, general and meteorological.

In **chapter seven**, the structural analysis of the large floating dock (Dock_VARD_Tulcea) is presented, based on the 1D equivalent beam model and the 3D-FEM full length extended model, under still water and quasi-static equivalent head - follow wave loads, with the evaluation of local - global strength and minim free board criteria. The analysis highlights the extreme loads for the operation of the large floating dock. The analysis includes five loading cases, all with the draught of 6,2 m ensured by a continuum assisted ballasting, according to the size of the quay within the yard: light, docked with a OSV ship with a docking mass of 19747 t, and for the maximum docking capacity of 27000 t, with uniform, sagging and hogging mass distribution.

Chapter eight presents the analysis of the dynamic behaviour in random waves of the large floating dock (Dock_VARD_Tulcea), for three ballast draughts 5,2 m, 6,2 m and 7,2 m, for the towing speed rage from 0 to 12 km/h, and heading angle 0 - 360º, for its relocation on river and costal routes between shipyards. From the evaluation of the seakeeping criteria results the operating restrictions in random waves of the large floating dock. In addition, the criteria for intact, general and meteorological (dynamic) transverse stability are analysed for the large floating dock.

In **chapter nine**, the navigation performance is analysed from the point of view of the seakeeping criteria of a 4000 H.P. river – costal tug, intended for the relocation operations of the three floating docks.

Chapter ten presents the final conclusions of the research which include the results of the comparative multicriterial study for the three types of floating docks subjected to extreme loads and with the influence of the restrictions from the river – costal tug, followed by the personal contributions to the research developed in this thesis.

Figure 1 presents the logical scheme of the research developed in this thesis, in correlation with the general and specific objectives formulated for the thesis topic.

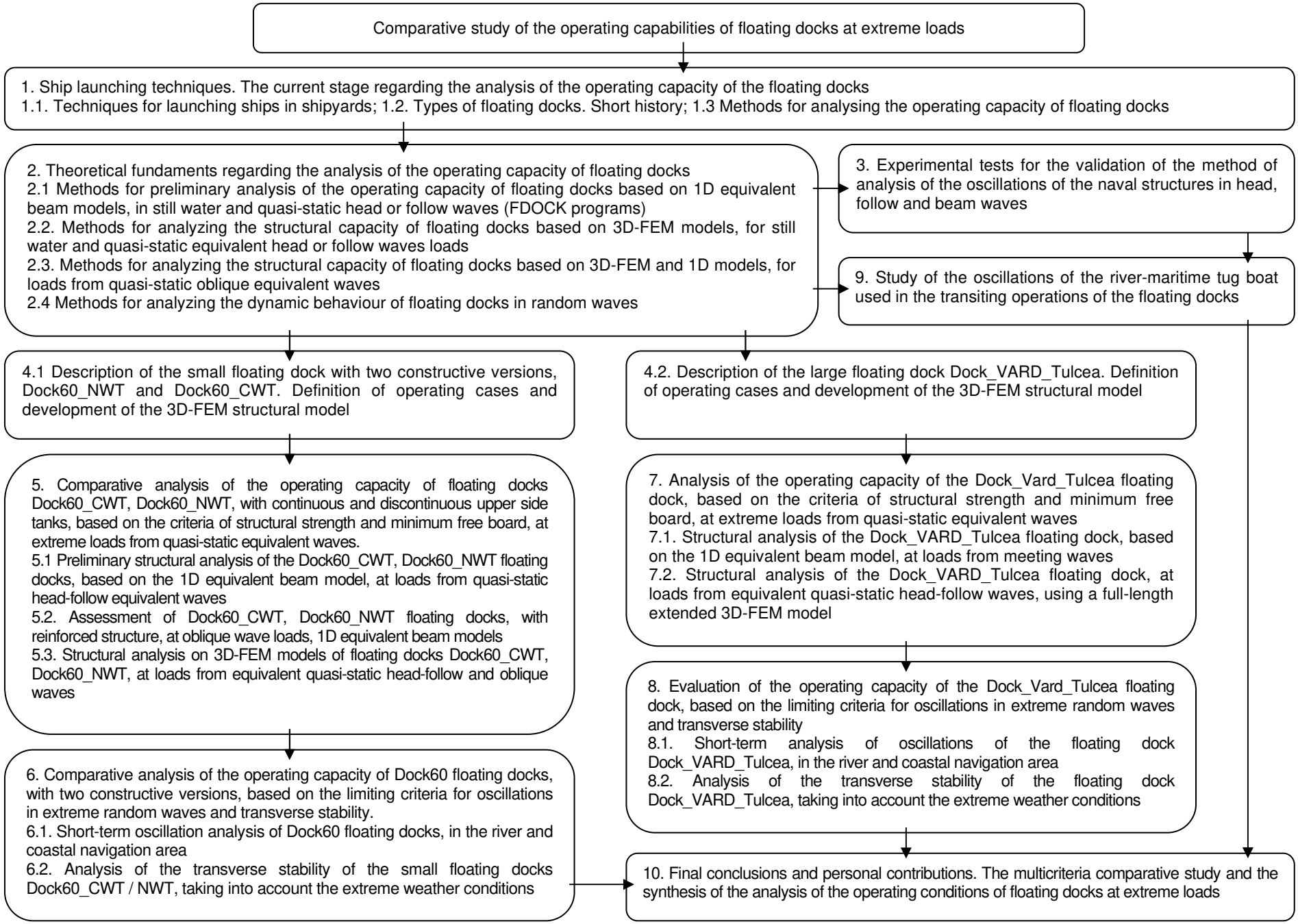

Figure 1*. The logical scheme of the research developed within the thesis*

CHAPTER 1

SHIP LAUNCHING TECHNIQUES. THE CURRENT STATE REGARDING THE ANALYSIS OF THE OPERATING CAPACITY OF THE FLOATING DOCKS.

This chapter is structured in three parts, including ship launch technologies, as well as the current stage in the structural analysis of floating docks. The first subchapter briefly presents the techniques of launching floating structures in shipyards, with the advantages and disadvantages of each launching technology. It continues with a brief history of floating docks and the different types of construction in operation. The last subchapter summarizes the current state of analysis methods for evaluating the safe operating capacity of floating docks, based on the criteria imposed by the norms of naval classification societies, as well as their own study directions according to the thesis objectives.

1.1. Techniques for launching ships in shipyards

Ship launching is one of the main stages in the ship manufacturing process. This is the technological phase of translating the ship built in the shipyard, from the slipway into the water [4], [5], [6], [7].

In recent years, this stage of ship construction has been modernized, taking into account the launch systems that ensure structural safety during these operations.

The two methods of launching a ship to water are [4], [5], [7]:

- when all the body assembly, equipment assembly and finishing work are done on the assembly line, the ship will be launched fully equipped;
- when only a certain volume of work on the ship, determined by the conditions of water-tightness, local and global resistance of the body and the extent of equipment installation is completed, but it is still necessary that some works of saturation and sealing of the body to be completed before the ship is launched.

The most used types of launching techniques in shipyards in Romania are:

- gravitational launch of ships on an inclined plane which implies launching under the influence of their own force of weight (method used for medium displacement vessels):
  - longitudinal launch
  - cross launch (S.N. DAMEN from Galați, S.N. VARD from Brăila)
  - launch by mechanized means (rolling stock - S.N. VARD from Brăila, cranes, synchrolifts, floating docks)
- launch of ships using air balloons - one of the newest launch techniques
- vertical launching
  - synchrolifts (S.N. VARD from Tulcea)
  - dry docks (S.N. Constanța, S.N. DAMEN from Galați, S.N. DAMEN from Mangalia)

- floating docks (S.N. Constanța, S.N. DAMEN from Galați, S.N. VARD from Tulcea, S.N. VARD from Turnu - Severin)

A floating dock is a metallic construction of a parallelepiped shape, with a "U" type structure, usually provided with superior lateral tanks for ballast [1], [2], [3], [4], [5]. These can be built by converting simple or modular type pontoons, by installing side ballast tanks. Floating docks (S.N. Constanța, S.N. DAMEN from Galați, S.N. VARD from Tulcea, S.N. VARD from Turnu - Severin), figures 1.1. – 10., they are equipped with high flow pumping installations for filling the ballast tanks during the launch operation. The ship is built on docking systems (keel blocks, metal scaffolding, scaffolding, hydraulic systems, etc.), located on the dock deck, launching into water by flooding the ballast tanks of the dock and therefore by diving it into the draft corresponding to the float of the ship that is docked for launch [6], [8].

For the case of loading/unloading of the floating constructions on the dock, laterally or through its stern, the construction to be launched must be aligned with the main deck of the floating dock. The construction is brought on board the dock by towing it on the existing tracks, on the dock deck (figure 1.4.a., b.). During loading / unloading, the ballast tanks will be filled / emptied, so that the transfer of the construction from the dock to the main deck of the dock is made as easy as possible (the trim of the ship must remain horizontal). In the case of launching and towing the docked ship, the floating dock will be submerged so that the docked buoyant construction can be towed by the pilot boats (figure 1.5.) from the field of the dock deck. In this respect, in chapters 7 and 8 of this thesis the analysis of the structure of a floating dock will be presented at extreme demands, figure 1.3., with the initial technical data made available by the VARD Shipyard in Tulcea [4], [9].

Figure.1.1. *ATLANTE II barge on the Danube, having docked a ship that was launched in the Black Sea [10]*

Figure. 1.2. *ATLANTE II barge totally submerged in the Black Sea during a launch [11]*

Figure. 1.3. *The floating dock Dock_VARD_Tulcea at the end of the total docking of the calculation case in the chapter 7.2.2. [12]*

a. b.

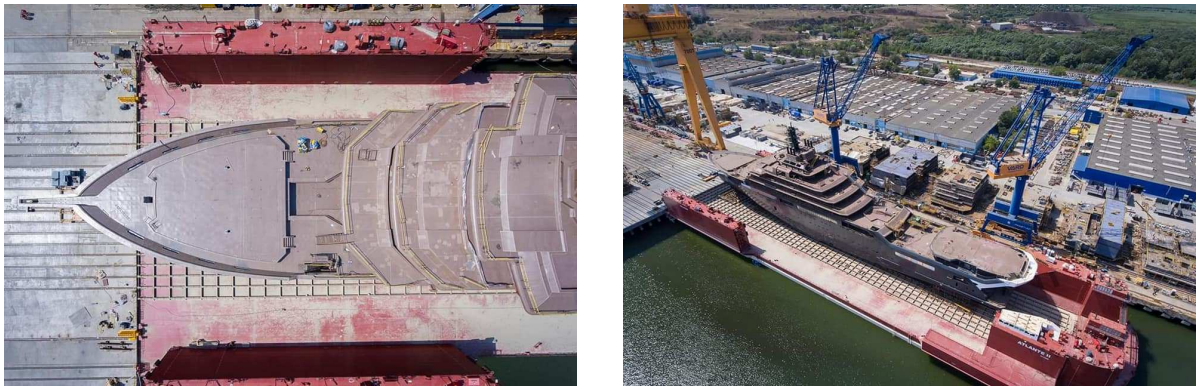

Figure 1.4. a., b. *The floating dock Dock_VARD_Tulcea aligned with the rails on the mounting way 2, at launch a. [13], b. [14]*

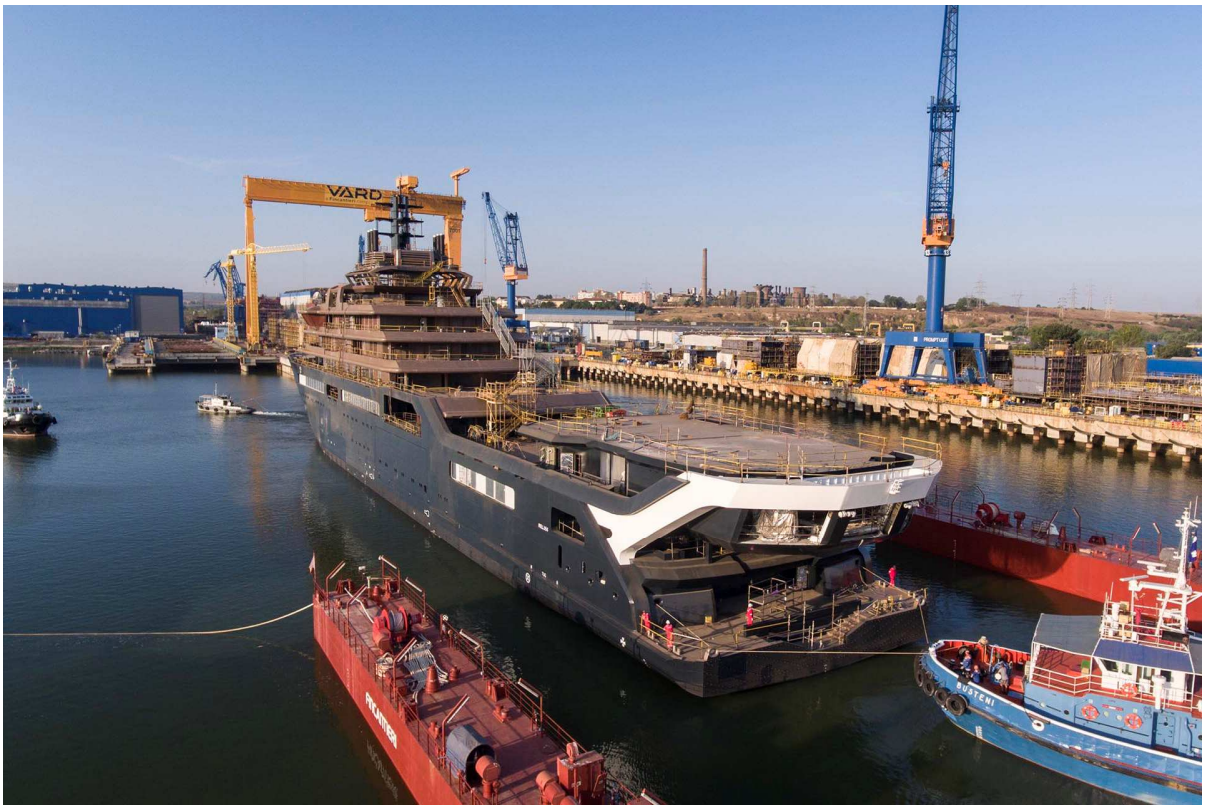

Figure 1.5. *The floating dock Dock_VARD_Tulcea maximum ballast for the towing of the ship being launched [15]*

1.2. Types of floating docks. Short history.

Based on the specialized literature, the current stage of the ship launch techniques in the shipyards is achieved with floating docks due to the multitude of advantages they benefit, as well as floating constructions but also for the shipyard.

The floating dock is a special construction, intended for docking ships for inspection and repair of the hull, but also for launching different marine structures, made in accordance with the norms of the classification societies. The main type of floating dock is the two-sided tower, with a U-shaped cross-section. The immersion and emergence of such a dock is done by ballasting or de-ballasting the pontoon tanks and the upper lateral ballast tanks on the docking deck [1], [6], [16], [17].

Floating docks have been in use for over 100 years, amounting today up to around 213 docks worldwide [18], [19]. Figures 1.6. – 1.10. present some of this multitude of floating docks of different sizes. They had great use during the Second World War, due to their mobility in relation to their capabilities, already known for several years at that time [20].

Figure. 1.6. *The floating dock ARD-1 constructive version from 1934 [21]*

Figure. 1.7. *The floating dock in operation S.N. VARD Vung Tau, Vietnam [22]*

Figure.1.8. *The 180 m floating dock – Norden Ship design House [23]*

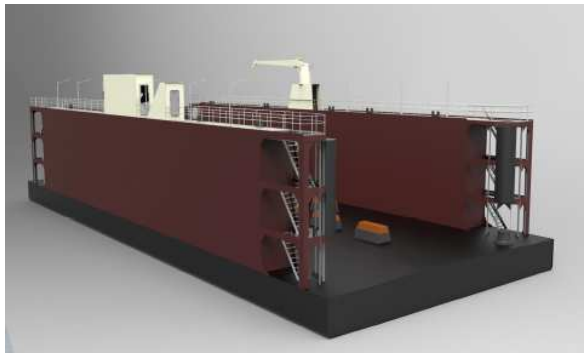

Figure. 1.9. *The 50 m floating dock – Norden Ship design House [24]*

Figure. 1.10. *The floating dock S.N. Geoje, South Korea (430mx84mx23,5m – 20800 t) [25]*

1.3. Methods of analysing the operating capacity of floating docks

The construction of floating docks is regulated by the classification companies in the shipping industry that are associated in IACS - International Association of Classification Societies (DNV-GL - Det Norske Veritas - Germanische Lloyd; ABS - American Bureau of Shipping, BV - Bureau Veritas; LRS - Lloyd's Register of Shipping; RINA – Registro Italiano Navale; NKK - Nippon Kaiji Kyokai, etc.) [1], [3]. In this thesis, in chapter 4, we will present the requirements of the norms regarding the permissible limit values when evaluating floating docks.

Obs. Details of the rules of the norms of the classification societies regarding the sizing of the structural elements of the floating docks, which will be subjected to analysis at extreme demands, are not included, not being a research component established by the scientific objectives of the thesis.

In the following we present, in summary, the current state of the types of analysis that will be addressed in the thesis for the evaluation of the operational safety of floating docks.

The requirements regulated by the ship classification companies for evaluating the safe operating capacity in extreme cases require the following analyses:

- selection of the constructive type of the floating dock according to the operating capacity;
- analysis of transverse stability and volumetry of the floating dock;
- analysing the global and local resistance of the floating docks structure;
- the analysis of the vertical bending moment at the ultimate resistance (overall stability);
- analysis of the dynamic behaviour of the dock (seakeeping) when relocating between shipyards.

Naval classification companies divide this type of floating structures into floating docks with a loading capacity less than or equal to 40,000 t and floating docks with ballast capacity for load capacities greater than 40,000 t. A special examination by the classification company should be carried out if a floating dock with ballast capability and a loading capacity greater than 40,000 tons must be loaded with two vessels side by side, or if the dock has a displacement of at least twice the total mass of the floating dock without docked and unbalanced mass (RINA, DNV-GL, BV, ABS) [1], [3].

From a constructive point of view, the floating docks can be of the caisson type, to which we find a basic pontoon and two upper lateral tanks that can be continuous (CWT) or discontinuous (NWT) along the entire length of the dock, or pontoon type, in which the basic pontoon consists of individual, discontinuous, permanently connected or detachable pontoons from the upper lateral ballast tanks.

Another classification of floating docks can be done from the point of view of the ballast mode: dock with uniform ballast or dock with controlled ballast. A dock with uniform ballast, is a dock that has the capacity that the tanks are loaded with ballast simultaneously at the same level. This system is beneficial, because in this case it is not possible to discuss the occurrence of bending moments or excessive deformations in the case of operation. In the case of a ballast with controlled ballast, each tank is ballast independently. This constructive solution allows the adjustment of the trim as well as the control of the efforts at all stages of operation. Floating docks must be equipped with *global deformation monitoring equipment* [3].

From the point of view of global and local resistance, evaluated on the basis of the admissible stresses criterion against the material flow limit, at any stage of the design it is necessary to develop 1D and 3D structural equivalent beam models, subject to quasi-static equivalent stresses from waves and calm water, based on long-term statistics, for the entire lifetime of the floating docks, according to the norms of international naval classification companies (RINA, BV, ABS, LR, DNV-GL, etc.) [1], [3].

The preliminary analysis of the global resistance is performed using the equivalent 1D elastic beam model of the floating dock body, using nonlinear iterative procedures for calculating the equilibrium conditions of the floating dock in waves, which allows for sectional efforts and maximum global tensions, the evaluation based on the allowable values

prescribed by the naval norms, as well as the calculation of the maximum global deformations. The main disadvantage of this model is the impossibility to include the structural details, respectively of the correct evaluation of the tension concentrators [26].

The evolution of numerical modelling in the field of analysis of naval structures has led to the development of three-dimensional structural models using the finite element method, 3D-FEM, which allow the elimination of the disadvantages generated by the use of 1D models of equivalent beam. The body structure of the floating dock is completely defined along the entire length, with the quasi-static equivalent stresses according to the naval norms, obtaining the state of extreme local and global tensions in all the floors of the dock, considerable computing resources are involved. The structural details are included, having a finer discretization for the evaluation of the tension concentrator factors with the corresponding accuracy [27]. The balancing parameters are taken from the analyses on 1D equivalent beam structural models. The main disadvantage of the fully extended 3D-FEM models over the entire length of the floating dock is that they cannot be used for structure analysis in the preliminary design phase.

In the thesis, different constructive models and docking capabilities of floating docks will be analysed.

In the evaluation of the global resistance, the criterion of the last resistance is applied, respectively based on the Smith method [28] the ultimate bending moment is calculated, corresponding to the loss of stability of the floating dock floors (DNV-GL, BV, ABS, etc.) [1], [3].

In order to evaluate the extreme cases in the operation of relocation of the docks, on internal or coastal waterways, dynamic analysis in random waves (seakeeping) is required, at vertical, pitch and roll oscillations [29], [30], [31], [32]. Floating docks have dominant prismatic forms that are suitable for linear analysis of oscillations, respectively the amplitude response functions on the oscillation components can be obtained by a direct solution in the frequency domain for regular waves. The dynamic response in random waves is obtained by a short-term statistical analysis, using the power spectral density functions of the random waves [33], [34].

Due to the significant variation of the dock masses at each stage of the docking operation, the norms require the evaluation of the operational safety and based on the criteria of intact transverse stability at large inclination angles, including on the meteorological criteria (BV, DNV-GL, ABS, etc.) [1], [3].

The following chapters will present the foundations of the theoretical models, i.e. in chapter 2, and analysing the safe operating capacity of a caisson type dock, with small dimensions, with two constructive variants, with continuous lateral tanks of continuous and discontinuous ballast, as well as a large dock, with technical data provided by the VARD Shipyard in Tulcea [9], [11], based on the criteria of global, local and ultimate resistance, of minimum free board, transverse stability and dynamic behaviour in random waves, i.e. in chapters 5-8.

CHAPTER 2

TEORETICAL FUNDAMENTS REGARDING THE ANALYSIS OF THE OPERATING CAPCACITY OF FLOATING DOCKS

This chapter presents the theoretical fundaments of the floating docks operating capacity analysis, including: methods of analysis of loads in still water and equivalent quasi–static head, follow and oblique waves on equivalent1D beam models, the freeboard limit criteria, preliminary global strength and intact transverse stability for large healing angle; methods for analysing the structural capacity for still water and head – follow equivalent quasi-static oblique wave, based on full extended 3D-FEM models along the length and one side, local and global strength criteria, including structural stability; methods for structural analysis in equivalent quasi-static oblique wave, based on full extended 3D-FEM models along length and both sides, with dock equilibrium parameters in oblique wave, based on 1D equivalent beam models, local – global strength and structural stability criteria, methods for analysing the dynamic behaviour of the floating docks in random waves, seakeeping criteria.

2.1. Methods for preliminary analysis of the operating capacity of floating docks based on 1D equivalent beam models, in still water and quasi – static head or follow waves (FDOCK programs).

The floating dock operating capabilities and safety must be assessed at any design and service stages for each working ship project by several criteria, according to the shipbuilding classification society rules [1].

For this purpose we have developed our own software package FDOCK [4], [35], making it possible to assess the following: the freeboard criterion corresponding to the floating and trim condition, the vertical global strength criteria by yielding stress and ultimate strength limits (global buckling), the general and weather transversal intact stability criteria.

In this section the modules of the FDOCK software package [4], [35] for operation criteria assessment, with the flowchart in figure 2.1., and the theoretical brief are presented. The software modules are developed by free Pascal Programming Language PPL [36] (Annexes 1 – 5)

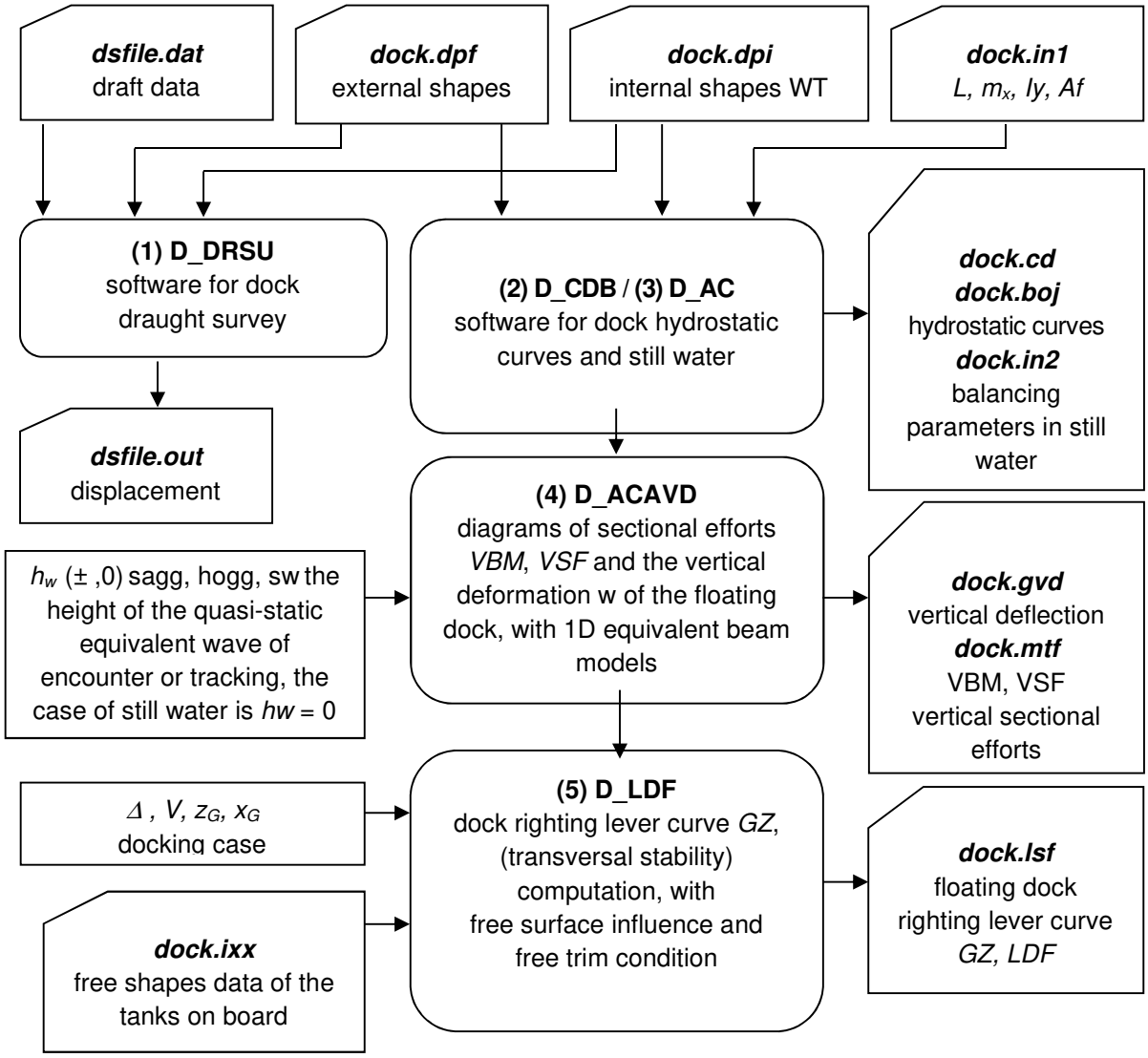

Figure.2.1. *Flowchart of the FDOCK software package [4], [35] modules for floating docks capability and operation safety assessment, input and output files*

2.1.1. The module for determining the displacement of floating docks based on the draughts recorded on full scale

The *D_DSRU module*, figure 2.1. (Annex 5), is developed for floating dock draught survey data processing, with trim and hull girder deflection [4], [35]. This module can be used for experimental evaluation of the floating dock displacement, longitudinal gravity centre position and vertical deflection, based on draught survey measurements, in still water condition.

2.1.2. Module for calculating the hydrostatic curves of the floating dock

The *D_CDB module*, figure 2.1. (Annex 1), is developed for the floating dock hydrostatic curves computation and the Bonjean diagram [4], [35] used for the initial evaluation of the dock freeboard and intact stability characteristics at each loading case.

2.1.3. Module for calculating the equilibrium parameters in still water

The *D_AC module*, figure 2.1. (Annex 2), is developed for the SW still water equilibrium parameters computation, based on a non-linear iterative procedure for floating and trim equilibrium [4], [27], [35], used for the freeboard criteria check according to the shipbuilding classification society rules. Besides the offset lines of the dock shape external and between the side wing tanks WT, as input data is required also the dock mass distribution per unit length m_x.

$$FB_{PD}(x) = D_p - T(x) \geq FB_{PDadm} \;\; ; \;\; FB_{UD}(x) = D - T(x) \geq FB_{UDadm} \tag{2.1}$$

$$T(x) = T_{pp} + (T_{pv} - T_{pp})\frac{x}{L}; \;\; x = 0, L \tag{2.2}$$

where: T(x) is the draught at x=0,L, L is the dock length, D_p, D are the pontoon deck and upper deck height, FB_{PD}, FB_{UD} are the freeboard at pontoon deck and upper deck, FB_{PDadm}, FB_{UDadm}, are the freeboard at pontoon deck and upper deck minim admissible value [1], [4], [35].

2.1.4. Module for calculating bending moments and shear forces at loads from quasi – static head or follow waves

The D_ACVAD module, figure 2.1. (Annex 3), is developed for the still water and design head equivalent quasi-static waves vertical bending moments VBM and vertical shear forces VSF computation, based on a non-linear iterative procedure [1], [4], [27], [35]. The length of the wave is considered equal to the dock length $\lambda = L$ [28]. The results based on this module are used for the assessment of the global strength criteria vertical bending moments (by Smith method [4], [28], [37]) and vertical shear force, global strength, yielding stress limit (admissible stress) and ultimate strength (global buckling) according to the shipbuilding classification society`s rules [34], [38]

Analogous to chapter 2.1.3., in the case of follow and head quasi-static waves, we use a non-linear iterative procedure with two parameters, to satisfy the balance conditions for the study case (Δ , x_G) [1], [4], [27], [28], [35], which must simultaneously ensure the intersection of the free surface of the wave with the outer and inner shell.

The maximum design equivalent quasi-static wave height h_{w_max} according to the shipbuilding classification society rules [4], [33], [35] is:

$$h_{w\_\max} \leq 2m \;\; \text{SW, IN(0.6), IN(1.2), IN(2.0) for inland operation} \tag{2.3}$$

$$h_{w\_\max} = 0.50 \cdot 0.0856 \cdot L \; ; \; L < 90 \; m$$

$$h_{w\_\max} = 0.50 \cdot \left[10.75 - \left(\frac{300 - L}{100} \right)^{3/2} \right] \;\; ; \;\; 90 \leq L \leq 300 \; m \qquad \text{RE(50\%) for costal harbour operation} \tag{2.4}$$

The following results are obtained based on the non-linear iterative procedure with two parameters:

$$Z(x) = T_{pp} + (T_{pv} - T_{pp})\frac{x}{L} \pm \frac{h_w}{2}\cos\left(\frac{2\pi x}{L}\right) \rightarrow A_t(x) \;\rightarrow p_x(x) = g \cdot m_x(x) - \rho_w g \cdot A_t(x) \;\; ; \;\; x \in [0, L]$$

$$VSF(x) = \int_0^x p_x(x)dx \leq AVSF \;\; ; \; VBM(x) = \int_0^x VSF(x)dx \leq \min\{AVBM, AUSVBM\} \tag{2.5}$$

$$w(x) \leq w_{adm} = L/400 \;\; ; \;\; x \in [0, L] \tag{2.6}$$

$$FB_{PD}(x)\big|_{Z(x)} = D_p - Z(x) \geq FB_{PDadm} \;\; ; \;\; FB_{UD}(x)\big|_{Z(x)} = D - Z(x) \geq FB_{UDadm} \tag{2.7}$$

where: T_{pp}, T_{pv} are the wave medium plane equilibrium parameters, $Z(x)$ is the wave free surface elongation, $m_x(x)$ the mass distribution, $A_t(x)$ transversal immersed areas, *AUSVBM* is the ultimate strength vertical bending moment according to the Smith method [35], [28], [37] using *DNVGL-Poseidon* program [39], *AVSF* admissible vertical shear forces and *AVBM* admissible vertical bending moment according to the shipbuilding classification society rules [27],[28], w the total dock girder deflection, w_{adm} the admissible vertical deflection.

2.1.5. Module for analysing the transverse stability of floating docks

The L_LDF module (Annex 4) is developed for the dock righting level curve GZ (transversal stability) computation with free surface influence and free trim condition, using a non-linear iterative procedure in the case of large heeling angles.

The results for this module are used for the assessment of the general transversal stability and weather stability criteria according to the shipbuilding classification society rules [4], [35], [78].

$$GM_0 = \frac{dGZ_c}{d\varphi}\Big|_{\varphi=0} \geq 1m\ ;\ GZ_c(\varphi_{ref}) \geq GZ_{ref}\ ;\ LDF_c(\varphi) = \int_0^{\varphi} GZ_c(\varphi)d\varphi\ ;\ K_{meteo}\left(LDF_{ref}(\varphi)\right) \geq 1 \quad (2.8)$$

where: GZ_c, , LDF_c are the righting lever curves without and with correction for the free surfaces of onboard tanks; φ heeling angle.

2.2. Methods for analysing the structural capacity of floating docks based on 3D-FEM models, at load from still water and quasi – static head and follow waves.

For the complex analysis of the floating docks, the classification society requires the use of 3D-FEM structural models, completely extended in length, so that the comparison with the 1D equivalent beam model (chapter 2.1.3., 2.1.4.) both of the overall strength can be simultaneously evaluated, with the structural details and masses included.

In case of 3D-FEM analysis, the floating dock equilibrium in head – follow equivalent quasi-static wave is obtained on the equivalent 1D beam model, because from the practical point of view, the implementation of non-linear procedures (chapter 2.1.3., 2.1.4.) in complex structural models would lead to long times for computation. In this case, it is necessary to ensure a correspondence with a high accuracy of shapes, equivalent rigidity and mass diagram from 3D-FEM models to 1D equivalent beam models

For global and local strength analysis of the floating docks, based on the global and local admissible stress, we have used several own program codes and user procedures implemented in Femap/NX Nastran [27], [41], [42], [43] linked as in the flowchart for figure 2.2.

1. *The floating dock design concept data.*
2. *The 3D-FEM model*. Based on the Femap NX/Nastran [42] CAD modelling facilities, the offset lines for the floating dock are first implemented. Using the data from the dock design concept, a 3D-CAD structural model is developed, including the main longitudinal panels, main and simple frames, longitudinal girders, stiffeners brackets, etc. Based on the Femap/NX Nastran meshing facilities, the numerical 3D-FEM model is obtained. The 3D-FEM model is fully extended over the length, in one board, figure 2.3. The dock structure is developed with finite elements of membrane and thick plate (Mindlin) triangular and square elements (PLATE). The edge conditions [44] applied to the 3D-FEM models are shown in table 2.1. and figure 2.3.

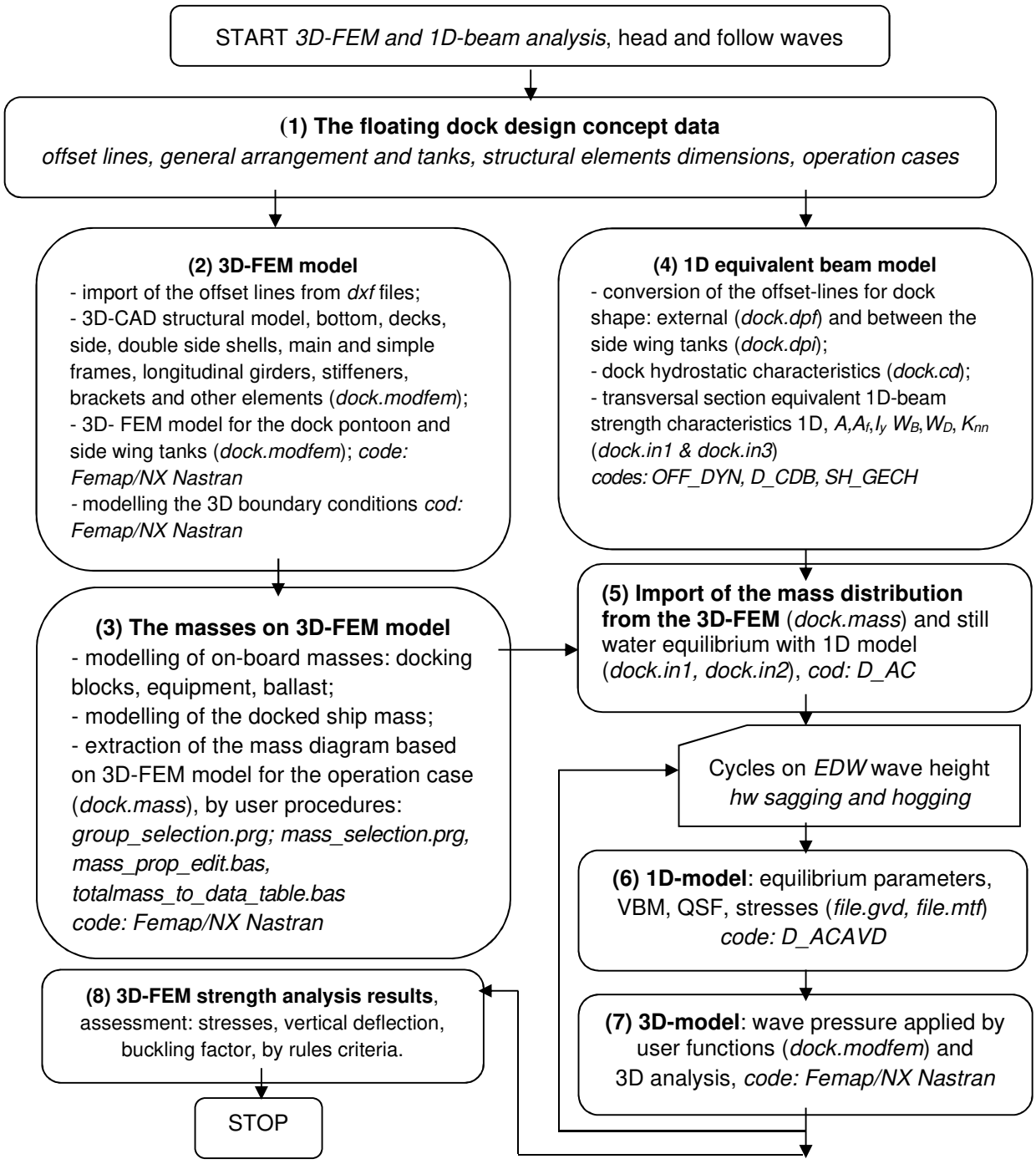

Figure 2.2. *The flowchart for the floating dock strength analysis by 3D-Fem and 1D-beam models [40], [41]*

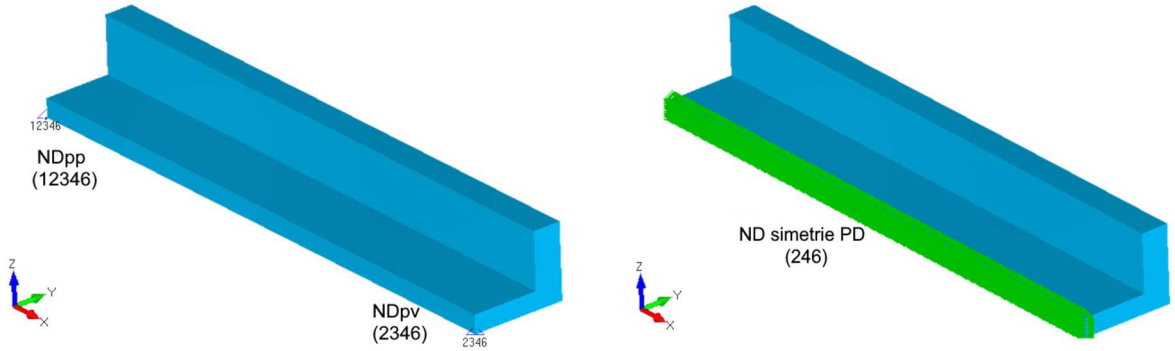

Figure 2.3 *The boundary conditions at 3D-FEM model, at head – follow equivalent quasi-static waves*

Table 2.1 *The boundary conditions for the 3D-FEM mode, at head – follow equivalent quasi-static waves* [44]

Boundary conditions	DOF degrees of freedom restraint					
	U_x (1)	U_y (2)	U_z (3)	R_x (4)	R_y (5)	R_z (6)
Symmetry at centre line	-	x	-	x	-	x
Master node stern ND_{pp}	x	x	x	x	-	x
Master node bow ND_{pv}	-	x	x	x	-	x

3. *The masses on 3D-FEM model*. Using the floating dock and the operation loading case data, the required-on board masses, ballast and docking ship type mass are obtained. Using lumped masses or un-structural mass elements from Femap/NX Nastran [42], the mass distribution on the 3D-Fem model is performed via own user procedures (*group_selection.prg; mass_selection.prg,mass_prop_edit.bas,totalmass_to_data_table.bas, (Annexes 6-9*) developed for Femap/NX Nastran [42], the mass distribution per unit length for the 1D-beam model is extracted.

4. The equivalent 1D-beam model includes: external and between side tanks offset lines (3D geometric) imported from *dxf.* Files using *OFF_DYN* [45] code, the dock hydrostatic curves by *D_CDB code (Annex 1)*, the transversal sections strength characteristics by SH_GECH code [46].

5. *Import of the mass distribution from the 3D-FEM*. Special care is needed to ensure the best correlation for the external hull shape and mass distribution between the 3D and 1D models used for the dock – wave equilibrium parameters (chapters 2.1.3., 2.1.4). Also, the still wave equilibrium condition is obtained by *D_AC code* (Annex 2), in order to check out the accuracy of the loading case idealization using the 3D/1D models.

6. *1D-model equilibrium parameters.* Using an iterative non-linear algorithm with two parameters (chapter 2.1.4.), the dock – EDW equilibrium position is obtained (T_{pp}, T_{pv}). The algorithm is implemented in *D_ACAVD* code (Annex 3).

Equation 2.9. presents the EDW head wave free surface equation and the EDW wave pressure at x and z position over the external and between sides dock shells.

$$\begin{aligned}&\textit{Pressure: max(0.000;(!ro*9.81*(-ZEL(!EL)+!Tpp+(!Tpv-!Tpp)*XEL(!EL)/!L}\pm\\&\pm\textit{!hw/2*COS((2*180*(XEL(!EL))/!L)))))}\end{aligned} \tag{2.9}$$

where: T_{pp} ,T_{pv} are the aft, fore and average vertical positions of EDW head wave medium plane and represents the draught values in the case of SW still water; h_w the wave height; *XEL*, *ZEL* are Femap/NX Nastran [42] functions for element *EL centre longitudinal x and vertical z position selection*; *L* the dock length, ± sagging or hogging wave.

7. *3D-model wave pressure*. Based on the function from equation 2.9. and the equilibrium parameters from step 6, corresponding to a wave height h_w, in sagging (+0 or hogging (-), by Femap/NX Nastran [42] program loading menu *Model / Load / Elemental / Pressure* on each element from the external and between side tanks shell the EDW wave pressure is applied automatically. Using the NX Nastran solver with static linear option, the 3D-FEM model is analysed. Also, using the buckling option the structural stability analysis is analysed.

$$\left[\overline{K}_g\right]\left\{\overline{u}_g\right\}=\left\{\overline{Q}_g\right\} \tag{2.10}$$

$$\left(\left[\overline{K}_g\right]+B\left[\overline{K}_g^{\sigma}\right]_{ref}\right)\left\{d\overline{u}_g\right\}=0 \tag{2.11}$$

where: $\left[\overline{K}_g\right]$ the stiffness matrix, $\left[\overline{K}_g^{\sigma}\right]_{ref}$ the geometric rigidity matrix, $\left\{\overline{Q}_g\right\}$ the external load vector, $\left\{\overline{u}_g\right\}$ vector for freedom degrees for 3D-FEM nodes, *B* structural stability factor (buckling).

In order to evaluate the accuracy of the equilibrium state of the dock-quasi-static wave reactions on vertical direction *RFZ* in the two master nodes (*NDpp*, *NDpv*) must tend to zero (equation 2.12.), which means the simultaneous satisfaction of the equilibrium conditions for buoyancy and longitudinal trim.

$$RFZ\left(ND_{pp}\right)\to 0 \qquad RFZ\left(ND_{pv}\right)\to 0 \tag{2.12}$$

8. *3D-FEM strength analysis results assessment*. For each operation case, the maximum EDW head wave height is selected according to the limits imposed by the freeboard criteria. Then the 3D-FEM model analysis results are assessed by the global – local strength criteria according to the rules [1], [50]: the admissible stress to the yield stress limit, the admissible buckling factor and the admissible global vertical deflection of the floating dock hull.

In our thesis, the procedure presented in this chapter is applied to the study of the structural capacity for requests from quasi-static head and follow extreme waves, for two small docks (L=60m) in chapters 5.1., 5.3. and for a large dock (L=209.2m) in chapter 7, using 3D-FEM structural models and 1D equivalent beam.

2.3. Methods for analysing the structural capacity of floating docks based on 3D-FEM and 1D models, at loads from quasi – static oblique waves

In case of requests from quasi-static equivalent oblique waves for the analysis of the general resistance on 3D-FEM models, analogue to the head or follow waves (chapter 2.2.), from the practical point view, non-linear iterative procedures for determining the equilibrium cannot be directly applied of the oblique wave system, because the running times would be excessively high. Consequently, in the case of oblique wave, we will resort to the 1D equivalent beam models for the floating dock, which allow the practical implementation of the procedures for determining the oblique equilibrium parameters (chapter 2.3.1.) which will be used in the analyses of local and global strength on 3D-FEM models (chapter 2.3.2.), from modelling oblique wave pressure.

2.3.1. Determination of the equilibrium parameters of the floating dock – quasi – static oblique wave system, based on 1D equivalent beam models

In the case of quasi-static equivalent waves, we considered the heading angle $\mu = 0^0$ - 180^0 (360^0), figure 2.4., taking into account the centre line symmetry of the floating dock. The length of the oblique wave is $\lambda = \lambda_r \cos\mu = L\cos\mu$, considering the relative length of the wave equal to the length of the dock $\lambda_r = L$, [28], [44], [51].

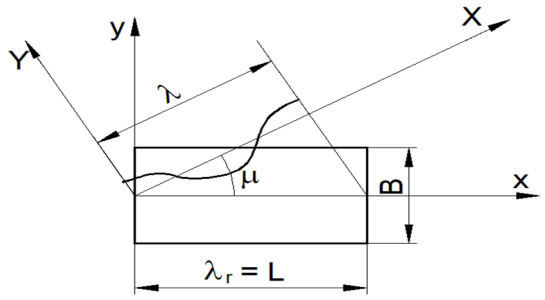

Figure 2.4. *Relative position of floating dock – quasi-static oblique wave. [28]*

The docking case is defined by the displacement Δ with the immersed volume V, the position of the centre of gravity $x_G \neq 0$, $y_G=0$ and the mass distribution along the length of the dock $m_x(x)$, x=0,L.

The free surface of the quasi-static oblique equivalent wave has the expression:

$$z_w(x,y) = T_m + (x - x_F)\cdot\theta + (y - y_F)\cdot tg(\varphi) \pm \frac{h_w}{2}\cos\left[\frac{2\pi}{\lambda}(x\cos\mu + y\sin\mu)\right] \quad x \in [0,L] \; y \in \left[-\frac{B}{2},\frac{B}{2}\right] \qquad (2.13)$$

where: T_m, θ, φ equilibrium parameters dock – EDW (transversal trim angle, vertical displacement, longitudinal trim angle); x_F, y_F the EDW oblique wave median plane centre position (*x,y*); h_w, λ height and length of EDW; *L*, *B* the dock length and breadth.

For the computation of the equilibrium conditions of the dock in oblique equivalent design waves, we have used a numerical code *P_QSW* [44], [52], using the Free Pascal language [36], that includes a non-linear iterative algorithm for three equilibrium parameters (chapter 2.1.3., 2.1.4.) sinkage T_m, longitudinal θ and transversal φ trim, that defines the relative position between the dock base plane and the medium plane of the EDW waves.

This study delivers as results the preliminary evaluation of the floating docks operating capabilities in terms of design wave height limits: global bending and torsion moments, shear forces and ultimate vertical bending moment criteria.

The parameters $T_m, \theta, \varphi, x_F, y_F, h_w, \mu, \lambda_1$ define the equilibrium in oblique wave and are used for applying the pressure of the wave on the shell of the dock with 3D-FEM model extended throughout the length and both edges (chapter 2.3.2.).

2.3.2. Methods for analysing the local and general strength of floating docks based on 3D-FEM models, at loads from equivalent quasi-static oblique waves

For the global strength analysis by equivalent beam models and 3D-FEM models, under equivalent design waves has the linked logical flowchart presented in figure 2.5.

1. *The floating dock data and operation cases parameters*. The input data for the dock operating case include the oblique equivalent design wave range, h_{wmax}, δh_w = 0.25m, the wave heading angle μ = 0 - 180^0 (360^0), $\delta\mu$ = 15^0, taking into account that the dock has plane symmetry at centre line. For the selection of the maximum oblique EDW wave height at each loading case, the freeboard restriction must be first taken into consideration.

2. *The 3D-CAD/FEM model*. In the case of oblique equivalent design waves EDW the pressure on the external shell is no longer symmetric on the sides as in the case of head waves. So, for the numerical analyses the 3D model has to be extended not only over the whole length but also from side to side, increasing the necessary number of nodes and elements. The FEM model is developed with quad and triangle shell elements, coupled membrane and Mindlin plate elements. The on-board masses are modelled as path distributed or lumped, including the wave ballast and dock structure, so the displacement Δ corresponds to the analysed loading case. The longitudinal and transversal position of the dock gravity centre remains unchanged for all the loading cases, x_G, y_G=0. For each constructive version, specific loading cases are considered, according to the floating dock rules [1], and also the shipyard capacities [9], [11]. The mass diagram over, for each loading case, is extracted from the 3D-FEM model using own developed subroutines (Annexes 6-9) implemented by command language of the Femap/NX Nastran program [42].

3. *Setup of the data for the floating dock and oblique EDW equilibrium procedure*. For each loading case the relative equilibrium position between the dock hull and the oblique wave must be computed, by a nonlinear iterative approach with three parameters (chapter 2.3.1.), covering modules 4.a., b., c. (figure 2.5.). in the case of EDW equivalent design waves, a direct implementation in the FEM program of the iterative approach has been

proven practically feasible only in the case of head waves (μ=180 degrees), so that for the oblique waves (μ=0-360 degrees), we have developed an external source program code P_QSW. For this program as input data we have to import from the floating dock data the offset lines 3D model and the mass diagram from the 3D-FEM model.

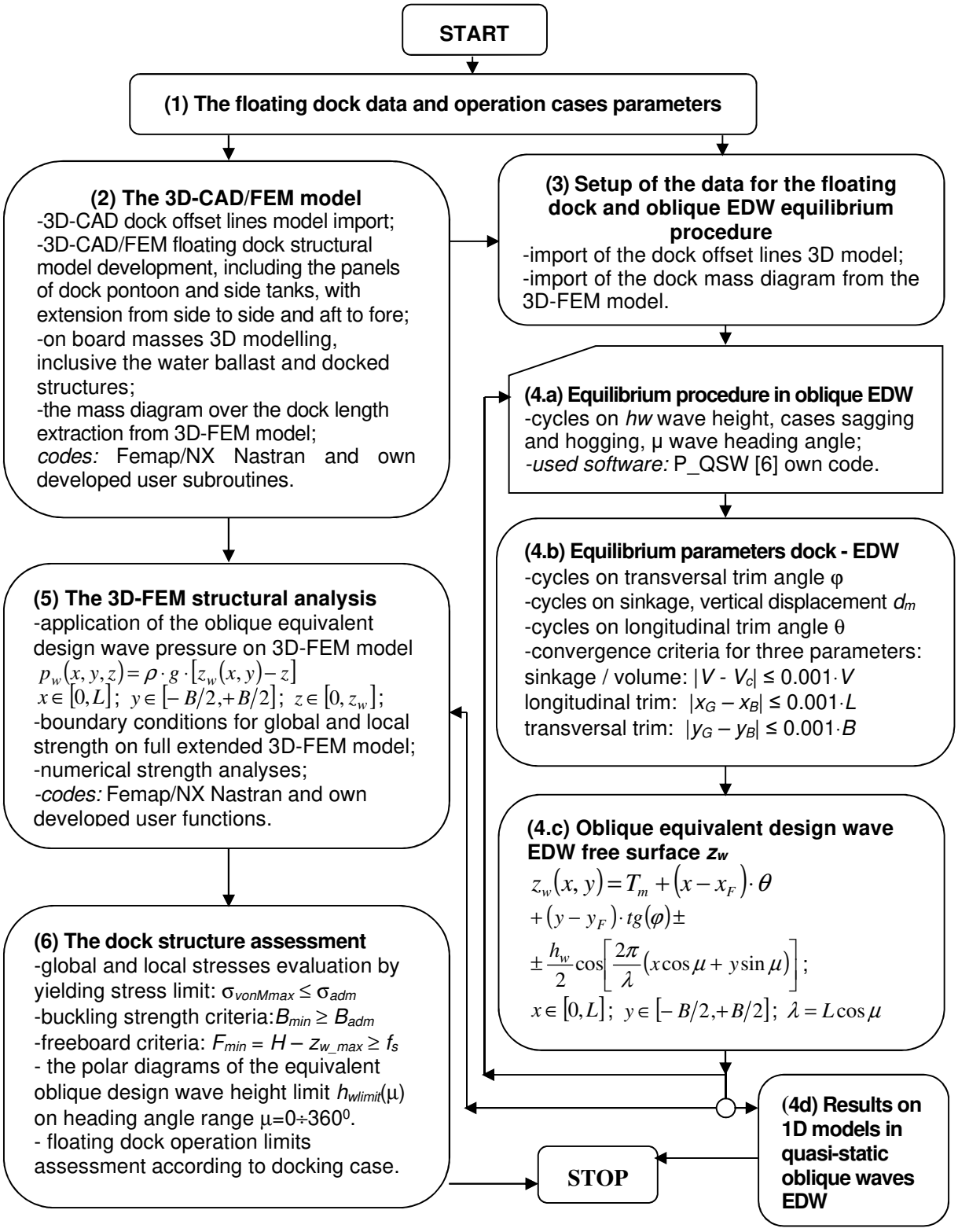

Figure 2.5. *The algorithm for floating dock structural analysis in oblique design waves by 3D-FEM approach [51]*

4.a., b., c., d. *Equilibrium procedure in oblique EDW. For each floating dock constructive version and loading case, using the P_QSW program [44], [52], the operation conditions are cycled for oblique EDW wave height h_w and heading angle* μ. Subsequently, for the 3D-FEM analysis only the cases that satisfy the minimum free board restrictions will be selected. Based on the three equilibrium parameters, the free surface of the quasi-static oblique wave is calculated (equation 2.14.)

$$\begin{aligned} &\textit{Pressure: max(0.000;(!ro*9.81*(-ZEL(!EL)+!Tm+} \\ &\textit{+(XEL(!EL)-!xf)*!teta*180/!PI+(YEL(!EL)-!yf)*TAN((!phi*180/!PI))±} \\ &\textit{±!hw/2*COS((XEL(!EL)*360*COS(!niu)/!lambda} \\ &\textit{+YEL(!EL)*360*SIN(!niu)/!lambda)))))} \end{aligned} \tag{2.14}$$

5. *The 3D-FEM structural analysis. The external pressure from the oblique equivalent design wave for each loading and operation case, is applied on the floating dock hull external shell by own developed user functions, implemented in the FEM program (equation 2.14.) Femap/NX Nastran [42].* Because the oblique wave pressure has an unsymmetrical distribution on the sides, at centre plane reference, special boundary conditions for the 3D-FEM models has to be considered (figure 2.6., table 2.2.), in four nodes, one at fore peak and three at aft peak. The numerical structural simulations involve: linear static analysis, under the assumption that the dock stresses are below the yielding stress limit, and first mode buckling iterative analysis [27], [28], [44], [53], [54], with specific solvers according to the FEM program [42].

6. The dock structure assessment. The global and local strength assessment is done by three criteria: yielding stress admissible value σ_{adm}, buckling admissible factor B_{adm} and freeboard safety value f_s according to [1], [3]. Based on the three criteria, for each floating dock constructive version the polar diagrams of the oblique EDW wave height limit, $h_{wlimit}(\mu)|_{load}$, over the whole wave heading angle range μ=0-360^0, are obtained.

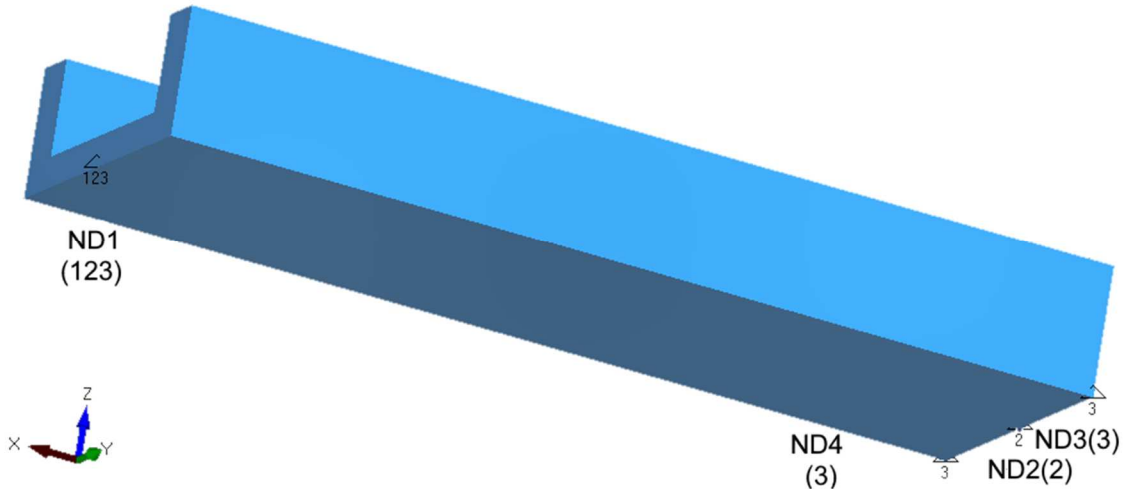

Figure 2.6 *Boundary conditions for the 3D-FEM model at oblique EDW waves*

Table 2.2 *Boundary conditions for the 3D-FEM model at oblique EDW waves [44]*

Position	NOD	x	y	z	U_x (1)	U_y (2)	U_z (3)	R_x (4)	R_y (5)	R_z (6)
Fore	ND_1	L	0	0	x	x	x	-	-	-
Aft	ND_2	0	0	0	-	x	-	-	-	-
	ND_3	0	B/2	0	-	-	x	-	-	-
	ND_4	0	-B/2	0	-	-	x	-	-	-

In the thesis, the procedure presented in this chapter is applied to the study of the structural capacity at requests form quasi-static oblique extreme waves, for two small floating docks (L=60m) in chapter 5.3., using 3D-FEM structural models and 1D equivalent beam model.

2.4. Methods for analysing the dynamic behaviour of floating docks in random waves

When operating floating docks, situations may arise when they need to be relocated between different shipyards, located on river or coastal routes. Normally the operation of relocation of the docks is performed without docked mass, ballasted at a medium draft dictated by the criteria of transversal stability and minimum freeboard. In this case, in addition to the assessment of the structural capacity of the floating docks (subchapters 2.1. - 2.3.), the rules of the dock classification societies [1], [3] require the analysis of the dynamic behaviour of the docks in oblique random waves (oscillations), for the evaluation of the limit criteria for seakeeping.

For the oscillation analysis of the floating docks we used the DYN software (OSC model) [30], [45] with the logic diagram in figure 2.9, based on a linear hydrodynamic model, the strip theory [55] and which is experimentally validated on a small-scale model of a ship at the fairing basin (chapter 3). The analysis of the dynamic response of the floating dock to the relocation operation includes the following main steps:

1. Development of the numerical model. The input data for the analysis of dock oscillations are taken from the 1D equivalent beam structural model. The speed range for dynamic analysis is established according to the drag resistance characteristics of the tug - floating dock convoy, where the maximum towing speed results v_{max}, and the minimum speed is v_{min}=0, which corresponds to the extreme case of damage of the tugboat. Depending on the route selected for the relocation of the dock, we considered routes on the Danube river, where the maximum significant wave height is H_s = 0.6; 1.2; 2 m. or routes on the Black Sea coast, between Sulina and Mangalia, where the maximum significant height of the irregular waves H_{smax} it is selected according to the norms of the classification societies [1],[3] for the coastal area RE(50%).

2. *Determining the RAO response amplitude functions*. Based on a 2D linear hydrodynamic potential flow model, according to the strip method, and with the cross sections parameterized by the transform according to three parameters, according to the Lewis method, the radiation terms are calculated, additional hydrodynamic masses and damping on the oscillation components of the floating dock [30], [55] depending on the ship-wave circular frequency ω_e (2.16), being constant over time with reference to the equilibrium position of the dock in still water. The diffraction terms are calculated for the excitation of the regular wave with unitary amplitude (a_w=h_w/2=1) [56]. For each towing speed the dock-wave heading angle is in the range of μ=0-360^0, $\delta\mu$=5^0, and the frequency of the wave is in the range ω=0-3 rad/s and $\delta\omega$=0,001 rad/s. The time domain the linearized motion equations system at the oscillations of the dock are linearized and for the excitation of the regular wave, with unitary amplitude, it has the expression:

$$([M]+[A(\omega_e)])\{\ddot{Q}(t)\}+[B(\omega_e)]\{\dot{Q}(t)\}+[C(\omega_e)]\{Q(t)\}=\{\overline{F}_w(\omega_e)\}e^{-i\,\omega_e t};\ \{Q(t)\}=\{\overline{Q}(\omega_e)\}e^{-i\cdot\omega_e t} \tag{2.15}$$

$$\omega_e=\omega-\omega^2/g\ v\cos\mu \tag{2.16}$$

where: $[M]$ the ship's own mass matrix; $[A(\omega_e)], [B(\omega_e)], [C(\omega_e)]$ are the hydrodynamic radiation (inertial and damping) and hydrostatic matrix; $\{\overline{F}_w(\omega_e)\}$ is hydrodynamic diffraction vector from the regular wave excitation; $\{\overline{Q}(\omega_e)\}$ is the motion amplitude; ω, ω_e are the wave and the encountering ship-wave circular frequencies; *g* is the gravity acceleration.

The time domain motion equations system for regular wave (2.15) is obtained directly in the frequency domain and for *j* motion components of response amplitude operators RAO_j:

$$[D(\omega_e)]\{\overline{Q}(\omega_e)\}e^{-i\,\omega_e t}=\{\overline{F}_w(\omega_e)\}e^{-i\,\omega_e t}\rightarrow\{\overline{Q}(\omega_e)\}=[D(\omega_e)]^{-1}\{\overline{F}_w(\omega_e)\};\qquad [D(\omega_e)]=-\omega_e^2([M]+[A(\omega_e)])-i\,\omega_e[B(\omega_e)]+[C(\omega_e)] \tag{2.17}$$

$$\{\overline{Q}(\omega_e)\}=\{Q_1(\omega_e)\}+i\{Q_2(\omega_e)\}\rightarrow q_j(t)=Q_{1j}(\omega_e)\cos\omega_e t+Q_{2j}(\omega_e)\sin\omega_e t\quad j=1,6 \tag{2.18}$$

$$q_j^a(\omega_e)=\sqrt{Q_{1j}^2(\omega_e)+Q_{2j}^2(\omega_e)}\rightarrow RAO_j(\omega_e)\Big|_{v,\omega,\mu}=\frac{q_j^a(\omega_e)}{a_w}\Big|_{aw=1}\quad j=1,6$$

For the main motions and accelerations components of the large floating dock: heave ζ (*j*=3), pitch θ (*j*=5) and roll φ (*j*=4).

3. *Determining the short-term statistical dynamic response (SSTR).* For the modelling of random waves we considered The short-term most probable statistical response in irregular waves with $S_w(\omega)$ spectrum with an ITTC parameter [57], [58], [59] (2.45.) for both navigation areas when relocating the docks, both for the Danube river area (Galați - Sulina) with the maximum wave significant height H_{smax}≤2m, as well as for the Black Sea coastal area (Sulina - Mangalia, figure 2.7), with the long-term histogram of the waves significant height in figure 2.8. [60], [61], [62], having the probability of 99,5% the occurrence of the significant wave height in the range of H_s=0-4m.

$$S_w(\omega)=\frac{\alpha}{\omega^5}e^{-\frac{\beta}{\omega^4}};\ \alpha=0{,}7795;\ \beta=\frac{3{,}11}{H_s^2};\ S_w^e(\omega_e)=S_w(\omega)\cdot\left|1-2\,\omega/g\ v\cos\mu\right|^{-1} \qquad (2.19)$$

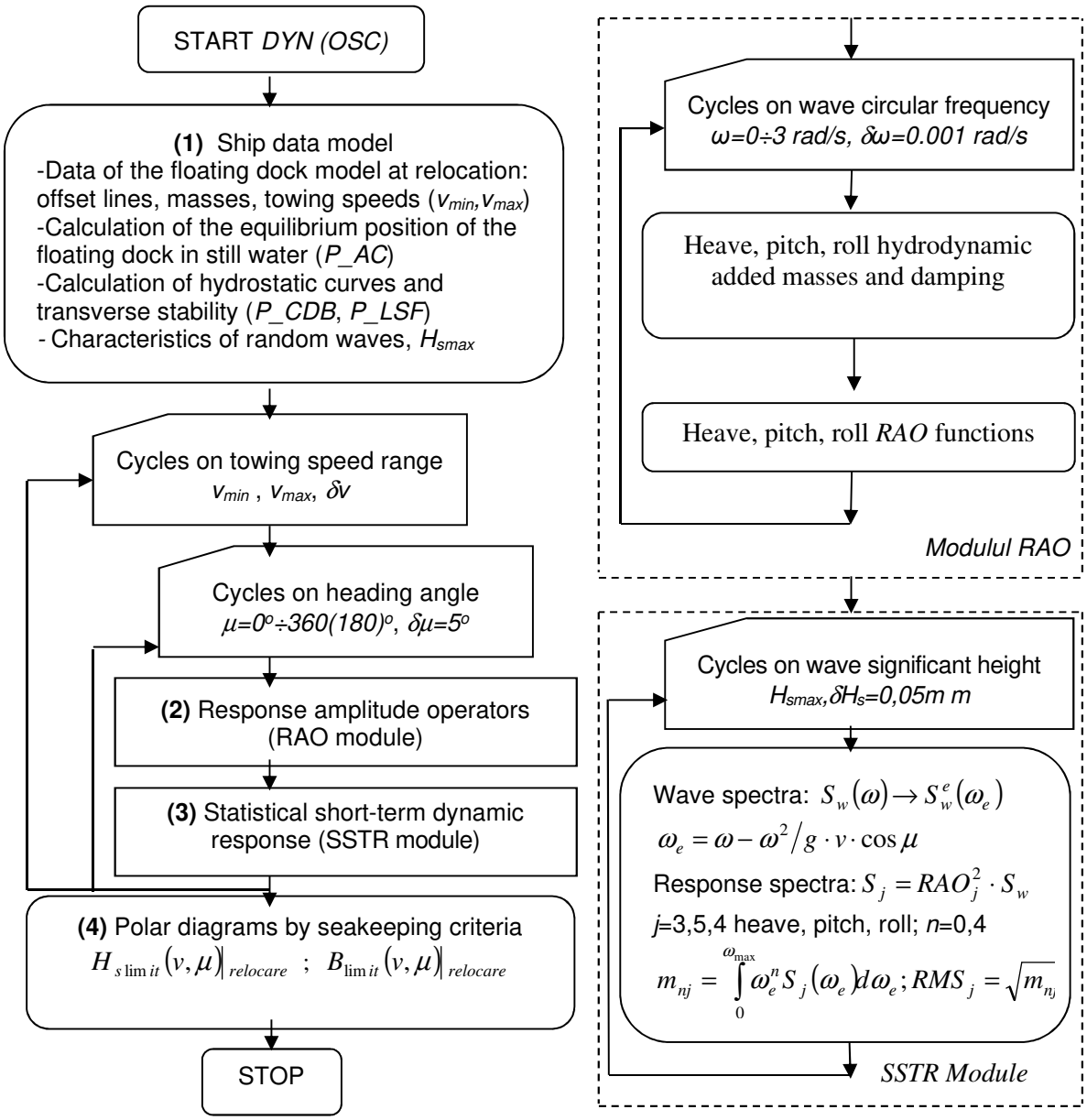

Figure 2.9. *Logical schematic of the DYN software (OSC module) [45], [62], [63] for analysing the dynamic response of floating docks at the relocation operation*

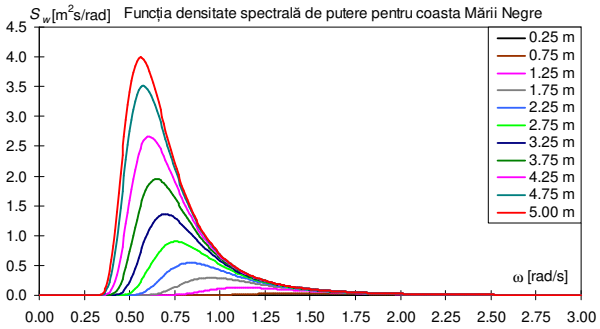

Figure 2.7. *Black Sea Romanian Costal average wave spectrum $S_w(\omega)$ [60]*

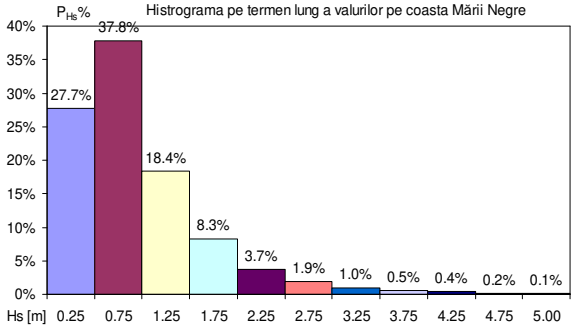

Figure 2.8. *Black Sea Romanian costal H_s, long term histogram P_H% [61]*

The power spectral density function of the dynamic response is obtained based on the amplitude response operator functions $RAO_j(\omega_e)$ and wave spectrum $S_w^e(\omega_e)$:

$$S_j(\omega_e) = RAO_j^2(\omega_e) \cdot S_w^e(\omega_e)\Big|_{v,\omega,\mu} \quad j = 1,6 \tag{2.20}$$

$$m_{0j} = \int_0^{\omega_{max}} S_j(\omega_e) d\omega_e \; ; \; m_{4j} = \int_0^{\omega_{max}} \omega_e^4 S_j(\omega_e) d\omega_e \quad j = 1,6 \tag{2.21}$$

$$q_j^{mp} = RMS_j = \sqrt{m_{0j}} \; ; \; q_{ac\,j}^{mp} = RMS_{ac\,j} = \sqrt{m_{4j}} \quad j = 1,6 \tag{2.22}$$

where the spectral moments result m_{0j}, m_{4j} the short-term static response, the most probable statistical motions amplitudes $q_j^{mp} = RMS_j$ and accelerations $q_{ac\,j}^{mp} = RMS_{ac\,j}$, used to evaluate seakeeping criteria.

4. *Determining the polar diagrams based on the seakeeping limit criteria*. In the last step, based on the DYN code (OSC module) [45], figure 2.9. the polar safety diagrams for the navigation of floating docks are determined, expressed in terms of significant wave height H_{slimit} (v, μ) and Beaufort level B_{limit} (v, μ). Polar diagrams are obtained based on the seakeeping limit criteria (2.23 - 2.25), also taking into account the criterion of the minimum freeboard, without flooding the pontoon's deck, being formulated as the admissible statistical most probable response values RMS_{adm} and applied to: vertical movements at the stern $RMS_z\big|_{pp}$, bow $RMS_z\big|_{pv}$, middle $RMS_z\big|_m$, results from the combination of vertical oscillations, pitch, roll at x=0, $L/2$, L and y=$B/2$; pitching movements RMS_θ and roll RMS_φ; vertical accelerations $RMS_{ac\zeta}$, pitch $RMS_{ac\theta}$ and roll $RMS_{ac\varphi}$. [64], [65], [66]

The study of the operating capacity under random wave conditions of the tugboat used to relocate floating docks on river or coastal routes is performed using the entire DYN software (OSC module) [144] (figure 2.9).

- heave motion at aft, bow and middle

$$\begin{gathered} RMS_{z\,adm}\Big|_{pp,pv,m} = D_{pp,pv,m} - f_s - T_{pp,pv,m} \geq RMS_z\Big|_{pp,pv,m} \\ RMS_z\Big|_{pp} = RMS_\zeta + x_F \cdot RMS_\theta + B/2 \cdot RMS_\varphi + H_s/4 \; ; \\ RMS_z\Big|_{pv} = RMS_\zeta + (L - x_F) \cdot RMS_\theta + B/2 \cdot RMS_\varphi + H_s/4 \\ RMS_z\Big|_{mid} = RMS_\zeta + B/2 \cdot RMS_\varphi + H_s/4 \end{gathered} \tag{2.23}$$

- pitch and roll motions

$$RMS_{\theta\,adm} \geq RMS_\theta \quad ; \quad RMS_{\varphi\,adm} \geq RMS_\varphi \tag{2.24}$$

- heave, pitch and roll accelerations

$$\begin{gathered} RMSac_{\zeta\,adm} \geq RMS_{ac\zeta} \; ; \qquad RMSac_{\varphi\,adm} = \overline{RMS}ac_{\varphi\,adm} \big/ (B/2) \geq RMSac_\varphi \\ RMSac_{\theta\,adm} = \overline{RMS}ac_{\theta\,adm} \big/ (\min\{x_F, (L - x_F)\}) \geq RMSac_\theta \end{gathered} \tag{2.25}$$

where: *L, B, D,* x_F they are the length, the width, the height at the pontoon deck and the floating centre of balance in still water; H_s is the significant height of the wave; *g* is gravitational acceleration; f_s is the minimum allowed value of the freeboard.

Table 2.3 The admissible values for the seakeeping criteria [60], [62], [63]

Criterion	$RMS_{z\,adm}\big\vert_{pp,pv,m}$	f_s	$RMS_{\theta\,adm}$	$RMS_{\varphi\,adm}$	$RMSac_{\zeta\,adm}$	$\overline{RMS}ac_{\theta\,adm}$	$\overline{RMS}ac_{\varphi\,adm}$
Dock60_CWT	relation (2.23) L=60m	0.075m	1^0	4^0	0.05·g	0.10·g	0.15·g
Dock60_NWT	relation (2.23) L=60m	0.300m	1^0	4^0	0.05·g	0.10·g	0.15·g
Dock_VARD_Tulcea	relation (2.23) L=209.2m	0.300m	2^0	4^0	0.10·g	0.10·g	0.10·g
TUG 4,000C.P.	relation (2.23) L=48m	0.300m	3^0	8^0	0.10·g	0.15·g	0.10·g

In this thesis we analysed the safe navigation conditions for three types of floating docks Dock60-CWT (*L*=60 m, continuous upper tanks, chapter 6), Dock60-NWT (*L*=60 m, discontinuous upper tanks, chapter 6), Dock_VARD_Tulcea (*L*=209.2 m, discontinuous upper tanks, chapter 8), with the technical data in chapter 4, as well as for the river and seagoing tugboat TUG 4,000 H.P., chapter 9, having selected the allowable limits for seakeeping criteria according to the norms of international naval classification companies [1], [3] presented in Table 2.3. The navigation classes are marked on the river area SW (still water), IN(0.6), IN(1.2), IN(2.0) and coastal C(2.5), C(3.0), C(4.0), depending on the wave height of 0–4 m.

CHAPTER 3

EXPERIMENTAL TESTS FOR THE VALIDATION OF THE METHOD OF ANALYZING THE OSCILATIONS OF THE NAVAL STRUCTURES IN HEAD, FOLLOWING AND BEAM WAVES

For the numerical analysis of the naval structures oscillations in regular and random waves, we used the program code DYN [45] based on the hydrodynamic model presented in subchapter To validate the DYN program code [45], we developed the experimental study in the hull basin of the Faculty of Naval Architecture in Galați, using a 1:16 scale model of a full-fledged fluvial research vessel, made available by SDG Company – Ship Design Group in Galați [168]. The experimental model is made of wood and fiberglass mounted on the trolley of the hull basin and it is equipped with transducers for measuring the oscillation movement in the vertical direction and the pitch and roll oscillation angles. The wave transducer is also mounted on the trolley. The experimental tests are performed for two reference speeds and some significant cases of the height of the head, following and transverse waves. **The results of this chapter are published and presented in the article in reference [68].**

3.1. Description of the experimental model

For the safety assessment in the case of floating docks navigation in the transition phase between locations (chapter 6, chapter 8), we will analyse the dock oscillations in regular and random waves using the program code DYN [45], with the hydrodynamic model presented in subchapter 2.4.

To validate the DYN program code [45], we considered in the experimental study a river-maritime survey vessel (SV), designed by SDG - Ship Design Group in Galați [67].

The experimental model of the research vessel is reduced to a 1:16 scale (figure 3.1.a., b.) and is made of wood and fiberglass extended only to the main deck. Figure 3.2. presents the design plan of the survey vessel [67]. Table 3.1. shows the main characteristics of the model on a natural scale and reduced to a scale of 1:16.

a.  b. 

Figure 3.1.a., b. *The experimental model at 1:16 scale of the river-maritime research vessel (a. – top view – for, b. – aft view with the bottom of the ship)*

Table 3.1. Main characteristics of the ship and the model of the survey vessel [67].

Symbol and units	Full scale	Model scale 1:16	Symbol and units	Full scale	Model scale 1:16
L_{max} [m]	46.4	2.9	C_B	0.791	
L_{CWL} [m]	44.151	2.759	C_M	0.991	
L_{Pp} [m]	43.2	2.7	C_W	0.941	
D_{Pp} [m]	3.25	0.203	N_C	80	
B_{WL} [m]	13.0	0.813	d_x [m]	0.6	0.037
T_M[m], T_{Pp}[m], T_{Pv}[m]	1.5	0.094	φ_{max} [°]	26	
x_G [m]	20.074	1.255	g [m/s^2]	9.81	
y_G [m]	1.992	0.125	ρ [kg/m^3]	1,010.0	998.9
GM_T [m]	8.950	0.559	*v[km], v[m/s]*	10	1.28
Δ [m^3]	680.97	0.166	F_n	0.246	

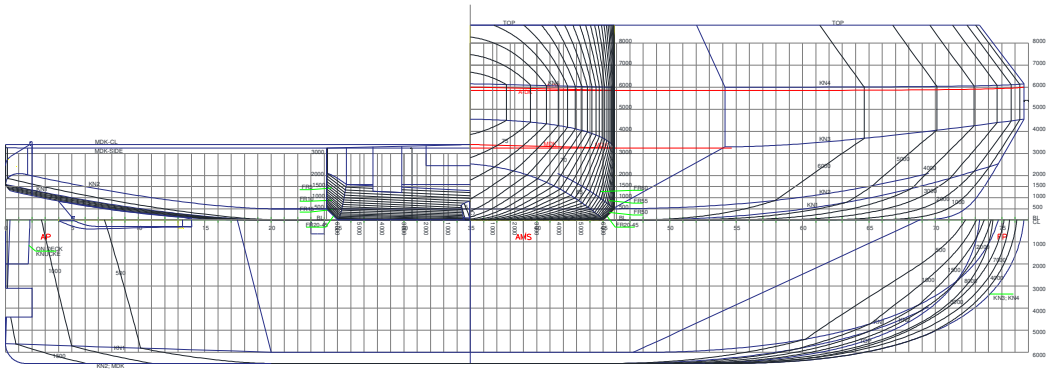

Figure 3.2. *The body plan of the research vessel [67]*

The experimental tests are developed in the hull basin of the Faculty of Naval Architecture, “Dunărea de Jos” University in Galați (figures 3.3.a., b., figures 3.4.a., b., figure 3.5., figure 3.6.), with the main dimensions 45x4x3 m and with a maximum traction speed of 4 m/s. The hull basin has an automated trolley for towing experimental models, produced by the company *Cussons Marine Technology Ltd [69]* with an integrated command and measurement system. The acquisition system is equipped with sensors (figures 3.4.a., b.) for measuring the vertical movements and pitching oscillations, if the model is placed longitudinally to the hull basin (figure 3.7.), respectively for measuring the movements of vertical and roller oscillations, if the model is arranged transversely to the hull basin (figure 3.8.). The wave transducer is also mounted on the trolley of the hull basin (figure 3.6.). Preliminarily all the translators were calibrated.

a.

b.

Figure 3.3.a., b. *The towing tank carriage system, Cussons Marine Technology Ltd. model [69]*

a.

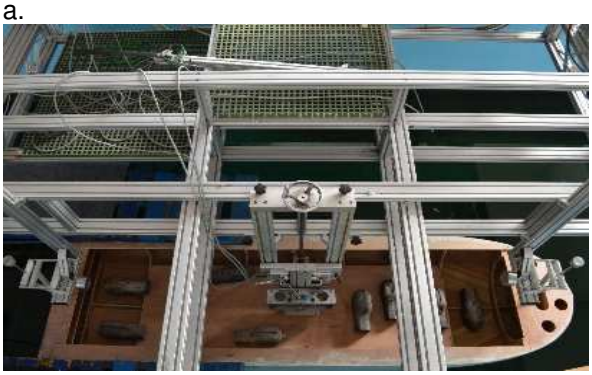

b.

Figure 3.4.a, b. *The transducers for heave, pitch or roll measurement*

Figure 3.5 *The regular wave generator*

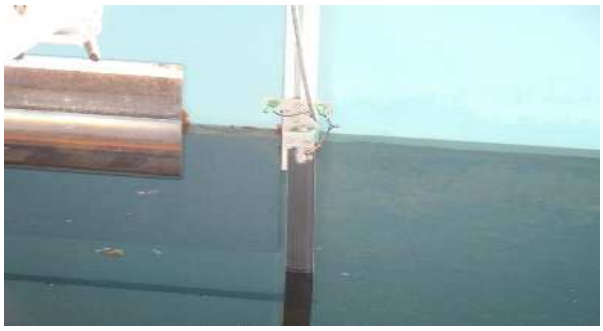

Figure 3.6. *the wave transducer*

For the experimental analysis, we considered in all cases an acquisition time of T_s = 30 s, with a sampling time step of δt = 0.1 s, which corresponds to the sampling frequency of $f_{sampling}$ = 10 Hz. It was taken into account that the recorded dynamic response has a maximum frequency of 2 Hz. The oscillations of the experimental model are produced by the mechanical generator of the hull basin (*figure 3.5.*), with regular head, following and transversal waves, with a frequency range f = 0.4 – 1.1 Hz. The experimental analysis of the oscillations of the scaled model is performed in compliance with the international ITTC procedures [58], [59].

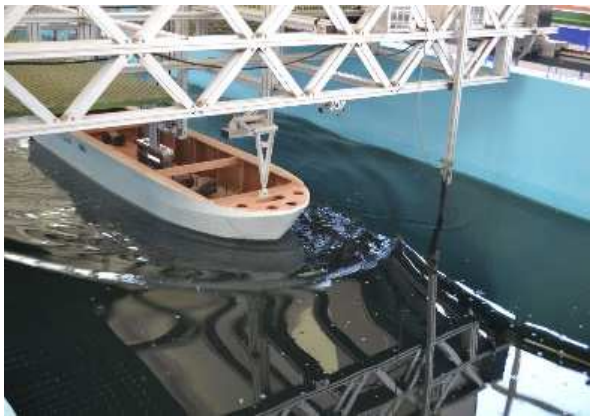

Figure 3.7. *The research vessel model at head wave condition*

Figure 3.8. *The research vessel model at beam wave condition*

3.2. Experimental analysis of the oscillations of the river – maritime research vessel

The program for the experimental analysis of the oscillations of the research vessel on the model reduced to a 1:16 scale, aims to determine the RAO response amplitude operator functions in regular waves (defined in subchapter *2.4., relation 2.18.*).

In table 3.2. the experimental test program for the study vessel model is presented. We considered four main cases depending on the wave propagation direction:

- Head wave μ = 180˚ and the speed of the model v = 1.28 m/s, F_n = 0.246;
- Head wave μ = 180˚ and the stationary model in the middle of the basin, v = 0 m/s, F_n = 0, longitudinally positioned relative to the axis of the hull basin and oriented with the stern towards the wave generator;

- Following wave $\mu = 0^{\circ}$ and the stationary model in the middle of the basin, $v = 0$ m/s, $F_n = 0$, longitudinally positioned relative to the axis of the hull basin and oriented with the stern towards the wave generator;
- Transverse wave $\mu = 90^{\circ}$ and the stationary model in the middle of the basin, $v = 0$ m/s, $F_n = 0$, placed transversely with respect to the axis of the hull basin.

The frequency of the waves generated in the hull basin are in the range $f = 0.427 – 1.086$ Hz, resulting in the model with the speed of $v = 1.28$ m/s frequency of the meeting of the ship - wave $f_e = 0.568 – 1.672$ Hz.

Table 3.2. The program of experimental tests for the model of the survey vessel and the amplitude values from the FFT spectral analysis

Case	μ [°]		v [m/s]	F_n	Frequency cases	f [Hz]	f_e [Hz]	A_{SW} [mm]	$A_{S\zeta}$ [mm]	$A_{S\theta}$ [°]	$A_{S\varphi}$ [°]
1	180	Head wave	1.28	0.246	T1	0.432	0.586	6.237	4.493	0.174	0.000
					T2	0.534	0.769	6.546	4.430	0.269	0.000
					T3	0.634	0.964	9.506	4.119	0.383	0.000
					T4 **Fig. 3.10.a. – h.**	0.743	1.196	9.623	1.388	0.217	0.000
					T5	0.849	1.440	12.302	0.211	0.083	0.000
					T6	0.943	1.672	10.215	0.491	0.010	0.000
2			0	0	T1	0.427	0.27	7.209	4.951	0.248	0.000
					T2	0.537	0.537	6.371	3.664	0.316	0.000
					T3	0.623	0.623	9.295	3.724	0.529	0.000
					T4 **Fig. 3.11.a. – h**.	0.732	0.732	14.655	2.307	0.714	0.000
					T5	0.830	0.830	15.046	2.197	0.398	0.000
					T6	0.928	0.928	10.486	1.679	0.018	0.000
3	0	Following wave	0	0	T1	0.427	0.427	6.924	4.740	0.232	0.000
					T2	0.525	0.525	6.674	3.981	0.297	0.000
					T3	0.647	0.647	9.081	3.014	0.443	0.000
					T4	0.745	0.745	8.279	0.977	0.281	0.000
					T5	0.830	0.830	14.647	1.097	0.236	0.000
					T6 **Fig. 3.12.a. – h.**	0.928	0.928	11.527	1.005	0.059	0.000
4	90	Beam wave	0	0	T1	0.427	0.427	7.346	5.796	0.000	0.275
					T2	0.525	0.525	8.810	6.905	0.000	0.502
					T3	0.623	0.623	7.496	5.489	0.000	0.656
					T4	0.732	0.732	12.721	9.162	0.000	1.393
					T5	0.830	0.830	14.041	8.876	0.000	1.927
					T6	0.964	0.964	14.439	6.011	0.000	2.541
					T7	1.025	1.025	16.853	5.369	0.000	3.244
					T8 **Fig. 3.13.a. – h.**	1.086	1.086	16.438	3.855	0.000	2.986

Figure 3.10.a. *Experimental SV model, v=1.28 m/s, T4, μ=180º, bow view*

Figure 3.10.b. *Experimental SV model, v=1.28 m/s, T4, μ=180º, stern view*

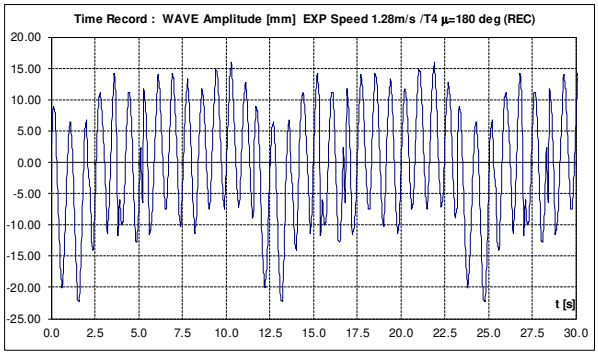

Figure. 3.10.c. *Recording of the elongation of the wave [mm], v=1.28 m/s, T4, μ=180º*

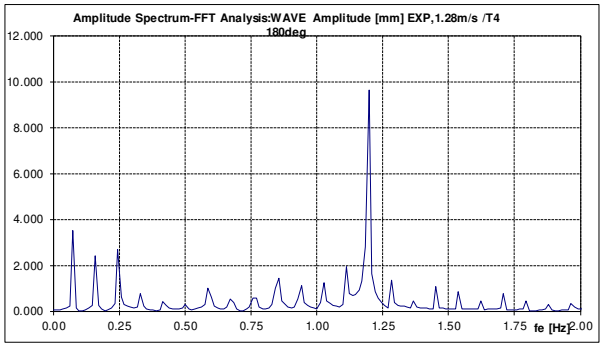

Figure. 3.10.d. *Amplitude spectrum (FFT) elongation of the wave [mm], v=1.28 m/s, T4, μ=180º*

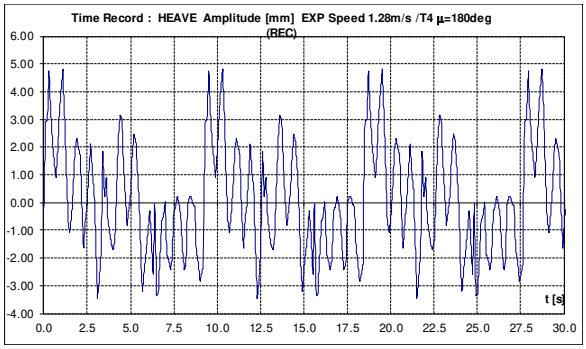

Figure. 3.10.e. *Vertical displacement recording [mm], v=1.28 m/s, T4, μ=180º*

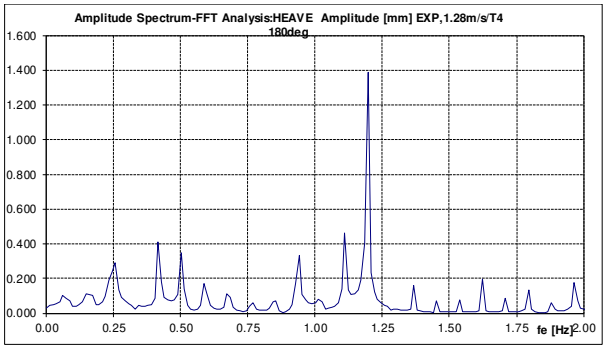

Figure. 3.10.f. *Amplitude spectrum (FFT) vertical displacement [mm], v=1.28 m/s, T4, μ=180º*

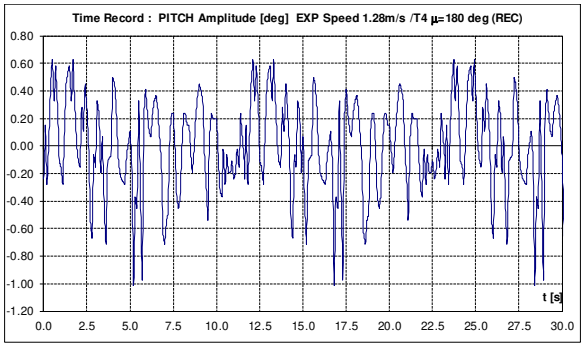

Figure. 3.10.g. *Recording the pitch angle [º], v=1.28 m/s, T4, μ=180º*

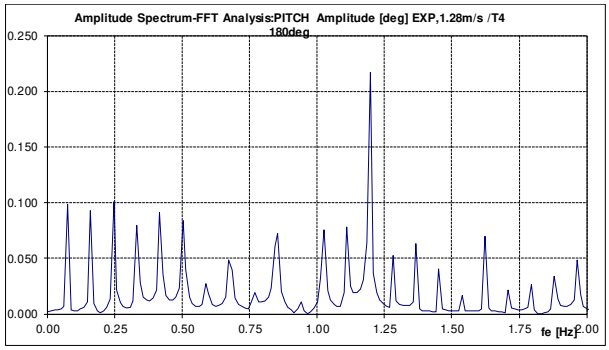

Figure. 3.10.h. *Amplitude spectrum (FFT) pitch angle [º], v=1.28 m/s, T4, μ=180º*

Figure 3.11.a. *Experimental SV model, v=0 m/s, T4, μ=180º, bow view*

Figure 3.11.b. *Experimental SV model, v=0 m/s, T4, μ=180º, stern view*

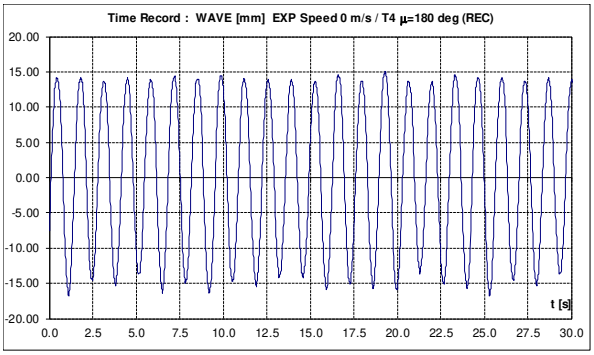

Figure. 3.11.c. *Recording of the elongation of the wave [mm], v=0 m/s, T4, μ=180º*

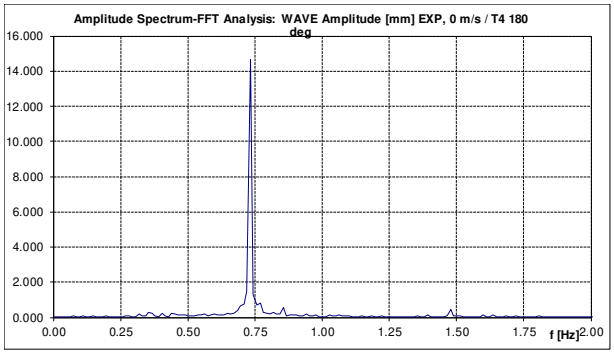

Figure. 3.11.d. *Amplitude spectrum (FFT) wave elongation [mm], v=0 m/s, T4, μ=180º*

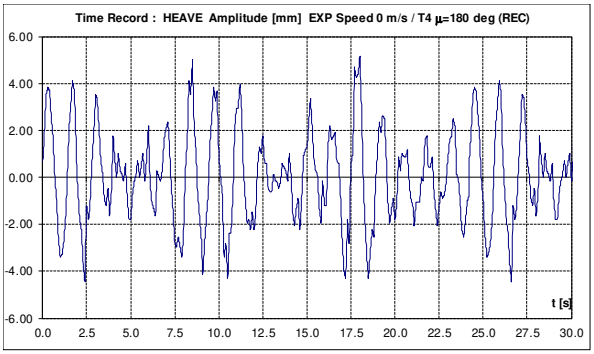

Figure. 3.11.e. *Vertical displacement recording [mm], v=0 m/s, T4, μ=180º*

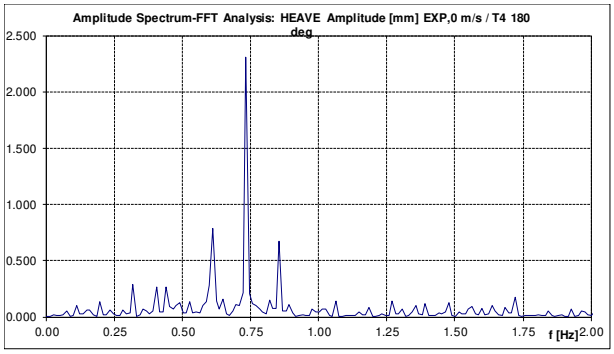

Figure. 3.11.f. *Amplitude spectrum (FFT) vertical displacement [mm], v=0 m/s, T4, μ=180º*

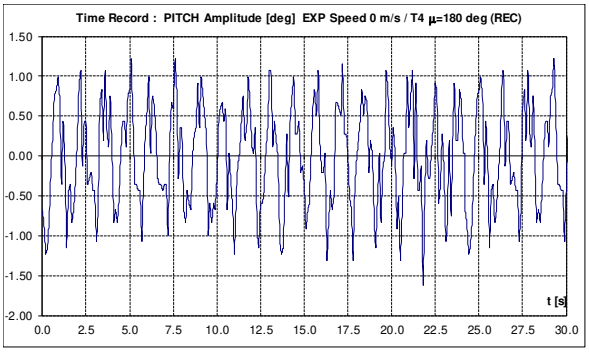

Figure. 3.11.g. *Recording the pitch angle [º], v=0 m/s, T4, μ=180º*

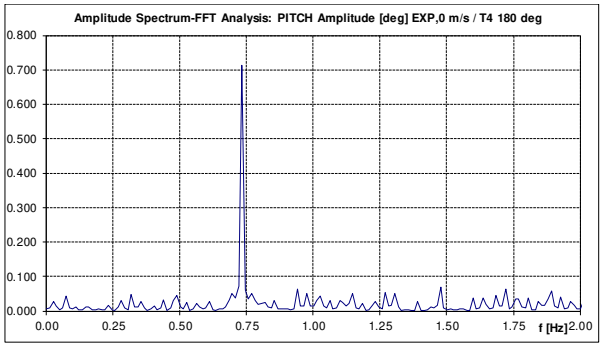

Figure. 3.11.h. *Amplitude spectrum (FFT) pitch angle [º], v=0 m/s, T4, μ=180º*

Figure 3.12.a. *Experimental SV model, v=0 m/s, T6, μ=0º, stern view*

Figure 3.12.b. *Experimental SV model, v=0 m/s, T6, μ=0º, bow view*

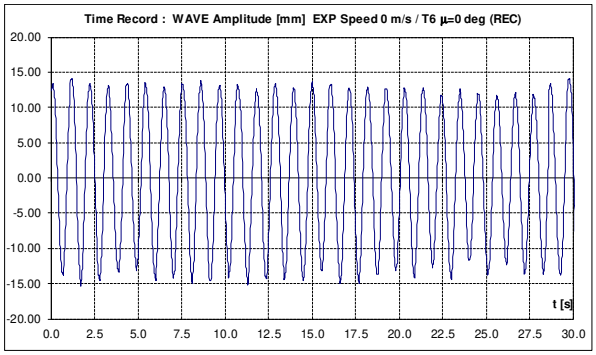

Figure. 3.12.c. *Recording of the elongation of the wave [mm], v=0 m/s, T6, μ=0º*

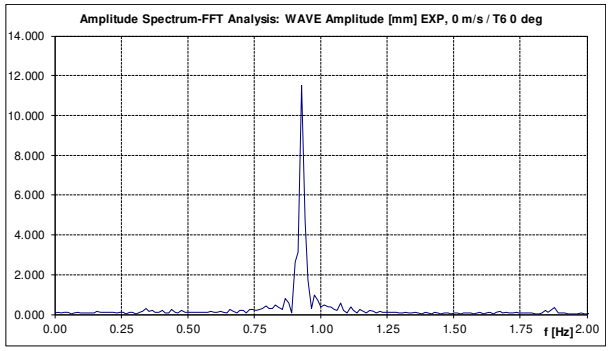

Figure. 3.12.d. *Amplitude spectrum (FFT) wave elongation [mm], v=0 m/s, T6, μ=0º*

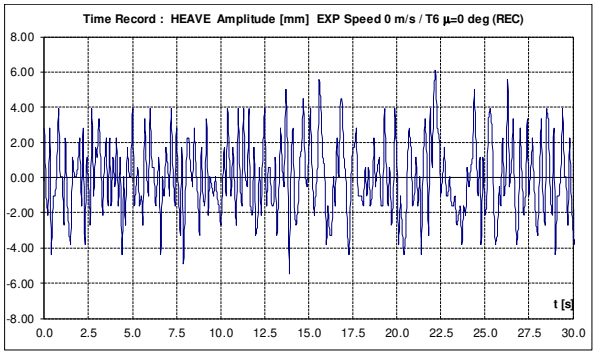

Figure. 3.12.e. *Vertical displacement recording [mm], v=0 m/s, T6, μ=0º*

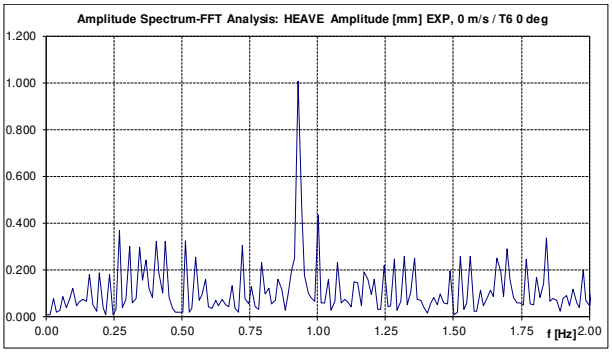

Figure. 3.12.f. *Amplitude spectrum (FFT) vertical displacement [mm], v=0 m/s, T6, μ=0º*

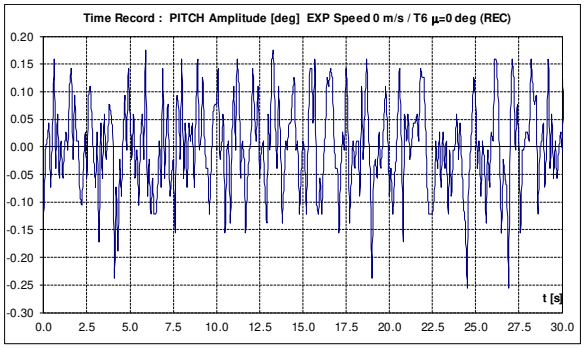

Figure. 3.12.g. *Recording the pitch angle [º], v=0 m/s, T6, μ=0º*

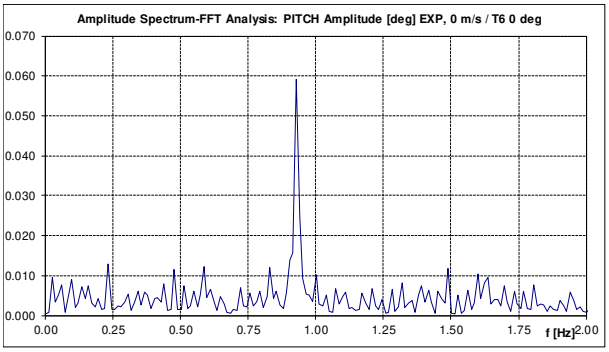

Figure. 3.12.h. *Amplitude spectrum (FFT) pitch angle [º], v=0 m/s, T6, μ=0º*

Figure 3.13.a. *Experimental SV model, v=0 m/s, T8, μ=90º, starboard view*

Figure 3.13.b. *Experimental SV model, v=0 m/s, T8, μ=90º, stern view*

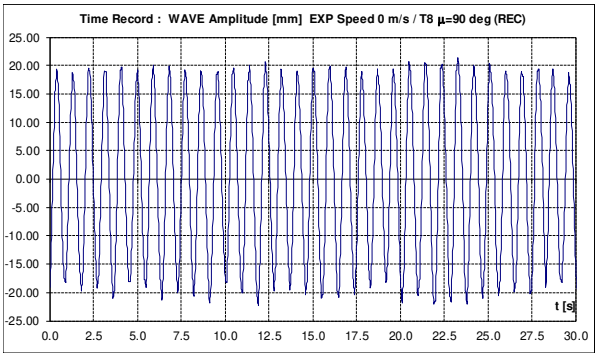

Figure. 3.13.c. *Recording the elongation of the wave [mm], v=0 m/s, T8, μ=90º*

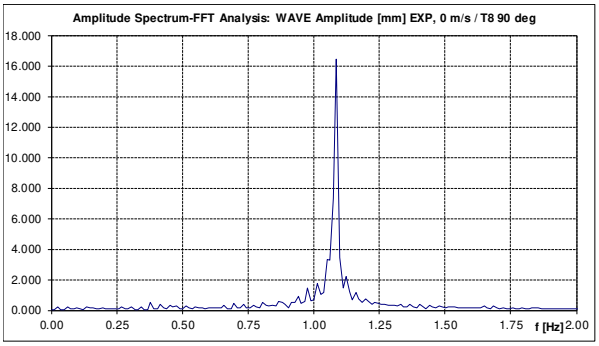

Figure. 3.13.d. *Amplitude spectrum (FFT) wave elongation [mm], v=0 m/s, T8, μ=90º*

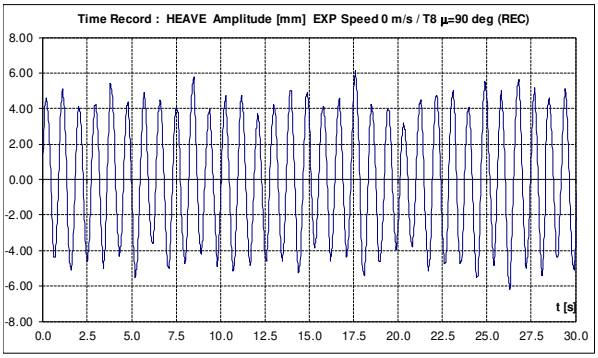

Figure. 3.13.e. *Vertical displacement recording [mm], v=0 m/s, T8, μ=90º*

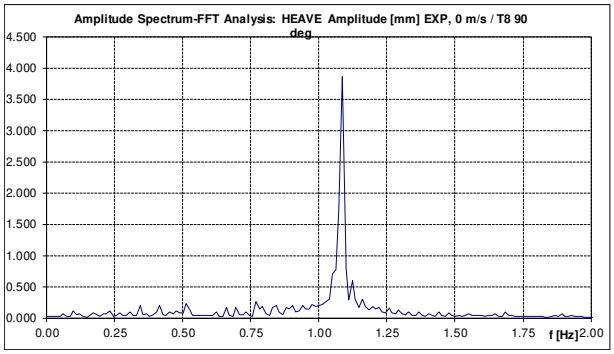

Figure. 3.13.f. *Amplitude spectrum (FFT) vertical displacement [mm], v=0 m/s, T8, μ=90º*

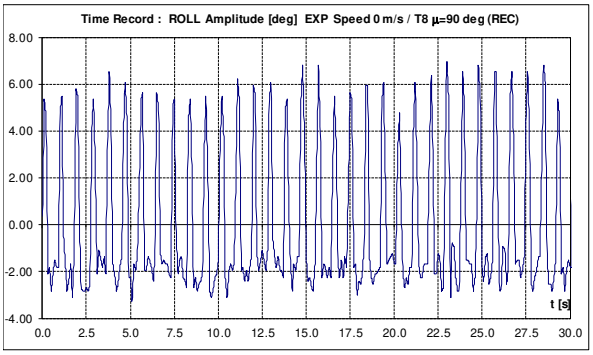

Figure. 3.13.g. *Roll angle recording [º], v=0 m/s, T8, μ=90º*

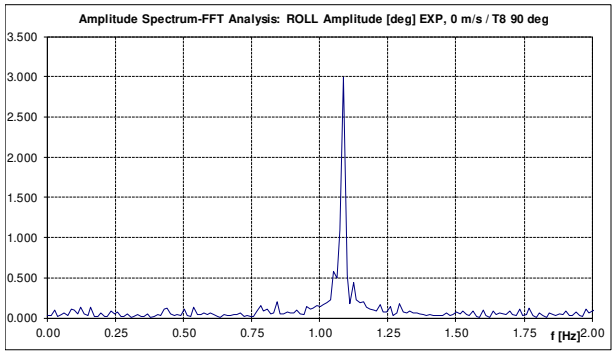

Figure. 3.13.h. *Amplitude spectrum (FFT) roll angle [º], v=0 m/s, T8, μ=90º*

The amplitude spectra are obtained for recordings in the time domain of wave elongation and dynamic response to oscillations (vertical displacement, pitch angle and roll angle) using Fast Fourier Transform - FFT [58],. To ensure the accuracy of the FFT procedure, all the records in the initial time domain are processed numerically, so the sampling step is brought to the value of δt = 0.01 s.

Figures 3.10. – 13.a., b. present selected frames from the films made during the experiments. Figures 3.10. – 13.c., d., e., f., g., h., present the recordings in the time domain and the amplitude spectra of wave A_{SW} [mm] and at oscillations: vertical displacement $A_{S\zeta}$ *[mm]*, pitch $A_{S\theta}$ *[˚]* and roll $A_{S\varphi}$ *[˚]* angles for the selected experimental cases (table 3.2.).

Based on the amplitude spectra resulting from the FFT processing of records in the time domain for all test sets (*table 3.2.*), in figures *3.14. – 17.a., b.* and tables *3.3. – 6.*, the experimental RAO amplitude response operators are presented for vertical oscillations, pitch and roll angles, calculated with the formula:

$$RAO_q^{\exp} = \frac{A_{S_q^{\exp}}}{A_{S_W^{\exp}}}\Big|_{freq}; q \in \{\xi, \theta, \phi\}; freq \in \{f; f_e\}; f = \frac{\omega}{2\pi} \tag{3.1.}$$

$$f_e = f - \frac{2\pi}{9.81} \cdot f^2 \cdot v \cdot \cos(\mu) \tag{3.2.}$$

Side effects on wave components (*figures 3.10. – 13.d.*) due to the reflection on the border of the hull basin as well as the own wave of the hull are neglected, so that from the amplitude spectra we consider in the calculation of the response amplitude operator functions RAO only the main component corresponding to the excitation wave.

For the 1:16 scale survey vessel model (table *3.1., figure 3.1. a., b.*), using the program code DYN [45], with the hydrodynamic model presented in subchapter 2.4., the numerical answer operators are obtained $RAO_q^{num}, q \in \{\zeta, \theta, \varphi\}$ (*figures 3.14. – 17. a., b.*) for the four sets of tests (*table 3.2.*). In the numerical analysis we considered as a source of excitation the regular wave with the unit amplitude a_w = 1 mm and pulsation ω = 0 – 9 rad/s (f_{max} = 1.432 Hz), $\delta\omega$ = 0.01 rad/s.

Tables 3.3. – 6. also present the average differences between the amplitude operators in response to vertical oscillations, pitch and roll angle, obtained experimentally and numerically, for the model reduced to scale 1:16 of the research vessel, defined as:

$$\delta_q = \left| 1 - \frac{1}{n_T} \sum_{j=1}^{n} \left(\frac{RAO_q^{\exp}}{RAO_q^{num}} \right)_j \right|; q \in \{\xi, \theta, \phi\} \tag{3.3.}$$

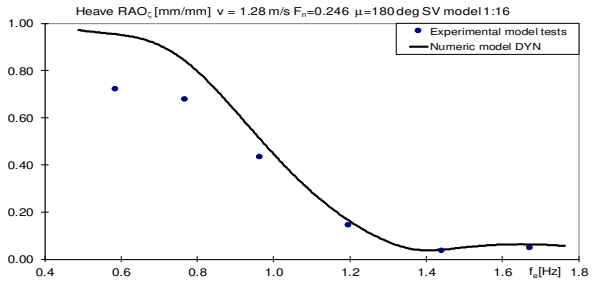

Figure 3.14.a. Heave RAO_ζ *[mm/mm], SV 1:16, μ=180⁰, v=1.28 m/s*

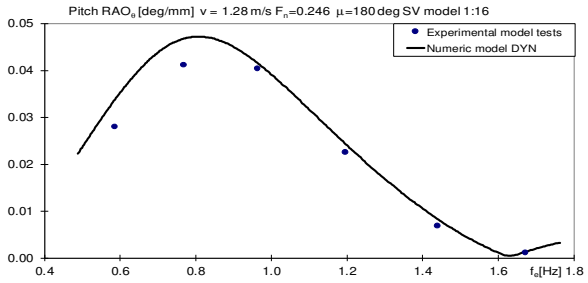

Figure 3.14.b. Pitch RAO_θ *[º/mm], SV 1:16, μ=180⁰, v=1.28 m/s*

Table 3.3. Heave & pitch RAO, SV model 1:16, *v*=1.28 m/s, ,μ=180⁰

Case	*f* [Hz]	f_e [Hz]	RAO_ζ [mm/mm]		RAO_θ [º/mm]	
			experiment	numeric	experiment	numeric
T1	0.432	0.586	0.720	0.954	0.028	0.034
T2	0.534	0.769	0.677	0.840	0.041	0.047
T3	0.634	0.964	0.433	0.511	0.040	0.042
T4	0.743	1.196	0.144	0.165	0.023	0.024
T5	0.849	1.440	0.034	0.040	0.007	0.008
T6	0.943	1.672	0.048	0.063	0.001	0.001
			$\delta\zeta = 18.17\%$		$\delta\theta = 13.28\%$	

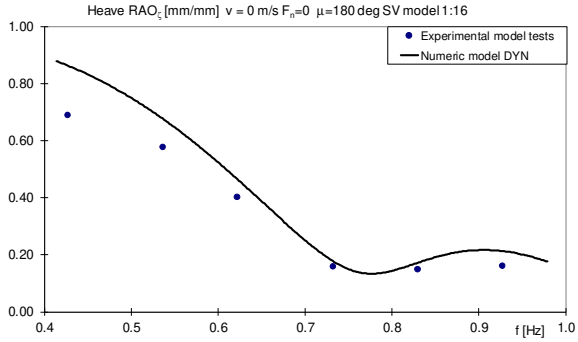

Figure 3.15.a. *Heave RAO_ζ [mm/mm], SV 1:16, μ=180^0, v=0 m/s.*

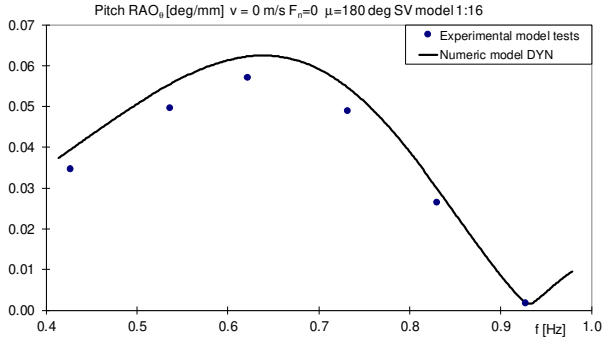

Figure 3.15.b. *Pitch RAO_θ [º/mm], SV 1:16, μ=180^0, v=0 m/s*

Table 3.4. Heave & pitch RAO, SV model 1:16, *v*=0m/s, ,μ=180^0

Case	*f* [Hz]	f_e [Hz]	RAO_ζ [mm/mm]		RAO_θ [º/mm]	
			experiment	numeric	experiment	numeric
T1	0.427	0.427	0.687	0.862	0.034	0.039
T2	0.537	0.537	0.575	0.675	0.050	0.055
T3	0.623	0.623	0.401	0.463	0.057	0.062
T4	0.732	0.732	0.157	0.177	0.049	0.054
T5	0.830	0.830	0.146	0.173	0.026	0.030
T6	0.928	0.928	0.160	0.213	0.002	0.002
			$\delta\zeta = 16.67\%$		$\delta\theta = 11.11\%$	

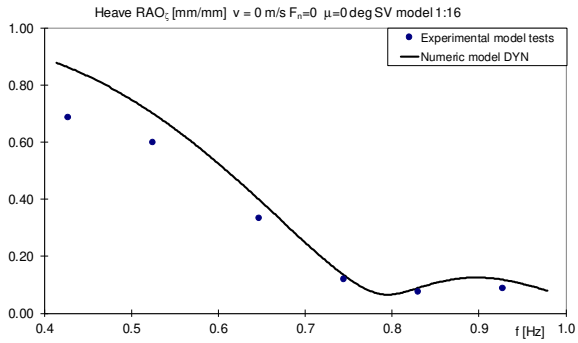

Figure 3.16.a. *Heave RAO_ζ [mm/mm], SV 1:16, μ=0^0, v=0 m/s.*

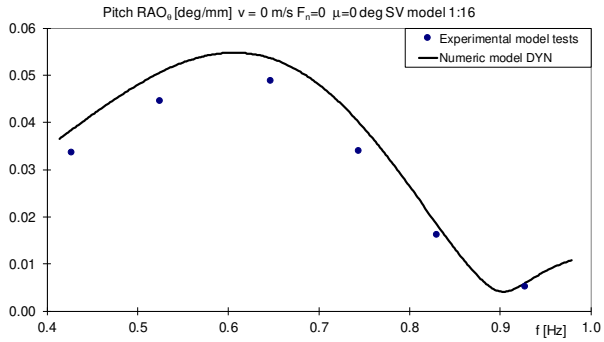

Figure 3.16.b. *Pitch RAO_θ [º/mm], SV 1:16, μ=0^0, v=0 m/s*

Table 3.5. Heave & pitch RAO, SV model 1:16, *v*=0m/s, ,μ=0^0

Case	*f* [Hz]	f_e [Hz]	RAO_ζ [mm/mm]		RAO_θ [º/mm]	
			experiment	numeric	experiment	numeric
T1	0.427	0.427	0.685	0.861	0.034	0.038
T2	0.525	0.525	0.597	0.700	0.044	0.051
T3	0.647	0.647	0.332	0.397	0.049	0.054
T4	0.745	0.745	0.118	0.134	0.034	0.040
T5	0.830	0.830	0.075	0.089	0.016	0.018
T6	0.928	0.928	0.087	0.117	0.005	0.006
			$\delta\zeta = 17.48\%$		$\delta\theta = 12.57\%$	

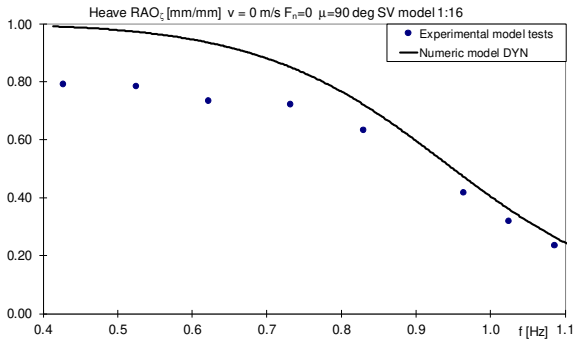

Figure 3.17.a. *Heave RAO_ζ [mm/mm], SV 1:16, μ=90^0, v=0 m/s.*

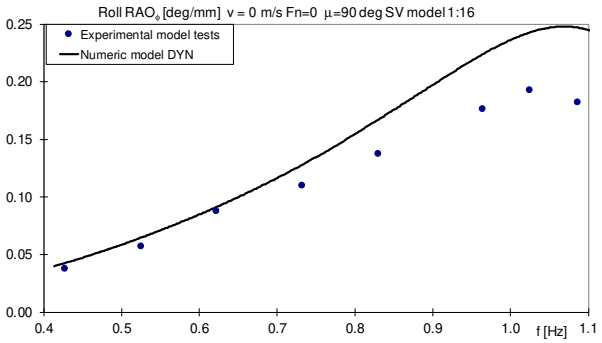

Figure 3.17.b. *Roll RAO_φ [º/mm], SV 1:16, μ=90^0, v=0 m/s.*

Table 3.6. Heave & roll, SV model 1:16, *v*=0m/s, ,μ=90^0

Case	*f* [Hz]	f_e [Hz]	RAO_ζ [mm/mm]		RAO_φ [º/mm]	
			experiment	numeric	experiment	numeric
T1	0.427	0.427	0.789	0.990	0.037	0.043
T2	0.525	0.525	0.784	0.972	0.057	0.065
T3	0.623	0.623	0.732	0.934	0.088	0.091
T4	0.732	0.732	0.720	0.850	0.110	0.128
T5	0.830	0.830	0.632	0.720	0.137	0.167
T6	0.964	0.964	0.416	0.471	0.176	0.224
T7	1.025	1.025	0.319	0.359	0.193	0.243
T8	1.086	1.086	0.235	0.263	0.182	0.247
			$\delta\zeta = 15.34\%$		$\delta\varphi = 16.15\%$	

3.3. The conclusions of the analysis on the experimental model

The results of the study in this chapter lead to the following conclusions regarding the validation of the DYN program code [45] and the related hydrodynamic model (subchapter 2.4.).

Comparing the values of the RAO amplitude operator functions (tables 3.3. – 6.) obtained for the four sets of tests (*table 3.2.*), differences between numerical and experimental results are obtained, with the following main causes:

- the numerical hydrodynamic model is considered linear in the 2D formulation of the potential linear flow with ideal fluid, corresponding to the strip theory (*subchapter 2.4.*) by neglecting the movement between two consecutive cross sections, instead, in nature, the flow is viscous 3D which induces a more pronounced hydrodynamic damping;
- the linear hydrodynamic numerical model does not include the interference components between the external excitation wave and the actual wave generated by the radiation at the hull movements, as well as other hydrodynamic nonlinearities, whereas in nature, the secondary components of the dynamic response are recorded experimentally (*Figures 3.10. – 13.d., f., h.*) and lead to an energy transfer from the main component of the amplitude spectrum to the secondary terms;
- secondary spectral components (*Figures 3.10. – 13.d., f., h.),* generated by the reflection on the border of the hull basin (*Figure 3.6., Figure 3.8., Figure 3.9.*), are not included in the linear hydrodynamic numerical model, so that differences between the two models, numerical and experimental, also occur.

The maximum differences between the numerical and the experimental model registered for the RAO response amplitude functions are: at vertical oscillations 15.34 – 18.17% with an average of 16.79%, at roll oscillations 16.15% and the slightest difference in pitch oscillations 11.11 – 13.28% with an average of 12.32%.

Only the case of the meeting wave μ=180˚ was also tested with a forward speed v=1.28 m/s (F_n = 0.246), when the maximum differences between the two models for the amplitude response functions are obtained, at vertical oscillation 18.17% and at pitch oscillation 13.28%.

In all the tested cases (figures 3.17. – 20.a., b.) the numerical response amplitude operator functions RAO are greater than the experimental ones, so we can say that the numerical model with linear hydrodynamic formulation through the strip theory leads to an overestimation of the dynamic response of the floating structure, representing a conservative approach to estimating the ship safety from the criteria for permissible seakeeping.

CHAPTER 4

DEFINING THE CHRACTERISTICS OF FLOATING DOCKS CONSIDERED IN THE STUDY OF EXTREME LOADS

For the studies developed in this thesis we have considered three variants of floating docks in order to analyse and compare different modes of behaviour of the structure in terms of its criteria for resistance structural and minimum freeboard under extreme stress from equivalent quasi-static waves (chapters 5 and 7), as well as from the criteria for oscillations in extreme random waves and transverse stability (chapters 6 and 8), using the theoretical models presented in chapter 2.

This chapter presents the main technical characteristics of floating docks, which constitute in the following chapters the case study. The characteristics of the preliminary structure of two types of docks with a total length of 60 m are presented. The large floating dock used by the VARD Naval Shipyard in Tulcea is also presented in this chapter. For all three constructive variants of docks, the operating cases and the criteria necessary for the analysis of small floating docks in two constructive versions will be presented, with continuous upper lateral tanks Dock60_CWT and with discontinuous upper lateral tanks Dock60_NWT, as well as for the floating dock found. in operation at the VARD Shipyard in Tulcea Dock_VARD_Tulcea [9]. Also presented are the 3D-FEM structural models made for the three constructive variants of the floating docks.

4.1. Description of the small floating dock with two constructive versions, Dock60_NWT and Dock60_CWT. Definition of the operating cases and development of the 3D-FEM structural model.

According to the norms of the naval classification societies (chapter 1) [1], [3], [56], there are two types of caisson floating docks, with continuous upper wing tanks. (CWT) and with discontinuous upper wing tanks (NWT).

We have developed two floating dock structures in accordance with the construction of floating docks, falling within the category of small floating dock, with a length of 60 m (see table 4.1.), In two constructive variants: a small-sized floating dock of caisson type with continuous upper wing tanks - Dock60_CWT (figure 4.2.a., b.) and a small-size floating dock with discontinuous upper wing tanks - Dock60_N WT (figure 4.1.a., b.), which we used for the numerical study of the operating capacity, based on the criteria of structural resistance and minimum freeboard at extreme demands from quasi-static equivalent waves (chapter 5) , as well as based on the limit criteria for oscillations in extreme random waves and cross-sectional stability (Chapter 6).

For the two constructive variants, based on the shapes in figures 4.1.b. and 4.2.b. we have obtained the *module D_CDB (Chapter 2,* Annex *3)*, the hydrostatic

curves, the displacement Δ and floating area A_w of figure 4.6 and 4.7. These diagrams emphasize the significant variations of shapes depending on the draft at the transition from the pontoon body to the upper wing tanks. Figure 4.1.a. and 4.2.a. present the cross section of the floating dock with the structural elements dimensioned according *to DNV - GL RU_FD rules* [1]. In the case of the Dock60_NWT constructive version (figure 4.1.a.), the tanks in the central area on the pontoon deck are removed.

Figures 4.4.a., b., c. and figures 4.5.a., b., c. show the diagrams of the vertical bending moment at the ultimate resistance (loss of overall stability) of USVBM, using the Smith method [26], [34]. The ultimate bending moment is calculated for both variants of the small-size floating docks Dock60 (NWT, CWT) using the program *DNV - GL Poseidon* [39], considering the frame distance $a_{FR} = [a_0, 2a_0, 4a_0]$, for reference at a regular distance $a_0 = 0.6m$. The maximum ultimate bending moment , USVBM, is obtained for the frame distance $a_{FR} = a_0$ [37], [40], and the structure of the docks with the frame distance of $a_{FR} = 2a_0$ [4], [35], [43] is analysed . Based on DNV - GL rules [1], in table 4. 3. table 4.4 and table 4.5. the limits of the permissible criteria for overall strength, global vertical deformation and minimum freeboard of two variants of the small floating docks Dock60_NWT/CWT.

For the structural analysis of the floating docks of small dimensions model of the equivalent 1D beam, at loads from equivalent quasi-static head – follow waves (chapter 5.1.), we considered two variants of docking blocks, short docking blocks - SB and long docking blocks - LB, with the characteristics of table 4.2. Each docking block is located on the main deck of the pontoon, at the intersection between the transverse and longitudinal reinforced beams according to the plan in figure 4.3.a. for short docking blocks (SB) and figure 4.3.b. for long docking blocks (LB).

Table 4.1. shows the main constructive characteristics of the two versions of small floating docks Dock60 _CWT/NWT. The maximum docking capacity of the small floating docks is, in the two constructive variants $M_s = 828t$. Thus for the analyses performed within the thesis, according to the norms of the classification society *DNV-GL RU-FD* [1] the maximum docking mass is arranged on the main deck in three variants: uniform distribution (figure 4.8.a.), sagging type distribution (figure 4.8.b.) and hogging type distribution (figure 4.8.c.). In addition to these three cases, docking at full capacity, I considered the light case and the maximum ballast case, which are the cases at the initial docking or after the launch of the docked mass. Table 4.6. and table 4. 7. presents displacement cases for the floating Dock60, NWT and CWT constructive cases, with short and long docking blocks and five loading cases: light, full ballast and the three testing distribution cases (uniform, sagging and hogging mass distribution), resulting a total of 20 main analysis sets. Also, in table 4.1. are presented the main characteristics of the equivalent 1D beam for the model of the two constructive versions of small floating docks.

Table 4.1. Dock60_CWT/NWT floating dock main characteristics [4], [35], [41], [37]

Dock 60 main dimensions/FD type (side WT type)			CWT	NWT	Material type		Steel grade A		
Length overall		*LOA* [m]	60		Section characteristics along the dock Dock60_NWT		*L*(1) [m] *L*(3) [m]	0-15 45-60	
Breadth		*B* [m]	20		Section characteristics along the dock Dock60_NWT		*L*(2) [m]	15 – 45	
Height pontoon		D_{Pp} [m]	2		Total area $a_{fr}=a_0$	(1)	*A*[m^2]	0.80700	0.80860
Height side WT		D_{WT} [m]	8			(2)			0.50400
Displacement	Light	$\Delta[t]$	1,152	960	Total area $a_{fr}=2a_0$	(1)		0.54700	0.54860
	M_{lift}[t]=828t		1,980	1,788		(2)			0.34000
Freeboard		f_s[mm]	300	75	Shear area $a_{fr}=a_0$	(1)	A_f[m^2]	0.36800	0.36960
Draught at aft, medium and bow stern	Light	T_M[m], T_{Pp}[m], T_{Pv}[m]	0.960	0.800		(2)			0.20400
	M_{lift}[t]=828t		1.650	1.490	Shear area $a_{fr}=2a_0$	(1)		0.23200	0.23360
Longitudinal position of free surface centre		*LCG* [m]	30			(2)			0.10000
Transversal position of free surface centre		*YCG* [m]	0		Bending moment of inertia $a_{fr}=a_0$	(1)	I_y[m^4]	5.23698	5.29335
No. of elements 3D-FEM	Head – follow EDW	N_{EL}	237,928	162,065		(2)			0.34768
	Oblique EDW		472,830	378,210	Bending moment of inertia $a_{fr}=2a_0$	(1)		3.75842	3.75842
Element type 3D-FEM		Shell (plate Mindlin) and mass				(2)			0.27333
No. of nodes 3D-FEM	Head – follow EDW	N_{ND}	201,153	190,618	Neutral axis vertical position	(1)	z_N[m]	2.72761	2.75669
	Oblique EDW		398,995	320,771		(2)			1.0000
Average EL length 3D-FEM			200		Section modulus of bottom $a_{fr}=a_0$	(1)	*WB*[m^3]	1.94078	1.94881
Frame distances		$a_0[mm]$	600			(2)			0.34768
		$2a_0[mm]$	1,200		Section modulus of bottom $a_{fr}=2a_0$	(1)		1.35274	1.36338
No nodes on 1D model		N_{EL}	300			(2)			0.27333
1D equivalent girder type		Timoshenko girder type			Section modulus at UD/PD $a_{fr}=a_0$	(1)	*WD*[m^3]	0.98781	1.00181
No. nodes 1D model		N_{ND}	301			(2)			0.34768
Yielding stress limit		R_{eH} [MPa]	235		Section modulus at UD/PD $a_{fr}=2a_0$	(1)		0.69982	0.71680
Elasticity module		*E* [MPa]	2.1 10^5			(2)			0.27333
Poisson ratio		ν	0.3		Hearing coefficient	(1)	K_{nn}[m^{-2}]	6.86328	6.86436
Material density		ρ_{mat}[t/m^3]	7.8			(2)			11.1942
Average El length 1D model		*dx* [m]	0.200		External condition		*Head – follow EDW* $\mu=0^0(180^g)$ *Oblique EDW* $\mu=0^0$-360^0		
Gravity acceleration		*g* [m/s^2]	9.81						

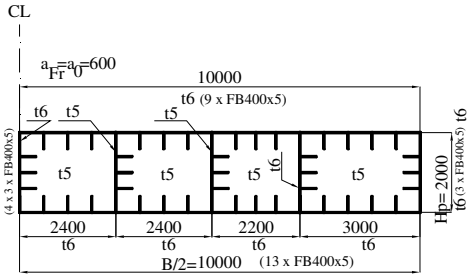

Figure 4.1.a. *Dock60_NWT amidships transversal floating dock structure*

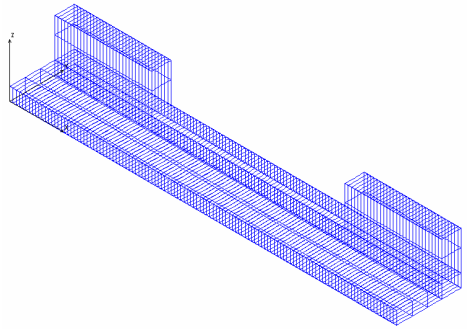

Figure 4.1.b. *Dock60_NWT offset lines non-continuous side wing tanks*

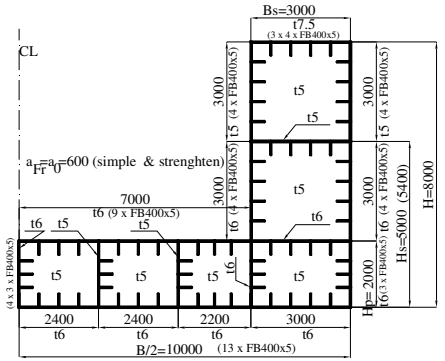

Figure 4.2.a. *Dock60_CWT amidships transversal floating dock structure*

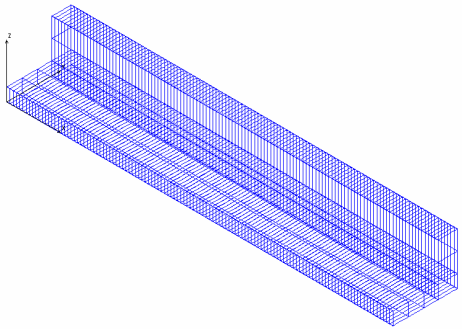

Figure 4.2.b. *Dock60_CWT offset lines continuous side wing tanks*

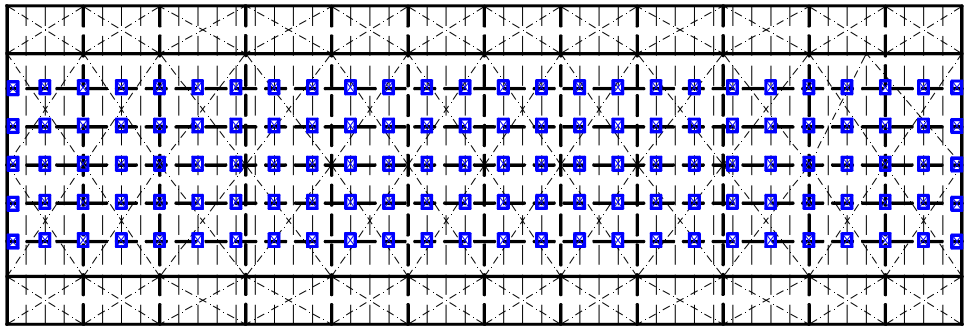

Figure 4.3.a. *Docking with short blocks SB (0,6 x 0,8 x 1,25, 1,212 t), 26 columns & 5 rows*

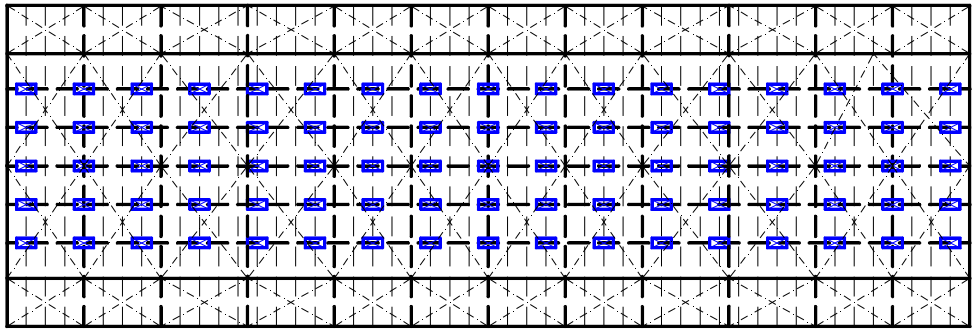

Figure 4.3.b. *Docking with long blocks LB (1,2 x 0,6 x 1,25, 1,818 t), 17 columns & 5 rows*

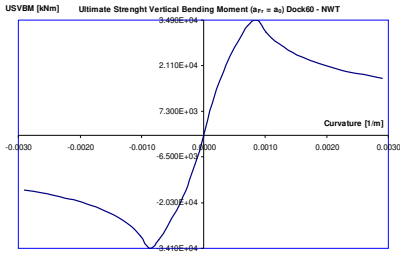

Figure 4.4.a. *Dock60_NWT USVBM [kNm]* $a_{FR} = a_0$

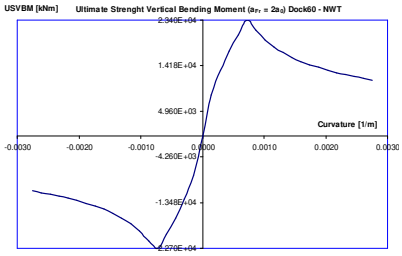

Figure 4.4.b. *Dock60_NWT USVBM [kNm]* $a_{FR} = 2a_0$

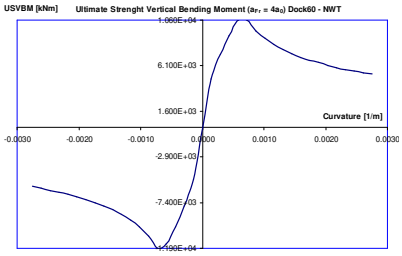

Figure 4.4.c. *Dock60_NWT USVBM [kNm]* $a_{FR} = 4a_0$

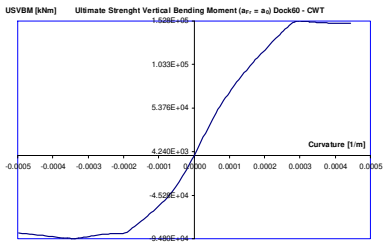

Figure 4.5.a. *Dock60_CWT USVBM [kNm]* $a_{FR} = a_0$

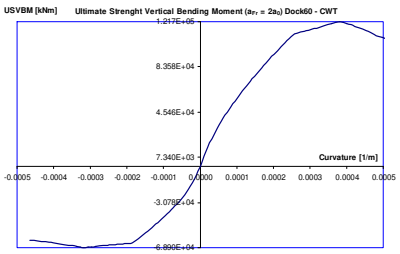

Figure 4.5.b. *Dock60_CWT USVBM [kNm]* $a_{FR} = 2a_0$

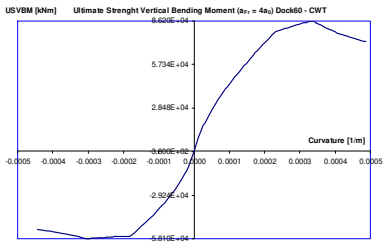

Figure 4.5.c. *Dock60_CWT USVBM [kNm]* $a_{FR} = 4a_0$

Table 4.2. Docking block characteristics (SB – short blocks, LB – long blocks)

Docking block type	SB	LB	Docking block type	SB	LB
$L_{bloc}[m]$	0.6	1.2	$\rho_{oak}[t/m^3]$	0.9	
$B_{bloc}[m]$	0.8	0.6	$M_{bloc}[t]$	1.212	1.818
$H_{bloc}[m]$	1.25		nr_L	nr_L	17
$H_{bloc\_concret}[m]$	1		nr_B	5	
$\rho_{concret}[t/m^3]$	2.3		$M_{bloc-total}[t]$	157.56	154.53
$H_{bloc\_oak}[m]$	0.25				

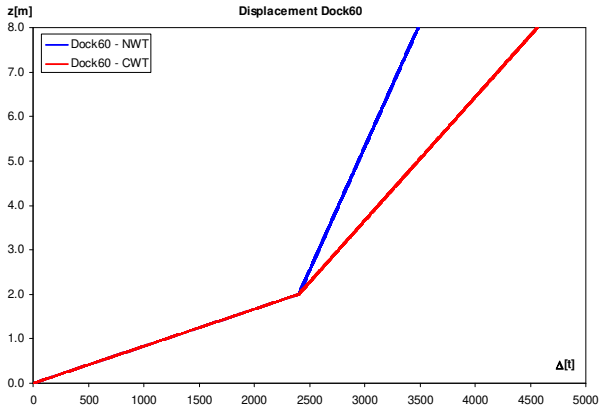

Figure 4.6. *Dock60_NWT / CWT displacement Δ[t]*

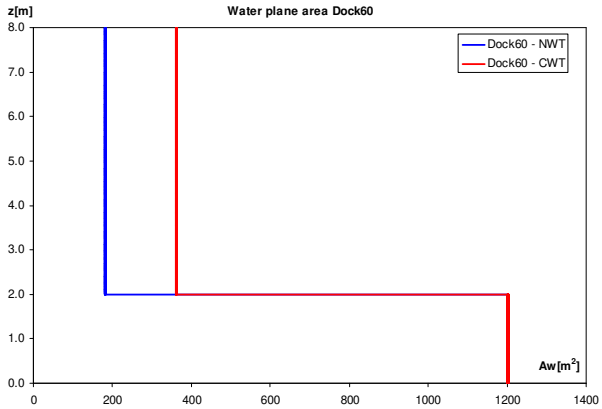

Figure 4.7. *Dock60_NWT / CWT* water plane area $A_w[m^2]$

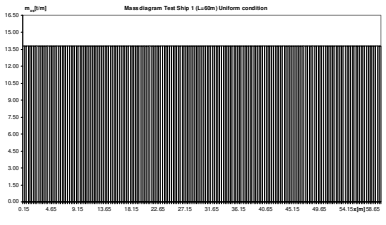

Figure 4.8.a *Mass diagram* $m_x[t/m]$*, test uniform mass distribution (*$M_s = 828t$*,* $x_s = 30m$*)*

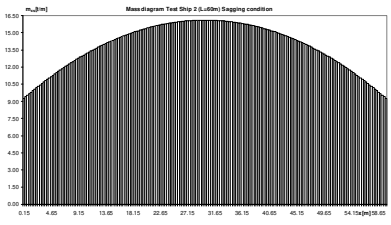

Figure 4.8.b. *Mass diagram* $m_x[t/m]$*, test sagging mass distribution (*$M_s = 828t$*,* $x_s = 30m$*)*

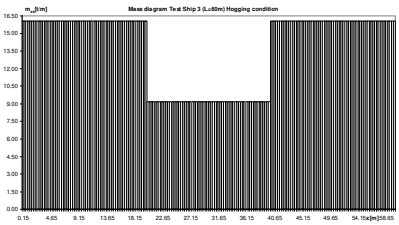

Figure 4.8.c. *Mass diagram* $m_x[t/m]$*, test hogging mass distribution (*$M_s = 828t$*,* $x_s = 30m$*)*

Table 4.3. Allowable limits for vertical deformation $w_{adm}[m]$, tensions, buckling factor and minimum free board $D_{adm}[m]$, for the two constructive versions of small floating docks Dock60_NWT/CWT, according to the rules of the ship classification companies [1]

Freeboard criterion	$D_{PD\_adm} = D_p - FB_{PD\_adm}[m]$ cases 1, 3, 4 and 5		$D_{UD\_adm} = D - FB_{UD\_adm}[m]$ case 2	
	Dock60_CWT	Dock60_NWT	Dock60_CWT	Dock60_NWT
	1.925	1.700	7.000	
Strength criterion	w_{adm} = 0.150 m	B_{adm} =1.5	σ_{adm} = 175 MPa	τ_{adm} = 110 MPa

Table 4.4. The allowable values from the criteria of the ultimate bending moment (safety factor c_s=1.2) and overall strength for the preliminary structure verification (a_{Fr}=$2a_0$) of the two constructive versions of small floating docks Dock60_NWT/CWT, with requests from meeting - following waves, for 1D equivalent beam models, according to the norms [1]

Dock60	a_{Fr}	Hogging		Sagging		*AVBM* [kNm] adm. rules	*AVSF* [kN] adm. rules
		USVBM [kNm]	*AUSVBM* [kNm] (*cs*=1.2)	*USVBM* [kNm]	*AUSVBM* [kNm] (*cs*=1.2)		
NWT	a_0	3.490E+04	2.908E+04	-3.410E+04	-2.842E+04	5.56E+04	3.14E+03
	$2a_0$	2.340E+04	1.950E+04	-2.270E+04	-1.892E+04		
	$4a_0$	1.060E+04	0.883E+04	-1.190E+04	-0.992E+04		
CWT	a_0	1.528E+05	1.273E+05	-9.480E+04	-7.900E+04	5.56E+04	3.14E+03
	$2a_0$	1.217E+05	1.014E+05	-6.890E+04	-5.742E+04		
	$4a_0$	8.620E+04	7.183E+04	-5.810E+04	-4.842E+04		

Table 4.5. The allowable values from the criteria of the ultimate bending moment (safety factor c_s=1.5) and overall strength for final structure verification (a_{Fr}=a_0) of the two constructive versions of small floating docks Dock60_NWT/CWT, with requests from oblique waves, for 1D equivalent beam models, according to the norms [1]

Constructive type	*USVBM* [kNm] ultimate	*AUSVBM* [kNm] (*cs*=1.5)	*VBM-adm* [kNm] rules	*AVBM* [kNm] combined	*AVSF* [kN] rules	*AHBM* [kNm] rules	*AHSF* [kN] rules	*AMT* [kNm] rules	*Fs* [m] rules
Dock60_NWT	3.41E+04	2.27E+04	5.56E+04	2.27E+04	3.14E+03	4.26E+03	2.11E+02	2.44E+04	0.300
Dock60_CWT	9.48E+04	6.32E+04	5.56E+04	5.56E+04	3.14E+03	5.11E+03	2.54E+02	2.44E+04	0.075

Table 4.6. Dock60_NWT displacement cases

Cases	Blocks	$M_{long}[t]$	$M_{Fr}[t]$	$M_{Eq+rezball}[t]$	$M_{bt}[t]$	$M_{ballast}[t]$	$M_{ship}[t]$	Δ [t]	$d_m[m]$	$x_G[m]$	$y_G[m]$	$z_G[m]$
(1) Light	SB	207.93	121.99	472.52	157.56	-	-	960	0.800	30	0	1.777
	LB			475.55	154.53							
(2) Full ballast	SB	207.93	121.99	472.52	157.56	2,292	-	3,252	6.733	30	0	1.738
	LB			475.55	154.53							
(3) Test case with uniform mass distribution	SB	207.93	121.99	472.52	157.56	-	828	1,788	1.49	30	0	2.691-6.395
	LB			475.55	154.53							
(4) Test case with sagging mass distribution	SB	207.93	121.99	472.52	157.56	-	828	1,788	1.49	30	0	2.691-6.395
	LB			475.55	154.53							
(5) Test case with hogging mass distribution	SB	207.93	121.99	472.52	157.56	-	828	1,788	1.49	30	0	2.691-6.395
	LB			475.55	154.53							

Table 4.7. Dock60_NWT displacement cases

Cases	Blocks	$M_{long}[t]$	$M_{Fr}[t]$	$M_{Eqrezball}[t]$	$M_{bt}[t]$	$M_{ballast}[t]$	$M_{ship}[t]$	Δ [t]	$d_m[m]$	$x_G[m]$	$y_G[m]$	$z_G[m]$
(1) Light	SB	256.00	151.16	587.28	157.56	-	-	1,152	0.960	30	0	3.891
	LB			590.31	154.53							
(2) Full ballast	SB	256.00	151.16	587.28	157.56	2,940	-	4,092	6.700	30	0	2.144
	LB			590.31	154.53							
(3) Test case with uniform mass distribution	SB	256.00	151.16	587.28	157.56	-	828	1,980	1.650	30	0	3.832- 7.177
	LB			590.31	154.53							
(4) Test case with sagging mass distribution	SB	256.00	151.16	587.28	157.56	-	828	1,980	1.650	30	0	3.832- 7.177
	LB			590.31	154.53							
(5) Test case with hogging mass distribution	SB	256.00	151.16	587.28	157.56	-	828	1,980	1.650	30	0	3.832- 7.177
	LB			590.31	154.53							

a.

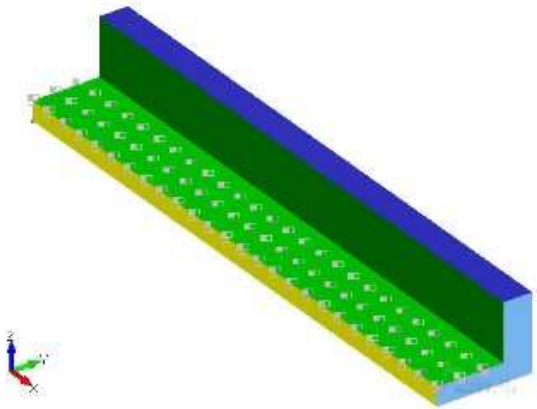

b.

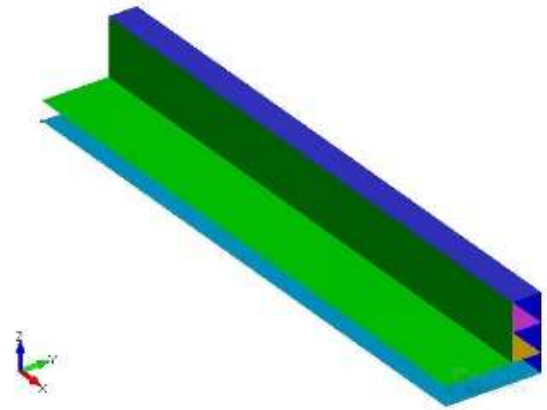

c.

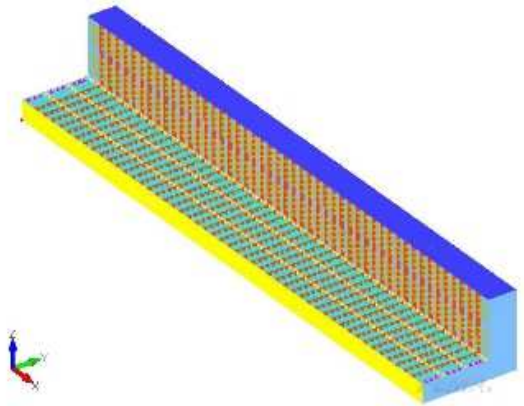

Figure 4.9.a., b., c. *Dock60_CWT 3D-CAD/FEM model*

a.

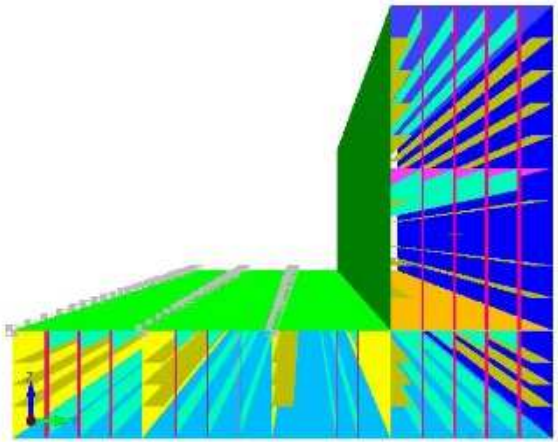

b.

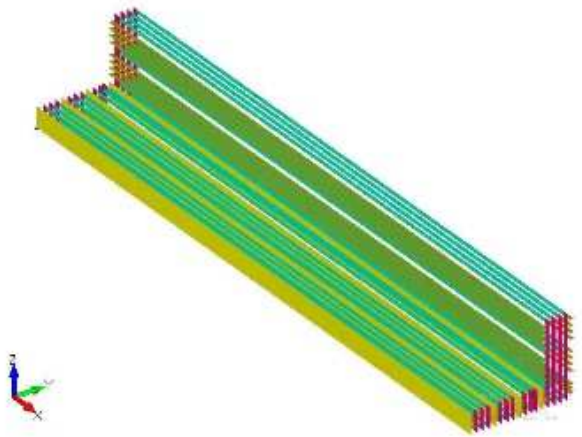

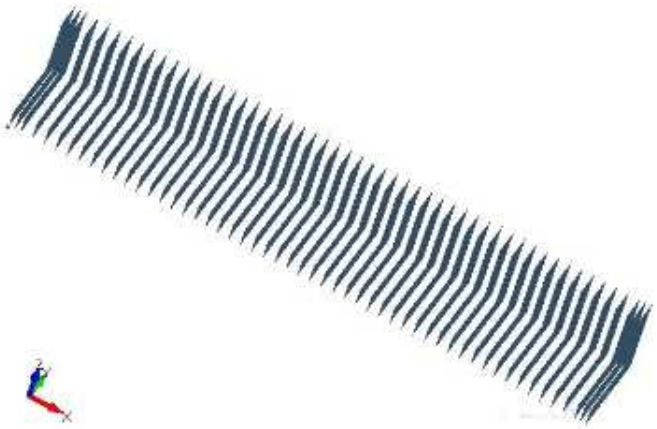

Figure 4.10.a., b. *Dock60_CWT 3D-CAD/FEM model, longitudinal elements*

Figure 4.11. *Dock60_CWT 3D-CAD/FEM model, frame*

a.

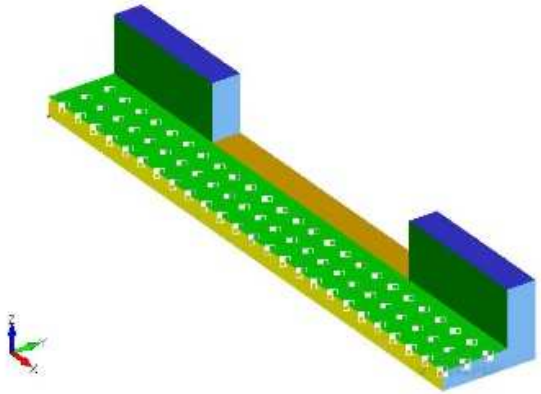

b.

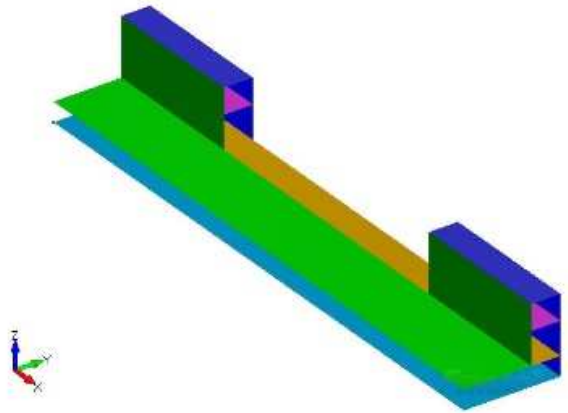

c.

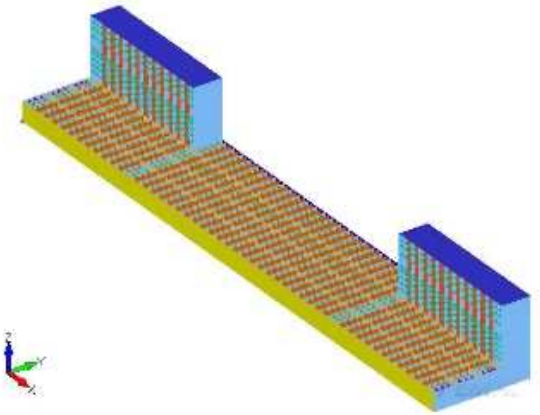

Figure 4.12.a., b., c. *Dock60_NWT 3D-CAD/FEM model*

a.

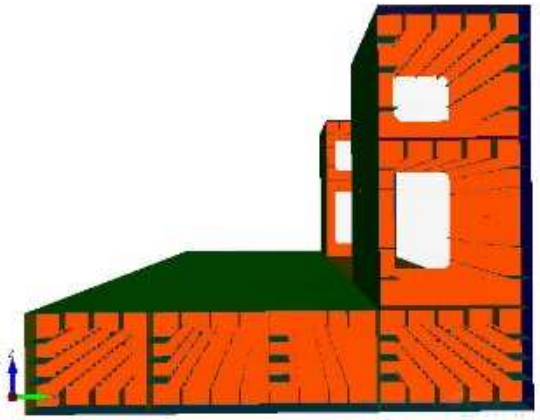

b.

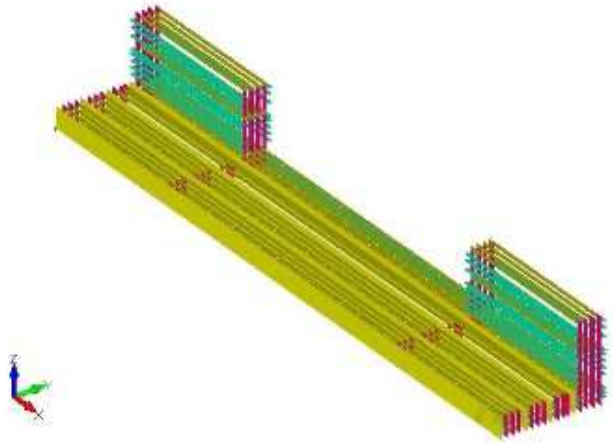

Figure 4.13.a., b. *Dock60_NWT 3D-CAD/FEM model, longitudinal elements*

Figure 4.14. *Dock60_NWT 3D-CAD/FEM model, frame*

Figure 4.15. *Dock60_CWT 3D-CAD/FEM model, longitudinal and frame elements*

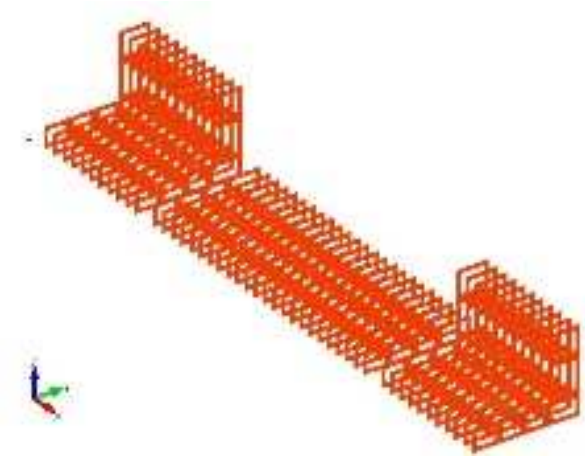

Figure 4.16. *Dock60_NWT 3D-CAD/FEM model, longitudinal and frame elements*

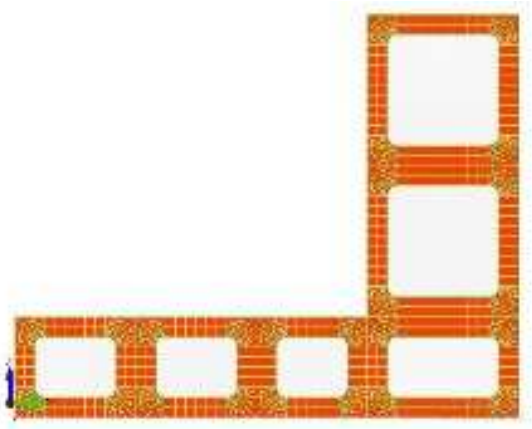

Figure 4.17. *3D-Fem model, simple frames elements*

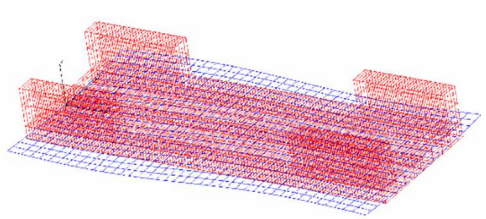

Figure 4.18.a *Dock60_NWT, light case, EDW wave hogging h_w=1.278m, quarte sea μ=45^0, and offset lines*

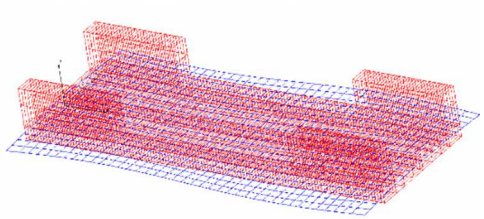

Figure 4.18.b *Dock60_NWT, light case, EDW wave sagging h_w=1.278m, quarte sea μ=45^0, and offset lines*

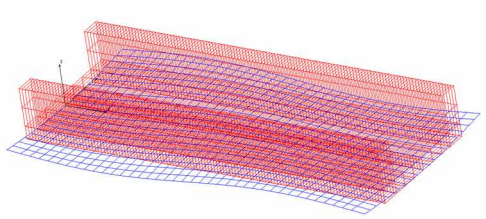

Figure 4.19.a *Dock60_CWT, light case, EDW wave hogging h_w=1.930m, quarte sea μ=45^0, and offset lines*

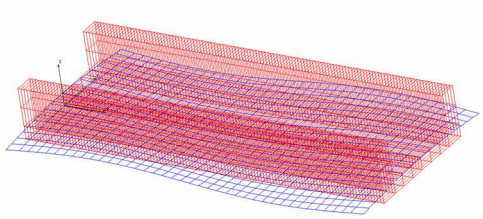

Figure 4.19.b *Dock60_CWT, light case, EDW wave sagging h_w=1.930m, quarte sea μ=45^0, and offset lines*

a. b.

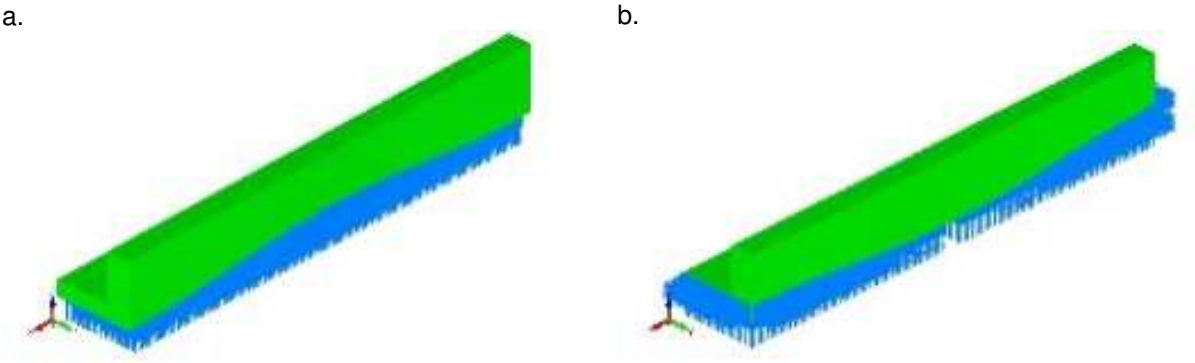

Figure 4.20.a., b. *The EDW pressure on Dock60_CWT, μ=0⁰(180⁰), hogging & sagging, h_w=1.930m, light case*

a. b.

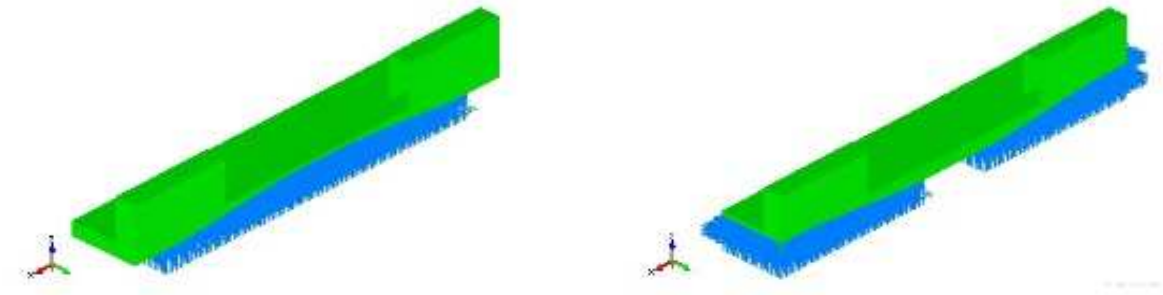

Figure 4.21.a., b. *The EDW pressure on Dock60_NWT, μ=0⁰(180⁰), hogging & sagging, h_w=1.930m, light case*

a. b.

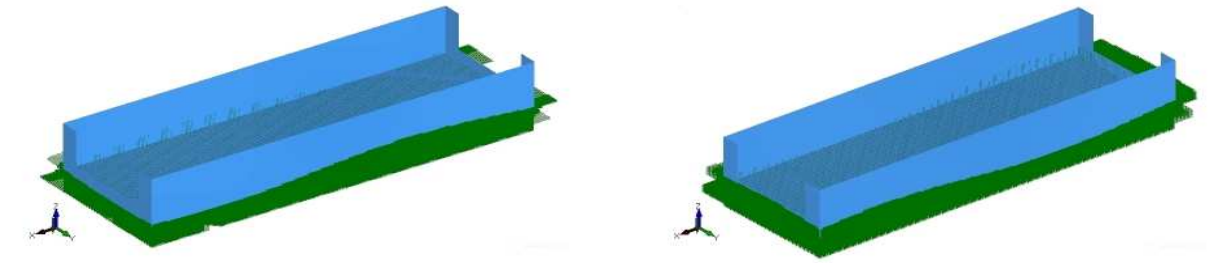

Figure 4.22.a., b. *The EDW pressure on Dock60_CWT, μ=45⁰, hogging & sagging, h_w=1.930m, light case*

Figures 4.18 .a., b. present the floating dock Dock60_NWT in equivalent quasi-static oblique wave system μ = 45 °, type sagging and hogging wave, with a wave height h_w= 1.278 m, in the light case. Figures 4.19 .a., b. show the floating dock Dock60_CWT in equivalent quasi - static oblique waves system μ = 45 °, type sagging and hogging wave , with a wave height of h_w=1.930 m, in the light case.

In the final version of the small floating dock structure ,Dock60 _NWT/ CWT, analysed in equivalent quasi - static oblique waves (chapter 5.2.), we reconsidered the intercostal distance to $a_{FR} = a_0 = 600mm$ from $a_{FR} = 2a_0 = 1200mm$. Also, to increase the resistance to the structural stability of the local stress, there whore added brackets and stiffeners (FB400 * 5), for ensuring finally a significant increase in the resistance of the global and local structure of the Dock60_NWT/CWT comparing to the preliminary version.

Table 4. 5. presents the allowable values, calculated according to the rules [1], [3] for the vertical bending moment VBM / AVBM [kNm], vertical shear force VSF / AVSF [kN], horizontal bending moment HBM / AHBM [kNm], horizontal shear force HSF / AHSF [kN], torque moment MT / AMT [kNm], ultimate strength vertical bending moment USVBM / ASVBM [kNm] and the minimum freeboard value $F_s[m]$ for the two constructive models of the small floating docks, having the frame distance $a_{FR} = a_0 = 600mm$ (final constructive version) [70], [71], [72].

The quasi – static equivalent head/follow and oblique waves, for which the small docks Dock60_CWT/NWT are analysed, have the height selected in accordance with DNV-GL [1] representing the maximum river class IN(2.0) (h_{wmax} *=2 m*) and coastal class RE(50%) (h_{wmax} *=2,568 m*).

Structural analysis on 3D-FEM models at requests from quasi - static and oblique equivalent waves (chapter 5.3.), required the development of the 3D structural models of the two types of small floating docks, Dock60_CWT/NWT. The two 3D-CAD/FEM models for the two types of construction, are developed over the entire length of the docks, being used in the case of head/follow waves, as well as their full width, for the structural analysis study in the case of oblique waves.

The main features of the two 3D-FEM models are presented in *table 4.1.*

The 3D-CAD/FEM models are developed with the program Femap/NX Nastran [42] and includes inner and outer shells, the longitudinal beams and transversal frames and the main and side relief with the corresponding holes and the local brackets.

The 3D-FEM models of the two constructive versions of small floating docks, Dock60_CWT/NWT, has shell, membrane and plate (Mindlin) elements, [42], [41], [73], [51], [43], [40], [44], with an average element size of 200 mm, suitable for global and local stress investigation, according rules [1], [3], plus the mass element for onboard mass groups. By adjusting the ballast and adding the docking mass, the displacement cases presented in table 4.5 are ensured. Figures 4.9. - 4.17. presents details of the 3D-CAD/FEM structural model for the two constructive versions of the small floating docks Dock60 with continuous (CWT) and discontinuous (NWT) side tanks.

Figures 4.20. - 22. presents examples of loading on 3D-FEM models with quasi-static equivalent head/follow wave pressure or oblique wave on the outer shell of the small floating docks Dock60, in the two construction versions (NWT/CWT).

4.1. Description of the large floating dock Dock_VARD_Tulcea. Definition of operating cases and development of the 3D-FEM structural model

To achieve numerical model of the large floating dock, obtained by converting a offshore barge, to carry out research, the data of the floating dock was provided by VARD Tulcea Shipyard (figure 4.24., figure 1.3., figure 4.23., figure 1.4.). The main changes made between the offshore barge and the floating dock are mentioned in table 4.8. and refers to the replacement of a portion of the pontoon between frame 0 and 60.5, the widening from 40.23m to 55.13m - 61.09m and the extension of the two upper ballast tanks, up to the length of about 39 m in the fore area. The floating dock Dock_VARD_Tulcea is designed to be able to dock and launch ships with a maximum width of 50 m and a maximum length of 195 m. The main deck of the dock is provided with a system of railway tracks, in number of 14 units (figure 1.3., figure 1.4.a., b.) , compatible with those on *Mounting Sheet No.2 from the VARD Tulcea Shipyard*, *figure 1.4.,* thus being able to carry out the transfer of the vessels from this mounting area to the floating dock, figure 1.4. *(table 4.10.)* [4], [9], [11].

Table 4.8. The main changes made to the offshore barge for the floating dock Dock_VARD_Tulcea [11]

Vessel type	**Offshore barge Figure 4.23.**	**The floating dock Dock_VARD_Tulea Figure 4.24.**
Class	RINA	
Total length (LOA):	168.20 m	209.20 m
Useful length of main deck	151.00 m	189.00 m
Width (*B*):	40.23 m	55.13 m
Maximum width between the aft towers	34.27 m	50.66 m
Maximum width (Bmax):	43.21 m	61.09 m
Height at main deck:	10.10 m	10.10 m
Intercostal distance:	0.750 m	0.750 m
Distance between longitudinal:	0.745 m	0.745 m
Distance between reinforced frames	3.00 m	3.00 m
Maximum transfer draft	7.58 m	6.20 m
Maximum draft at launch	21.10 m	20.00 m
Mass of the dock without load	12,967 t	19,855 t
Mass of parts to be removed	3,498 t	-
Mass of parts to be added		10,396 t
Maximum mass that can be docked		27,000 t
Extreme position of the centre of gravity of the dock		25.25m
Position of the vertical centre of gravity		13.20m
The draft during the docking / launching operations		5.6 – 20 m
Total ballast capacity		116,138 t

The body structure of the floating dock is mainly in longitudinal frame system, similar to figure 4.25. and figure 4.26. The structure of the dock is mixed, both longitudinal and transverse. The whole body is made of steel, in accordance with the requirements of RINA - Registro Italiano Navale [9], [11].

The dock is equipped with two service tanks for diesel, with a capacity that ensures autonomy of diesel generators at maximum power for at least 48 hours. The technical water tanks, have a capacity of about 10 t, these having exits to the pump room, the diesel compartments of the generators located at the level of deck 2, the compartment of the workshop at the level of deck 3, the "Shelter area" compartment of the crew from the port as well as at level of corridors [9], [11].

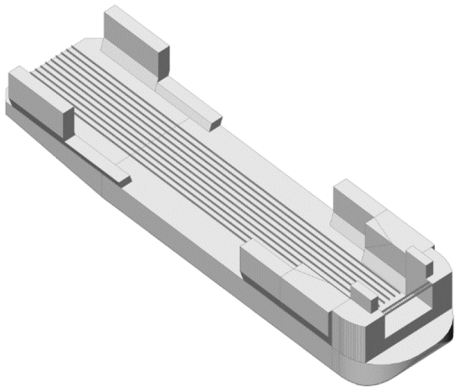

Figure 4.23. *Offshore barge (3D-CAD model).[9]*

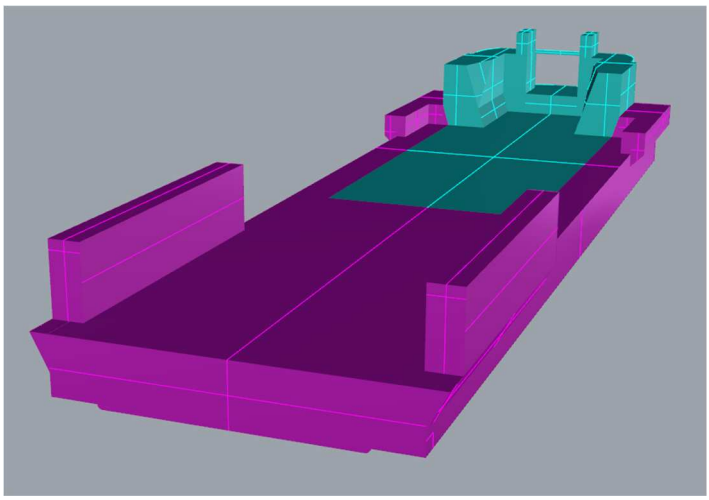

Figure 4.24. *Dock_VARD_Tulcea floating dock (3D-CAD model) [9], [11]*

The floating dock is equipped with a ballast loading, unloading and transfer system, served by six pumps with a flow of 2400 m³/h, located in the pump room and two pumps with a flow of 1600 m³/h located outside the pump room. The pumping chambers and the electricity generator chambers are equipped with forced extraction/ventilation means [9], [11].

The construction material of the body is made of high strength steel with flow limit R_{eh} =355 N/mm², AH36 and DH36, according to RINA standards [9], [11].

Inside, the floating dock, is divided by ten transverse watertight walls, which extend across the entire width of the body and two longitudinal watertight walls arranged symmetrically with to the centre line. Also, a non-leaking longitudinal wall is located in the CL. The strength of the structure is ensured locally, through additional stiffening elements, in correspondence with the anchoring and towing equipment [9], [11].

The docking deck has a length of 189 m. At the time of docking, at the longitudinal position of the deck cargo, the largest portion of the docked vessel must be located between frame 15+500 mm and frame 161+250 mm, one part remaining in console. The distance between the main deck of the dock and the bottom of the docked ship is approximately 2 m, with the system on the dock [9], [11].

The draft and stability during launch are controlled by ballast in the lower and upper tanks in the stern and the bow. The upper towers are built for the purpose of ballast tanks in order to be able to make a dive as fast as possible up to the maximum draft of 20 m, remaining a reserve of 2,765 m until the dive operation can be made.

The ballast system is dimensioned so as to carry out immersion in the draft of 5.6 m to 20 m in less than 4 hours, following a succession of sequences defined to comply with the safety of the operations on board the floating dock, and ensuring the integrity of the construction that is docked on board the dock [9], [11].

The floating dock is equipped with a trim control system to verify ballast transfer and handling. The control is assisted by an on-board computer that automatically manages the docking and launching operations, ensuring always the position on the right hull of the dock [9], [11].

In figure 4.27., it is represented the body plan of the floating dock made available by the VARD Tulcea Shipyard [9], [11].

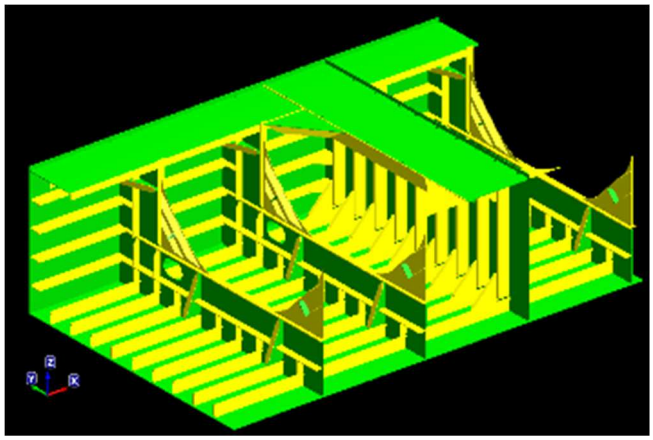

Figure 4.25. *3D-CAD model of a section with longitudinal and transverse frame system the structure of the floating dock Dock_VARD_Tulcea – view from AVEVA Marine [9]*

Figures 4.30.a., b., c. shows how the launch is made for an internal order of the shipyard. The floating dock is brought to the 6.2 m draft, necessary for coupling the rails on the docking deck, with the rails on the mounting area (figure 1.4 .). The ship to be docked is towed in several stages, to achieve the clearing without significant differences of the draft at the stern, centre and the sample in front of the reference of 6.2 m, figure 4.30.a. After completing the docking and positioning in the safety zone - figure 4.30.b., the floating dock is ballasted until the draft of 20 m is provided for the launch of the ship, 4.30.c. For such a case, of a docked mass of 19747 t (figure 4.29a., b.), with 7 docking steps, the shipyard provided the level of ballast of the tanks at each stage and the distribution of the docked ship mass. Also, we analysed the floating dock Dock_VARD_Tulcea in the limit cases: light ballasted to ensure the draft of 6.2 m and docked to the maximum capacity of 27000 t, with the distribution of uniform, type sagging and type hogging mass, according to classification norms of ship [1], [3].

A selection of the characteristic data of this constructive model can be found in *table 4.9*. *Figure 4.31.a., b.,* shows the dock in quasi - static head sagging and hogging waves, with a maximum height of h_w = 4,492 m. The frame distance is $a_{Fr} = 4a_0$ = 3000 mm [9]. *Figure 4.28.* shows the diagram of the ultimate bending moment according to the Smith method [38], [34], for the structure at the middle of the pontoon in *figure 4.26*.

Table 4.10 . presents the allowable values, according to the rules [1], for the vertical bending moment *VBM* [kNm], the vertical shear force *VSF* [kN], as well as the ultimate strength vertical bending moment USVBM / ASVBM [kNm], used to evaluate the general strength of the dock on a 1D equivalent beam model at demands of quasi – static in head / follow equivalent waves.

The 3D-FEM structure of the floating dock Dock_VARD_Tulcea is developed in one board (for requests of head/follow waves) extend over the entire length, using the program Femap/NX Nastran [42] (*Figure 4.33. - 38.).* The 3D-FEM model includes mostly quadric elements, but also triangular, membrane and thick plate (Mindlin) finite elements for the body structure, as well as concentrated mass on finite elements for modelling equipment, ballast mass and docked mass. The average dimension of the elements is about 187.5 mm (see details in *figure 4.34.*), so that the model corresponds to the local and global structural analysis. The main steps of the modelling for the 3D-FEM model are:

- Import from the CAD model in AVEVA Marine of the outer surface of the floating dock using a *.iges* file in the Femap/NX Nastran program as a separate layer [9].
- Generation of the list of layers according to the class .dwg [9] (shell, decks, stringers, longitudinal, frames, stiffeners, brackets), 190 layers
- Generation of the list of materials according to class .dwg A, A36, B36 and D36
- Generation of the list of properties according to the types of dimensions existing in the class .dwg (16 properties) [9]
- Generation of the 3D-CAD model and then the 3D- FEM model of the structural model of the ship [9], using the program Femap/NX Nastran, with 399922 points (PT), 394138 curves (CR), 99341 surfaces (SF), 1834221 nodes (ND), 1353139 elements (EL), over 11 million degrees of freedom (DOF).
- The application of boundary conditions on the 3D-FEM model (see table 2.1.)

- Modelling of the masses on board the ship [9], equipment, ballast, docked ship, using finite element type concentrated mass.
- It is applied to the outer shell the pressure of the equivalent quasi - static wave, using the users' function, the parameters of the equilibrium parameters computation doc - wave are calculated on the basis of its equivalent 1D beam. The dock can operate in both river and coastal areas, so that the maximum wave height varies between 2 m and 4,942 m, according to the rules of the ship classification companies [1].
- It is analysed structurally the model of the dock subjected to requests from equivalent quasi - static head – follow waves, using the NX/NASTRAN solver [105], using local and global resistance criteria, as well as the minimum freeboard criterion (study made in chapter 7).

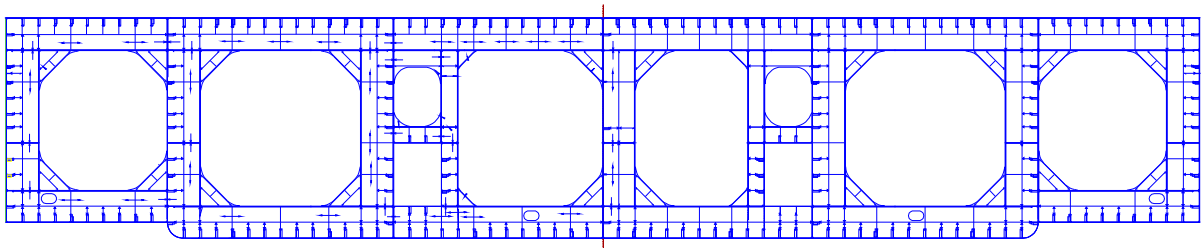

Figure 4.26. *Dock_VARD_Tulcea amidships transversal floating dock structure [9]*

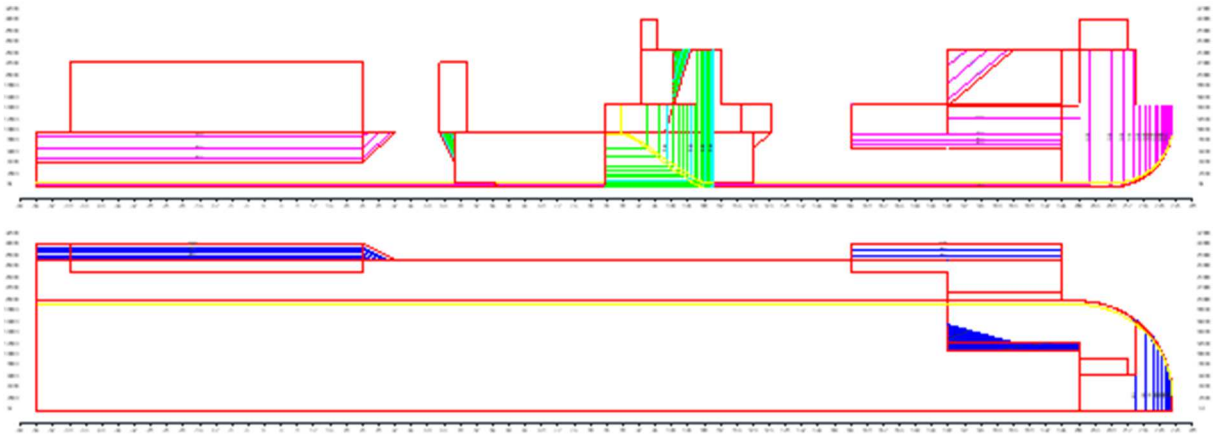

Figure 4.27. *Body plan of Dock_VARD_Tulcea [9]*

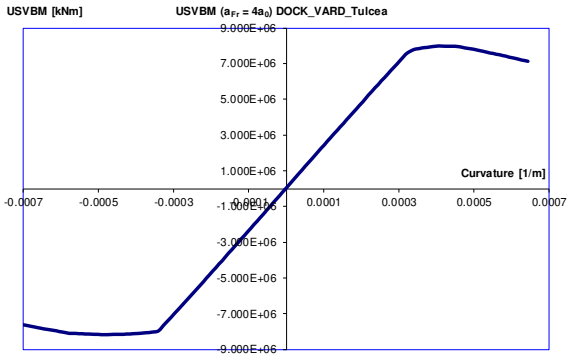

Figure 4.28. *USVBM [kNm] Dock_VARD_Tulcea diagram*

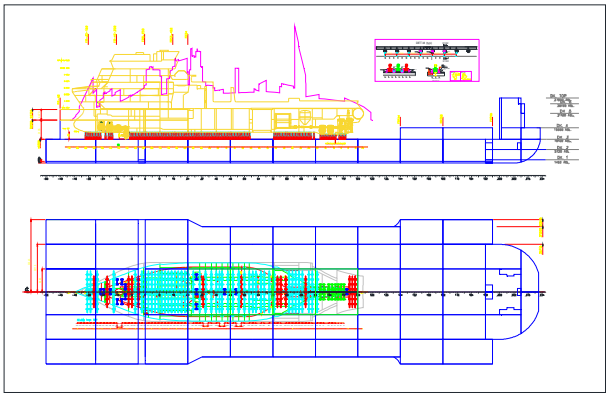

Figure 4.29.a. *Docking scheme of OSV type vessel of 19,747 t, along the entire length of the rails (122.79 m) from the main deck of the FD in the VARD Shipyard basin in Tulcea [9]*

Table. 4.9. The main features of the floating dock Dock_VARD_Tulcea [9], [73], [60].

Overall length	*LOA* [m]	209.20			Number of elements of the 1D model equivalent beam	N_{EL}	280
Width	*B* [m]	61			Type of elements of the 1D model equivalent beam	Timoshenko type elastic beam elements	
Height at the main deck	D_P [m]	10.10			The number of nodes of the 1D model equivalent beam	N_{ND}	281
Height of side tanks	D_{WT} [m]	Upper side tank stern 4.90, upper side tank bow12.66			The average element size of the 1D equivalent model beam	*dx* [mm]	750
Medium draft	T_m [m]	7.2	6.2	5.2	Material flow limit	R_{eH} [MPa]	355
Displacement	Δ [t]	77,587	66,324	55,162	Admissible von Mises tensions	σ_{adm} [MPa]	292
Longitudinal position of the centre of gravity	*LCG* [m]	100.103	100.139	100.120	Young's modulus of elasticity	*E* [MPa]	$2.1\ 10^5$
Waterline length	Lc_{WL} [m]	100.103	100.139	100.120			
The vertical position of the centre of gravity	*KG*[m](z_G)	6; 8; 10; 12; 14; 16			Poisson's ratio	ν	0.3
The floating area	Ac_{WL} [m^2]	11,287	11,211	11,132	Material density	ρ_{mat} [t/m^3]	7.8
Number of elements of the 3D-FEM model	N_{EL}	1,353,139			The allowable vertical deformation	w_{adm} [mm]	418
The number of nodes of the 3D-FEM model	N_{ND}	1,834,221			The value of the minimum allowable free board	F_{min} [mm]	300
The average size of the finite elements	*ds* [mm]	187.5			Longitudinal and transverse position of the centre of gravity and of the hull	$x_G = x_B$ [m]	100.148
The distance between the web frames	a_{Fr} [mm]	3,000				$y_G = y_B$ [m]	0
Intercostal distance	a_0 [mm]	750			Gravitational acceleration	*g* [m/s^2]	9.81
The type of finite elements of the 3D-FEM model	Membrane type elements + thick plate (Mindlin), concentrated mass				Extreme conditions from quasi-static equivalent waves	Meeting / following $\mu=0^0(180^0)$ with the maximum height h_w=4.492m	
Material	High quality steel AH36						

Table. 4.10. The allowable values from the criteria of the ultimate bending moment (safety factor c_s=1.5) and global resistance for checking the structure of the floating dock Dock_VARD_Tulcea, with requests from meeting – following waves, for 1D equivalent beam models, according to the norms [1], [3]

USVBM [kNm] ultimate	*AUSVBM* [kNm] (cs=1,5)	*VBM-adm* [kNm] rules	*AVBM* [kNm] combined	*AVSF* [kN] rules	*Fs* [m] rules
7.97E+06	5.32E+06	3.44E+06	3.44E+06	5.70E+04	0.300

a. b. c.

***Figure 4.30.a., b., c.**. Docking of a ship and launching it into the harbour of the shipyard [74], [75], [76]*

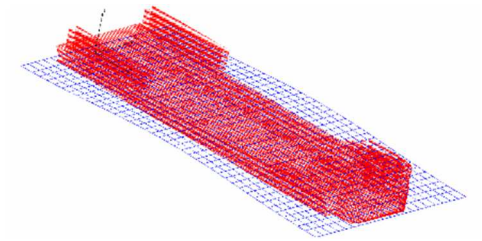

***Figure 4.31.a** 3D-CAD model of Dock_VARD_Tulcea GD in quasi static equivalent head - follow waves, hogging type, h_w=4.492m, at T_m=6,2m draft, light case [37]*

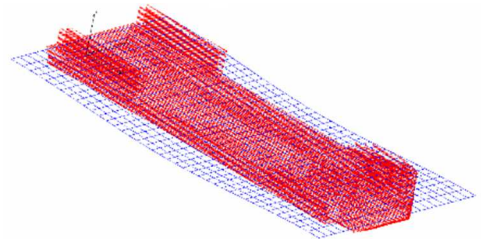

***Figure 4.31.b** 3D-CAD model of Dock_VARD_Tulcea GD in quasi static equivalent head - follow waves, sagging type, h_w=4.492m, at Tm=6,2m draft, light case [37]*

a. b.

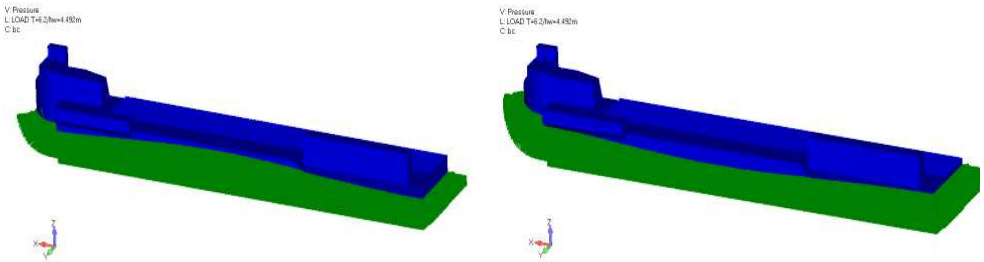

***Figure 4.32.a., b.** the pressure applied to the shell of the Dock_VARD_Tulcea from quasi-static EDW head – follow, a. hogging type and b. sagging type, h_w=4.492m, at T_m=6.2m draft, light case*

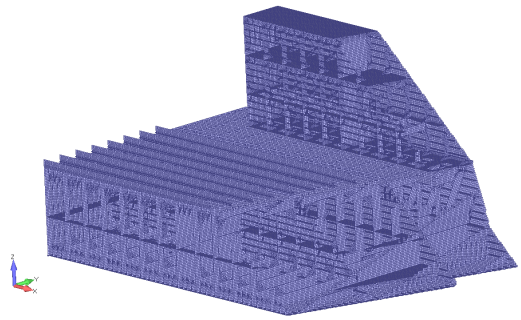

Figure 4.33. *Detail of the 3D-FEM model for the stern tower, Dock_VARD_Tulcea*

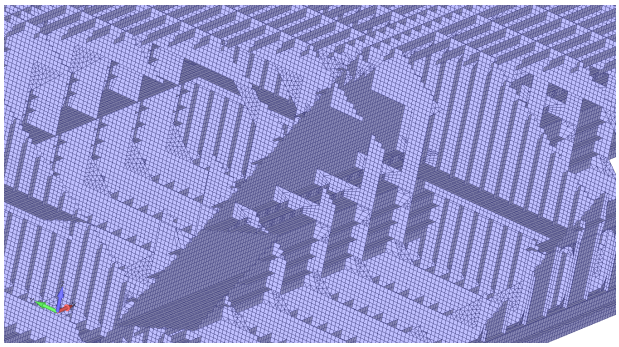

Figure 4.34. *Detail of the 3D-FEM model for frames and longitudinal structure, Dock_VARD_Tulcea*

a. b.

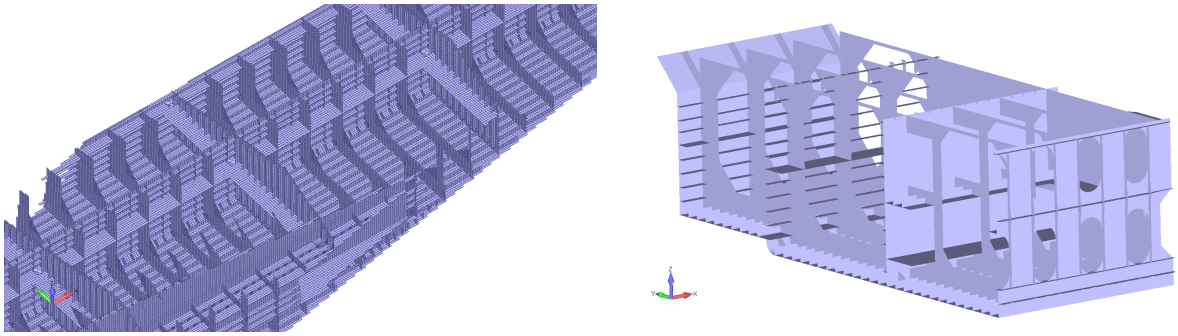

Figure 4.35.a., b. *3D-FEM model of the middle area, Dock_VARD_Tulcea*

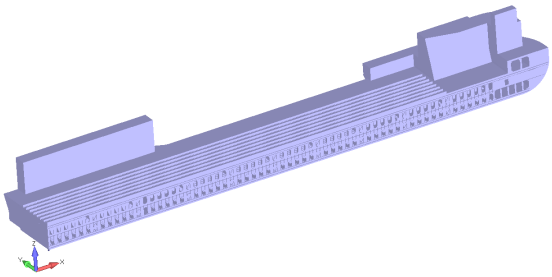

Figure 4.36. *The 3D-FEMmodel of the FD Dock_VARD_Tulcea*

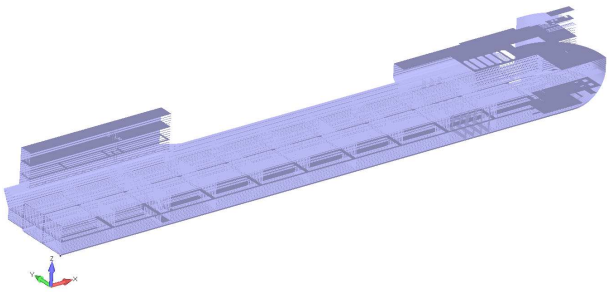

Figure 4.37. *The 3D-FEM model of the FD Dock_VARD_Tulcea, horizontal and longitudinal plate sections*

a. b.

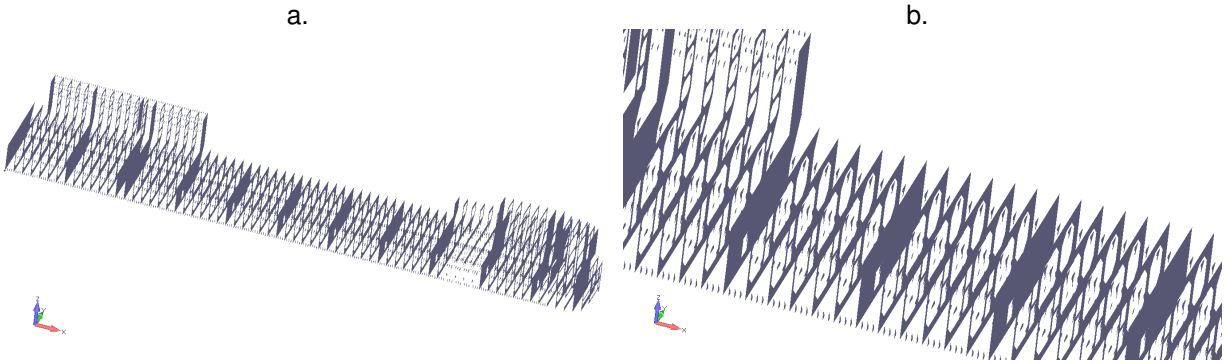

Figure 4.38.a., b. *3D-FEM model of the FD Dock_VARD_Tulcea, frame sections*

CHAPTER 5

COMPARATIVE ANALYSIS OF THE OPERATING CAPACITY OF THE DOCK60_CWT, DOCK60_NWT FLOATING DOCKS, WITH CONTINUOUS AND DISCONTINUOUS UPPER SIDE TANKS, BASED ON THE CRITERIA OF STRUCTURAL STRENGTH AND MINIMUM FREEBOARD, AT EXTREME LOADS FROM QUASI – STATIC WAVES

The study in this chapter presents the structural analysis and the minimum freeboard restrictions, of the small floating docks, with two constructive variants, with continuous upper side tanks (Dock60_CWT) and discontinuous (Dock60_NWT), using full-length 3D-FEM models, in a single board for the case of head and following waves, respectively over the entire width of the dock for the case of oblique waves, according to the procedures presented in chapter 2. With the help of 1D equivalent beam models, the equilibrium parameters of the quasi-static equivalent wave-dock system are determined. The height of the equivalent wave is considered maximum h_{wmax} ≤ 2 m , SW, IN(0.6), IN(1.2), IN(2.0), for the case of river navigation, and in the case of coastal navigation h_{wmax} ≤ 2.568 m, according to the rules of the ship classification companies [1]. For the loading cases described in chapter 4.1., The following will present the numerical results obtained from the analysis of the general resistance on a 1D equivalent beam model, as well as 3D-FEM models, in the case of quasi-static head/follow and oblique waves. For the consistency of the presentation, each of the three subchapters included the related conclusions.

Results on 1D equivalent beam model, quasi- static head/follow equivalent wave, are published and presented in the article in the reference [35]. The results on 1D equivalent beam model, quasi – static equivalent oblique wave, are published and presented in the article in the reference [37]. The results on the 3D-FEM models for the quasi-static head and follow equivalent waves are presented and published in the reference article [41]. The results on 3D-FEM models, in the case of quasi-static oblique waves, are presented and published in the article in the reference [51].

5.1. Preliminary structural analysis ($a_{Fr}=2a_0$) of the floating docks Dock60_CWT, Dock60_NWT, based on the 1D equivalent beam model, at loads from equivalent quasi – static head – follow waves

For the preliminary structural analysis of the small floating docks Dock60, with the two constructive versions NWT and CWT (chapter 4.1.), we considered the criteria of global resistance (initial structure $a_{Fr}=2a_0$) based on the allowable values of the vertical bending moment and shear force AVBM, AVSF, the ultimate strength vertical bending moment AUSVBM, as well as the maximum allowable vertical deflection w_{adm} (table .4.3., table 4.4. and table 4.5.). The dock loads correspond to the still water condition SW h_w = 0 m in the protected harbour, IN(2.0) h_w = 2 m and RE(50%) h_w = 2.568 m, conditions of navigation on river routes respectively coastal, for the cases of relocation of the floating dock, without or with docked mass, with the step of the wave height $\delta h_w = 0.1 \div 0.25m$, according to the rules of the ship classification companies [1].

Based on the D_ACVAD module, chapter 2.1.4., annex 3, the following numerical results are obtained:

- the vertical deflection diagrams of the floating dock 1D beam $w[m]$ in calm water conditions and quasi-static equivalent sagging and hogging waves, as well as the allowable deflection $w_{adm}[m]$ (table 4.3., figure 5.1.1.a. – Dock60_NWT_SB, figure 5.1.1.b. – Dock60_NWT_LB, figure 5.1.2.a. – Dock60_CWT_SB, figure 5.1.2.b. – Dock60_CWT_LB);
- diagrams of vertical bending moment $VBM[kNm]$ of the floating docks in calm water conditions and quasi-static equivalent sagging and hogging waves, as well as allowable limits AVBM and AVSUVBM (table 4.4., figure 5.2.1.a. – Dock60_NWT_SB, figure 5.2.1.b. – Dock60_NWT_LB, figure 5.2.2.a. – Dock60_CWT_SB, figure 5.2.2.b. – Dock60_CWT_LB);
- diagrams of the vertical shear forces of the floating dock $VSF[kN]$ under calm water conditions and quasi-static equivalent sagging and hogging waves, as well as allowable limits AVSF (table 4.4., figure 5.3.1.a. – Dock60_NWT_SB, figure 5.3.1.b. – Dock60_NWT_LB, figure 5.3.2.a. – Dock60_CWT_SB, figures 5.3.2.b. – Dock60_CWT_LB).

Tables 5.1. a., b. – Dock60_NWT_SB/LB and tables 5.2. a., b. – Dock60_CWT_SB/LB, presents the structural capability of floating docks Dock60_CWT/NWT formulated by the environmental conditions, the limit height of the quasi-static equivalent encounter heave/follow wave a h_w, to the criteria of resistance and global deformation (table 4.3., table 4.4.). There are no major differences between cases of short (SB) and long (LB) docking blocks, as a fact that calculations on 1D equivalent beam model for oblique wave and 3D-FEM models will be done only for short docking blocks.

Table 5.1.a. Limits values according to strength, deflection and freeboard criteria

Dock60_NWT_SB		Hogging				Sagging			
Criteria	**Limit**	***T_m*[m]**	***w*[m]**	***VBM*[kNm]**	***VSF*[kN]**	***T_m*[m]**	***w*[m]**	***VBM*[kNm]**	***VSF*[kN]**
1	IN(0.38)	0.776	-0.150	1.95E+04	2.86E+03	0.776	0.128	-1.89E+04	1.347E+03
hw[m]	0.378	1.848	0.922	0.378	2.568	1.848	2.568	1.844	2.568
2	IN(0.33)	6.837	-0.029	5.41E+03	3.38E+02	6.266	-0.012	2.45E+03	2.55E+02
hw[m]	0.326	0.326	2.568	2.568	2.568	1.468	2.568	2.568	2.568
3	IN(0.25)	1.490	-0.150	1.95E+04	2.52E+03	1.490	0.095	-1.89E+04	1.28E+03
hw[m]	0.252	0.420	0.781	0.252	2.568	0.420	2.568	2.476	2.568
4	IN(0.42)	1.490	-0.150	1.95E+04	2.19E+03	1.490	0.135	-1.89E+04	1.57E+03
hw[m]	0.420	0.420	1.309	0.664	2.568	0.420	2.568	1.724	2.568
5	SW	1.490	-0.150	1.95E+04	2.79E+03	1.490	0.076	-1.54E+04	9.41E+02
hw[m]	0.000	0.420	0.569	0.000	2.568	0.420	2.568	2.568	2.568
hw[m]	**0.000**	**Class SW**							

Table 5.1.b. Limit values according to strength, deflection and freeboard criteria

Dock60_NWT_LB		Hogging				Sagging			
Criteria	**Limit**	***T_m*[m]**	***w*[m]**	***VBM*[kNm]**	***VSF*[kN]**	***T_m*[m]**	***w*[m]**	***VBM*[kNm]**	***VSF*[kN]**
1	IN(0.39)	0.776	-0.150	1.95E+04	2.84E+03	0.776	0.129	-1.89E+04	1.350E+03
hw[m]	0.388	1.848	0.933	0.388	2.568	1.848	2.568	1.824	2.568
2	IN(0.33)	6.837	-0.028	5.23E+03	3.26E+02	6.266	-0.011	2.28E+03	2.61E+02
hw[m]	0.326	0.326	2.568	2.568	2.568	1.468	2.568	2.568	2.568
3	IN(0.34)	1.490	-0.150	1.95E+04	2.47E+03	1.490	0.103	-1.89E+04	1.35E+03
hw[m]	0.335	0.420	0.871	0.335	2.568	0.420	2.568	2.329	2.568
4	IN(0.42)	1.490	-0.150	1.95E+04	2.17E+03	1.490	0.135	-1.89E+04	1.62E+03
hw[m]	0.420	0.420	1.325	0.679	2.568	0.420	2.568	1.702	2.568
5	SW	1.490	-0.150	1.95E+04	2.73E+03	1.490	0.077	-1.57E+04	1.00E+03
hw[m]	0.015	0.420	0.584	0.015	2.568	0.420	2.568	2.568	2.568
hw[m]	**0.015**	**Class SW**							

Table 5.2.a. Limit values according to strength, deflection and freeboard criteria

Dock60_CWT_SB		Hogging				Sagging			
Criteria	**Limit**	***T_m*[m]**	***w*[m]**	***VBM*[kNm]**	***VSF*[kN]**	***T_m*[m]**	***w*[m]**	***VBM*[kNm]**	***VSF*[kN]**
1	IN(1.93)	0.958	-0.025	5.40E+04	3.08E+03	0.958	0.012	-2.67E+04	1.394E+03
hw[m]	1.934	1.934	2.568	2.568	2.568	1.934	2.568	2.568	2.568
2	IN(0.60)	6.700	-0.004	7.54E+03	3.77E+02	6.700	0.009	-2.00E+04	1.16E+03
hw[m]	0.600	0.600	2.568	2.568	2.568	0.600	2.568	2.568	2.568
3	IN(0.55)	1.650	-0.023	4.73E+04	2.77E+03	1.650	-0.023	-1.54E+04	1.09E+03
hw[m]	0.549	0.549	2.568	2.568	2.568	0.549	2.568	2.568	2.568
4	IN(0.55)	1.650	-0.019	4.00E+04	2.45E+03	1.650	0.010	-2.28E+04	1.38E+03
hw[m]	0.549	0.549	2.568	2.568	2.568	0.549	2.568	2.568	2.568
5	IN(0.55)	1.650	-0.024	5.17E+04	3.04E+03	1.650	0.005	-1.10E+04	7.53E+02
hw[m]	0.549	0.549	2.568	2.568	2.568	0.549	2.568	2.568	2.568
hw[m]	**0.549**	**Class IN(0.55)**							

Table 5.2.b. Limit values according to strength, deflection and freeboard criteria

Dock60_CWT_LB		Hogging				Sagging			
Criteria	**Limit**	***T_m*[m]**	***w*[m]**	***VBM*[kNm]**	***VSF*[kN]**	***T_m*[m]**	***w*[m]**	***VBM*[kNm]**	***VSF*[kN]**
1	IN(1.93)	0.958	-0.025	5.38E+04	3.03E+03	0.958	0.013	-2.69E+04	1.393E+03
hw[m]	1.934	1.934	2.568	2.568	2.568	1.934	2.568	2.568	2.568
2	IN(0.60)	6.700	-0.003	7.37E+03	3.63E+02	6.700	0.009	-2.02E+04	1.19E+03
hw[m]	0.600	0.600	2.568	2.568	2.568	0.600	2.568	2.568	2.568
3	IN(0.55)	1.650	-0.022	4.59E+04	2.69E+03	1.650	0.007	-1.68E+04	1.16E+03
hw[m]	0.549	0.549	2.568	2.568	2.568	0.549	2.568	2.568	2.568
4	IN(0.55)	1.650	-0.019	3.98E+04	2.38E+03	1.650	0.010	-2.30E+04	1.43E+03
hw[m]	0.549	0.549	2.568	2.568	2.568	0.549	2.568	2.568	2.568
5	IN(0.55)	1.650	-0.024	5.15E+04	2.98E+03	1.650	0.005	-1.13E+04	8.05E+02
hw[m]	0.549	0.549	2.568	2.568	2.568	0.549	2.568	2.568	2.568
hw[m]	**0.549**	**Class IN(0.55)**							

In the case of Dock60_CWT, the criteria of resistance and global deformation do not impose restrictions regarding the environmental conditions, $h_{w_{\lim it}} = 2{,}568m$. In the case of the dock Dock60_NWT, the strength criteria and the global deformations lead to the following restrictions for each displacement case (table 4.3., table 4.4.):

- The criterion of the permissible vertical shear force VSF does not impose restrictions in any case;
- For cases 1, 3 and 4 (table 4.6.), according to the criterion of the ultimate bending moment USBVM results in the limit height of the quasi-static wave equivalent at hogging $h_{w_{\lim it}} = 0{,}25 \div 0{,}68m$ and at saggging $h_{w_{\lim it}} = 1{,}70 \div 2{,}48m$;
- For case 5 (table 4.6.) according to the criterion of the ultimate strength vertical bending moment USBVM resulting the limit height of the quasi-static equivalent wave at hogging $h_{w_{\lim it}} = 0 \div 0{,}015m$ and unrestricted at sagging $h_{w_{\lim it}} = 2{,}568m$;
- Maximum allowable deflection criterion $w[m]$ does not impose restrictions in the case of quasi-static sagging wave;
- For cases 1, 3 and 4 (table 4.7.) according to the criterion of the maximum permissible deflection the limit height of the quasi-static equivalent hogging wave results $h_{w_{\lim it}} = 0{,}78 \div 1{,}32m$;
- For case 5 (table 4.7.) according to the criterion of the maximum permissible deflection, the limit height of the quasi-static hogging wave results $h_{w_{\lim it}} = 0{,}57 \div 0{,}58m$;
- For case 2 (table 4.7.) there are no restrictions according to the criteria of resistance and global deformation, $h_{w_{\lim it}} = 2{,}568m$;

In conclusion, we can state that from the criteria of global strength and deflection, in the case of floating dock with discontinuous tanks NWT (table 4.6.), the extreme scenario is represented by case 5 $h_{w_{\lim it}} = 0m$ (SW – still water), without restrictions in case 2 $h_{w_{\lim it}} = 2{,}568m$ and with restrictions for cases 1, 3 and 4, $h_{w_{\lim it}} = 0{,}25 \div 2{,}48m$, in these three cases it is necessary to operate in a protected port.

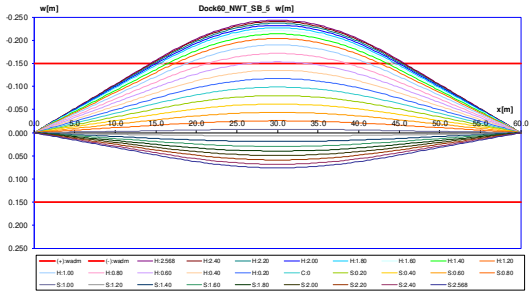

Figure 5.1.1.a. *Vertical deflection diagram w[m] for the 1D beam girder for Dock60_NWT, with short docking blocks (SB), docking case at maximum capacity of 828 t with hogging distribution, initial structure $a_{Fr}=2a_0$*

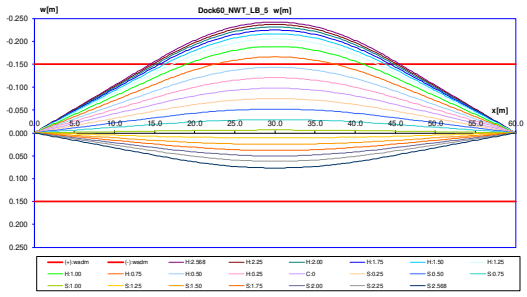

Figure 5.1.1.b. *Vertical deflection diagram w[m] for the 1D beam girder for Dock60_NWT, with long docking blocks (LB), docking case at maximum capacity of 828 t with hogging distribution, initial structure $a_{Fr}=2a_0$*

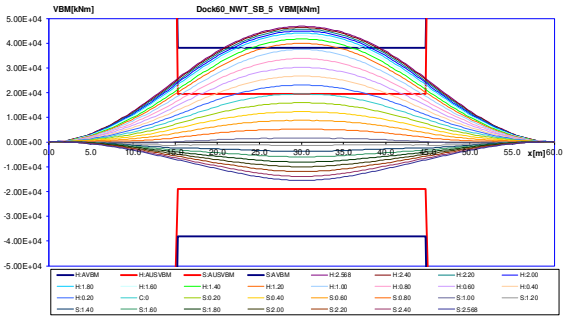

Figure 5.2.1.a. *Vertical bending moment diagram VBM[kNm] for the 1D beam girder for Dock60_NWT, , with short docking blocks (SB), docking case at maximum capacity of 828 t with hogging distribution, initial structure $a_{Fr}=2a_0$*

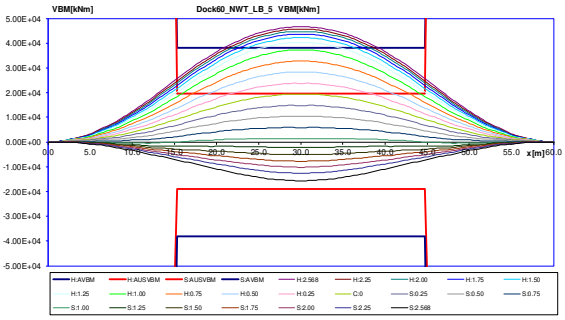

Figure 5.2.1.b. *Vertical bending moment diagram VBM[kNm] for the 1D beam girder for Dock60_NWT, with long docking blocks (LB), docking case at maximum capacity of 828 t with hogging distribution, initial structure $a_{Fr}=2a_0$*

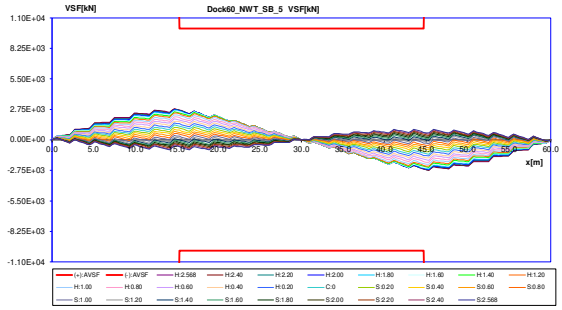

Figure 5.3.1.a. *Vertical shear force VSF[kN] for the 1D beam girder for Dock60_NWT, , with short docking blocks (SB), docking case at maximum capacity of 828 t with hogging distribution, initial structure $a_{Fr}=2a_0$*

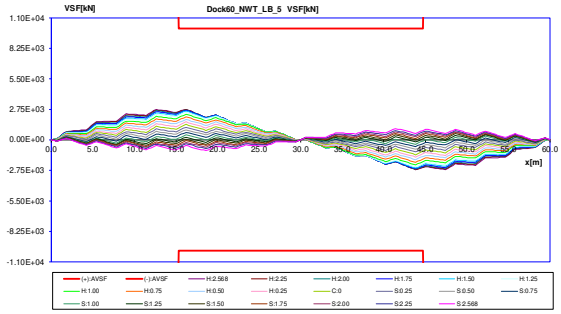

Figure 5.3.1.b. *Vertical shear force VSF[kN] for the 1D beam girder for Dock60_NWT, with long docking blocks (LB), docking case at maximum capacity of 828 t with hogging distribution, initial structure $a_{Fr}=2a_0$*

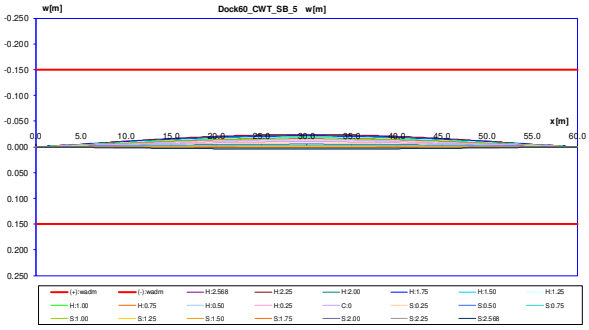

Figure 5.1.2.a. *Vertical deflection diagram w[m] for the 1D beam girder for Dock60_CWT, with short docking blocks (SB), docking case at maximum capacity of 828 t with hogging distribution, initial structure $a_{Fr}=2a_0$*

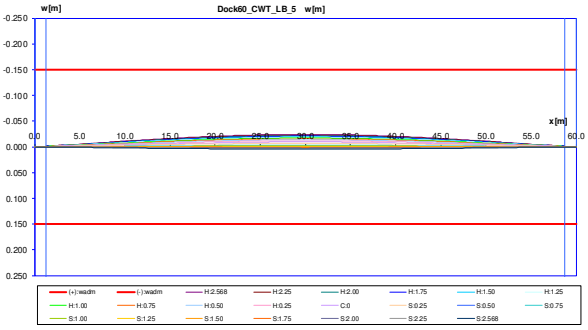

Figure 5.1.2.b. *Vertical deflection diagram w[m] for the 1D beam girder for Dock60_CWT, with long docking blocks (LB), docking case at maximum capacity of 828 t with hogging distribution, initial structure $a_{Fr}=2a_0$*

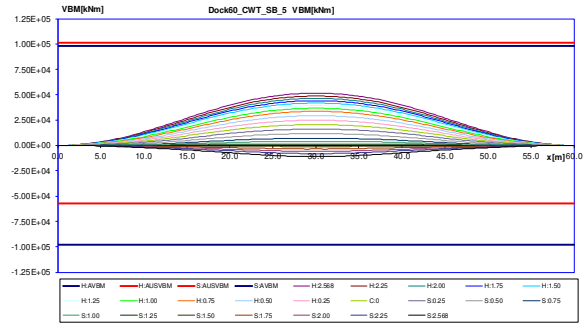

Figure 5.2.2.a. *Vertical bending moment diagram VBM[kNm] for the 1D beam girder for Dock60_CWT, , with short docking blocks (SB), docking case at maximum capacity of 828 t with hogging distribution, initial structure $a_{Fr}=2a_0$*

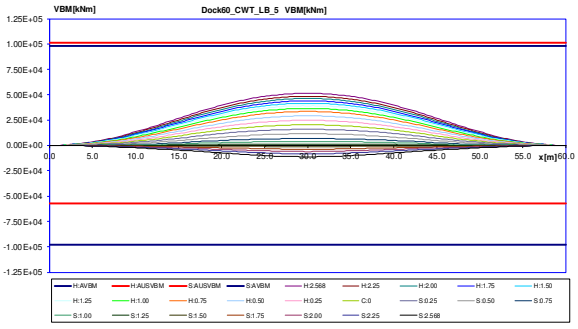

Figure 5.2.2.b. *Vertical bending moment diagram VBM[kNm] for the 1D beam girder for Dock60_CWT, with long docking blocks (LB), docking case at maximum capacity of 828 t with hogging distribution, initial structure $a_{Fr}=2a_0$*

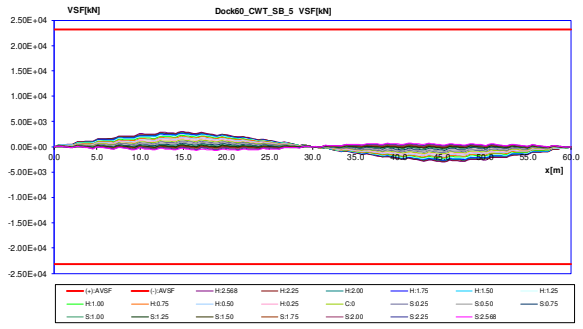

Figure 5.3.2.a *Vertical shear force VSF[kN] for the 1D beam girder for Dock60_CWT, , with short docking blocks (SB), docking case at maximum capacity of 828 t with hogging distribution, initial structure $a_{Fr}=2a_0$*

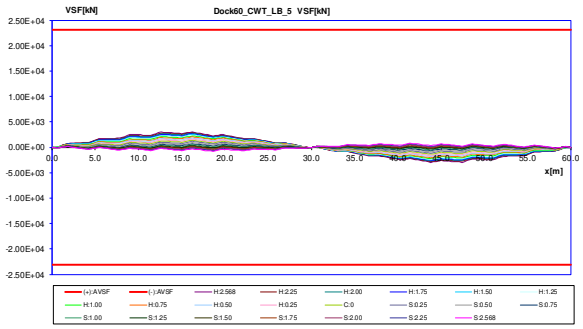

Figure 5.3.2.b. *Vertical shear force VSF[kN] for the 1D beam girder for Dock60_CWT, with long docking blocks (LB), docking case at maximum capacity of 828 t with hogging distribution, initial structure $a_{Fr}=2a_0$*

Considering only the minimum freeboard criterion, the following restrictions are obtained (wave height limit):

- Dock60_NWT: case 1 $h_{w_{\lim it}} = 1.85m$, cases 2 – 5 $h_{w_{\lim it}} = 0.33 \div 0.42m$ - table 5.7.a., b.;
- Dock60_CWT: case 1 $h_{w_{\lim it}} = 1.93m$, cases 2 – 5 $h_{w_{\lim it}} = 0.55 \div 0.60m$ - table 5.8.a., b.

From the numerical results of this chapter (table 5.2.a., b., table 5.3.a., b.) it turns out that the operating restrictions of the floating docks Dock60_CWT/NWT regarding the environmental conditions (the limit height of the wave) are imposed by the criteria of the ultimate bending moment USVBM and the minimum freeboard.

In summary, for the 20 displacement cases (table 4.6., table 4.7. – chapter 4.1.), in table 5.3. the operating capacity of the floating docks Dock60_CWT/NWT is presented from the criteria of resistance, global deformations and minimum freeboard. The extreme situation is the case 5, having the mass docked to the maximum capacity of 828 t, with a hogging distribution, for the constructive version with discontinuous upper side tanks Dock60_NWT, where extreme values have been reached for the criterion of ultimate global strength in the case of the initial structure $a_{Fr}=2a_0$.

Table 5.3. Safe operating capacity of floating docks Dock60_CWT/NWT, based on the criteria of resistance, global deformations and minimum freeboard

Loading case	Dock60_NWT $h_{w\lim}[m]$		Dock60_CWT $h_{w\lim}[m]$	
	SB blocks	LB blocks	SB blocks	LB blocks
Light displacement	0.38	0.39	1.93	1.93
Full ballast displacement	0.33	0.33	0.60	0.60
Maximum lifting capacity 828 t, with uniform mass distribution	0.25	0.34	0.55	0.55
Maximum lifting capacity 828 t, with sagging mass distribution	0.42	0.42	0.55	0.55
Maximum lifting capacity 828 t, with hogging mass distribution	0	0.015	0.55	0.55
Cases 2 - 5 The docking and ballast operation	In the case of a protected harbour still water condition		Unprotected / protected port ≈ IN(0.6) wave height 0.6m	
Case 1 The relocation operation	Only in inland waters, with the special approval of the navigation authorities (h_w<0.38 m)		≈ IN(2.0) inland navigation throughout the field of navigation Coastal navigation only with special approvals (h_w<1.93m)	

Based on the analyses in this chapter, the following conclusions are summarized in Table 5.4.:

- From the assessment of floating docks Dock60_CWT/NWT according to the global resistance criterion, for the height of the quasi-static extreme wave $h_{w\lim} \le 2{,}568m$, it turns out that for the CWT constructive version there are no restrictions. For the NWT constructive version, except for case 2 maximum ballast capacity, in other cases there are restrictions (cases 1, 3 and 4 $h_{w\lim} \ge 0{,}25m$) with the extreme condition for case 5, with docked mass at maximum capacity of 828 t with hogging distribution, where $h_{w\lim} \approx 0$ (SW still water). Restrictions are induced by the criterion of the vertical bending moment to the ultimate resistance. In the case Dock60_NWT, at the centre of the pontoon, because the upper lateral tanks are discontinuous, the overall resistance is significantly reduced, compared to the CWT variant, which has continuous lateral superior tanks along the entire length of the floating dock.
- From the assessment of the Dock60 floating dock according to the minimum free board criterion, in case 1 without docked table there is a significant free board reserve. In case 1 it is possible to relocate the dock, corresponding to the conditions of inland navigation without restrictions IN (2.0). For the other displacement cases 2 - 5 restrictions are $h_{w\lim} \le 0{,}42m$ (NWT) and $h_{w\lim} \ge 0{,}55m \approx 0{,}6m$ (CWT) approximately corresponding to the conditions of river navigation IN(0.6).
- The floating dock Dock60_CWT - caisson type with continuous upper lateral tanks has the greater operating capacity (without restrictions from the criterion of global resistance) compared to the constructive variant Dock60_NWT – with discontinuous lateral top tanks.

Table 5.4. The floating dock Dock60_CWT/NWT operation capabilities in safety conditions

Loading case	Dock60_NWT version (SB/LB blocks) non-continous side WT	Dock60_CWT version (SB/LB blocks) continuous side WT
1.Light displacement	- operation is sheltered harbour (SW), (h_{wlim}<0,38m) - relocation only on inland waterways with special approval of the inland navigation authorities	- operation in unsheltered ≈IN(2.0) / sheltered harbour (SW) (h_{wlim}<1,93m) - relocation on inland waterways without restrictions and for costal with special approval of the maritime navigation authorities
2. Full ballast displacement	- sheltered harbour (SW) (calm water conditions due to the stability criterion) - no relocation allowed	- sheltered harbour (SW) (calm water conditions due to the stability criterion) - no relocation allowed
3. Maximum lifting capacity 828 t, with uniform mass distribution	- operation in sheltered harbour (SW), (h_{wlim}<0,25m) - not designed for relocation operation with lifted ship onboard	- operation in unsheltered harbour ≈IN(0.6) / sheltered harbour (SW), (h_{wlim}<0,55m) - not designed for relocation operation with lifted ship onboard
4. Maximum lifting capacity 828 t, with sagging mass distribution	- operation in sheltered harbour (SW), (h_{wlim}<0,42m) - not designed for relocation operation with lifted ship onboard	- operation in unsheltered harbour ≈IN(0.6) / sheltered harbour (SW), (h_{wlim}<0,55m) - not designed for relocation operation with lifted ship onboard
5. Maximum lifting capacity 828 t, with hogging mass distribution	- operation in sheltered harbour (SW), (h_{wlim}≈0 m), the extreme loading case (strength limits) - not designed for relocation operation with lifted ship	- operation in unsheltered harbour ≈IN(0.6) / sheltered harbour (SW), (h_{wlim}<0,55m) - not designed for relocation operation with lifted ship

5.2. Evaluation of floating docks Dock60_CWT, Dock60_NWT, with reinforced structure ($a_{Fr}=a_0$), based on the 1D equivalent beam model, at oblique wave loads

This subchapter presents the analysis of the general resistance on 1D equivalent beam models for small floating docks, Dock60_CWT/NWT, having the reinforced structure $a_{Fr}=a_0$, for four of the operating cases presented in the previous subchapter. The case without maximum ballast is not analysed, due to the restrictions highlighted in the previous subchapter, the operation in this case being allowed only under still water conditions. For oblique waves, we took into account the fact that the small floating docks, Dock60_NWT/CWT, they have a double symmetry (figures 4.1. – 4.2.b., figures 4.13. – 4.16. - chapter 4.1.), so the heading angle of the wave can be considered for the values $\mu = 0 \div 90°$, for a step of $\delta\mu = 15°$. General resistance analysis on 1D equivalent beam models, in oblique waves, for the two constructive versions of floating docks Dock60_NWT/CWT, is done with the help of the P_QSWD software (chapter 2) [44]. In tables 5.5. – 5.6. a. – d and figures 5.4. – 5.8. presents the results of the analysis of the general resistance based on the 1D equivalent beam models of the Dock60_NWT / CWT floating docks, as well as checking the minimum free board criterion. For each docking case, 52 sub-cases were analysed.

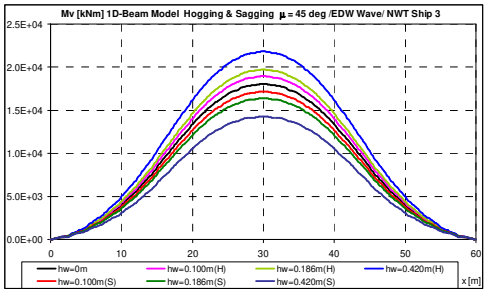

Figure 5.4.1. *Vertical bending moment [kNm], model 1D, docking case at maximum capacity of 828 t with hogging distribution, FD Dock60_NWT, oblique sagging(S) & hogging (H) EDW μ=45⁰, reinforced structure $a_{Fr}=a_0$*

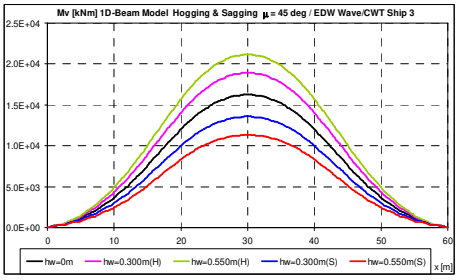

Figure 5.4.2. *Vertical bending moment [kNm], model 1D, docking case at maximum capacity of 828 t with hogging distribution, FD Dock60_CWT, oblique sagging(S) & hogging (H) EDW μ=45⁰, reinforced structure $a_{Fr}=a_0$*

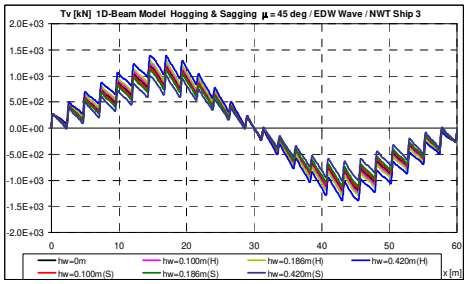

Figure 5.5.1. *Vertical shear force [kN], model 1D, docking case at maximum capacity of 828 t with hogging distribution, FD Dock60_NWT, oblique sagging(S) & hogging (H) EDW μ=45⁰, reinforced structure $a_{Fr}=a_0$*

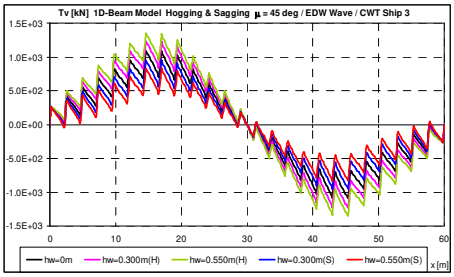

Figure 5.5.2. *Vertical shear force [kN], model 1D, docking case at maximum capacity of 828 t with hogging distribution, FD Dock60_CWT, oblique sagging(S) & hogging (H) EDW μ=45⁰, reinforced structure $a_{Fr}=a_0$*

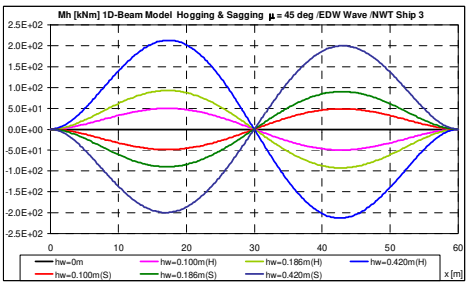

Figure 5.6.1. *Horizontal bending moment [kNm], model 1D, docking case at maximum capacity of 828 t with hogging distribution, FD Dock60_NWT, oblique sagging(S) & hogging (H) EDW μ=45⁰, reinforced structure $a_{Fr}=a_0$*

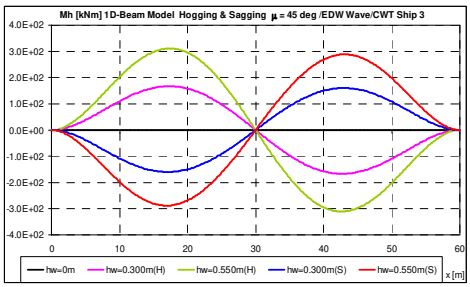

Figure 5.6.2. *Horizontal bending moment [kNm], model 1D, docking case at maximum capacity of 828 t with hogging distribution, FD Dock60_CWT, oblique sagging(S) & hogging (H) EDW μ=45⁰, reinforced structure $a_{Fr}=a_0$*

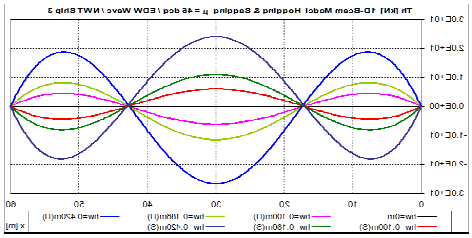

Figure 5.7.1. *Horizontal shear force [kN], model 1D, docking case at maximum capacity of 828 t with hogging distribution, FD Dock60_NWT, oblique sagging(S) & hogging (H) EDW μ=45^0, reinforced structure a_{Fi}=a_0*

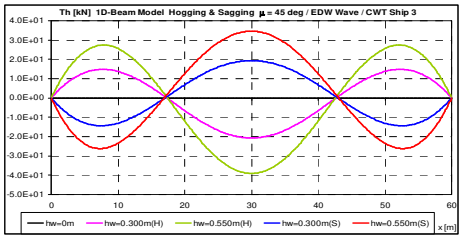

Figure 5.7.2. *Horizontal shear force [kN], model 1D, docking case at maximum capacity of 828 t with hogging distribution, FD Dock60_CWT, oblique sagging(S) & hogging (H) EDW μ=45^0, reinforced structure a_{Fi}=a_0*

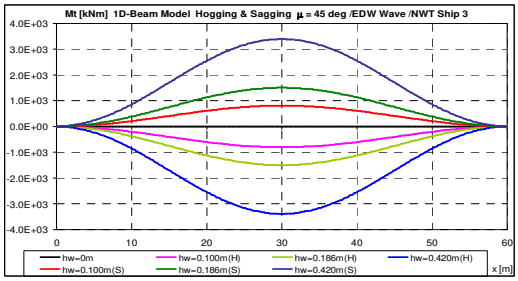

Figure 5.8.1. *Torque moment [kNm], model 1D, docking case at maximum capacity of 828 t with hogging distribution, FD Dock60_NWT, oblique sagging(S) & hogging (H) EDW μ=45^0, reinforced structure a_{Fi}=a_0*

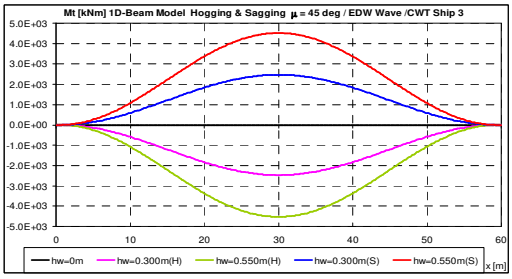

Figure 5.8.2. *Torque moment [kNm], model 1D, docking case at maximum capacity of 828 t with hogging distribution, FD Dock60_CWT, oblique sagging(S) & hogging (H) EDW μ=45^0, reinforced structure a_{Fi}=a_0*

Tables 5.5.a. – d. and 5.6. a. – d. presents the maximum values of the bending moments, the shear forces and the torsion moment for the two constructive versions of small floating docks, for the range of heading angles dock - wave from 0º to 90º. Also, according to the data in the tables, in figures 5.4. – 8. The sectional effort value diagrams for the 1D equivalent beam models of the two constructive versions of the small floating docks Dock60_CWT/NWT are selected, in the case of docking to the maximum capacity of 828 t, with the hogging distribution of the mass.

Figures 5.9. – 5.13. a., b. presents the diagrams of the maximum values of the shear forces, bending and torsional moments for the two constructive versions of the small floating docks Dock60_CWT / NWT.

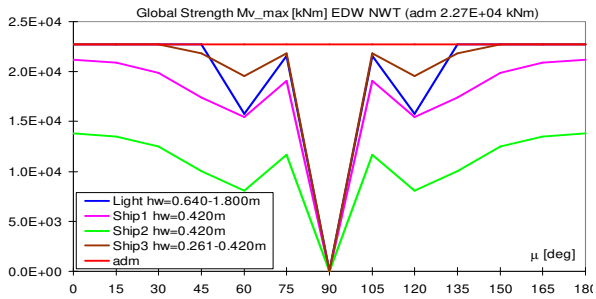

Figure 5.9.a. *Maximum values of the vertical bending moment for the FD Dock60_NWT, 1D model, reinforced structure a_{Fi}=a_0*

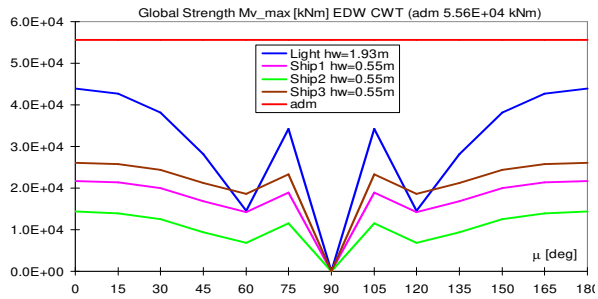

Figure 5.9.b. *Maximum values of the vertical bending moment for the FD Dock60_CWT, 1D model, reinforced structure a_{Fi}=a_0*

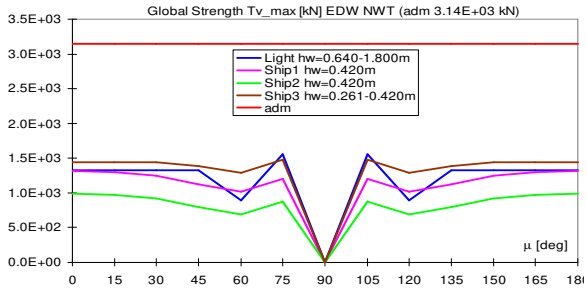

Figure 5.10.a. *Maximum values of the vertical shear force for the FD Dock60_NWT, 1D model, reinforced structure a_{Fi}=a_0*

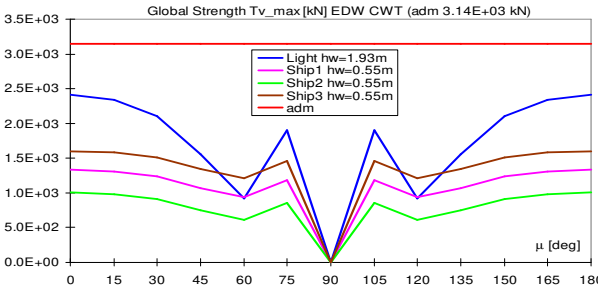

Figure 5.10.b. *Maximum values of the vertical shear force for the FD Dock60_VWT, 1D model, reinforced structure a_{Fi}=a_0*

Table 5.5.a. Maximum values of sectional efforts, 1D model, and verification of the minimum free board criterion for Dock60_NWT, in light case

NWT in light case Δ[t] = 960 ; $x_G = x_f$ [m] = 30 ; $y_G = y_f$ [m] =0 ; T_m[m] = 0,800 ; θ [rad] = 0 ; φ [rad] = 0															
1D	μ[deg]	0	max/ adm	15	max/ adm	30	max/ adm	45	max/ adm	60	max/ adm	75	max/ adm	90	max/ adm
h_{wlim}[m]	wave	0.640		0.666		0.778		1.278		1.800		1.800		1.800	
Fs [m]	sw	1.200	>1	*Fs* [m] = 0.300											
	hogg	0.880	>1	0.867	>1	0.811	>1	0.561	>1	0.300	**1.00**	0.300	**1.00**	0.300	**1.00**
	sagg	0.880	>1	0.867	>1	0.811	>1	0.561	>1	0.300	**1.00**	0.300	**1.00**	0.300	**1.00**
VBM [kNm] max.	sw	1.13E+4	0.50	*AVBM* [kNm] = 2.27E+04											
	hogg	2.27E+4	**1.00**	2.27E+4	**1.00**	2.27E+4	**1.00**	2.27E+4	**1.00**	1.01E+4	0.45	6.43E+3	0.28	0	0
	sagg	2.99E+2	0.01	2.99E+2	0.01	2.96E+2	0.01	3.03E+2	0.01	1.58E+4	0.69	2.16E+4	0.95	0	0

Table 5.5.b. Maximum values of sectional efforts, model 1D, and verification of the minimum free board criterion for Dock60_NWT, in case of the mass docked to the maximum capacity with uniform distribution

NWT uniform distribution Δ[t] = 1788 ; $x_G = x_f$ [m] = 30 ; $y_G = y_f$ [m] =0 ; T_m[m] = 1,490 ; θ [rad] = 0 ; φ [rad] = 0															
1D	μ[deg]	0	max/ adm	15	max/ adm	30	max/ adm	45	max/ adm	60	max/ adm	75	max/ adm	90	max/ adm
h_{wlim}[m]	wave	0.420		0.420		0.420		0.420		0.420		0.420		0.420	
Fs [m]	sw	0.510	1.70	*Fs* [m] = 0.300											
	hogg	0.300	**1.00**	0.300	**1.00**	0.300	**1.00**	0.300	**1.00**	0.300	**1.00**	0.300	**1.00**	0.300	**1.00**
	sagg	0.300	**1.00**	0.300	**1.00**	0.300	**1.00**	0.300	**1.00**	0.300	**1.00**	0.300	**1.00**	0.300	**1.00**

Table 5.5.c. Maximum values of sectional efforts, model 1D, and verification of the minimum free board criterion for Dock60_NWT, in case of the docked mass at maximum capacity with sagging distribution

NWT sagging distribution Δ[t] = 1788 ; $x_G = x_f$ [m] = 30 ; $y_G = y_f$ [m] =0 ; T_m[m] = 1,490 ; θ [rad] = 0 ; φ [rad] = 0															
1D	μ[deg]	0	max/ adm	15	max/ adm	30	max/ adm	45	max/ adm	60	max/ adm	75	max/ adm	90	max/ adm
h_{wlim}[m]	wave	0.420		0.420		0.420		0.420		0.420		0.420		0.420	
Fs [m]	sw	0.510	1.70	*Fs* [m] = 0.300											
	hogg	0.300	**1.00**	0.300	**1.00**	0.300	**1.00**	0.300	**1.00**	0.300	**1.00**	0.300	**1.00**	0.300	**1.00**
	sagg	0.300	**1.00**	0.300	**1.00**	0.300	**1.00**	0.300	**1.00**	0.300	**1.00**	0.300	**1.00**	0.300	**1.00**

Table 5.5.d. Maximum values of sectional efforts, 1D model, and verification of the minimum free board criterion for Dock60_NWT, in case of the mass docked to the maximum capacity with hogging distribution.

NWT hogging distribution Δ[t] = 1788 ; $x_G = x_f$ [m] = 30 ; $y_G = y_f$ [m] =0 ; T_m[m] = 1,490 ; θ [rad] = 0 ; φ [rad] = 0															
1D	μ[deg]	0	max/ adm	15	max/ adm	30	max/ adm	45	max/ adm	60	max/ adm	75	max/ adm	90	max/ adm
h_{wlim}[m]	wave	0.261		0.272		0.318		0.420		0.420		0.420		0.420	
Fs [m]	sw	0.510	1.70	*Fs* [m] = 0.300											
	hogg	0.379	1.26	0.374	1.24	0.351	1.17	0.300	**1.00**	0.300	**1.00**	0.300	**1.00**	0.300	**1.00**
	sagg	0.379	1.26	0.374	1.24	0.351	1.17	0.300	**1.00**	0.300	**1.00**	0.300	**1.00**	0.300	**1.00**

VBM [kNm] max.	sw	1.81E+4	0.79	*AVBM* [kNm] = 2.27E+04											
	hogg	2.27E+4	**1.00**	2.27E+4	**1.00**	2.27E+4	**1.00**	2.18E+4	0.96	1.63E+4	0.72	1.27E+4	0.56	0	0
	sagg	1.34E+4	0.59	1.34E+4	0.59	1.34E+4	0.59	1.43E+4	0.63	1.96E+4	0.86	2.18E+4	0.96	0	0

Table 5.6.a. Maximum values of sectional efforts, 1D model, and verification of the minimum free board criterion for Dock60_CWT, in light case

CWT light Δ[t] = 1152 ; $x_G = x_f$ [m] = 30 ; $y_G = y_f$ [m] =0 ; T_m[m] = 0,960 ; θ [rad] = 0 ; φ [rad] = 0															
1D	μ[deg]	0	max/ adm	15	max/ adm	30	max/ adm	45	max/ adm	60	max/ adm	75	max/ adm	90	max/ adm
h_{wlim}[m]	wave	1.930		1.930		1.930		1.930		1.930		1.930		1.930	
Fs [m]	sw	1.040	>1	*Fs* [m] = 0,075											
	hogg	0.075	**1.00**	0.075	**1.00**	0.075	**1.00**	0.075	**1.00**	0.075	**1.00**	0.075	**1.00**	0.075	**1.00**
	sagg	0.075	**1.00**	0.075	**1.00**	0.075	**1.00**	0.075	**1.00**	0.075	**1.00**	0.075	**1.00**	0.075	**1.00**

Table 5.6.b. Maximum values of sectional efforts, 1D model, and verification of the minimum free board criterion for Dock60_CWT, in case 1 with the mass docked to the maximum capacity with uniform distribution

CWT uniform distribution Δ[t] = 1980 ; $x_G = x_f$ [m] = 30 ; $y_G = y_f$ [m] =0 ; T_m[m] = 1,650 ; θ [rad] = 0 ; φ [rad] = 0															
1D	μ[deg]	0	max/ adm	15	max/ adm	30	max/ adm	45	max/ adm	60	max/ adm	75	max/ adm	90	max/ adm
h_{wlim}[m]	wave	0.550		0.550		0.550		0.550		0.550		0.550		0.550	
Fs [m]	sw	0.350	>1	*Fs* [m] = 0.075											
	hogg	0.075	**1.00**	0.075	**1.00**	0.075	**1.00**	0.075	**1.00**	0.075	**1.00**	0.075	**1.00**	0.075	**1.00**
	sagg	0.075	**1.00**	0.075	**1.00**	0.075	**1.00**	0.075	**1.00**	0.075	**1.00**	0.075	**1.00**	0.075	**1.00**

Table 5.6.c. Maximum values of sectional efforts, 1D model, and verification of the minimum free board criterion for Dock60_CWT, in case 2 with the docked mass at the maximum capacity with sagging distribution

CWT sagging distribution Δ[t] = 1980 ; $x_G = x_f$ [m] = 30 ; $y_G = y_f$ [m] =0 ; T_m[m] = 1,650 ; θ [rad] = 0 ; φ [rad] = 0															
1D	μ[deg]	0	max/ adm	15	max/ adm	30	max/ adm	45	max/ adm	60	max/ adm	75	max/ adm	90	max/ adm
h_{wlim}[m]	wave	0.550		0.550		0.550		0.550		0.550		0.550		0.550	
Fs [m]	sw	0.350	>1	*Fs* [m] = 0.075											
	hogg	0.075	**1.00**	0.075	**1.00**	0.075	**1.00**	0.075	**1.00**	0.075	**1.00**	0.075	**1.00**	0.075	**1.00**
	sagg	0.075	**1.00**	0.075	**1.00**	0.075	**1.00**	0.075	**1.00**	0.075	**1.00**	0.075	**1.00**	0.075	**1.00**

Table 5.6.d. Maximum values of sectional efforts, 1D model, and verification of the minimum free board criterion for Dock60_CWT, in case 3 with the mass docked to the maximum capacity with hogging distribution

CWT hogging distribution Δ[t] = 1980 ; $x_G = x_f$ [m] = 30 ; $y_G = y_f$ [m] =0 ; T_m[m] = 1,650 ; θ [rad] = 0 ; φ [rad] = 0															
1D	μ[deg]	0	max/ adm	15	max/ adm	30	max/ adm	45	max/ adm	60	max/ adm	75	max/ adm	90	max/ adm
h_{wlim}[m]	wave	0.550		0.550		0.550		0.550		0.550		0.550		0.550	
Fs [m]	sw	0.350	>1	*Fs* [m] = 0.075											
	hogg	0.075	**1.00**	0.075	**1.00**	0.075	**1.00**	0.075	**1.00**	0.075	**1.00**	0.075	**1.00**	0.075	**1.00**
	sagg	0.075	**1.00**	0.075	**1.00**	0.075	**1.00**	0.075	**1.00**	0.075	**1.00**	0.075	**1.00**	0.075	**1.00**

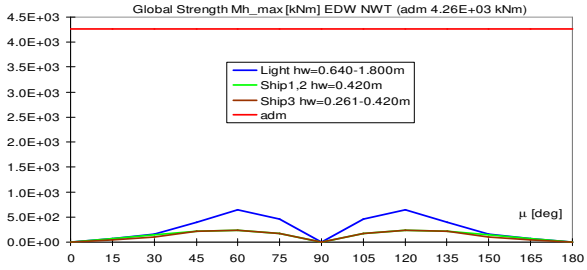

Figure 5.11.a. *Maximum values of the horizontal bending moment for the FD Dock60_NWT, 1D model, reinforced structure $a_{Fr}=a_0$*

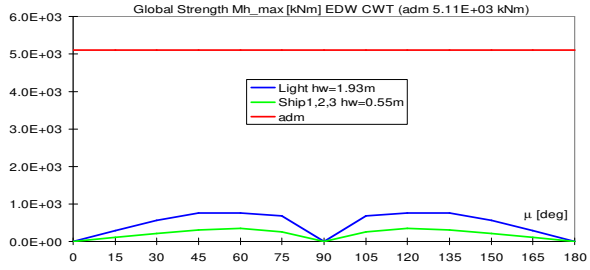

Figure 5.11.b. *Maximum values of the horizontal bending moment for the FD Dock60_CWT, 1D model, reinforced structure $a_{Fr}=a_0$*

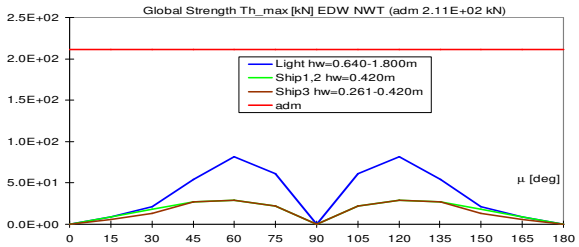

Figure 5.12.a. *Maximum values of the horizontal shear force for the FD Dock60_NWT, 1D model, reinforced structure $a_{Fr}=a_0$*

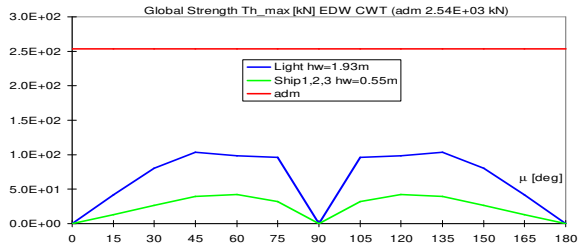

Figure 5.12.b. *Maximum values of the horizontal shear force for the FD Dock60_CWT, 1D model, reinforced structure $a_{Fr}=a_0$*

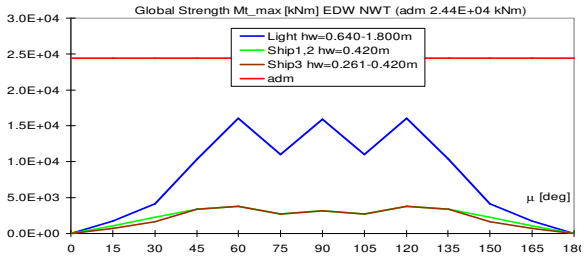

Figure 5.13.a. *Maximum values of the torque moment for the FD Dock60_NWT, 1D model, reinforced structure $a_{Fr}=a_0$*

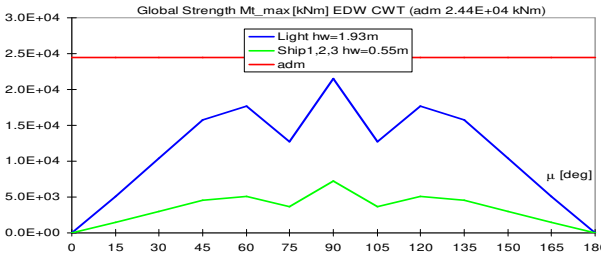

Figure 5.13.b. *Maximum values of the torque moment for the FD Dock60_CWT, 1D model, reinforced structure $a_{Fr}=a_0$*

From the analysis on 1D models to requests in equivalent quasi-static oblique waves of the two constructive versions for the small floating docks Dock60_NWT/CWT with reinforced structure $a_{Fr}=a_0$ the following conclusions are drawn:

- For the small dock Dock60_NWT, depending on the heading angle of the wave $\mu = 0 \div 90°(360°)$, the following limits of the maximum wave height have been set, for the case without docked mass (table 5.5.a.) $h_{w\,\lim} = 0.640 \div 1.278\ m$ - with restrictions of the allowable vertical bending moment criterion for $\mu = 0 \div 60°(120 \div 180°, 180 \div 240°, 300 \div 360°)$ in the case of hogging type waves, and $h_{w\,\lim} = 1.800\ m$ - with restrictions from the minimum freeboard criterion for $\mu = 60 \div 90°(90 \div 120°, 240 \div 300°)$; docking case at maximum capacity of 828t with uniformly distributed mass and sagging type mass (tables 5.5.b. and c.) $h_{w\,\lim} = 0.42\ m$ - with restrictions from the minimum freeboard criterion for the entire range of heading angles dock - wave; the docking case at the maximum capacity of 828 t with the distributed hogging mass (table 5.5.d.) $h_{w\,\lim} = 0.261 \div 0.318\ m$ - with restrictions from the vertical bending moment criterion for $\mu = 0 \div 30°(150 \div 210°, 330 \div 360°)$ for hogging type waves $h_{w\,\lim} = 0.420\ m$ - with restrictions from the minimum freeboard criterion for $\mu = 45 \div 90°(90 \div 135°, 225 \div 315°)$. The synthesis results of the 1D model analysis for the Dock60_NWT are presented in the polar diagram in figure 5.14.a. and in table 5.7.

- For Dock60_CWT floating dock, the maximum limits without docked mass is $h_{w\,\lim} = 1.930\ m$ (table 5.6.a.) and for the case with docking mass at maximum capacity is $h_{w\,\lim} = 0.550\ m$ (tables 5.6.b. – d.), for the entire range of heading angles $\mu = 0 \div 90°(360°)$, the restrictions being due to the minimum freeboard criterion. The synthesis results of the 1D model analysis for Dock60_NWT are presented in the polar diagram of figure 5.14.b. and in table 5.7.
- For both cases of small floating docks, the most restrictive case remains the head/follow wave, $\mu = 0°(180°)$. The floating dock Dock60_NWT has significant restrictions on river navigation, still water (SW) – IN(0.64) and in the coastal case it should be operated only in sheltered harbours. Floating dock Dock60_CWT, has fewer restrictions on waterway routes, IN(0.55) – IN(1.93), and for the coastal area, relocation is allowed only in the case without the dock with special approvals RE(37%). The constructive case with continuous upper lateral tanks, allows the operation with the maximum docking capacity of 828 t in the three modes of distribution (uniform, sagging type and hogging type) only in sheltered harbours.

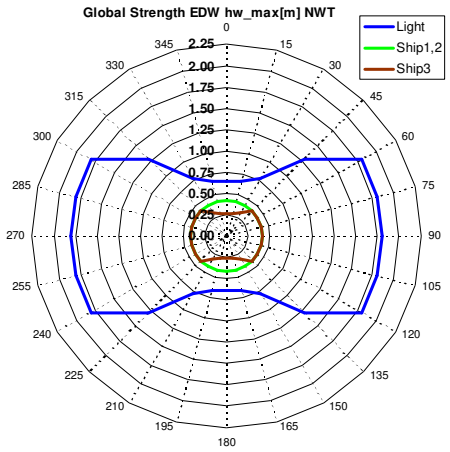

Figure 5.14.a. *Dock60_NWT polar diagram of EDW wave height limit, all four loading cases, beam model, reinforced structure $a_{Fr}=a_0$*

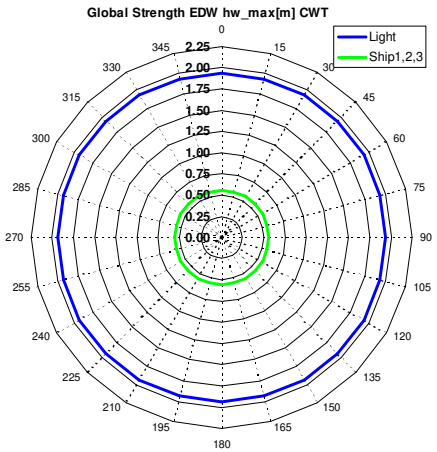

Figure 5.14.b. *Dock60_CWT polar diagram of EDW wave height limit, all four loading cases, beam model, reinforced structure $a_{Fr}=a_0$*

Thus, the main conclusion of this subchapter is that floating docks with discontinuous side tanks have much more restrictions in the operational cases, being recommended for operations only in sheltered harbours.

Table 5.7. The results obtained for the cases of docking of small floating docks Dock60_CWT / NWT, model 1D equivalent beam, in equivalent quasi-static oblique waves, reinforced structure $a_{Fr}=a_0$

Case	Dock60_NWT				Dock60_CWT			
	Light	*Docking case at maximum capacity of 828 t* with uniform mass distribution	*Docking case at maximum capacity of 828 t* with sagging mass distribution	*Docking case at maximum capacity of 828 t* with hogging mass distribution	Light	*Docking case at maximum capacity of 828 t* with uniform mass distribution	*Docking case at maximum capacity of 828 t* with sagging mass distribution	*Docking case at maximum capacity of 828 t* with hogging mass distribution
$h_{w\,limit}$ [m]	0.640	0.420	0.420	0.261	1,930	0,550	0,550	0,550
criterion	Restriction form strength criteria	Restrictions form freeboard criteria		Restriction form strength criteria	Restrictions from the minimum free board criterion at the level of the main dock of the floating dock			
inland	IN(0.64)	IN(0.42)	IN(0.42)	SW	IN(1.93)	IN(0.55)	IN(0.55)	IN(0.55)
coastal	Operations only in sheltered harbour				RE(37%)	Operations only in sheltered harbour		

5.3. Structural analysis on 3D-FEM models of floating docks Dock60_CWT, Dock60_NWT, at loads from equivalent quasi – static head – follow and oblique waves

This subchapter presents the evaluation of the minimum freeboard criteria, the permissible stresses and strains for the two constructive versions of the Dock60_CWT/NWT small floating docks, on fully extended 3D-FEM models:

- For the analysis in quasi-static equivalent head – following waves, the operating cases used are presented in in subchapter 5.1.
- For the analysis in quasi-static equivalent oblique waves, the operating cases used in subchapter 5.2 will be analysed.

The 3D-FEM model is developed for both types of wave requests with the FEMAP NX/Nastran software [42] (figure 4.13 - 4.21), using finite elements of thick plate (Mindlin) and membrane, rectangular and triangular, for the structure of the steel body, as well as finite mass elements concentrated for modelling the equipment, the ballast mass and the mass of the docked vessel. *The analysis includes from the beginning the variant with reinforced structure $a_{Fr}=a_{0,}$ of the two constructive variants of floating docks Dock60_CWT/NWT.* In table 5.8. loading cases for the small floating docks are presented.

Table 5.8. Load cases for small floating docks Dock60_CWT/NWT

Type		Light	Full ballast	*Docking case at maximum capacity of 828 t* with uniform mass distribution	*Docking case at maximum capacity of 828 t* with sagging mass distribution	*Docking case at maximum capacity of 828 t* with hogging mass distribution
CWT	$\Delta[t]$	1,152	4,092	1,980		
	$d_m[m]$	0.960	6.700	1.650		
	$LCG\ [m]$	30	30	30		
NWT	$\Delta[t]$	960	3,252	1,788		
	$d_m[m]$	0.80	6.733	1.490		
	$LCG\ [m]$	30	30	30		

5.3.1. Case of head – follow waves

In the first part of this subchapter, we analyse the structural response to requests from quasi-static head – following waves, with 3D-FEM structural model extended in a single board (figure 4.13. – 4.16.a., b., c.)

Figures 5.15.1., 2., a. and b. presents the docking case at the maximum capacity of 828 t, with the hogging distribution of the mass, out of a total of 66 cases analysed, for the values of von Mises equivalent stress (vonM [MPa]) for the state of sagging and hogging of the meeting waves, in all cases of docking, for the two constructive versions of the floating docks Dock60_CWT/NWT with 3D-FEM model.

Figures 5.15.1.,2.,c.,d. and e. presents the distributions of normal tensions ($\sigma_x[MPa]$) and the vertical deflection ($w[mm]$) in the case of still water conditions, sagging wave type and hogging wave type, for constructive versions of Dock60_CWT/NWT floating docks, in the case of docking at a maximum capacity of 828 t, with the mass distribution hogging, for 3D-FEM models and 1D equivalent beam.

Figures 5.16.a. – b., presents the way of losing the structural stability and the values of the associated buckling factor ($B_{buckling}$) for sagging type and hogging head – following wave type, in the case of docking at a maximum capacity of 828 t, with the mass hogging distribution for 3D-FEM models, with structural loose in the transverse frame for the constructive case with continuous lateral tanks (CWT), and with structural loose on the girders for the case of construction with discontinuous side tanks (NWT).

Tables 5.9. and 5.11. presents the maximum tension and the vertical deflection evaluated by the criteria in table 4.3., in both constructive versions, for all five operating cases

in table 4.6. and table 4.7. for 3D-FEM models and 1D equivalent beam, at heading and following waves.

Following the checks for both constructive variants of small floating docks, Dock60_NWT/CWT, subjected to requests from still water and quasi-static equivalent head – follow waves, up to the height limits of the waves imposed by the criterion of the minimum freeboard (table 4.3.), the most restrictive operations are for the docking case of the maximum capacity of 828 t, in the three cases, the mass distribution in the case of complete ballast (table 5.6. table 5.7.), resulting in limit values of wave height $h_{w\lim} = 0.550 \div 0.600\ m$ for Dock60_CWT and $h_{w\lim} = 0.326 \div 0.420\ m$ for Dock60_NWT, requiring operating conditions in sheltered harbours IN(0.6). In the case without docked mass, from the criterion of the minimum freeboard, the limit values of the wave height of the $h_{w\lim} = 1.930\ m$ for Dock60_CWT and $h_{w\lim} = 1.829\ m$ for Dock60_NWT, therefore it is allowed to operate in a maximum inland navigation area of IN(1.8).

In the case of Dock60_CWT floating dock, the structural stability criterion does not add any additional restrictions, the limitations being imposed only by the minimum freeboard criterion for the hogging type wave with the height of $h_{w\lim} = 1.930\ m$. The criteria of the von Mises equivalent stresses and of the allowable vertical deformations do not impose restrictions on this constructive case.

In the case of the small floating dock with discontinuous upper side tanks, Dock60_NWT, the criterion of loss of structural stability induces significant restrictions for the case without docked mass, $h_{w\lim} = 0.582\ m$, and for the case of docking at a maximum capacity of 828 t with the hogging mass distribution $h_{w\lim} = 0.186\ m$. The buckling criterion does not impose restrictions for the docking case to the maximum capacity with the sagging mass distribution, and for the uniform distribution, we have restrictions only from the minimum freeboard criterion. For the conditions of equivalent wave heading - following with wave height already reduced by the criteria of minimum freeboard and structural stability, the criteria of equivalent von Mises stresses and of the allowable vertical deformations do not induce additional restrictions.

Summarizing the results of this subchapter, table 5.12. presents the operating conditions resulting from the 3D-FEM structural analysis, with requests from equivalent quasi-static head-following waves, for the two constructive versions of the small floating docks Dock60_NWT/CWT. The comparison between 3D-FEM and 1D equivalent beam models highlights areas with tension concentrators.

Table 5.9. The von-Mises equivalent stresses and the structural stability factor from the 3D-FEM model Dock60_CWT

No	Case	Wave	h_w[m]	d_m[m]	Z[m]	$Z/adm \le 1$	σ_{vM}[MPa]	$\sigma_{vM}/adm \le 1$	$B_{buckling}$	$B/adm \ge 1$
adm		-	-	-	1.925(7.0) m	-	175 MPa	-	1.50	-
1	Light	hogg.	1.00	0.96	1.460	0.758	32.16	0.184	2.347	1.565
			1.93		**1.925**	**1**	48.30	0.276	**1.518**	**1.012**
2	Full ballast	hogg.	0.30	6.70	6.850	0.979	43.82	0.250	3.037	2.025
			0.60		**7.000**	**1**	44.98	0.257	2.953	1.969
3	*Docking case at maximum capacity of 828 t* with uniform mass distribution	hogg.	0.30	1.65	1.800	0.935	31.26	0.178	3.464	2.309
			0.55		**1.925**	**1**	31.26	0.179	2.849	1.899
4	*Docking case at maximum capacity of 828 t* with sagging mass distribution	hogg.	0.30	1.65	1.800	0.935	30.85	0.176	4.702	3.135
			0.55		**1.925**	**1**	31.47	0.180	3.995	2.663

5	*Docking case at maximum capacity of 828 t* with hogging mass distribution	hogg.	0.30	1.65	1.800	0.935	30.95	0.177	2.838	1.892
			0.55		**1.925**	**1**	31.08	0.178	2.411	1.607

Table 5.10. The von-Mises equivalent stresses and the structural stability factor from the 3D-FEM model Dock60_NWT

No	Case	Wave	h_w[m]	d_m[m]	Z[m]	$Z/adm\leq1$	σ_{VM}[MPa]	$\sigma_{VM}/adm\leq1$	$B_{buckling}$	$B/adm\geq1$
adm		-	-	-	1.700(7.0) m	-	175 MPa	-	1.50	-
1	Light	hogg.	0.378	0,80	0.989	0.582	74.35	0.425	1.801	1.201
			0.582		1.091	0.642	89.30	0.510	**1.503**	**1.001**
			1.829	0,7853	**1.700**	**1**	**173.10**	**0.99**	**0.765**	**0.510**
2	Full ballast	hogg.	0.150	6,7811	6.8561	0.979	106.9	0.611	2.356	1.571
			0,326	6,8370	**7.000**	**1**	106.4	0.608	2.303	1.535
3	*Docking case at maximum capacity of 828 t* with uniform mass distribution	hogg.	0.252	-	1.616	0.951	86.63	0.495	1.740	1.160
			0.420		**1.700**	**1**	98.97	0.566	**1.503**	**1.001**
4	*Docking case at maximum capacity of 828 t* with sagging mass distribution	hogg.	0.250	-	1.615	0.950	62.94	0.360	2.856	1.904
			0.420		**1.700**	**1**	66.82	0.382	2.264	1.509
5	*Docking case at maximum capacity of 828 t* with hogging mass distribution	hogg.	0.186	-	1.583	0.931	84.36	0.482	**1.501**	**1**
			0.420		**1.700**	**1**	101.50	0.580	**1.263**	**0.842**

Table 5.11. Comparison between maximum equivalent voltages and vertical warping on 3D-FEM models and 1D equivalent beam for Dock60_NWT

No	Case	Wave	h_w[m]	σ_{xD} [MPa] (3D)	σ_{xD} [MPa] (1D)	*3D/1D* (σ_{xD})	$\sigma_{xD(3D)}/adm\leq1$	w[mm] *(3D)*	w[mm] *(1D)*	*3D/1D* *(w)*	$w_{(3D)}/adm\leq1$
adm		-	-	175 MPa		-	-	150 mm		-	-
1	Light	sw.	0	36.092	32.461	1.112	0.206	48.55	45.88	1.058	0.324
		sagg.	0.378	16.103	13.010	1.238	0.092	19.33	18.94	1.021	0.129
			0.582	6.016	3.031	1.985	0.034	3.866	3.52	1.098	0.026
			1.829	68.255	58.407	1.169	0.390	89.02	80.71	1.103	0.593
		hogg.	0.378	56.068	51.912	1.080	0.320	77.76	72.81	1.068	0.485
			0.582	66.846	62.410	1.071	0.382	93.54	87.34	1.071	0.535
			1.829	129.38	123.329	1.049	0.739	**184.6**	**171.3**	**1.078**	**1.231**

a. b.

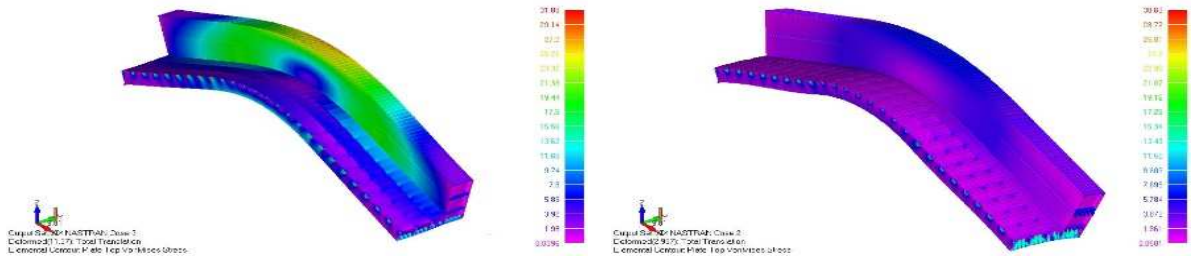

Figure 5.15.1.a.,b. *3D-FEM model , von Mises equivalent stress, docking case at maximum capacity of 828 t* with hogging mass distribution*, a. hogging type wave $\mu=0(180^0)$ h_w= 0.550m, Dock60_CWT, b. sagging type wave $\mu=0(180^0)$ h_w=0.550m, Dock60_CWT*

a. b.

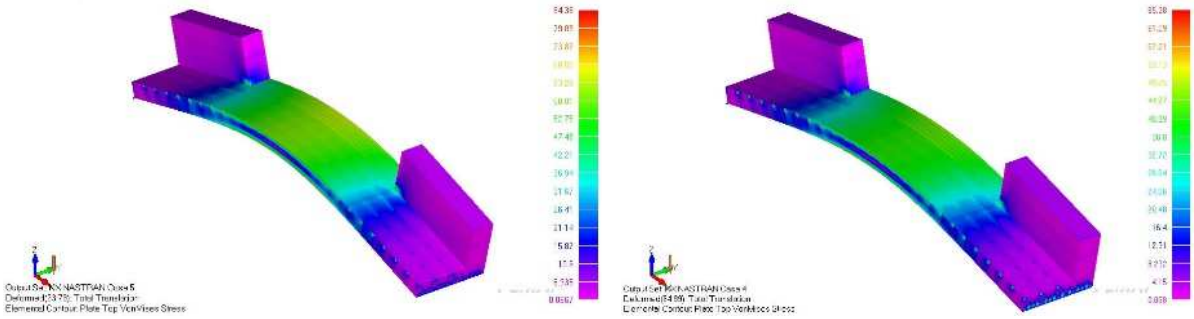

Figure 5.15.2.a.,b. *3D-FEM model , von Mises equivalent stress, docking case at maximum capacity of 828 t* with hogging mass distribution*, a hogging type wave μ=0(180⁰) h_w= 0.186m, Dock60_NWT, b. sagging type wave μ=0(180⁰) h_w= 0.186m, Dock60_NWT*

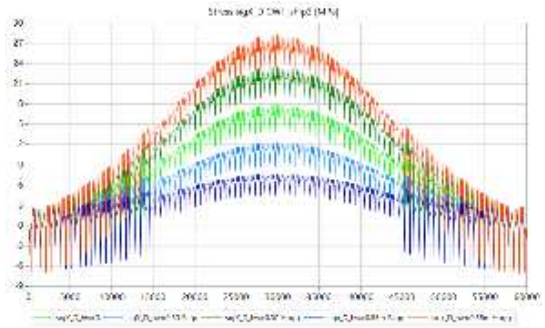

Figure 5.15.1.c. *Normal stress distribution diagram σ_x docking case at maximum capacity of 828 t* with hogging mass distribution*, 3D-FEM model of Dock60_CWT, all cases of wave heights μ=0(180⁰)*

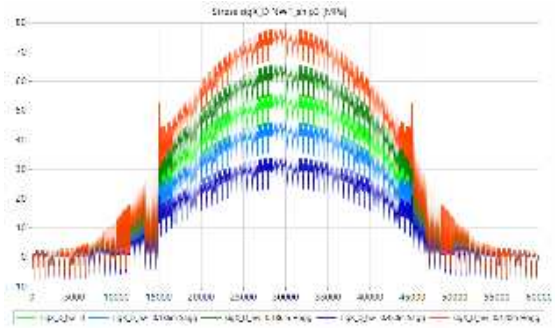

Figure 5.15.2.c. *Normal stress distribution diagram σ_x docking case at maximum capacity of 828 t* with hogging mass distribution*, 3D-FEM model of Dock60_NWT, all cases of wave heights μ=0(180⁰)*

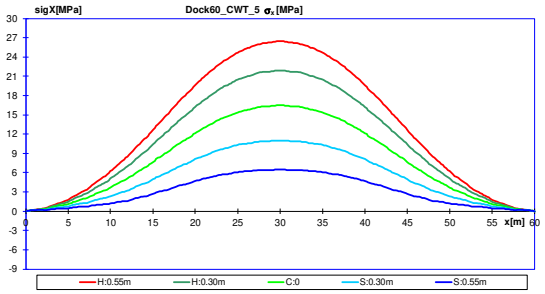

Figure 5.15.1.d. *Normal stress distribution diagram σ_x docking case at maximum capacity of 828 t* with hogging mass distribution*, 1D beam model of Dock60_CWT, all cases of wave heights μ=0(180⁰)*

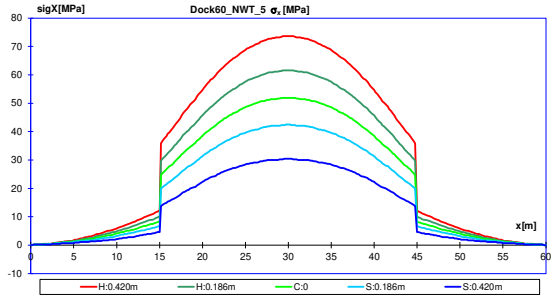

Figure 5.15.2.d. *Normal stress distribution diagram σ_x docking case at maximum capacity of 828 t* with hogging mass distribution*, 1D beam model of Dock60_NWT, all cases of wave heights μ=0(180⁰)*

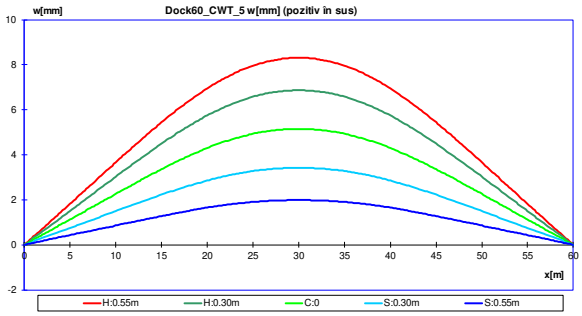

Figure 5.15.1.e. *Vertical deformation diagram for docking case at maximum capacity of 828 t* with hogging mass distribution*, 1D beam model of Dock60_CWT, all cases of wave heights μ=0(180⁰)*

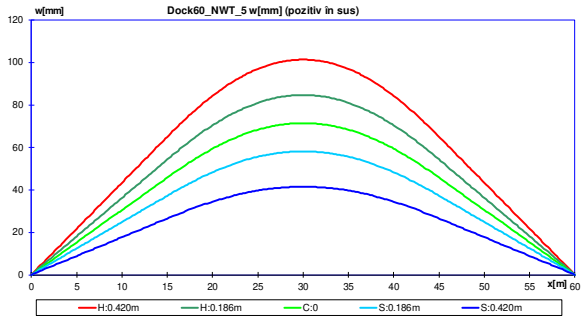

Figure 5.15.2.e. *Vertical deformation diagram for docking case at maximum capacity of 828 t* with hogging mass distribution*, 1D beam model of Dock60_NWT, all cases of wave heights μ=0(180⁰)*

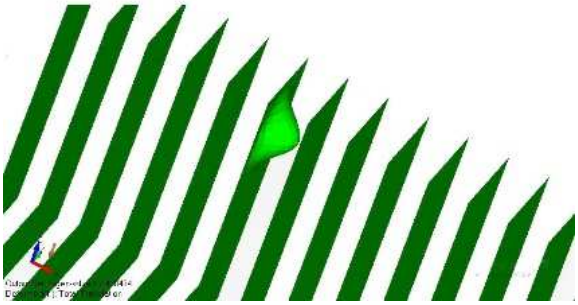

Figure 5.16.a. *Verification of the structural stability criterion (B=2,411), docking case at maximum capacity of 828 t* with hogging mass distribution*, hogging type wave μ=0(180⁰) h_w= 0.550m, Dock60_CWT*

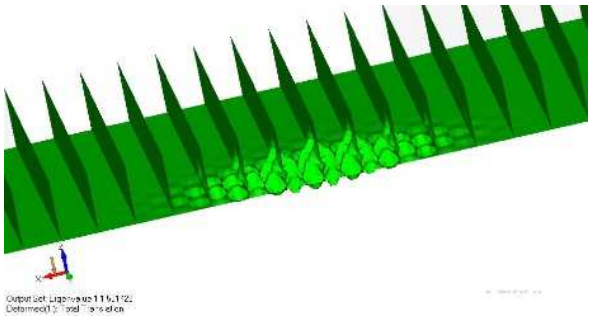

Figure 5.16.b. *Verification of the structural stability criterion (B=1,501), docking case at maximum capacity of 828 t* with hogging mass distribution*, hogging type wave μ=0(180⁰) h_w= 0.186m, Dock60_NWT*

Table 5.12. Operating limit conditions resulting from structural analysis on 3D-FEM models, with requests from quasi-static equivalent head – follow waves μ=0(180⁰), for the two constructive versions of the small floating docks Dock60_NWT / CWT

Type		Light	Full ballast	*Docking case at maximum capacity of 828 t* with uniform mass distribution	*Docking case at maximum capacity of 828 t* with sagging mass distribution	*Docking case at maximum capacity of 828 t* with hogging mass distribution
CWT	$h_{w\,\lim}\ [m]$	1.930	0.600	0.550	0.550	0.550
	Criterion	Minimum free board criterion and buckling criterion	Minimum free board criterion	Minimum free board criterion	Minimum free board criterion	Minimum free board criterion
	Inland operation	≈IN(2.0)	IN(0.6)	≈IN(0.6)	≈IN(0.6)	≈IN(0.6)
	Costal operation	Special approval	Protected port			
NWT	$h_{w\,\lim}\ [m]$	0.582	0.326	0.420	0.420	0.186
	Criterion	Buckling criterion	Minimum free board criterion	Minimum free board criterion and buckling criterion	Minimum free board criterion	Buckling criterion
	Inland operation	≈IN(0.6)	SW	SW	SW	SW
	Costal operation	Special approval	Protected port			

5.3.2. Case of oblique waves

For numerical study in the case of quasi-static oblique equivalent waves, the two 3D-FEM models (figures 4.13. – 4.16., 4.24. – 4.25.), for the two versions of small floating docks Dock60_CWT/NWT, they are taken over the entire length of the floating docks, as well as their full width. For the structural analysis we used the cases presented in subchapter 5.2., the case of the docks without docked mass and without ballast, and three cases of docking at the maximum capacity of the dock of 828 t, in three cases of mass distribution, namely, uniform distribution, sagging type and hogging type. In all operating cases, the Dock60_CWT/NWT floating docks have the same transverse and longitudinal hull centre.

Table 5.13. Minimum free board, maximum von Mises equivalent tensions, maximum vertical deformations and the value of the structural stability factor for the 3D-FEM model of the Dock60_CWT floating dock

Case	h_w[m]	T_m[m]	θ[rad]	φ[rad]	F_{min}[m]	σ_{vonM} /B	hogg/sagg	0	15	30	45	60	75	90	sw
Light	1.930 (0)	0.960	0	0	**0.075** (1.040)	$\sigma_{vonM\ max}$ [N/mm^2]	hogg.	56.95	56.98	56.93	56.20	54.46	42.92	35.30	23.99
							sagg.	46.17	47.53	50.49	53.50	51.38	44.04	47.42	
						B_{min} [-]	hogg.	1.518	1.530	1.571	1.714	2.169	2.874	4.234	5.550
							sagg.	2.828	2.636	2.365	2.149	1.982	2.947	3.667	
Docking case at maximum capacity of 828 t with uniform mass distribution	0.550 (0)	1.650	0	0	**0.075** (0.350)	$\sigma_{vonM\ max}$ [N/mm^2]	hogg.	47.76	47.79	47.79	47.74	47.54	46.80	46.26	46.68
							sagg.	46.93	46.93	46.95	47.00	47.10	47.20	47.25	
						B_{min} [-]	hogg.	2.849	2.864	2.914	3.045	3.443	3.785	4.162	4.511
							sagg.	3.844	3.742	3.653	3.592	3.672	4.153	4.703	
Docking case at maximum capacity of 828 t with sagging mass distribution	0.550 (0)	1.650	0	0	**0.075** (0.350)	$\sigma_{vonM\ max}$ [N/mm^2]	hogg.	53.92	53.97	54.02	54.09	54.17	53.96	53.91	53.73
							sagg.	54.40	54.40	54.39	54.37	54.28	53.99	54.01	
						B_{min} [-]	hogg.	3.995	4.024	4.120	4.121	3.768	3.734	4.031	4.377
							sagg.	3.738	3.650	3.575	3.527	3.599	4.495	4.739	
Docking case at maximum capacity of 828 t with hogging mass distribution	0.550 (0)	1.650	0	0	**0.075** (0.350)	$\sigma_{vonM\ max}$ [N/mm^2]	hogg.	56.63	56.64	56.61	56.52	56.29	55.66	55.06	55.37
							sagg.	54.21	54.25	54.32	54.45	54.75	55.59	55.82	
						B_{min} [-]	hogg.	2.410	2.421	2.459	2.552	2.835	3.867	3.586	3.606
							sagg.	3.909	3.812	3.726	3.667	3.755	3.303	3.627	

Table 5.14. Minimum free board, maximum von Mises equivalent tensions, maximum vertical deformations and the value of the structural stability factor for the 3D-FEM model of the Dock60_NWT floating dock

Case	h_w[m]	T_m[m]	θ[rad]	φ[rad]	F_{min}[m]	σ_{vonM} /B	hogg/sagg	0	15	30	45	60	75	90	sw
Light	0.582 ÷ 1.800	0.800	0	0	**0.300** ÷ 0.909	$h_{w\ limit}$[m]		0.582	0.587	0.615	0.696	1.041	1.800	1.800	0
						F_{min}[m]		0.909	0.907	0.893	0.852	0.680	**0.300**	**0.300**	1.200
						$\sigma_{vonM\ max}$ [N/mm^2]	hogg.	73.58	73.46	73.42	73.44	77.33	55.33	53.73	41.10
							sagg.	23.68	23.89	24.46	31.71	54.17	89.65	54.84	
						B_{min} [-]	hogg.	**1.503**	**1.506**	**1.505**	**1.503**	**1.502**	2.317	2.746	2.833
							sagg.	5.391	5.327	5.104	4.514	3.412	**1.502**	2.346	
Docking case at maximum capacity of 828 t with uniform mass distribution	0.420 (0)	1.490	0	0	**0.300** (0.510)	$\sigma_{vonM\ max}$ [N/mm^2]	hogg.	80.59	80.29	79.14	76.38	69.36	54.44	60.53	57.52
							sagg.	35.36	36.75	38.96	42.67	50.16	63.79	57.56	
						B_{min} [-]	hogg.	**1.503**	**1.510**	1.534	1.596	1.782	2.408	2.263	2.278
							sagg.	3.398	3.254	3.068	2.816	2.466	2.070	2.292	
Docking case at maximum capacity of 828 t with sagging mass distribution	0.420 (0)	1.490	0	0	**0.300** (0.510)	$\sigma_{vonM\ max}$ [N/mm^2]	hogg.	60.81	60.52	59.47	56.90	50.82	35.76	41.90	38.59
							sagg.	31.69	31.75	31.92	32.29	34.73	44.94	38.65	
						B_{min} [-]	hogg.	2.264	2.279	2.333	2.460	2.594	3.910	3.666	3.799
							sagg.	4.452	4.387	4.346	4.354	4.071	3.372	3.933	
Docking case at maximum capacity of 828 t with hogging mass distribution	0.186 ÷ 0.420	1.490	0	0	**0.300** ÷ 0.417	$h_{w\ limit}$[m]		0.186	0.186	0.192	0.220	0.350	0.420	0.420	0
						F_{min}[m]		0.417	0.417	0.414	0.400	0.335	**0.300**	**0.300**	0.510
						$\sigma_{vonM\ max}$ [N/mm^2]	hogg.	79.46	79.31	79.08	78.94	78.51	66.09	72.05	69,17
							sagg.	58.94	59.13	59.46	59.87	61.66	75.39	69.25	
						B_{min} [-]	hogg.	**1.501**	**1.504**	**1.508**	**1.507**	**1.501**	1.915	1.759	1,767
							sagg.	2.147	2.141	2.132	2.133	2.131	1.640	1.776	

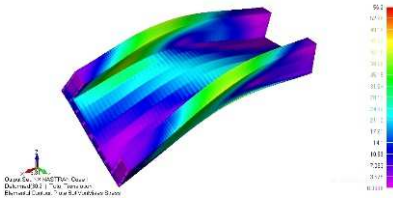

Figure 5.17.a. *3D-FEM model , von Mises equivalent strength, light case, hogging wave h_w=1.930m, Dock60_CWT, $\mu = 45°$*

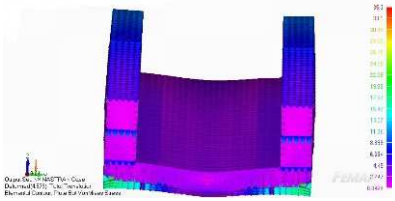

Figure 5.17.b. *3D-FEM model , von Mises equivalent strength, light case, hogging wave h_w= 1.930m, Dock60_CWT, $\mu = 90°$*

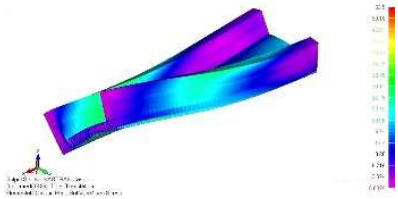

Figure 5.17.c. *3D-FEM model , von Mises equivalent strength, light case, sagging wave h_w= 1.930m, Dock60_CWT, $\mu = 45°$*

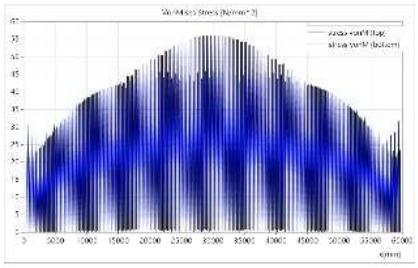

a.

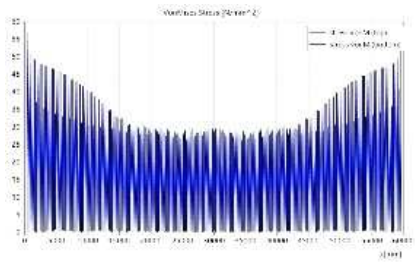

b.

Figure 5.18.a., b. *Equivalent Von Mises stress diagram, light case, Dock60_CWT, $\mu = 45°$, wave height h_w= 1.930m a. hogging type wave, b. sagging wave type*

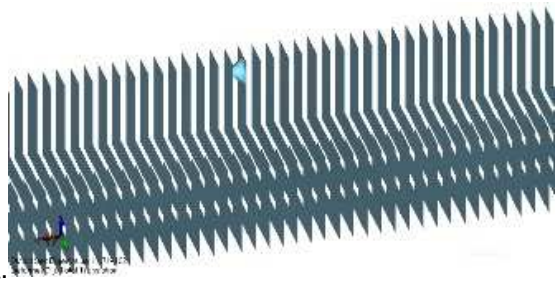

a.

b.

Figure 5.19.a., b. *Buckling criteria verification, light case, Dock60_CWT, $\mu = 45°$, wave height de h_w= 1.930m a. hogging type wave, b. sagging wave type*

a.

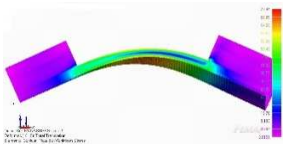

b.

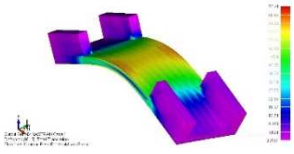

c.

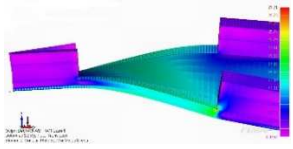

d.

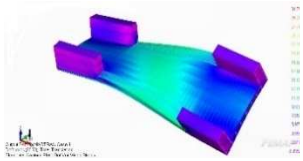

Figure 5.20.a., b., c., d. *3D-FEM model , von Mises equivalent strength, docking case at maximum capacity of 828 t with sagging mass distribution,, wave height h_w= 0,696m, Dock60_NWT, $\mu = 45°$, a., b., hogging type wave, c., d. sagging type wave*

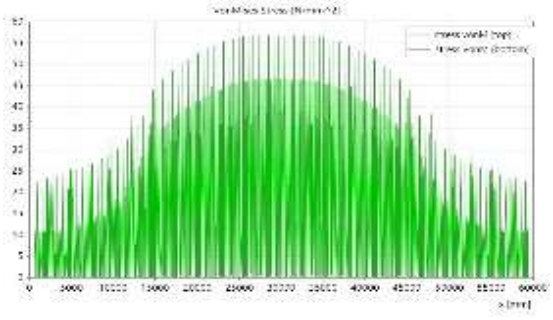

e.

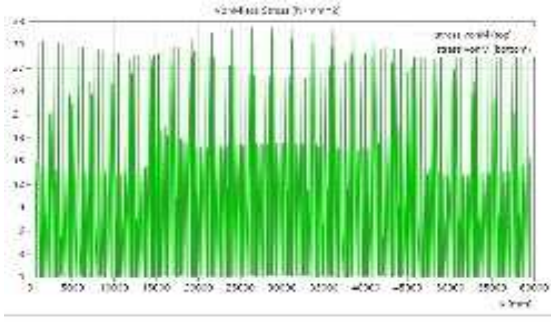

f.

Figure 5.21.e., f. *Equivalent Von Mises stress diagram, docking case at maximum capacity of 828 t with sagging mass distribution, Dock60_NWT, $\mu = 45°$, wave height h_w= 0,420 m e. hogging type wave, f. sagging type wave*

e. f.

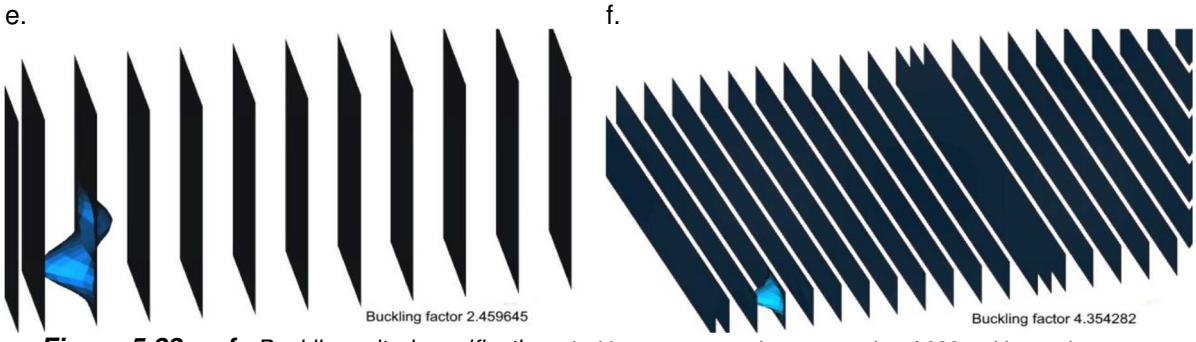

Figure 5.22.e., f., *Buckling criteria verification, docking case at maximum capacity of 828 t with sagging mass distribution, Dock60_NWT, $\mu = 45°$, wave height h_w= 0,420 m e. hogging type wave, f. sagging type wave*

The results for the 112 cases studied are summarized below, for the global and local analysis of the structure of the two constructive versions of the small floating docks Dock60_CWT/NWT, from requests in quasi-static equivalent oblique waves, using 3D-FEM structural models.

Tables 5.13. – 5.14. shows the values of the equivalent von Mises maximum stress, of the structural stability factor and of the freeboard for the analysed cases of the two constructive versions for the small floating docks Dock60. Most restrictions appear in the case of the dock with discontinuous upper tanks (table 5.15) Dock60_NWT, from the criterion of the minimum freeboard in the case without docked mass and in the case of docking at a maximum capacity of 828 t, with the hogging distribution of the mass, and from the criterion of structural stability for the case without docked mass.

Figures 5.17. and 5.20. presents a selection of von Mises equivalent tensions in oblique waves obtained on 3D-FEM models for the two Dock60 build versions. Figures 5.18. and 5.21. presents the von Mises equivalent stress diagrams for the cases with the highest restrictions, according to tables 5.13. and 5.14. Structural stability criterion (table 5.13., table 5.14.), imposes significant restrictions only on the small floating dock with discontinuous side tanks Dock60_NWT. The loss of structural stability occurs in the vast majority of cases in the cross-sectional elements.

Figures 5.23. – 5.36 presents the maximum values of the von Mises equivalent stresses and of the factor of loss of structural stability versus the allowable values, for the two constructive versions of the small floating docks Dock60_CWT, Dock60_NWT.

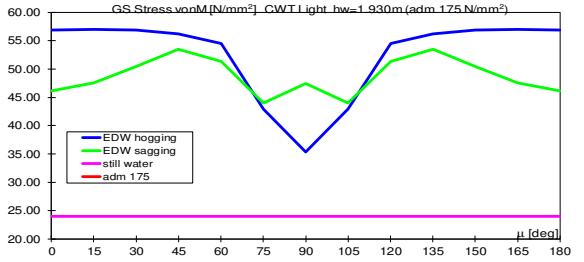

Figure 5.23.1.a. *3D-FEM model, maximum von Mises stress values, light case, Dock60_CWT, oblique waves μ=0-180⁰*

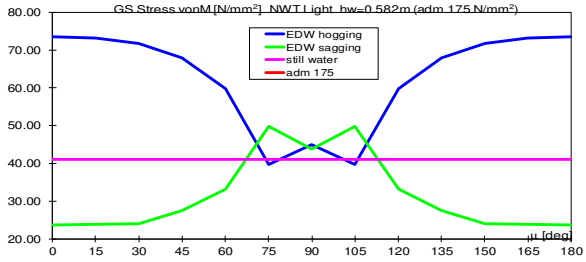

Figure 5.23.2.a. *3D-FEM model, maximum von Mises stress values, light case, Dock60_NWT, oblique waves μ=0-180⁰*

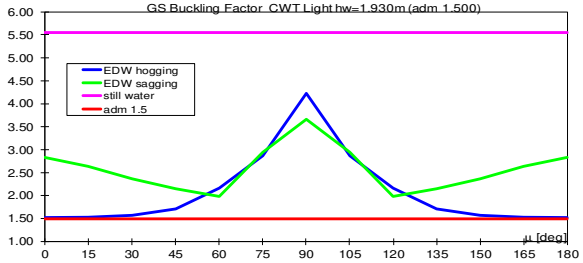

Figure 5.23.1.b. *3D-FEM model, buckling maximum values, light case, Dock60_CWT, oblique waves μ=0-180⁰*

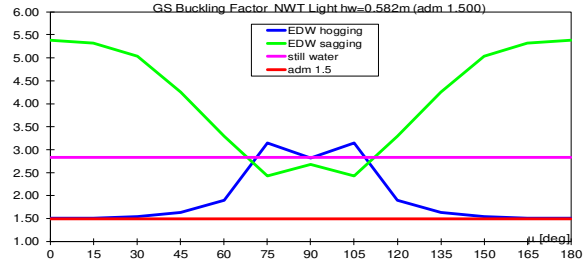

Figure 5.23.2.b. *3D-FEM model, buckling maximum values, light case, Dock60_NWT, oblique waves μ=0-180⁰*

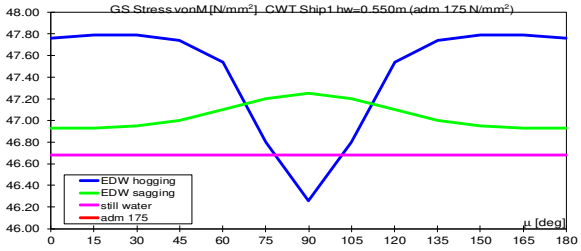

Figure 5.24.1.a *3D-FEM model, maximum von Mises stress values for docking case at maximum capacity of 828 t with uniform mass distribution, Dock60_CWT, oblique waves μ=0-180⁰*

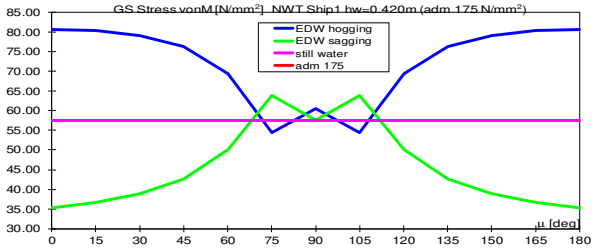

Figure 5.24.2.a. *3D-FEM model, maximum von Mises stress values for docking case at maximum capacity of 828 t with uniform mass distribution, Dock60_NWT, oblique waves μ=0-180⁰*

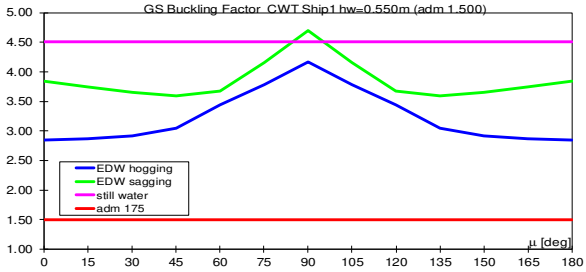

Figure 5.24.1.b. *3D-FEM model, buckling maximum values for docking case at maximum capacity of 828 t with uniform mass distribution, Dock60_CWT, oblique waves μ=0-180⁰*

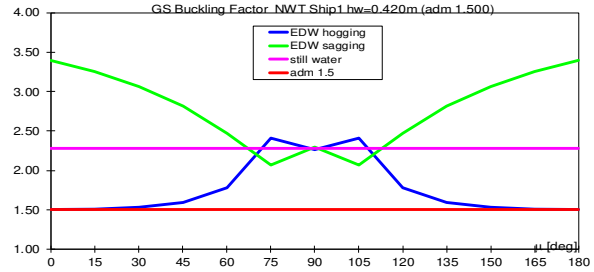

Figure 5.24.2.b. *3D-FEM model, buckling maximum values for docking case at maximum capacity of 828 t with uniform mass distribution, Dock60_CWT, oblique waves μ=0-180⁰*

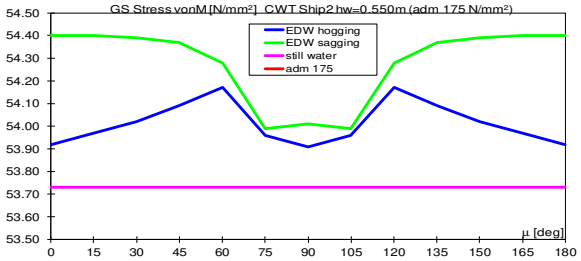

Figure 5.25.1.a. *3D-FEM model, maximum von Mises stress values for docking case at maximum capacity of 828 t with sagging mass distribution, Dock60_CWT, oblique waves μ=0-180⁰*

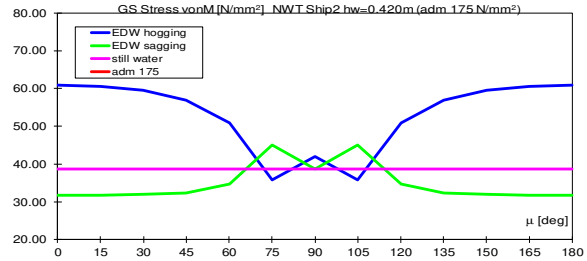

Figure 5.25.2.a. *3D-FEM model, maximum von Mises stress values for docking case at maximum capacity of 828 t with sagging mass distribution, Dock60_NWT, oblique waves μ=0-180⁰*

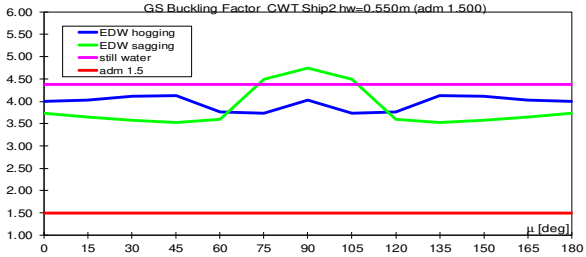

Figure 5.25.1.b. *3D-FEM model, buckling maximum values for docking case at maximum capacity of 828 t with sagging mass distribution, Dock60_CWT, oblique waves μ=0-180⁰*

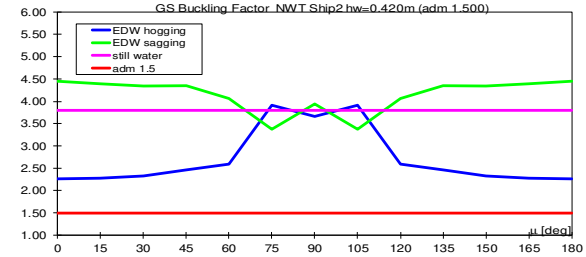

Figure 5.25.2.b. *3D-FEM model, buckling maximum values for docking case at maximum capacity of 828 t with sagging mass distribution, Dock60_NWT, oblique waves μ=0-180⁰*

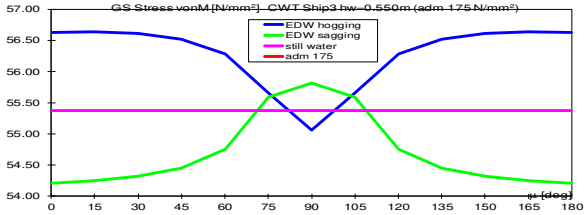

Figure 5.26.1.a. *3D-FEM model, maximum von Mises stress values for docking case at maximum capacity of 828 t with hogging mass distribution, Dock60_CWT, oblique waves μ=0-180⁰*

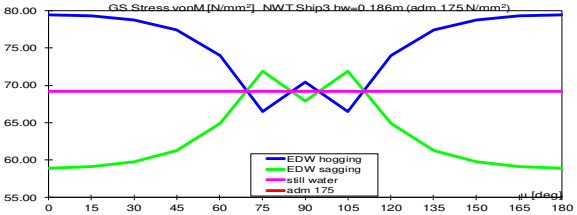

Figure 5.26.2.a. *3D-FEM model, maximum von Mises stress values for docking case at maximum capacity of 828 t with hogging mass distribution, Dock60_NWT, oblique waves μ=0-180⁰*

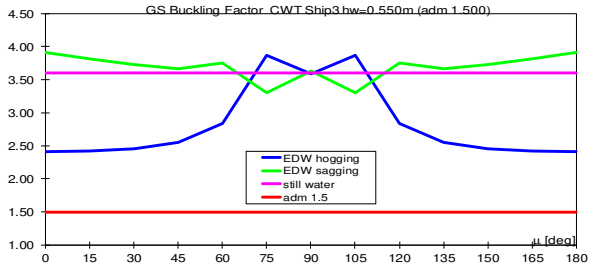

Figure 5.26.1.b. *3D-FEM model, buckling maximum values for docking case at maximum capacity of 828 t with hogging mass distribution, Dock60_CWT, oblique waves μ=0-180⁰*

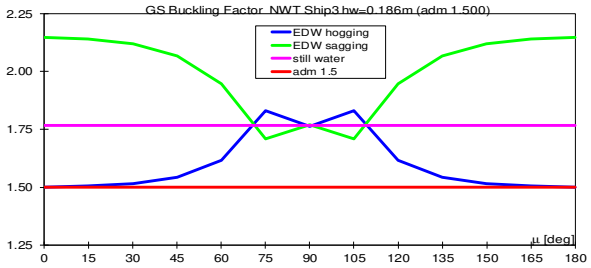

Figure 5.26.2.b. *3D-FEM model, buckling maximum values for docking case at maximum capacity of 828 t with hogging mass distribution, Dock60_NWT, oblique waves μ=0-180⁰*

Combining the criteria of resistance and minimum freeboard (table 5.13., table 5.14.), for the two constructive versions of small floating docks, with continuous upper side tanks Dock60_CWT and with discontinuous upper side tanks Dock60_NWT, the polar diagrams are obtained based on the significant wave height $h_{w_{\lim it}}$, shown in figures 5.27.a., b.

For the case of the floating dock Dock60_CWT, for all three docking cases, the only restrictions that appear are from the minimum free board criterion (table 5.13). The meeting angle dock - wave does not influence the height limit of the wave $h_{w_{\lim it}} = 1{,}93m$ in the case of the vessel without docked and unbalanced mass and $h_{w_{\lim it}} = 0{,}55m$ for cases with a maximum mass of 828 tonnes docked.

In the case of the floating dock Dock60_NWT (table 5.14.), the allowable stress criterion does not impose restrictions on any docking case. The criteria of loss of structural stability and minimum free board impose restrictions, resulting in the wave height limit $h_{w_{\lim it}} = 0{,}582 \div 1{,}800m$ for the case without docked mass and $h_{w_{\lim it}} = 0{,}186 \div 0{,}420m$ in the case of the mass of 828 t having a hogging distribution. For docking cases with a maximum capacity of 828 t with uniform mass distribution and sagging type, the restrictions are from the minimum free board criterion, resulting in the wave height limit $h_{w_{\lim it}} = 0{,}420m$

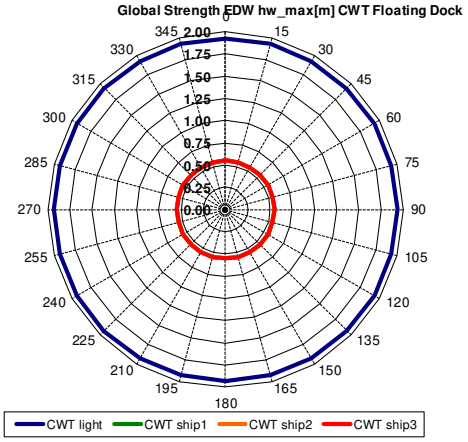

Figure 5.27.a. *3D-FEM model, polar diagram for Dock60_CWT, in oblique EDW, limit wave height, all cases of docking*

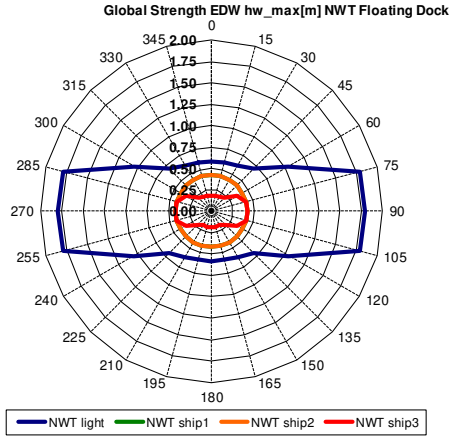

Figure 5.27.b. *3D-FEM model, polar diagram for Dock60_NWT, in oblique EDW, limit wave height, all cases of docking*

CHAPTER 6

COMPARATIVE ANALYSIS OF THE OPERATING CAPACITY OF THE FLOATING DOCKS DOCK60_CWT, DOCK60_NWT, WITH TWO CONSTRUCTIVE VERSIONS, BASED ON THE LIMITING CRITERIA FOR OSCILLATIONS IN EXTREME RANDOM WAVES AND TRANSVERSAL STABILITY

This chapter studies, in the first part, the transit condition, for the river and maritime navigation of the two small floating docks, with continuous upper side tanks – Dock60_CWT and with discontinuous upper side tanks – Dock60_NWT, by the criteria of dynamics of the ship in the real sea - seakeeping. Random waves from the navigation scenario, are modelled in the short term, using the power spectral density function with a parameter, type ITTC [58], [59], with the maximum significant wave height of 2 m and 2.568 m, for the conditions of river and coastal navigation, according to the norms of the naval classification societies [1]. The speed of transit of the floating docks, when relocating between two ports, is of maximum 18 km/h, the numerical analysis being performed for five different cases of speeds, namely: 0; 5; 10; 15 and 18 km/h. This is done using the DYN software [45], based on the hydrodynamic model presented in subchapter 2.4. The seakeeping criteria are interpreted in static terms of allowable values of the amplitude of the movement and the acceleration. **The numerical results of this study are published and presented in the article, in the reference [63].**

The second part of the chapter, studies the assessment of the safe operating capacity of Dock60_CWT/NWT floating docks, based on the criterion of intact transverse stability, according to the rules [1], [3], using the D_LDF software (Annex 4), based on the theoretical model presented in subchapter 2.1.5., for the same scenarios from the structural analysis of the preliminary concept of the two docks, chapter 4.1. **The numerical results of this subchapter are published and presented in the article in the reference [35]**.

6.1. Short term oscillation analysis of floating docks Dock60_CWT, Dock60_NWT, in the river and costal navigation area

In this subchapter we analyse the safety of relocation operations of small floating docks, with two constructive variants (figures 4.1.b., 4.2.b., 4.13., 4.16., 4.24., 4.25.), without docked mass, for inland waterways of the Danube (figure 2.7.), with wave heights of 0.6 m; 1.2 m and 2 m, as well as for the coastal areas of the Black Sea, with a maximum height of 2.568 m (figure 2.8.), height correlated with the length of the floating docks according to the norms of the naval classification societies [1], [3]. The results present the evaluation of the dynamic behaviour in random waves, based on the seakeeping criteria (navigation) [30], [57] and of the theoretical model presented in subchapter 2.4.

Towing for the small floating docks, Dock60_CWT and Dock60_NWT, it is considered to be made with the help of a 4,000 H.P. river – maritime tugboat [43], [77], [62] (chapter 9). The drag resistance of the tugboat - dock system is analysed with a theoretical model [55], with the tow cable long enough that it allows the hypothesis of the decoupled analysis of the dynamics of the floating dock when relocating.

Figure 6.1. presents the diagram of the drag resistance of the tugboat and the two constructive versions of Dock60_CWT/NWT floating docks during navigation operations in still water. From the analysis of the drag resistance of the tugboat-dock system, a maximum towing speed of 18 km/h results the analysis included the cases of 0; 5; 10 and 15 km/h. During relocation operations, small floating docks are considered to have no docked mass, with characteristic values according to table 4.6. and 4.7., for each constructive type. Due to

the significant difference in the position of the centre of gravity of the two constructive versions, there are considerable differences in cross-sectional stability characteristics, presented in table 4.6. and table 4.7., as well as in figure 6.2. The numerical analysis of the two variants of small floating docks during the relocation on the river or coastal route is performed using the DYN software [45].

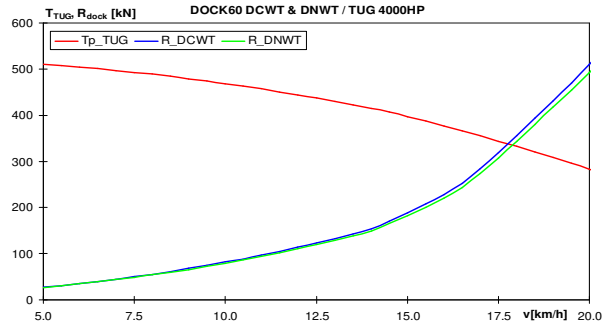

Figure 6.1. *GZ [m] stability diagram for Dock60_CWT/NWT*

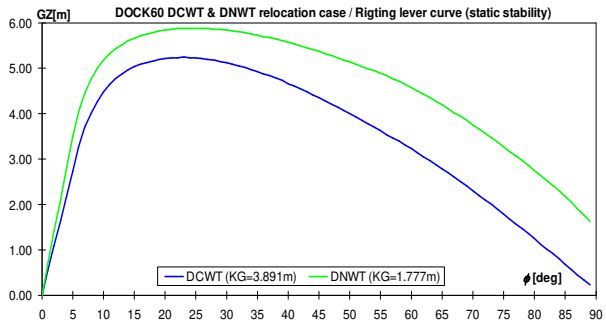

Figure 6.2. *DOCO – TUG resistance prediction*

Navigation safety for river and coastal transit operations, in the case of navigation without docked mass, for the two constructive variants Dock60_CWT/NWT, according to table 4.6. and 4.7., it is evaluated from the point of view of the significant height of the wave $H_{s\lim it}[m]$ and the boundary intensity of the sea state in Beaufort degrees $B_{\lim it}$. The limit criteria are formulated in terms of the most probable values admissible response values RMS for the amplitudes of the oscillations and accelerations at the heave, pitch and roll oscillations of the floating docks (table 6.1.).

Table 6.1. Seakeeping criteria for Dock60 floating docks, formulated for components at heave, pitch and roll oscillations

	$RMS_{z\,max}$ [m]	$RMS_{\theta\,max}$ [rad]	$RMS_{\varphi\,max}$ [rad]	RMS_{axzmax} [m/s^2]	$RMS_{ac\theta\,max}$ [rad/s^2]	$RMS_{ac\varphi\,max}$ [rad/s^2]
Dock60_CWT	0.965	0.01745	0.06981	0.49050	0.03270	0.14715
Dock60_NWT	0.900					

6.1.1. Determination of the response amplitude operators RAO to oscillations for small floating docks, in two constructive variants

Using the DYN software [45], based on the theoretical model, equations 2.18. and the histogram of the significant wave height, figures 2.7. - 2.8., RAO response amplitude operators are obtained for the two constructive versions of the Dock60_CWT/NWT floating docks (figure 4.19. - 4.12, table 4.1.).

Both build versions of Dock60_CWT/NWT floating docks, is in transit on a river - sea route, for five test speeds, v = 0; 5; 10; 15 and 18 km/h. The case with zero speed represents the tugboat damage situation during the relocation of the floating docks. Floating docks are considered to be without docked mass. The meeting angle dock - wave is considered in the range $\mu = 0 - 360°$, with the step $\delta\mu = 5°$, taking into account the double symmetry of the two constructive versions. The RAO response amplitude operator functions for heave, pitch and roll oscillations are calculated for the pulse wave range ω=0 - 3 rad / s and step δω= 0.001 rad / s.

Figures 6.3. – 6.4. a., b. presents the RAO functions at vertical oscillations for the two constructive variants of floating docks, at test speeds of 0 km / h and 18 km / h, for the dock - wave angle in the range 0 - 180º. From the analysis of the RAO functions at vertical oscillations (10 cases), it is found that the maximum value appears in the case of the transverse wave for both constructive variants and for the entire speed range. Due to the prismatic shapes, it is observed that for the speeds tested, there are no significant differences in the case of RAO functions in the vertical oscillations.

Figures 6.5. – 6.6. a., b. presents like the vertical oscillations, the RAO response amplitude operator functions to roll oscillations. From figures 6.5. - 6.6. b., it turns out that the maximum values for the roll, for the constructive variant of the floating dock with discontinuous side tanks is in the case of the transverse wave. In the case of small floating dock with continuous side tanks, RAO functions at roll oscillations, they have maximum values for the traverse wave at a speed of 0 km/h. For speeds of 5, 15 and 18 km/h there are recorded maximum values for bow – stern oblique waves and cross waves. In the case of the speed of 10 km/h, maximum and approximately equal values are observed for the case of oblique and transverse waves, and very low in the case of oblique waves of 70º.

Figures 6.7. -6.8. a., b. presents the RAO response amplitude operator functions for pitch oscillations. From figures 6.7. - 6.8.a., b. for both constructive variants and for the entire range of speeds tested, significant values are observed in the case of following and meeting waves.

The differences between the RAO response amplitude operator functions for the roll oscillations and the similar functions for the pitch oscillations are also justified by the own pulsations of the fluctuations of the floating docks, presented in table 6.2.

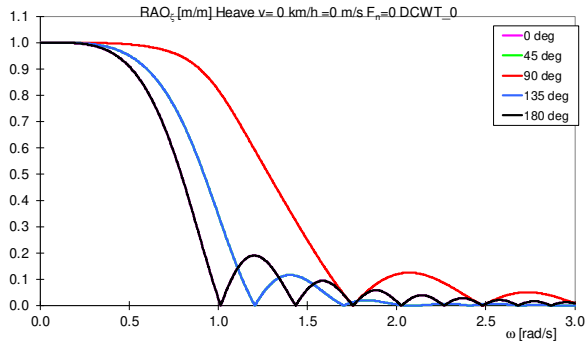

Figure 6.3.a. *RAO_ζ [m/m], heave, Dock60_CWT, v=0km/h, μ=0 - 180^0*

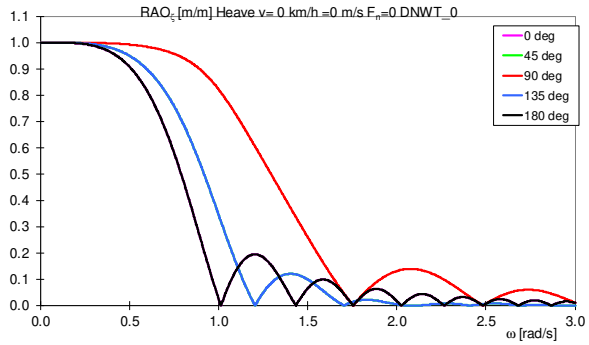

Figure 6.3.b. *RAO_ζ [m/m], heave, Dock60_NWT, v=0km/h, μ=0 - 180^0*

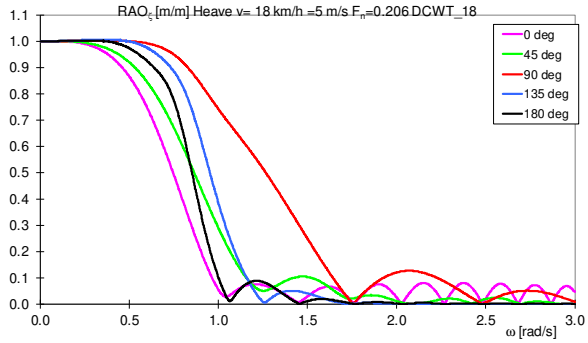

Figure 6.4.a. *RAO_ζ [m/m], heave, Dock60_CWT, v=18km/h, μ=0 - 180^0*

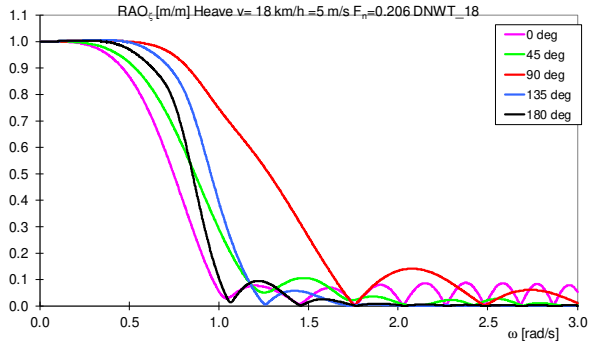

Figure 6.4.b. *RAO_ζ [m/m], heave, Dock60_NWT, v=18km/h, μ=0 - 180^0*

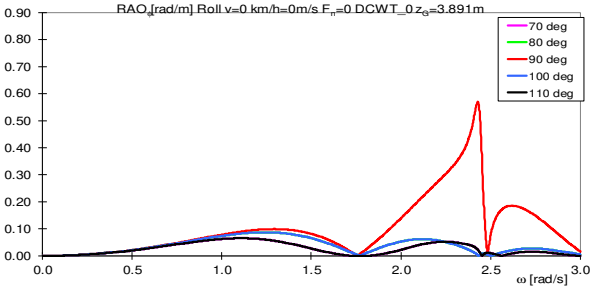

Figure 6.5.a *RAO$_\phi$ [rad/m], roll, Dock60_CWT, v=0km/h, μ=0 - 180^0*

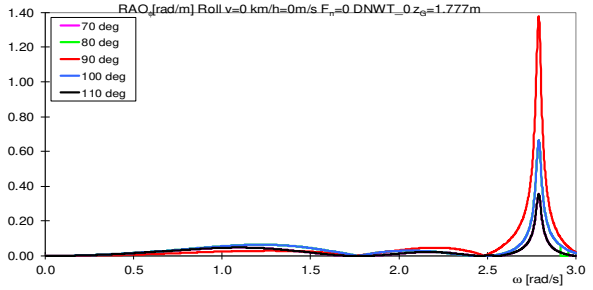

Figure 6.5.b *RAO$_\phi$ [rad/m], roll, Dock60_NWT, v=0km/h, μ=0 - 180^0*

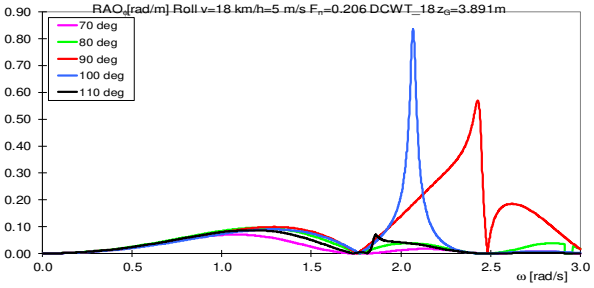

Figure 6.6.a *RAO$_\phi$ [rad/m], roll, Dock60_CWT, v=18km/h, μ=0 - 180^0*

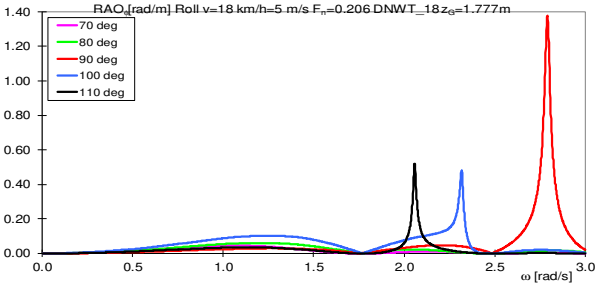

Figure 6.6.b *RAO$_\phi$ [rad/m], roll, Dock60_NWT, v=18km/h, μ=0 - 180^0*

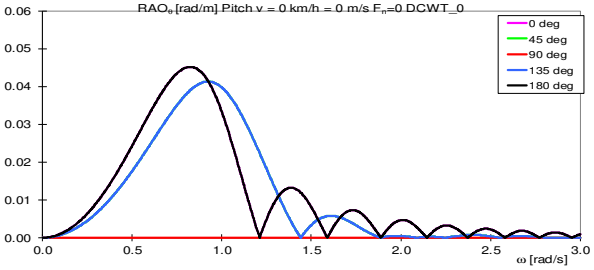

Figure 6.7.a. *RAO$_\theta$ [rad/m], pitch, Dock60_CWT, v=0km/h, μ=0 - 180^0*

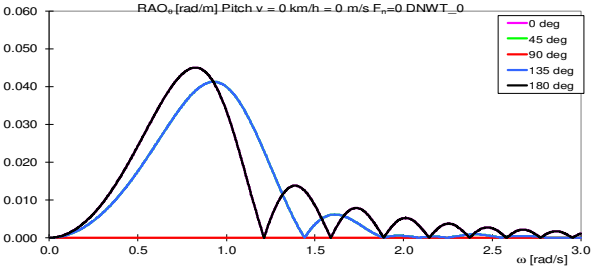

Figure 6.7.b. *RAO$_\theta$ [rad/m], pitch, Dock60_NWT, v=0km/h, μ=0 - 180^0*

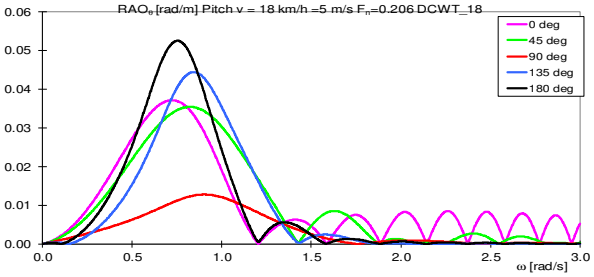

Figure 6.8.a. *RAO$_\theta$ [rad/m], pitch, Dock60_CWT, v=18km/h, μ=0 - 180^0*

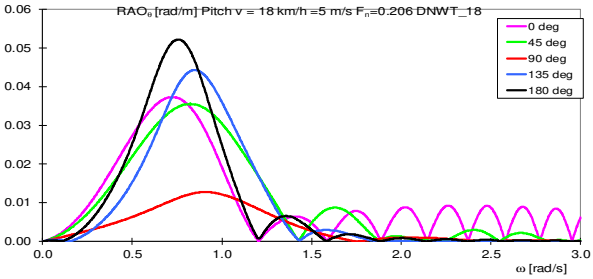

Figure 6.8.b. *RAO$_\theta$ [rad/m], pitch, Dock60_NWT, v=18km/h, μ=0 - 180^0*

Table 6.2. Own pulsations and periods of oscillation of small floating docks in the two constructive variants

FD type	Motion	Heave	Pitch	Roll
Dock60_CWT	$\omega_p[rad/s]$	0.860	0.825	2.428
	$T_p[s]$	7.306	7.616	2.588
Dock60_NWT	$\omega_p[rad/s]$	0.862	0.825	2.790
	$T_p[s]$	7.289	7.616	2.252

6.1.2. Analysis of the short-term statistical response for the two constructive versions of small floating docks.

Evaluation of the dynamics of the two constructive variants of small floating docks Dock60_CWT (figure.4.21.) and Dock60_NWT (figure 2.20.) in random waves, according to the river-maritime navigation scenario described in chapter 4, requires obtaining the most likely RMS statistical response values for heave, pitch and roll oscillations, as well as their accelerations, based on the RAO response amplitude functions of the previous subchapter and the power spectral density function of the ITTC wave (equations 2.19., figures 2.7. – 2.8.).

Considering the speed in the 0 -18 km/h range, and the extreme navigational condition with a maximum height of 2,568 m, are presented in tables 6.3. and 6.4. the allowable values of the seakeeping criteria (equations 2.23. - 2.25.) and the maximum statistical response most likely for the movements and accelerations at the oscillations of the two versions of small floating docks. The greatest influence of the speed is recorded for the movements of the combined vertical oscillations, for both constructive variants of docks.

Figures 6.9. – 14. a., b. presents the most probable statistical answer for the combined vertical movements, for the angles of oscillation at pitch and roll, as well as for their accelerations for the two constructive variants of the Dock60_CWT/NWT floating docks.

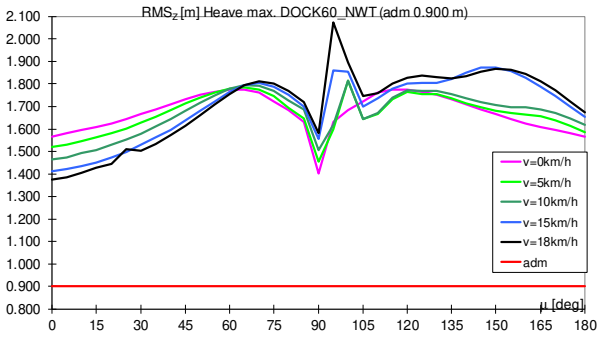

Figure 6.9.a. *Maximum most probable amplitudes RMSz[m] heave motions, for Dock60_NWT, v=0 – 18 km/h*

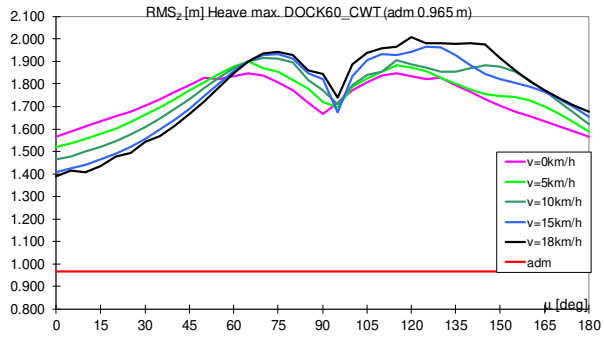

Figure 6.9.b. *Maximum most probable amplitudes RMSz[m] heave motions, for Dock60_CWT, v=0 – 18 km/h*

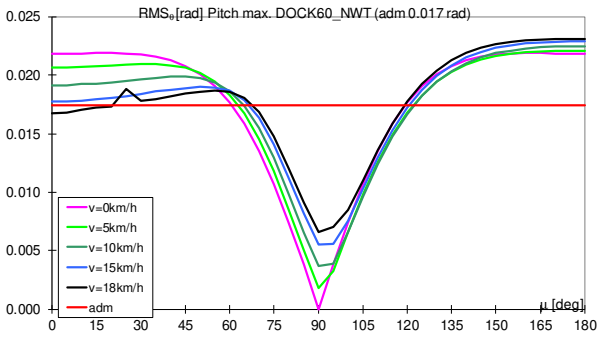

Figure 6.10.a. *Maximum most probable amplitudes for pitch motion RMSθ[rad], Dock60_NWT, v=0 – 18 km/h*

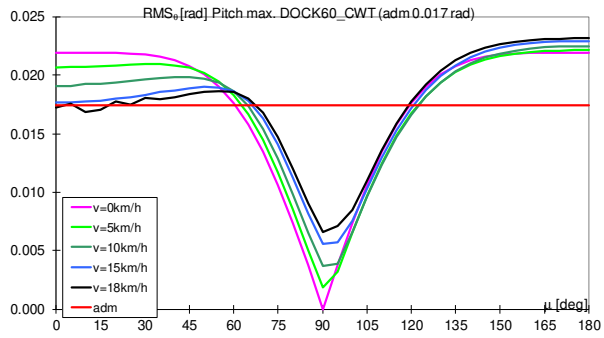

Figure 6.10.b. *Maximum most probable amplitudes for pitch motion RMSθ[rad], Dock60_CWT, v=0 – 18 km/h*

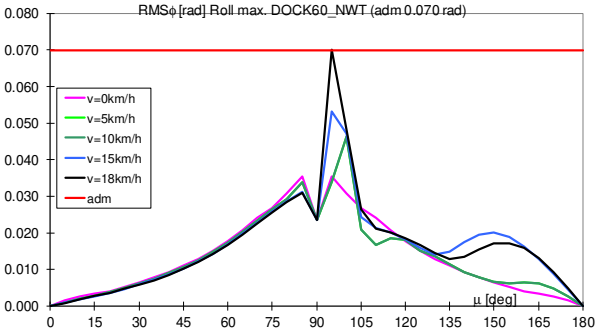

Figure 6.11.a. *Maximum most probable amplitudes for roll motion RMSφ [rad], Dock60_NWT, v=0 – 18 km/h*

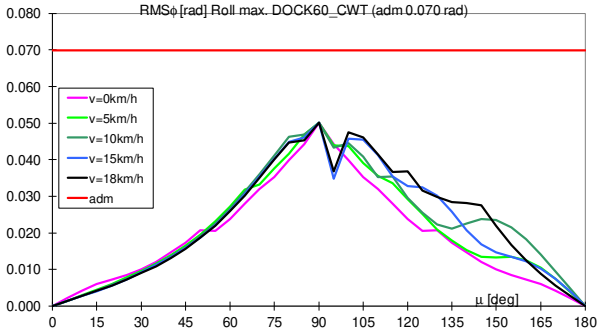

Figure 6.11.b. *Maximum most probable amplitudes for roll motion RMSφ [rad], Dock60_CWT, v=0 – 18 km/h*

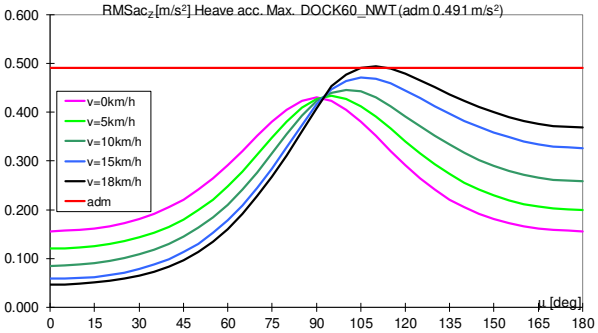

Figure 6.12.a. *Maximum most probable amplitudes for heave acceleration RMSacz[m] Dock60_NWT, v=0 – 18km/h*

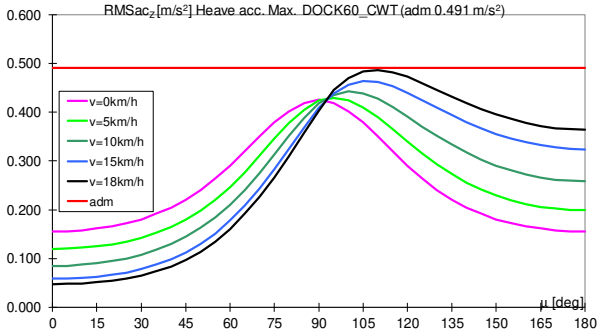

Figure 6.12.b. *Maximum most probable amplitudes for heave acceleration RMSacz[m] Dock60_CWT, v=0 – 18km/h*

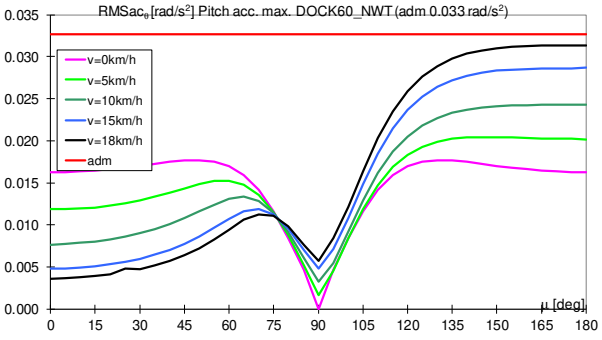

Figure 6.13.a. *Maximum most probable amplitudes for pitch acceleration RMSacθ[rad], Dock60_NWT, v=0 – 18 km/h*

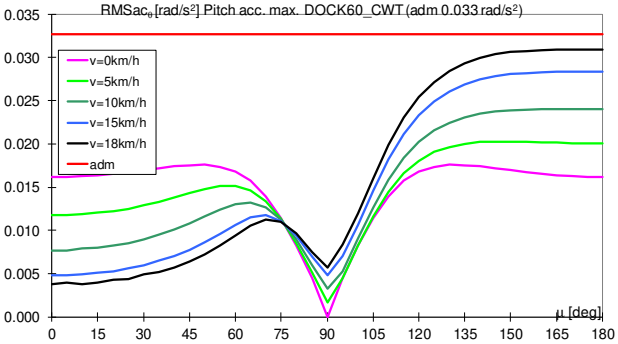

Figure 6.13.b. *Maximum most probable amplitudes for pitch acceleration RMSacθ[rad], Dock60_NWT, v=0 – 18 km/h*

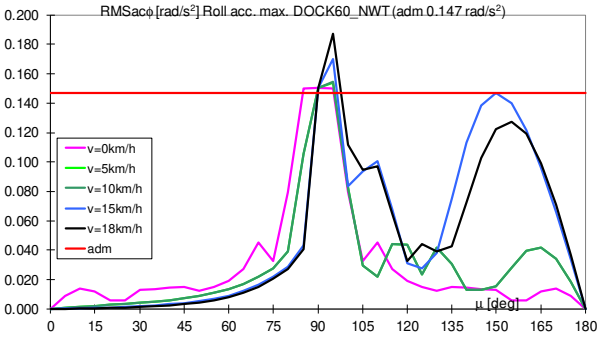

Figure 6.14.a. *Maximum most probable amplitudes for roll acceleration RMSacφ[rad], Dock60_NWT, v=0 – 18 km/h*

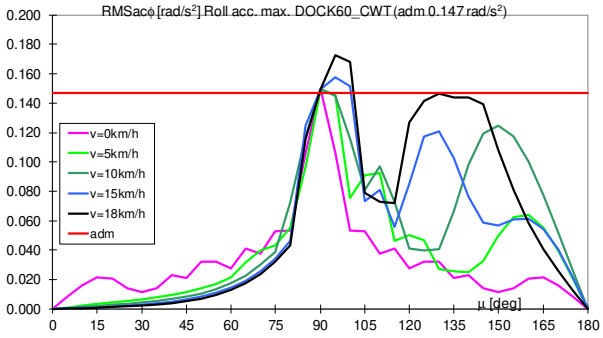

Figure 6.14.b. *Maximum most probable amplitudes for roll acceleration RMSacφ[rad], Dock60_CWT, v=0 – 18 km/h*

Table 6.3. Maximum values of dynamic RMS response for Dock60_CWT floating dock

RMS	$RMS_{z\ max}$ [m]	$RMS_{\theta\ max}$ [rad]	$RMS_{\varphi\ max}$ [rad]	RMS_{axzmax} [m/s^2]	$RMS_{ac\theta max}$ [rad/s^2]	$RMS_{ac\varphi max}$ [rad/s^2]
Adm	0.965	0.017	0.070	0.491	0.033	0.147
0 km/h	1.846	0.022	0.050	0.425	0.018	0.149
(max)	91.27%	25.54%	-28.22%	-13.26%	-46.26%	1.55%
5 km/h	1.898	0.022	0.050	0.429	0.020	0.149
(max)	96.71%	26.83%	-28.22%	-12.51%	-37.92%	1.55%
10 km/h	1.917	0.022	0.050	0.442	0.024	0.149
(max)	98.68%	28.89%	-28.22%	-9.92%	-26.41%	1.55%
15 km/h	1.966	0.023	0.050	0.464	0.028	0.157
(max)	103.75%	31.34%	-28.22%	-5.40%	-13.18%	7.00%
18 km/h	2.007	0.023	0.050	0.487	0.031	0.173
(max)	108.00%	32.55%	-28.22%	-0.71%	-5.35%	17.31%

Table 6.4. Maximum values of dynamic RMS response for Dock60_NWT floating dock

RMS	$RMS_{z\ max}$ [m]	$RMS_{\theta\ max}$ [rad]	$RMS_{\varphi\ max}$ [rad]	RMS_{axzmax} [m/s^2]	$RMS_{ac\theta max}$ [rad/s^2]	$RMS_{ac\varphi max}$ [rad/s^2]
Adm	0.900	0.017	0.070	0.491	0.033	0.147
0 km/h	1.775	0.022	0.035	0.430	0.018	0.151
(max)	97.19%	25.34%	-49.28%	-12.35%	-45.84%	2.31%
5 km/h	1.815	0.022	0.046	0.433	0.020	0.154
(max)	101.68%	26.72%	-33.81%	-11.65%	-37.45%	4,58%
10 km/h	1.816	0.022	0.046	0.446	0.024	0.155
(max)	101.73%	28.84%	-33.81%	-9.11%	-25.70%	5.04%
15 km/h	1.874	0.023	0.053	0.471	0.029	0.170
(max)	108.24%	31.13%	-23.71%	-3.91%	-12.30%	15.78%
18 km/h	2.073	0.023	0.070	0.494	0.031	0.187
(max)	130.33%	32.46%	0.45%	0.75%	-3.95%	27.25%

Table 6.5. Limit values of significant wave height and sea state in Beaufort degrees for safe navigation of the two constructive versions of small floating docks at relocation operations

		Dock60_CWT										*Dock60_NWT*									
v[km/h]		0		5		10		15		18		0		5		10		15		18	
μ[º]		H_{smt}	B_{mt}	H_{smt}	B_{mt}	H_{smt}	B_{mt}	H_{smt}	B_{mt}	H_{smt}	B_{mt}	H_{smt}	B_{mt}	H_{smt}	B_{mt}	H_{smt}	B_{mt}	H_{smt}	B_{mt}	H_{smt}	B_{mt}
0		1.821	4.21	1.856	4.28	1.915	4.40	1.981	4.54	2.003	4.58	1.739	4.04	1.769	4.10	1.825	4.21	1.889	4.35	1.939	4.45
15		1.750	4.06	1.804	4.17	1.861	4.29	1.928	4.43	1.963	4.50	1.696	3.92	1.732	4.02	1.785	4.13	1.850	4.27	1.880	4.33
30		1.696	3.91	1.724	4.01	1.774	4.11	1.830	4.23	1.843	4.25	1.640	3.72	1.667	3.81	1.711	3.97	1.768	4.10	1.799	4.16
45		1.601	3.59	1.617	3.64	1.648	3.75	1.695	3.91	1.723	4.00	1.563	3.45	1.575	3.50	1.602	3.59	1.649	3.75	1.676	3.84
60		1.518	3.30	1.494	3.22	1.499	3.24	1.514	3.29	1.526	3.33	1.479	3.16	1.474	3.15	1.475	3.15	1.490	3.20	1.502	3.25
75		1.457	3.09	1.435	3.01	1.404	2.86	1.400	2.84	1.398	2.83	1.442	3.04	1.434	3.01	1.422	2.96	1.417	2.93	1.412	2.29
90		1.459	3.10	1.420	2.95	1.389	2.79	1.364	2.66	1.353	2.60	1.071	0.97	1.071	0.97	1.071	0.97	1.071	0.97	1.071	0.97
Navigation limit	min	1.456	3.09	1.418	2.93	1.382	2.75	0.990	0.89	0.652	0.59	1.071	0.97	0.988	0.89	0.938	0.85	0.708	0.64	0.626	0.56
	max	1.821	4.21	1.856	4.28	1.915	4.40	1.981	4.54	2.003	4.58	**1.739**	**4.04**	1.769	4.10	**1.825**	**4.21**	1.889	4.35	1.939	4.45

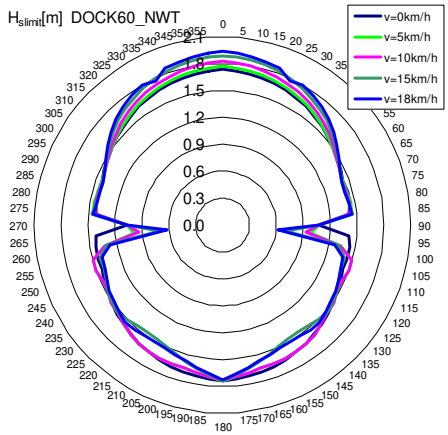

Figure 6.15.a. *Polar diagram for navigation safety limits H_{slimt} wave height, for all tested speeds Dock60_NWT*

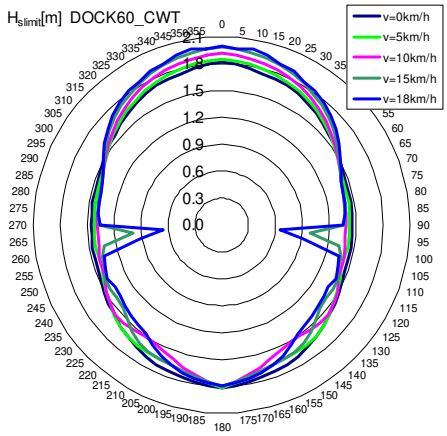

Figure 6.15.b. *Polar diagram for navigation safety limits H_{slimt} wave height, for all tested speeds Dock60_CWT*

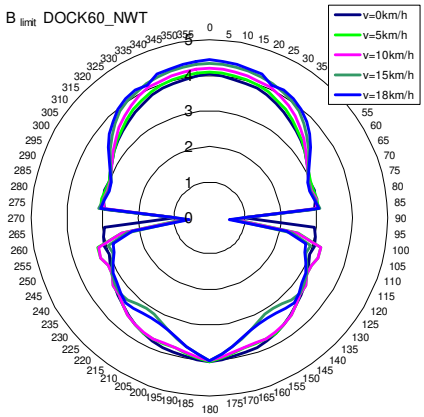

Figure 6.16.a. *Polar diagram for navigation safety expressed in the sea state limit Beaufort value degrees B_{limit}, all tested speeds Dock60_NWT*

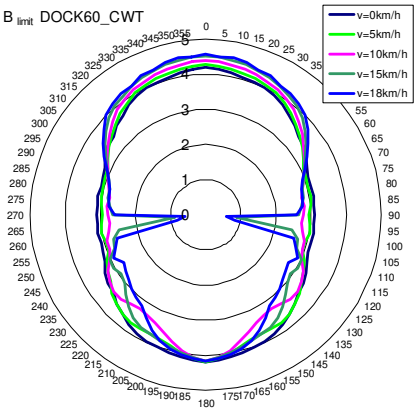

Figure 6.16.b. *Polar diagram for navigation safety expressed in the sea state limit Beaufort value degrees B_{limit}, all tested speeds Dock60_CWT*

Figures 6.15. – 16. a., b. presents the polar diagrams regarding the safety of navigation according to the seakeeping criteria, expressed in limit values of the significant wave height H_{slimit} and the sea state limit value in Beaufort degrees B_{slimit}. Table 6.5. presents the limit values of significant wave height and sea state in Beaufort degrees to ensure the safety of navigation when relocating small floating docks.

6.2. Analysis of the transverse stability of small floating docks Dock60_CWT, Dock60_NWT, taking into account the extreme weather conditions

In order to be able to evaluate the safe operating capacity of the Dock60 floating dock, with the NWT and CWT construction options, based on the criterion of intact transverse stability according to the rules of the ship classification companies [1], we used the D_LDF module *(Annex 4)*.

Because the values of displacement $\Delta[t]$ and of the draft $T_m[t]$ are the same for cases 3, 4 and 5, for each constructive variant (NWT, CWT), I considered for the test ship a series of values z_{GS} = 0.5 – 8.5 m for the position of the vertical centre of gravity of the docked vessel. When assessing the intact transverse stability of *Dock60_NWT/CWT* floating docks the type of docking blocks, SB and LB, has no influence.

- Table 6.6. includes the evaluation of the general stability criterion and the dynamic - meteorological stability criterion (wind and roll) for the version with Dock60_NWT discontinuous upper side tanks, for all five displacement cases;
- Table 6.7. includes the evaluation of the general stability criterion and the dynamic - meteorological stability criterion (wind and roll) for the version with continuous upper lateral tanks Dock60_CWT, for all five displacement cases.

The general criterion of intact transverse stability is met very well in cases 1, 3, 4 and 5 and almost to the limit in case 2 with complete ballast.

The dynamic - meteorological stability criterion (wind and roll) has variation depending on the cases of displacement, as follows:

- case 1 – without docked mass, for NWT $K_{meteo} = 1.63 > 1$ and for CWT $K_{meteo} = 1.11 > 1$, the criterion is satisfied and the Dock60 floating dock can operate in an unprotected port or be relocated;
- case 2 – maximum ballast, for NWT $K_{meteo} = 0.44 < 1$ and for CWT $K_{meteo} = 0.39 < 1$, the criterion is not met, so the Dock60 floating dock can only operate in a protected port and cannot be relocated;
- cases 3, 4 and 5 – test with docked ship at maximum lifting capacity of 828 t, z_{GS} = 0.5 – 7.5 m for NWT $K_{meteo} = 1.05 \div 1.84 > 1$ and for CWT $K_{meteo} = 1.02 \div 1.57 > 1$ the criterion is satisfied and can operate in an unprotected port;
- cases 3, 4 and 5 – test with docked ship at maximum lifting capacity of 828 t,, z_{GS} = 8.5 m for NWT $K_{meteo} = 0.99 < 1$ and for CWT $K_{meteo} = 0.98 < 1$, the criterion is not satisfied and can operate only in a protected port.

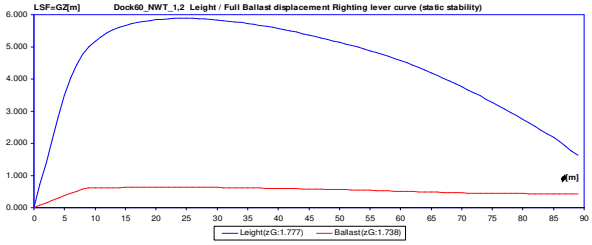

Figure 6.17.a. *Righting lever curve Dock60_NWT, cases 1 &2, light and full ballast cases*

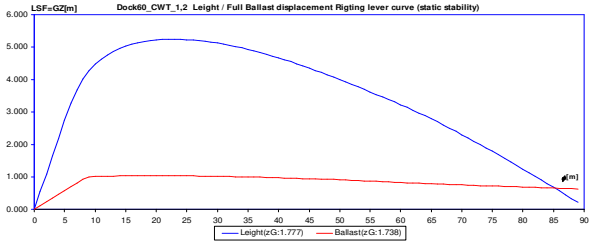

Figure 6.17.b. *Righting lever curve Dock60_NWT, cases 1 & 2, light and full ballast cases*

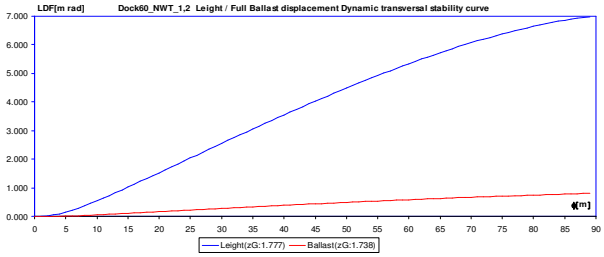

Figure 6.18.a. *Dynamic stability diagram Dock60_NWT, cases 1 & 2, light and full ballast cases*

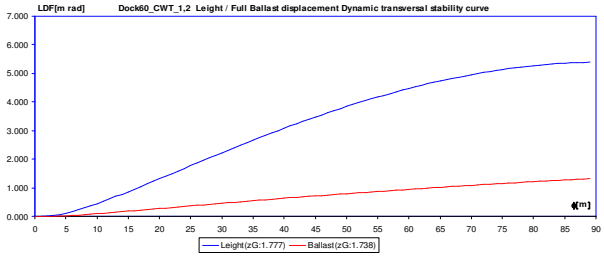

Figure 6.18.b. *Dynamic stability diagram Dock60_CWT, cases 1 & 2, light and full ballast cases*

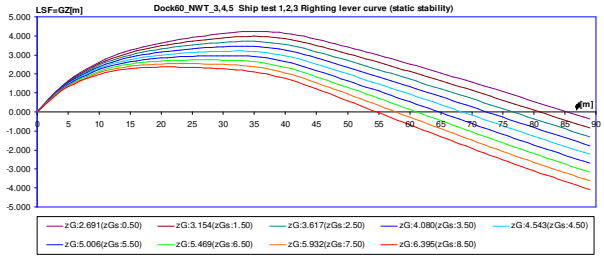

Figure 6.19.a. *Righting lever curve Dock60_NWT, cases 3, 4 & 5,* maximum lifting capacity 828 t, with uniform, sagging and hogging mass distribution

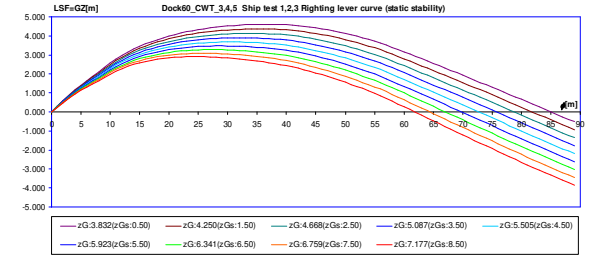

Figure 6.19.b. *Righting lever curve Dock60_CWT, cases 3, 4 & 5,* maximum lifting capacity 828 t, with uniform, sagging and hogging mass distribution

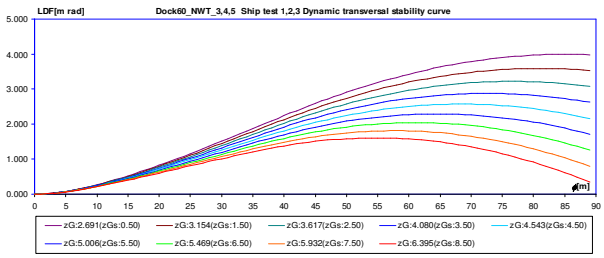

Figure 6.20.a. *Dynamic stability diagram Dock60_NWT, cases 3, 4 & 5,* maximum lifting capacity 828 t, with uniform, sagging and hogging mass distribution

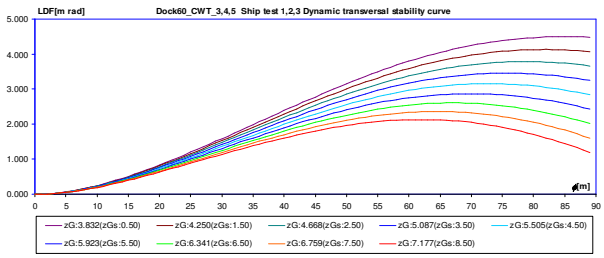

Figure 6.20.b. *Dynamic stability diagram Dock60_NWT, cases 3, 4 & 5,* maximum lifting capacity 828 t, with uniform, sagging and hogging mass distribution

Table 6.6. Checking the intact transverse stability criterion and the initial free board criterion for the Dock60_NWT floating dock

Case	Dock60_NWT_1	Dock60_NWT_2	Dock60_NWT_3,4,5								
	Light	Full ballast	z_{GS1}	z_{GS2}	z_{GS3}	z_{GS4}	z_{GS5}	z_{GS6}	z_{GS7}	z_{GS8}	z_{GS9}
Δ [t]	960	3252	1788	1788	1788	1788	1788	1788	1788	1788	1788
V[m^3]	960	3252	1788	1788	1788	1788	1788	1788	1788	1788	1788
Water density [t/m^3]	1,000	1,000	1,000	1,000	1,000	1,000	1,000	1,000	1,000	1,000	1,000
z_G[m]	1,777	1,738	2,691	3,154	3,617	4,080	4,543	5,006	5,469	5,932	6,395
z_{Gs}[m] (test ship 828 t)	-	-	0,5	1,5	2,5	3,5	4,5	5,5	6,5	7,5	8,5
Hp[m]	2	2	2	2	2	2	2	2	2	2	2
H[m]	8	8	8	8	8	8	8	8	8	8	8
T_m [m]	0,800	6,733	1,490	1,490	1,490	1,490	1,490	1,490	1,490	1,490	1,490
Pontoon deck freeboard	1,200	-	0,510	0,510	0,510	0,510	0,510	0,510	0,510	0,510	0,510
>=0,3 m	DA	-	DA	DA	DA	DA	DA	DA	DA	DA	DA
Upper deck freeboard	7,200	1,267	6,510	6,510	6,510	6,510	6,510	,.510	6,510	6,510	6,510
>=1 m	YES	YES	YES	YES	YES	YES	YES	YES	YES	YES	YES
$h_0 = GM_0[m]$	40,059	4,080	20,282	19,819	19,356	18,893	18,430	17,967	17,504	17,041	16,578
>=1 m	YES	YES	YES	YES	YES	YES	YES	YES	YES	YES	YES
LSF (30) = *GZ* (30) [m]	5.838	0.626	4,122	3,890	3,659	3,412	3,196	2,964	2,738	2,501	2,270
>=0,20 m	YES	YES	YES	YES	YES	YES	YES	YES	YES	YES	YES
LDF(15deg)[mrad]	1,02390	0,11632	0,52393	0,50816	0,49238	0,47660	0,46083	0,44505	0,42928	0,41350	0,39772
>=0,070 mrad	YES	YES	YES	YES	YES	YES	YES	YES	YES	YES	YES
LDF(30deg)[mrad]	2,65327	0,29246	1,57821	1,51208	1,44595	1,37982	1,31369	1,24756	1,18143	1,11530	1,04917
>=0,055 mrad	YES	YES	YES	YES	YES	YES	YES	YES	YES	YES	YES
LDF(40deg)[mrad]	3,54984	0,38883	2,23955	2,13123	2,02291	1,91459	1,80628	1,69796	1,58964	1,48132	1,37300
>=0,090 mrad	YES	YES	YES	YES	YES	YES	YES	YES	YES	YES	YES
φ_st_max[^{0}]	25	22	35	35	34	33	33	30	27	24	21
>=15 º	YES	YES	YES	YES	YES	YES	YES	YES	YES	YES	YES
LSF(φ_max)=*GZ*(φ_max)[m]	5,883	0,633	4,242	3,977	3,717	3,461	3,209	2,964	2,744	2,546	2,370
>=0,25 m	YES	YES	YES	YES	YES	YES	YES	YES	YES	YES	YES
LDF(φ_st_max) [mrad]	2,03961	0,19343	-	-	-	-	-	-	0,99035	0,80682	0,64292
if φ_st_max < 30 º	0,06	0,063	-	-	-	-	-	-	0,058	0,061	0,064
	YES	YES	-	-	-	-	-	-	YES	YES	YES
$\varphi\_stationary$	0,0685	0,0375	0,1079	0,1104	0,1130	0,1158	0,1187	0,1217	0,1249	0,1283	0,1318
<=2 º	YES	YES	YES	YES	YES	YES	YES	YES	YES	YES	YES
K_weather (wind & roll) (b/a)	1,63156	0,44099	1,84285	1,63909	1,48158	1,35624	1,27186	1,18614	1,11450	1,05427	0,99187
>=1	YES	**NO**	YES	YES	YES	YES	YES	YES	YES	YES	**NO**

Table 6.7. Checking the intact transverse stability criterion and the initial free board criterion for the Dock60_CWT floating dock

Case	Dock60_CWT_1	Dock60_CWT_2	Dock60_CWT_3,4,5								
	Light	Full ballast	z_{GS1}	z_{GS2}	z_{GS3}	z_{GS4}	z_{GS5}	z_{GS6}	z_{GS7}	z_{GS8}	z_{GS9}
Δ [t]	1152	4092	1980	1980	1980	1980	1980	1980	1980	1980	1980
V[m^3]	1152	4092	1980	1980	1980	1980	1980	1980	1980	1980	1980
Water density [t/m^3]	1,000	1,000	1,000	1,000	1,000	1,000	1,000	1,000	1,000	1,000	1,000
z_G[m]	3,891	2,144	3,832	4,250	4,668	5,087	5,505	5,923	6,341	6,759	7,177
z_{Gs}[m] (test ship 828 t)	-	-	0,5	1,5	2,5	3,5	4,5	5,5	6,5	7,5	8,5
Hp[m]	2	2	2	2	2	2	2	2	2	2	2
H[m]	8	8	8	8	8	8	8	8	8	8	8
T_m [m]	0,960	6,700	1,650	1,650	1,650	1,650	1,650	1,650	1,650	1,650	1,650
Pontoon deck freeboard	1,040	-	0,350	0,350	0,350	0,350	0,350	0,350	0,350	0,350	0,350
>=0,3 m	YES	-	YES	YES	YES	YES	YES	YES	YES	YES	YES
Upper deck freeboard	7,040	1,300	6,350	6,350	6,350	6.350	6,350	6,350	6,350	6,350	6,350
>=1 m	YES	YES	YES	YES	YES	YES	YES	YES	YES	YES	YES
$h_0 = GM_0[m]$	31,124	6,824	17,086	16,668	16,250	15,831	15,413	14,995	14,577	14,159	13,741
>=1 m	YES	YES	YES	YES	YES	YES	YES	YES	YES	YES	YES
LSF (30) = *GZ* (30) [m]	5,122	1,019	4,518	4,309	4,100	3,891	3,682	3,473	3,264	3,055	2,846
>=0,20 m	YES	YES	YES	YES	YES	YES	YES	YES	YES	YES	YES
LDF(15deg)[mrad]	0,86703	0,18899	0,50547	0,49122	0,47698	0,46270	0,44846	0,43422	0,41998	0,40573	0,39149
>=0,070 mrad	YES	YES	YES	YES	YES	YES	YES	YES	YES	YES	YES
LDF(30deg)[mrad]	2,31400	0,47634	1,66213	1,60243	1,54272	1,48288	1,42318	1,36347	1,30377	1,24407	1,18437
>=0,055 mrad	YES	YES	YES	YES	YES	YES	YES	YES	YES	YES	YES
LDF(40deg)[mrad]	3,08304	0,63307	2,38378	2,28599	2,18819	2,09017	1,99238	1,89459	1,79680	1,69901	1,60121
>=0,090 mrad	YES	YES	YES	YES	YES	YES	YES	YES	YES	YES	YES
φ_st_max[^{0}]	23	20	37	36	34	32	30	29	27	26	25
>=15 º	YES	YES	YES	YES	YES	YES	YES	YES	YES	YES	YES
LSF(φ_max)=*GZ*(φ_max)[m]	5,241	1,033	4,614	4,365	4,126	3,899	3,682	3,475	3,278	3,091	2,912
>=0,25 m	YES	YES	YES	YES	YES	YES	YES	YES	YES	YES	YES
LDF(φ_st_max) [mrad]	1,58976	0,27906	-	-	-	-	-	1,24229	1,07551	0,97603	0,88294
dacă φ_st_max < 30 º	0,062	0,065	-	-	-	-	-	0,056	0,058	0,059	0,06
	YES	YES	-	-	-	-	-	YES	YES	YES	YES
φ_stationary	0,1379	0,0337	0,1317	0,1350	0,1385	0,1421	0,1459	0,1500	0,1543	0,1588	0,1636
<=2 º	YES	YES	YES	YES	YES	YES	YES	YES	YES	YES	YES
K_weather (wind & roll) (b/a)	1,10830	0,39641	1,57573	1,45281	1,35053	1,26407	1,19054	1,12733	1,07267	1,02522	0,98399
>=1	YES	**NO**	YES	YES	YES	YES	YES	YES	YES	YES	**NO**

In *table 6.8.* a summary of the results obtained for the intact transverse stability criterion is found.

Table 6.8. Safe operating capacity of Dock60_CWT / NWT floating docks, with the two constructive variants, evaluated on the basis of intact transverse stability criteria

Case	General stability criterion	Dynamic - meteorological criterion (wind and roll)	The safe operating capacity of the floating dock
1	satisfied	1,11 ÷ 1,63 >1	Unprotected port, can be relocated
2	satisfied	not satisfied	Protected port, cannot be relocated
3, 4, 5	satisfied	1,02 ÷ 1,84 > 1	(z_{GS}=0,5÷7,5 m) unprotected harbour
3, 4, 5	satisfied	not satisfied	(z_{GS}=8,5 m) protected harbour

6.3. Conclusions on the dynamic analysis and transverse stability of floating docks Dock60_CWT, Dock60_NWT, with two constructive versions

For the assessment of safety conditions when relocating small floating docks with continuous and discontinuous upper tanks, Dock60_CWT / NWT (figures. 4.9., 4.12., table 4.1., 4.6, 4.7.), we developed a model with 200 cross sections (chapter 4.1.) and using the DYN program [45], with the linear hydrodynamic formulation using the strip method (subchapter 2.4.), we have determined the functions of the RAO response amplitude functions for the main components of oscillation of the dock, heave, pitch and roll. For a transit scenario on a river-maritime route, we modelled random waves using the power spectral density function ITTC [58], [59]. Based on the seakeeping criteria (equation 2.23. – 2.25., table 6.1.), formulated in terms of the most probable allowable statistical values for the amplitude of the movements and the accelerations of the combined vertical oscillations, of pitch and roll, the operating limits of the floating docks are obtained statistically in the short term, with a summary in table 6.5.

Due to the prismatic shapes of the floating dock, the RAO amplitude response functions for vertical and pitch oscillations are similar (figures 6.3. – 6.4. a., b.). Also, their own pulsations at the vertical and pitch oscillations are similar (table 6.2.). Due to the characteristics of transverse stability (Figure 6.2.), the RAO response amplitude operator function for the roll oscillation (figure 6.8. - 6.9.a., b.) records significant differences for the two constructive versions of the Dock60_CWT/NWT floating docks. Because their own pulsation in the case of roll oscillation is greater than 2 rad / s (table 6.2.), hydrodynamic damping is very low, resulting in significant values of the RAO response amplitude operator function to the roll oscillations. Significant influences on RAO response amplitude functions are observed due to changes in wave pulsation, angle between dock and wave, as well as towing speed.

The most likely RMS statistical response is compared with the limits of the seakeeping criteria, for the wave reference with the maximum significant height of 2.568 m. The permissible values for seakeeping are exceeded as follows (tables 6.3. - 6.4.):

- Vertical oscillations combined at the stern, middle and bow 91.19 – 130.3% (figures 6.9 – 6.11.a., b.);
- Pitch oscillation 25.34 – 32.55% (figures 6.12.a., b.);
- Accelerations from roll oscillation 1.55 – 27.25% (figures 6.13.a., b.);
- The roll oscillation and the acceleration of the combined vertical movements have the smallest exceedances of the permissible limit, 0.45 – 0.75% for Dock60_NWT and without overshoot for the Dock60_CWT variant

From the polar diagrams, the limits of the navigation result in terms of the significant height limit of the wave H_s=0.626 – 2.003 m, mainly due to the restrictions generated by the reduced freeboard (figures 6.15. – 16.a., b.). For the safety of relocating the floating docks, a low towing speed must be considered, the transverse waves should be avoided as far as possible and a special approval is required in the case of navigation on coastal routes.

From the evaluation of the Dock60_CWT/NWT floating docks according to the general transverse stability criterion (subchapter 6.2.) results without restrictions for all displacement and construction cases. Dynamic - meteorological stability criterion (wind and roll) is not fulfilled for case 2 – with full ballast and also for cases 3,4,5 – with docked vessel having the vertical position of the centre of gravity $z_{GS} > 7.5m$ (compared to the basic plan of the docked ship).

CHAPTER 7

ANALYSIS OF THE OPERATING CAPACITY OF THE FLOATING DOCK DOCK_VARD_TULCEA, BASED ON THE CRITERIA OF STRUCTURAL STRENGTH AND MINIMUM FREEBOARD, AT EXTREME LOADS FROM QUASI-STATIC EQUIVALENT WAVES

The study in this chapter presents the structural analysis and restrictions of the free floating dock at the VARD Naval Shipyard in Tulcea [9], [11], of large size, using a 3D-FEM model, extended over the entire length of the dock, in a single board, according to the procedure of chapter 2.3.2., subject to requests from quasi-static meeting – following waves. Using the 1D equivalent beam models, the balancing parameters of the equivalent dock - wave system are determined. The height of the quasi-static equivalent wave is considered within the range h_w = 0 – 4.492 m (equation 2.4.), according to naval classification rules [1], [3]. According to the loading cases described in chapter 4.2., the numerical results obtained after the analysis of the general resistance on the equivalent beam model 1D and 3D-FEM will be presented below.

The results of the 1D equivalent beam analysis are published and presented in the reference article [37]. The results of the 3D-FEM model analysis are published and presented in the reference article [73].

7.1. Structural analysis of the floating dock Dock_VARD_Tulcea, based on the 1D equivalent beam model, at loads from head and follow waves

This subchapter presents the numerical results obtained from the analysis of the general resistance on 1D equivalent beam models, for the Dock_VARD_Tulcea floating dock, for five different operating cases, according to the data in subchapter 4.2.

General resistance analysis based on the equivalent model of Dock_VARD_Tulcea, using the **D_ACVAD software (chapter 1.4., annex 3)** [35], leads to a preliminary assessment of the criteria of global strength and minimum freeboard, which are presented in tables 7.1.a. – g.

For the analysis of the general resistance of the dock, in all the five operating cases, considering requests from quasi-static equivalent waves of meeting as well as requests from still water, a total of 103 cases results.

Table 7.1.a. presents the balancing parameters of the wave system, based on the 1D equivalent beam model, at still water and equivalent wave demands, according to the model in subchapter 2.1., as well as the values of the freeboard. Due to the fact that, through the ballast system of the dock, it is balanced at the same displacement Δ=66,324 t, with a draft of $T_m = T_{Pp} = T_{Pv}$=6,2 m, the balancing parameters dock - wave and the values of the freeboard resulting in the same for all cases.

In table 7.1.b., based on the 1D equivalent beam model, the maximum values of the sectional efforts at the global resistance are presented, in the case without docked mass.

In table 7.1.c. and d., based on the 1D equivalent beam model, the maximum values of the sectional efforts to the global resistance are presented, in the case of loading provided by the VARD Shipyard in Tulcea [9], [11]. Figures 7.1.a.-b., presents the effort diagrams for the cases in the table 7.1.c., representative of the transition of the docked vessel from the quay to the dock, and for the table 7.1.d., the effort diagrams for the presented cases are shown in the figures 7.2.a.-d., representative for the final stage of docking, with the ship having a total mass of 19,747 t. For the case of docking at the capacity of 197474 t, in the range of design waves, the criteria of global resistance are met, which allows the dock to be relocated on a river and coastal route with the docked ship.

In table 7.1.e.-g., based on the 1D equivalent beam model, the maximum values of the sectional efforts at the global resistance are presented, in the case of docking to the maximum operating capacity 27,000 t, with three different types of mass distribution, namely uniform distribution, sagging distribution and hogging distribution, according to the norms of the ship classification company [1], [3]. Figures 7.3.a.-d., presents the sectional effort diagrams for the cases in tables 7.1.g.

For the case of docking at maximum capacity with uniform mass distribution, restrictions of the global resistance criterion for sagging wave cases, at the wave height of over 3.213 m, appear.

Table 7.1.a. Checking the minimum freeboard criterion for Dock_VARD_Tulcea at the reference draft T=6.2 m , F_s=0.300 m

EDW	h_w[m]	0	0.500	1.000	1.500	2.000	2.500	3.000	3.500	4.000	4.492
hogging	T_m[m]	6.200	6.191	6.182	6.174	6.165	6.156	6.147	6.138	6.128	6.118
	trim[rad]	0.00000	0.00028	-0.00058	0.00089	0.00120	-0.00151	0.00182	0.00213	0.00244	0.00275
	x_F[m]	100.104	100.107	100.110	100.114	100.117	100.120	100.124	100.128	100.132	100.135
	T_{pp}[m]	6.200	6.219	6.240	6.263	6.285	6.307	6.330	6.351	6.372	6.394
	T_{pv}[m]	6.200	6.160	6.119	6.077	6.034	5.992	5.949	5.905	5.862	5.819
	F_{aft}[m]	3.900	4.131	4.360	4.587	4.815	5.043	5.270	5.499	5.728	5.952
	F_m[m]	3.900	3.661	3.420	3.180	2.940	2.700	2.461	2.222	1.983	1.748
	F_{fore}[m]	3.900	4.190	4.481	4.773	5.066	5.358	5.651	5.945	6.238	6.527
	F_{min}[m]	3.900	3.661	3.420	3.180	2.940	2.700	2.461	2.222	1.983	1.748
	F_{min}/F_s	>1	>1	>1	>1	>1	>1	>1	>1	>1	>1
sagging	T_m[m]	6.200	6.207	6.215	6.222	6.229	6.236	6.243	6.250	6.256	6.262
	trim[rad]	0.00000	0.00032	0.00063	0.00095	0.00126	0.00157	0.00189	0.00220	0.00251	0.00282
	x_F[m]	100.104	100.100	100.097	100.094	100.092	100.089	100.086	100.084	100.081	100.079
	T_{pp}[m]	6.200	6.175	6.152	6.127	6.103	6.079	6.054	6.029	6.005	5.980
	T_{pv}[m]	6.200	6.242	6.284	6.326	6.367	6.407	6.449	6.490	6.530	6.570
	F_{aft}[m]	3.900	3.675	3.448	3.223	2.997	2.771	2.546	2.321	2.095	1.874
	F_m[m]	3.900	4.142	4.382	4.624	4.865	5.107	5.349	5.591	5.833	6.071
	F_{fore}[m]	3.900	3.608	3.316	3.024	2.733	2.443	2.151	1.860	1.570	1.284
	F_{min}[m]	3.900	3.608	3.316	3.024	2.733	2.443	2.151	1.860	1.570	1.284
	F_{min}/F_s	>1	>1	>1	>1	>1	>1	>1	>1	>1	>1

Table 7.1.b. The maximum values of the sectional efforts, model 1D, at the overall resistance in meeting waves, for the case without docked mass, ballasted at the reference draft T=6.2m

EDW	h_w[m]	0	0.500	1.000	1.500	2.000	2.500	3.000	3.500	4.000	4.492
					AVBM [kNm] = 3.44E+06		*AVSF* [kN] = 5.70E+04				
hogging	VBM_{max} [kNm]	5.11E+05	3.26E+05	3.41E+05	5.96E+05	8.53E+05	1.11E+06	1.37E+06	1.63E+06	1.89E+06	2.15E+06
	max/adm	0.15	0.09	0.10	0.17	0.25	0.32	0.40	0.47	0.55	0.63
	VSF_{max} [kN]	2.11E+04	1.87E+04	2.27E+04	2.68E+04	3.08E+04	3.48E+04	3.89E+04	4.29E+04	4.69E+04	5.08E+04
	max/adm	0.37	0.33	0.40	0.47	0.54	0.61	0.68	0.75	0.82	0.89
sagging	VBM_{max} [kNm]	5.11E+05	7.70E+05	1.03E+06	1.30E+06	1.57E+06	1.84E+06	2.12E+06	2.39E+06	2.67E+06	2.94E+06
	max/adm	0.15	0.22	0.30	0.38	0.46	0.54	0.62	0.70	0.77	0.85
	VSF_{max} [kN]	2.11E+04	2.36E+04	2.60E+04	2.85E+04	3.11E+04	3.36E+04	3.61E+04	3.86E+04	4.11E+04	4.40E+04
	max/adm	0.37	0.41	0.46	0.50	0.54	0.59	0.63	0.68	0.72	0.77

Table 7.1.c. The maximum values of the sectional efforts, model 1D, for the case of the docked ship's transition from the quay to the dock's deck, Ld=0-122.79 m, h_w = 0 m at the reference draft T=6.2 m

Ld[m]		SW	0	10	20	40	60	80	100	122.79
					AVBM [kNm] = 3.44E+06		*AVSF* [kN] = 5.70E+04			
docking	VBM_{max} [kNm]	3.37E+05	5.11E+05	4.14E+05	5.11E+05	4.13E+05	4.15E+05	4.06E+05	4.23E+05	4.29E+05
	max/adm	0.098	0.149	0.120	0.149	0.120	0.121	0.118	0.123	0.125
	VSF_{max} [kN]	6.13E+03	2.11E+04	1.64E+04	2.11E+04	1.64E+04	1.65E+04	1.62E+04	1.66E+04	1.68E+04
	max/adm	0.108	0.370	0.288	0.370	0.287	0.289	0.284	0.291	0.294

Table 7.1.d. Maximum values of sectional efforts, model 1D, for the final case of docking with the ship having a total mass of 19,747t ,Ld_{max}=122.79 m at the reference draft T=6.2 m

EDW	h_w[m]	0	0.500	1.000	1.500	2.000	2.500	3.000	3.500	4.000	4.492
					AVBM [kNm] = 3.44E+06		*AVSF* [kN] = 5.70E+04				
hogging	VBM_{max}[kNm]	4.29E+05	3.07E+05	4.18E+05	6.82E+05	9.47E+05	1.21E+06	1.48E+06	1.75E+06	2.01E+06	2.28E+06
	max/adm	0.12	0.09	0.12	0.20	0.28	0.35	0.43	0.51	0.58	0.66
	VSF_{max}[kN]	1.68E+04	1.88E+04	2.29E+04	2.69E+04	3.09E+04	3.50E+04	3.90E+04	4.30E+04	4.70E+04	5.10E+04
	max/adm	0.29	0.33	0.40	0.47	0.54	0.61	0.68	0.75	0.83	0.89
sagging	VBM_{max}[kNm]	4.29E+05	5.65E+05	7.95E+05	1.06E+06	1.34E+06	1.61E+06	1.89E+06	2.16E+06	2.44E+06	2.71E+06
	max/adm	0.12	0.16	0.23	0.31	0.39	0.47	0.55	0.63	0.71	0.79
	VSF_{max}[kN]	1.68E+04	1.92E+04	2.17E+04	2.42E+04	2.69E+04	3.10E+04	3.51E+04	3.92E+04	4.32E+04	4.73E+04
	max/adm	0.29	0.34	0.38	0.42	0.47	0.54	0.62	0.69	0.76	0.83

Table 7.1.e. Maximum values of sectional efforts, 1D model, for the case of docking at the maximum capacity of 27,000t, with uniform mass distribution, at the reference draft T=6.2 m

EDW	h_w[m]	0	0.500	1.000	1.500	2.000	2.500	3.000	**3.213**	**3.908**	4.492
					AVBM [kNm] = 3.44E+06		*AVSF* [kN] = 5.70E+04				
hogging	VBM_{max}[kNm]	1.28E+06	1.01E+06	7.40E+05	5.72E+05	4.34E+05	3.07E+05	4.12E+05	5.24E+05	8.92E+05	1.20E+06
	max/adm	0.37	0.29	0.22	0.17	0.13	0.09	0.12	0.15	0.26	0.35
	VSF_{max}[kN]	3.09E+04	2.69E+04	2.29E+04	1.89E+04	1.49E+04	1.89E+04	2.29E+04	2.46E+04	3.02E+04	3.49E+04
	max/adm	0.54	0.47	0.40	0.33	0.26	0.33	0.40	0.43	0.53	0.61
sagging	VBM_{max}[kNm]	1.28E+06	1.55E+06	1.83E+06	2.10E+06	2.38E+06	2.66E+06	2.93E+06	3.05E+06	**3.44E+06**	3.77E+06
	max/adm	0.37	0.45	0.53	0.61	0.69	0.77	0.85	0.89	**1.00**	1.09
	VSF_{max}[kN]	3.09E+04	3.49E+04	3.90E+04	4.30E+04	4.71E+04	5.12E+04	5.53E+04	**5.70E+04**	6.27E+04	6.75E+04
	max/adm	0.54	0.61	0.68	0.76	0.83	0.90	0.97	**1.00**	1.10	1.18

Table 7.1.f Maximum values of sectional efforts, 1D model, for the case of docking at the maximum capacity of 27,000t, with hogging mass distribution, at the reference draft T=6.2 m

EDW	h_w[m]	0	0.500	1.000	1.500	2.000	2.500	3.000	**3.769**	4.000	4.492
					AVBM [kNm] = 3.44E+06		*AVSF* [kN] = 5.70E+04				
hogging	VBM_{max}[kNm]	9.91E+05	7.67E+05	5.61E+05	3.84E+05	4.97E+05	7.55E+05	1.01E+06	1.42E+06	1.54E+06	1.79E+06
	max/adm	0.29	0.22	0.16	0.11	0.14	0.22	0.29	0.41	0.45	0,.2
	VSF_{max}[kN]	2.71E+04	2.32E+04	1.93E+04	2.30E+04	2.70E+04	3.11E+04	3.51E+04	4.13E+04	4.32E+04	4.71E+04
	max/adm	0.48	0.41	0.34	0.40	0.47	0.55	0.62	0.72	0.76	0.83
sagging	VBM_{max}[kNm]	9.91E+05	1.23E+06	1.47E+06	1.73E+06	1.99E+06	2.25E+06	2.52E+06	2.93E+06	3.06E+06	3.33E+06
	max/adm	0.29	0.36	0.43	0.50	0.58	0.66	0.73	0.5	0.89	0.97
	VSF_{max}[kN]	2.71E+04	3.10E+04	3.50E+04	3.89E+04	4.29E+04	4.69E+04	5.09E+04	**5.70E+04**	5.89E+04	6.28E+04
	max/adm	0.48	0.54	0.61	0.68	0.75	0.82	0.89	**1.00**	1.03	1.10

Table 7.1.g. Maximum values of sectional efforts, 1D model, for the case of docking at the maximum capacity of 27,000t, with sagging mass distribution, at the reference draft T=6.2 m

EDW	h_w[m]	0	0.500	1.000	1.500	2.000	**2.197**	3.000	**3.176**	4.000	4.492
					AVBM [kNm] = 3.44E+06		*AVSF* [kN] = 5.70E+04				
hogging	VBM_{max}[kNm]	1.68E+06	1.40E+06	1.13E+06	9.35E+05	7.80E+05	7.21E+05	5.00E+05	4.56E+05	5.11E+05	7.77E+05
	max/adm	0.49	0.41	0.33	0.27	0.23	0.21	0.15	0.13	0.15	0.23
	VSF_{max}[kN]	3.92E+04	3.52E+04	3.11E+04	2.71E+04	2.31E+04	2.15E+04	1.73E+04	1.87E+04	2.54E+04	2.93E+04
	max/adm	0.69	0.62	0.55	0.48	0.41	0.38	0.30	0.33	0.44	0.51
sagging	VBM_{max}[kNm]	1.68E+06	1.96E+06	2.23E+06	2.51E+06	2.79E+06	2.90E+06	3.34E+06	**3.44E+06**	3.90E+06	4.17E+06
	max/adm	0.49	0.57	0.65	0.73	0.81	0.4	0.97	**1.00**	1.13	1.21
	VSF_{max}[kN]	3.92E+04	4.32E+04	4.73E+04	5.13E+04	5.54E+04	**5.70E+04**	6.35E+04	6.50E+04	7.17E+04	7.57E+04
	max/adm	0.69	0.76	0.83	0.90	0.97	**1.00**	1.11	1.14	1.26	1.33

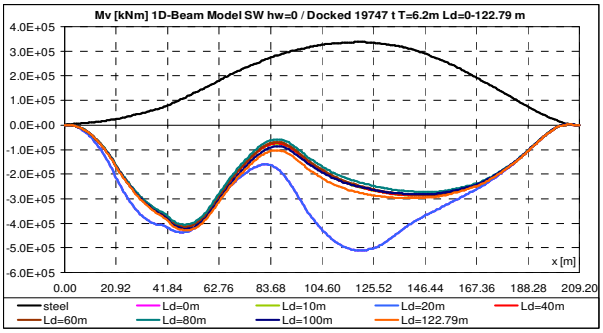

Figure 7.1.a. *Vertical bending moment VBM[kNm] for 1D beam girder of Dock_VARD_Tulcea, for docking step cases of a mass 19,747 t operation case in SW*

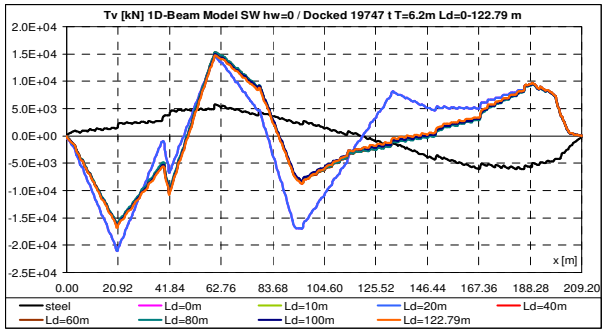

Figure 7.1.b. *Vertical shear force VSF[kN] for 1D beam girder of Dock_VARD_Tulcea, for 1D beam girder of Dock_VARD_Tulcea, for docking step cases of a mass 19,747 t operation case in SW*

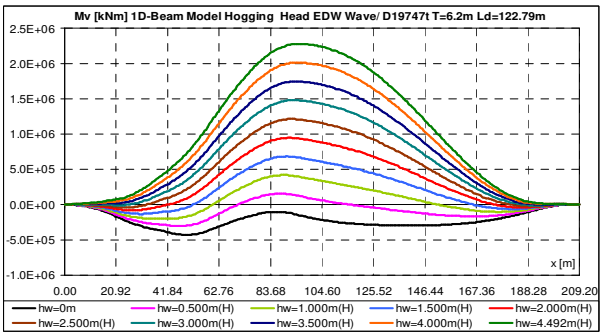

Figure 7.2.a. *Vertical bending moment VBM[kNm] for 1D beam girder of Dock_VARD_Tulcea, for docking mass 19.747t, hogging wave type*

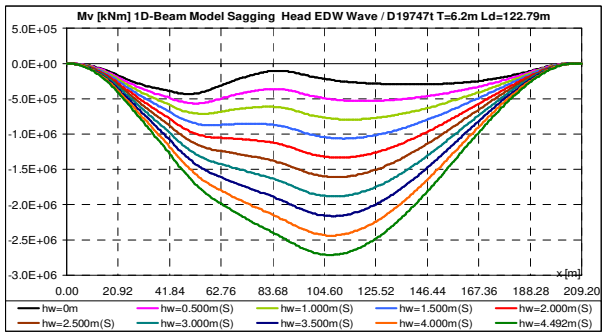

Figure 7.2.c. *Vertical bending moment VBM[kNm] for 1D beam girder of Dock_VARD_Tulcea, for docking mass 19.747t, sagging wave type*

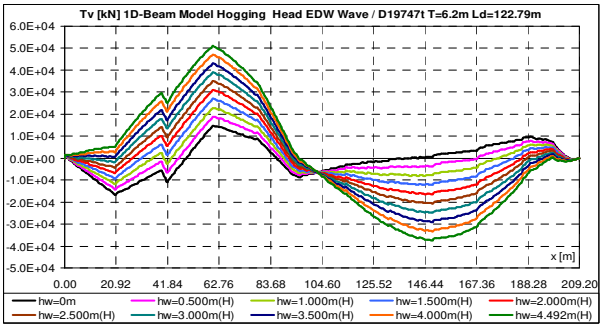

Figure 7.2.b. *Vertical shear force VSF[kN] for 1D beam girder of Dock_VARD_Tulcea, for docking mass 19.747t, hogging wave type*

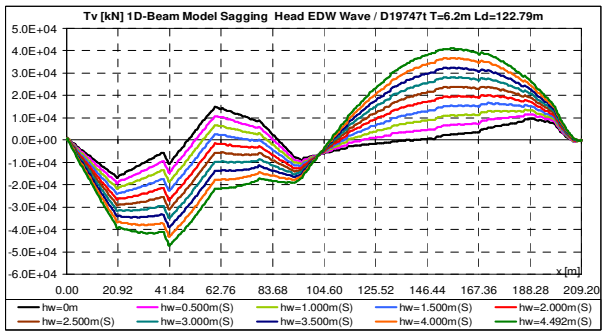

Figure 7.2.d. *Vertical shear force VSF[kN] for 1D beam girder of Dock_VARD_Tulcea, for docking mass 19.747t, hogging wave type*

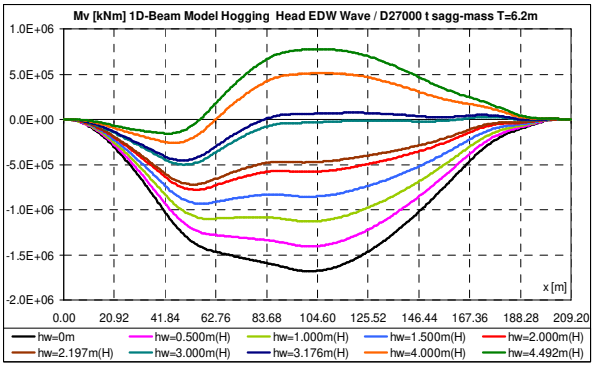

Figure 7.3.a. *Vertical bending moment VBM[kNm] for 1D beam girder of Dock_VARD_Tulcea, for maximum docking capacity operation case of 27,000t sagging distribution, hogging wave type*

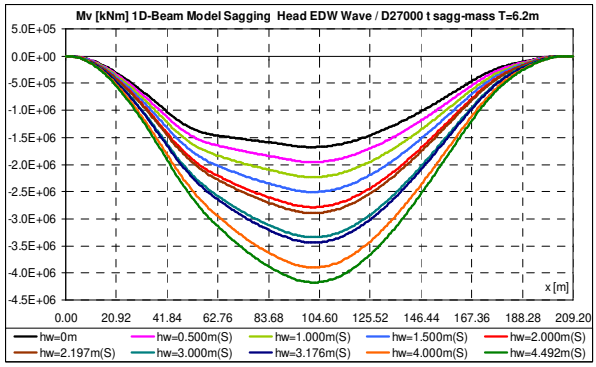

Figure 7.3.c. *Vertical bending moment VBM[kNm] for 1D beam girder of Dock_VARD_Tulcea, for maximum docking capacity operation case of 27,000t sagging distribution, sagging wave type*

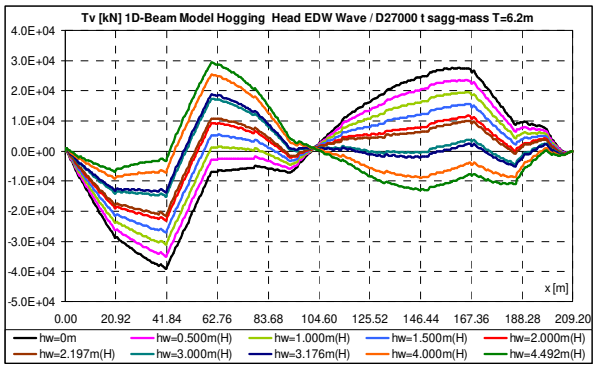

Figure 7.3.b. *Vertical shear force VSF[kN] a for 1D beam girder of Dock_VARD_Tulcea, for maximum docking capacity operation case of 27,000t sagging distribution, hogging wave type*

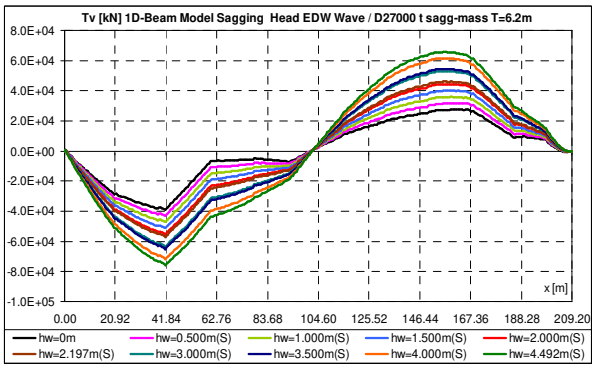

Figure 7.3.d. *Vertical shear force VSF[kN] for 1D beam girder of Dock_VARD_Tulcea, for maximum docking capacity operation case of 27,000t sagging distribution, sagging wave type*

For the case of docking to the maximum capacity of 27,000 t, with hogging distribution of the mass, restrictions of the criterion of the global resistance for the cases of wave type sagging, at heights of over 3.769 m appear.

In the case of docking at a maximum capacity of 27,000 t with sagging mass distribution, restrictions of the global resistance criterion for sagging wave cases, at heights of over 2.197 m, appear.

From the analysis on 1D models, it turns out that in the case of the large floating dock, Dock_VARD_Tulcea [37], there are no restrictions on the criterion of the minimum freeboard (table 7.1.a.). In the case without docked mass (table 7.1.b.) and in the case of the docked 19,747t vessel from the quay (tables 7.1.c., d.), there are no restrictions in terms of resistance, so the maximum wave height limit is $h_{w\lim it} = 4.492m$, the dock can be operated fluvially with class IN (2.0) and coastal with a class restriction RE (50%). For extreme cases of docking a maximum mass of 27,000t, the restrictions appear from the allowable values for shear forces under sagging wave conditions (tables 7.1.e. – g.), with an allowable wave height $h_{w\lim it} = 2.197 \div 3.769m$, without limitations for river operation IN (2.0), but with restrictions RE(24% - 40%) for coastal operation. A summary of all the results for the meeting waveform, 1D models, are presented in table 7.2. For the large dock, the case of oblique waves is no longer analysed, as we have shown in the case of the small dock with discontinuous side tanks Dock60_NWT, chapter 5.1., the extreme cases are obtained for the meeting waves, being identical in the case of following quasi-static equivalent waves.

Table 7.2. The results obtained for the cases of docking of the Dock_VARD_Tulcea floating dock, 1D model beam equivalent, in quasi-equivalent meeting-following waves

Docking case	Light *T*6.2	D19747t *T*6.2	D27,000t hogg. *T*6.2	D27,000t unif. *T*6.2	D27,000t sagg. *T*6.2
$h_{w\ limit}$ [m]	4.492	4.492	3.769	3.213	2.197
Criterion	No restrictions		AVSF admissible global strength, sagging EDW condition		
Inland	IN(2.0)	IN(2.0)	IN(2.0)	IN(2.0)	IN(2.0)
Costal	RE(50%)	RE(50%)	≈RE(40%)	≈RE(35%)	≈RE(24%)

In the following are presented the structural analysis of the floating dock Dock_VARD_Tulcea on the 3D-FEM model, to identify the areas with stress concentrators.

7.2. Structural analysis of the Dock_VARD_Tulea floating dock, at loads from equivalent quasi-static head-follow waves, using a full extended 3D-FEM model

This subchapter analyses the docking cases presented in subchapter 7.1. (1D model), using a 3D-FEM structural model, extended in a single board, over the entire length of the large Dock_Vard_Tulcea floating dock [9], [11]. The 3D-FEM model is developed with the FEMAP NX/Nastran software [42] (figure 7.4.), using finite elements of thick plate (Mindlin) [73], [57] and membrane, rectangular and triangular, for the structure of the steel body, as well as finite mass elements concentrated for modelling the equipment, the ballast mass and the mass of the docked vessel.

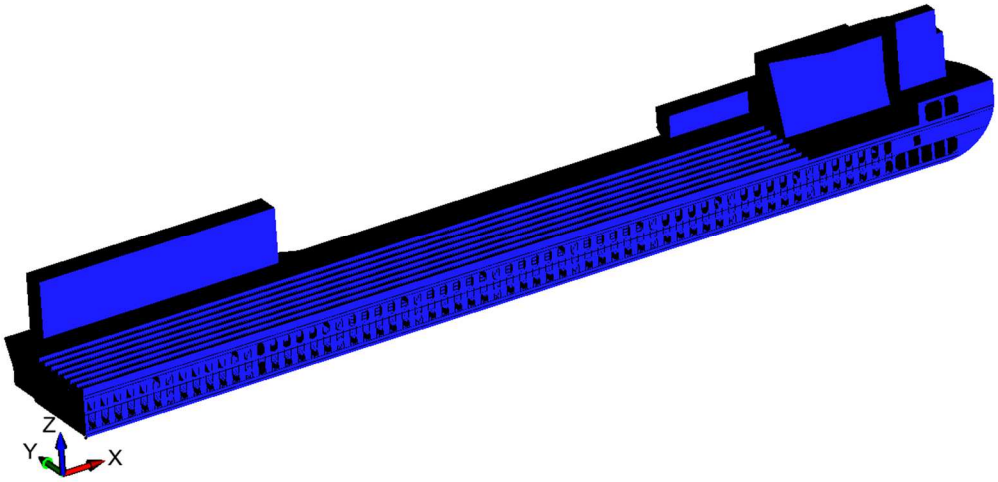

Figure 7.4. Dock_VARD_Tulcea 3D-FEM model

7.2.1. 3D-FEM structural analysis for the light operation of the large floating dock Dock_VARD_Tulcea

The unloaded case corresponds to the situation where the dock does not have a docked mass, but it is ballasted, to ensure a draft of 6.2 m, with the displacement of 66,324 t (table 4.9.). This case also corresponds to the standard dock relocation case between shipyards. In the following figures and in table 7.3., are presented the results of the 3D-FEM structural analysis for the range of meeting – following waves with the height from 0 m to 4.492 m with:

- the distribution of von Mises equivalent stresses, in figures 7.5.a., b., along the entire length of the rails (main deck) and on the area without side tanks in the central area of the dock
- vertical deformation, in figures 7.5.c.,

the distribution of stresses and vertical deformations of the 3D-FEM model in the case of the limit wave with the height of 3.867 m, in figures 7.6., 7.7.

Table 7.3. presents the evaluation of the minimum freeboard criteria, the vertical deformed and the permissible stresses in the case without docked table, at the hogging type wave, with the limit height of the wave $h_{w\lim it} = 4.014\ m$ (restriction from the vertical deformation criterion), but also the evaluations of the limit criteria for the sagging wave type, with the wave height limit $h_{w\lim it} = 3.867\ m$ (restriction from the vertical deformation criterion) and $h_{w\lim it} = 4.301\ m$ (restriction of the allowable stress criterion). The minimum freeboard criterion is not exceeded.

Table 7.3. The values of the minimum freeboard, the maximum von Mises equivalent stresses and the maximum vertical deformation, for the case without the docked mass, at demands in still water and from the head - follow wave - hogging and sagging type

Case	$h_w[m]$	$T_{Pp}[m]$	$T_{Pv}[m]$	$F_{Pp}[m]$	$\frac{F_{Pp}}{adm}$	$F_m[m]$	$\frac{F_m}{adm}$	$F_{Pv}[m]$	$\frac{F_{Pv}}{adm}$	$\sigma_{vM}[MPa]$	$\frac{\sigma_{vM}}{adm}$	$w[mm]$	$\frac{w}{adm}$
Sw	0	6.200	6.200	3.900	>1	3.900	>1	3.900	>1	252.790	0.866	-41	0.098
hogging	**4.014**	**6.373**	**5.861**	**5.734**	**>1**	**1.976**	**>1**	**6.246**	**>1**	**254.868**	**0.873**	**418**	**1.000**
sagging	**3.867**	**6.011**	**6.520**	**2.155**	**>1**	**5.768**	**>1**	**1.647**	**>1**	**275.825**	**0.944**	**-418**	**1.000**
	4.301	**5.990**	**6.554**	**1.960**	**>1**	**5.978**	**>1**	**1.395**	**>1**	**292.000**	**1.000**	**-464**	**1.110**

Figures 7.5. – 7.7., presents the von Mises equivalent stress diagrams and the vertical deformations on the 3D-FEM model of the rail area and the central area (without tanks on deck), for wave height $h_{w\lim it} = 3.867\ m$, in the case of sagging and hogging meeting wave for large floating dock without docked mass. In figures 7.10. it is presented the verification of the structural stability criterion for the wave with $h_{w\lim it} = 3.867\ m$.

a. b.

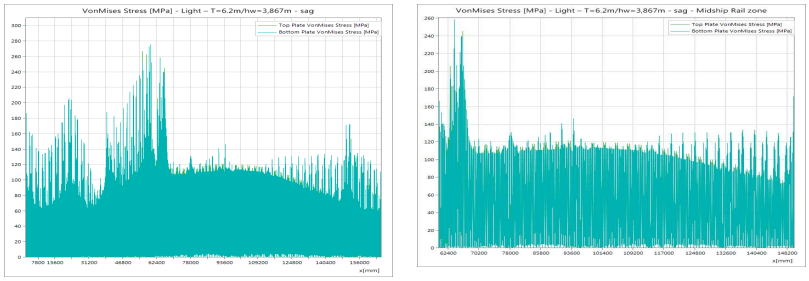

Figure 7.5.a., b. *Equivalent von Mises stress diagram, light case, T=6.2 m, hw=3.867 m, sagging wave type, a. length of rail b. midship zone*

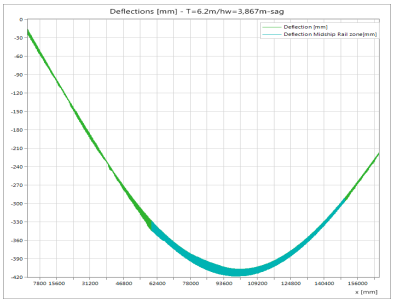

Figure 7.5.c. *Deflection diagram, T=6.2 m, hw=3.867m, sagging wave type*

a. b. c.

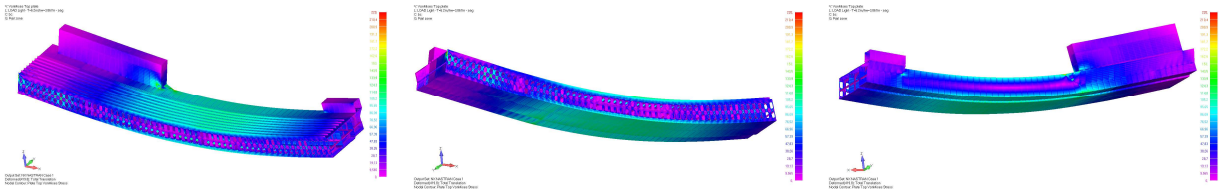

Figure 7.6.a., b., c. *3D-FEM model, equivalent von Mises stress, light case, T=6.2 m, hw=3.867 m, sagging wave type, a. deck view, b. bottom view, c. Shell view*

b.

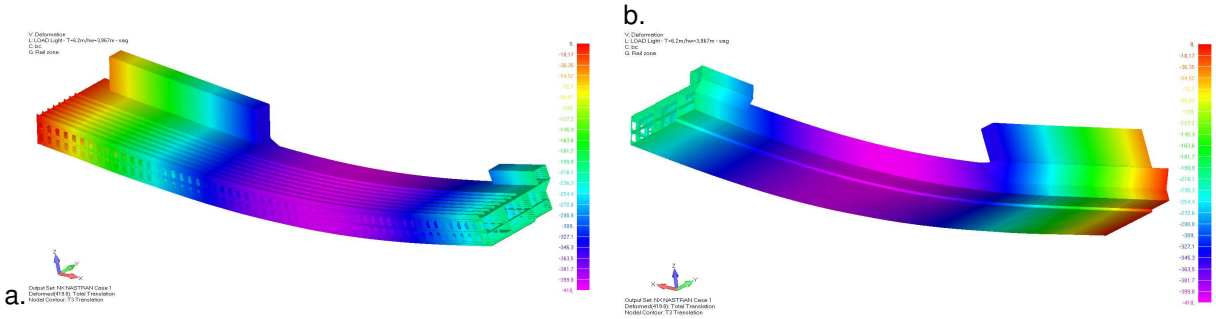

a.

Figure 7.7.a., b. *3D-FEM model, vertical deflection in light case, T=6.2m, hw=3.867m sagging wave type, a. deck view, b. shell view*

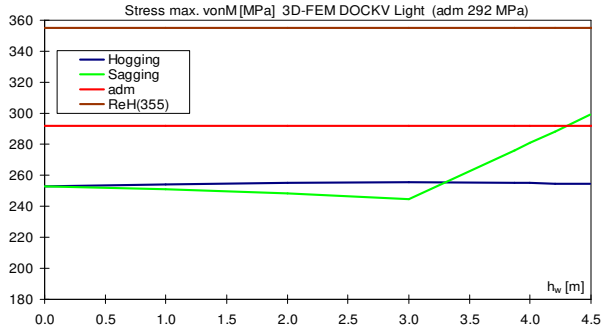

Figure 7.8. *Maximum von Mises stress , light case, 3D-FEM Dock-Vard Tulcea model*

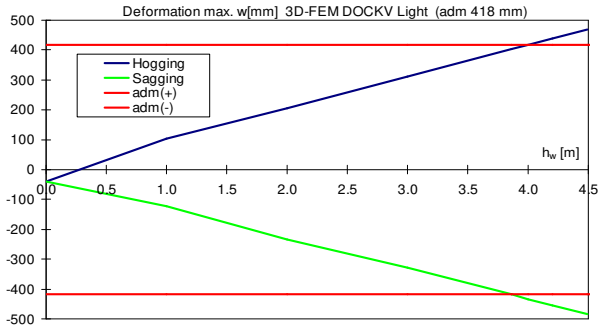

Figure 7.9. *Maximum deformation in light case, 3D-FEM Dock-Vard Tulcea model*

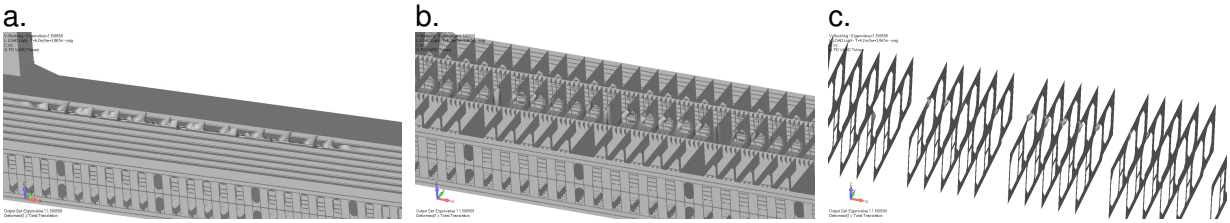

Figure 7.10.a., b., c. *Buckling criterion verification (B=1.500509), light case, sagging wave type, hw=3.867m, collapse at FR. 96 – FR. 160*

7.2.2. 3D-FEM structural analysis for the floating dock operating case Dock_VARD_Tulcea, with the docked ship of 19,747 t

The docking case of a mass of 19,747t, was made available by the VARD Shipyard in Tulcea (subchapter 4.2.). The transfer of the ship from the quay to the deck of the floating dock is done only under calm water conditions, in a protected harbour ($h_w = 0\ m$).

For the final case of docking of the 19,747t ship, it is also considered the extreme situation of relocation of the loading dock, with wave demands. From these results are selected:

- von Mises equivalent stress (figures 7.8.a., b.)
- vertical deformations (figure 7.8.c.) in the case of the wave height limit $h_w = 3.851\ m$ from the criteria of global and local resistance.

Table 7.5. presents the evaluation of the criteria of the minimum freeboard and of the allowable stresses in the final case of docking with the ship having a total mass of 19,747t, with restrictions on wave type hogging $h_{w\lim it} = 4.024\ m$ (the criterion of vertical deformation), but also restrictions on wave type sagging $h_{w\lim it} = 3.851\ m$ (vertical deformation criterion) and $h_{w\lim it} = 4.284\ m$ (the criterion of allowable stresses). In all cases, the criterion of the minimum freeboard is satisfied. Figures 7.11. – 7.13. presents the diagram of von Mises equivalent stresses, the vertical deformation diagram, the von Mises equivalent stress distribution and the vertical deformation on the 3D-FEM model in the rail area, for wave height of $h_{w\lim it} = 3.851m$, in the cases of waves type sagging and hogging for the final case of docking with the ship having a total mass of 19,747t. In Figures 7.16. – 17. is presented the verification of the criterion of structural stability for the wave with the height $h_{w\lim it} = 3.851m$.

Table 7.4. Minimum freeboard, von Mises equivalent stresses and maximum vertical deformation, for the cases of docked ship transition from the quay to the dock, in still water

	$L_{nava\_andocată}[m]$	10m	20m	40m	60m	80m	100m	122.79m
$T_{Pp} = T_{Pv} = 6{,}200m$ $F_{Pp} = F_{Pv} = 3{,}900m$	$\sigma_{vM}[MPa]$	197.835	198.130	197.736	198.390	195.597	197.799	198.965
	$\frac{\sigma_{vM}}{adm}$	0.6775	0.6785	0.6772	0.6794	0.6698	0.6774	0.6813
	$w[mm]$	-38.54	-38.43	-38.32	-37.93	-37.76	-38.34	-41.85
	$\frac{w}{adm}$	0.0933	0.0909	0.0909	0.0909	0.0909	0.0909	0.1005

Table 7.5. The minimum freeboard, the von Mises equivalent stresses and the maximum vertical deformation, for the operating case of the floating dock with the docked ship of 19,747 t, with requests from quasi-static equivalent waves type hogging and sagging

Case	$h_w[m]$	$T_{Pp}[m]$	$T_{Pv}[m]$	$F_{Pp}[m]$	$\frac{F_{Pp}}{adm}$	$F_m[m]$	$\frac{F_m}{adm}$	$F_{Pv}[m]$	$\frac{F_{Pv}}{adm}$	$\sigma_{vM}[MPa]$	$\frac{\sigma_{vM}}{adm}$	$w[mm]$	$\frac{w}{adm}$
Sw	0	6.200	6.200	3.900	>1	3.900	>1	3.900	>1	198.965	0.681	-42	0.100
hogging	**4.024**	**6.374**	**5.860**	**5.739**	**>1**	**1.971**	**>1**	**6.252**	**>1**	**232.330**	**0.796**	**418**	**1.000**
sagging	**3.851**	**6.012**	**6.518**	**2.163**	**>1**	**5.760**	**>1**	**1.656**	**>1**	**275.780**	**0.944**	**-418**	**1.000**
	4.284	**5.990**	**6.553**	**1.968**	**>1**	**5.970**	**>1**	**1.405**	**>1**	**292.000**	**1.000**	**-464**	**1.110**

a. b.

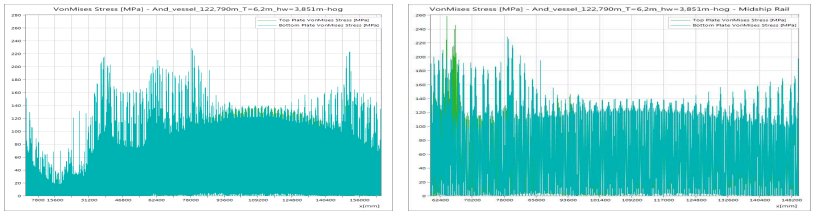

Figure 7.11.a., b. *Equivalent von Mises stress diagram, final case of docked 19,747 t mass, T=6.2 m, hw=3.851 m hogging type wave a. length of rail b. midship zone*

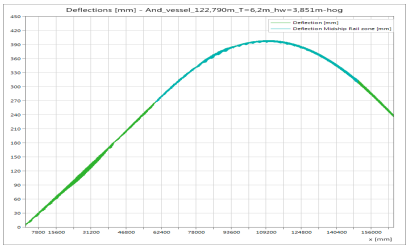

Figure 7.11.c. *Vertical deformation for final case of docked 19,747 t mass, T=6.2 m, hw=3.851 m hogging wave type*

a. b. c.

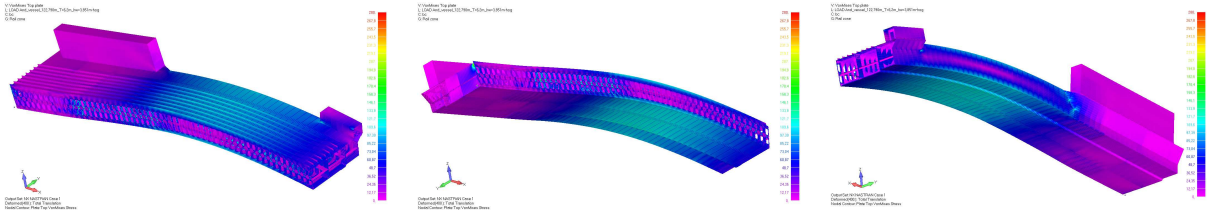

Figure 7.12.a., b., c. *3D-FEM model, equivalent von Mises stress for final case of docked 19,747 t mass, T=6.2 m, hw=3.851 m hogging wave type a. deck view, b. bottom view, c. shell view*

a. b.

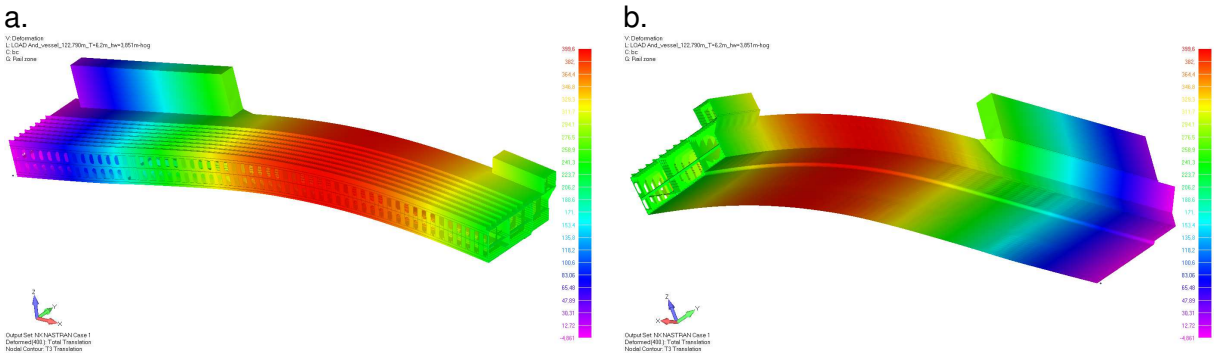

Figure 7.13.a., b. 3D-FEM model, vertical deflection in *final case of docked 19,747 t mass*, *T*=6.2 m, *hw*=3.851 m, hogging wave type, a. deck view, b. shell view

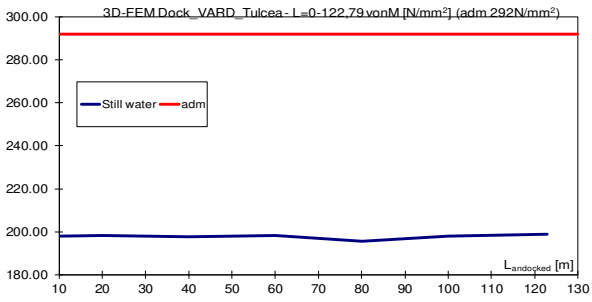

Figure 7.14.a. Maximum von Misses stress, *transit cases of docked 19,747 t mass*, SW

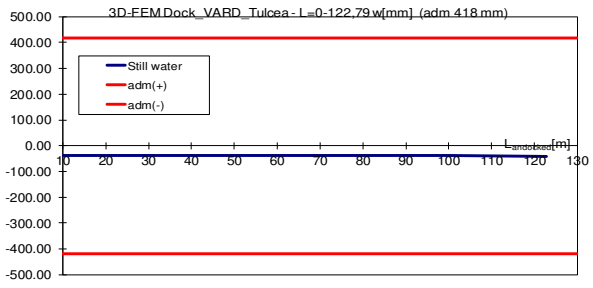

Figure 7.15.a. Maximum vertical deflection, *transit cases of docked 19,747 t mass*, SW

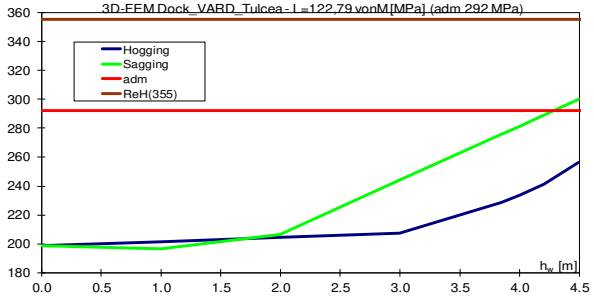

Figure 7.14.b. Maximum von Misses stress *final case of docked 19,747 t mass*

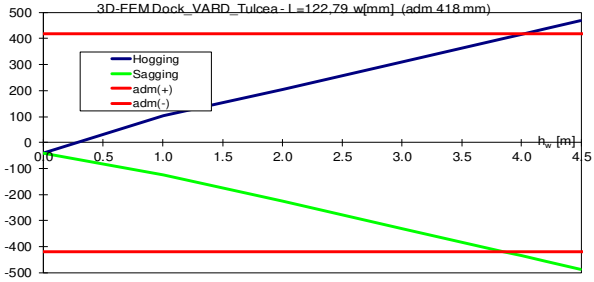

Figure 7.15.b. Maximum vertical deflection *final case of docked 19,747 t mass*

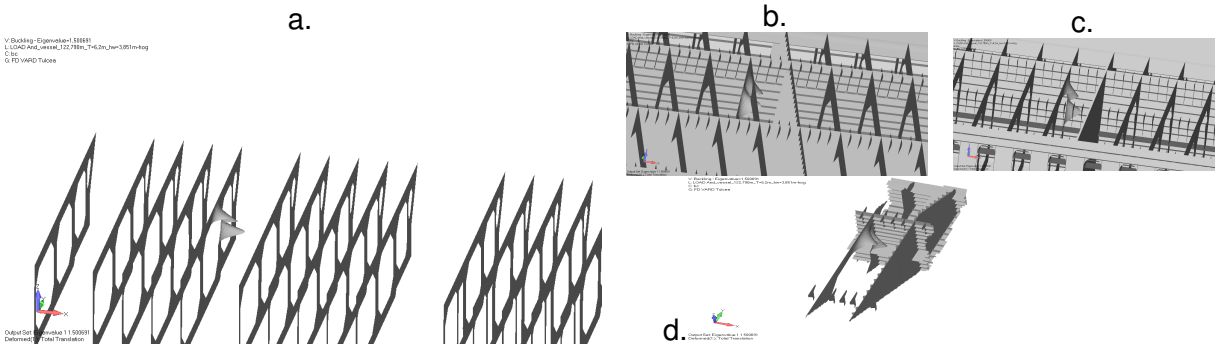

Figure 7.16.a., b., c., d. *Buckling criterion verification* (B=1.506910), *final case of docked 19,747 t mass, hogging wave type*, *hw*=3.851 m, *collapse at* FR. 24

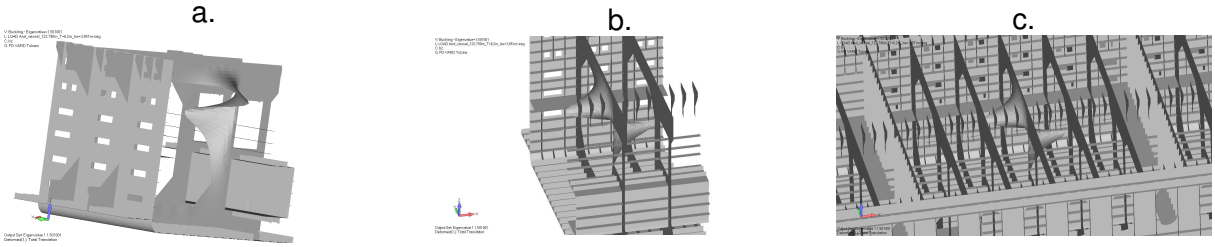

Figure 7.17.a., b., c. *Buckling criterion verification* (B=1.501001), *final case of docked 19,747 t mass, sagging wave type*, *hw*=3,851 m, *collapse at* FR. 92

7.2.3. 3D-FEM structural analysis for the case of docking at maximum capacity of 27,000 t

Tables 7.6. – 7.8., presents the evaluation of the criteria of the minimum freeboard and of the allowable stresses for the docking case at a maximum capacity of 27,000 t, in the following operating variants:

- Uniformly distributed mass (table 7.6.): No restrictions occur in the hogging type wave, and in the case of the sagging type wave, the restrictions are $h_{w\lim it}=2.173\ m$ (the criterion of allowable stresses), $h_{w\lim it}=2.271\ m$ (the criterion of vertical deformations), $h_{w\lim it}=3.668\ m$ (material flow limit);
- Mass with hogging distribution (table 7.7.): In the hogging type wave there are no restrictions, and in the case of the sagging type wave, the restrictions are: $h_{w\lim it}=3.471\ m$ (the criterion of allowable stresses), $h_{w\lim it}=3.048\ m$ (the criterion of vertical deformations),
- Mass with sagging distribution (table 7.8.): In the hogging type wave there are no restrictions, and in the case of the sagging type wave the restrictions are: $h_{w\lim it}=1.008\ m$ (the criterion of allowable stresses), $h_{w\lim it}=1.606\ m$ (the criterion of admissible deformations), $h_{w\lim it}=2.501\ m$ (material flow limit).

Figures 7.18. – 7.23, presents the von Mises equivalent stress diagrams and the vertical deformation diagram along the length of the ship, the distribution of the von Mises equivalent stresses and the vertical deformations on the 3D-FEM model in the rail area, for the wave height corresponding to the notations in tables 7.6 - 7.8., in the cases of sagging and hogging type waves, for each of the three docking scenarios with a maximum capacity of 27,000 t.

Table 7.6. Minimum freeboard, von Mises equivalent stresses and maximum vertical deformations, for the case of docking at a maximum capacity of 27,000 t, with a uniform distribution of the mass, with requests from equivalent quasi-static hogging and sagging waves

Case	$h_w[m]$	$T_{Pp}[m]$	$T_{Pv}[m]$	$F_{Pp}[m]$	$\frac{F_{Pp}}{adm}$	$F_m[m]$	$\frac{F_m}{adm}$	$F_{Pv}[m]$	$\frac{F_{Pv}}{adm}$	$\sigma_{vM}[MPa]$	$\frac{\sigma_{vM}}{adm}$	$w[mm]$	$\frac{w}{adm}$
SW	0	6.200	6.200	3.900	>1	3.900	>1	3.900	>1	223.285	0.534	-185	0.442
hogging	3.668	6.358	5.891	5.576	>1	2.141	>1	6.043	>1	232.337	0.795	221	0.529
sagging	2.173	6.095	6.381	2.919	>1	4.949	>1	2.632	>1	292.000	1.000	-408	0.976
	3.668	6.021	6.503	2.245	>1	5.672	>1	1.173	>1	355.000	1.215	-564	1.49

Table 7.7. Minimum freeboard, von Mises equivalent stresses and maximum vertical deformations, for the case of docking at a maximum capacity of 27,000 t, with a hogging distribution of the mass, with requests from quasi-static hogging and sagging waves

Case	$h_w[m]$	$T_{Pp}[m]$	$T_{Pv}[m]$	$F_{Pp}[m]$	$\frac{F_{Pp}}{adm}$	$F_m[m]$	$\frac{F_m}{adm}$	$F_{Pv}[m]$	$\frac{F_{Pv}}{adm}$	$\sigma_{vM}[MPa]$	$\frac{\sigma_{vM}}{adm}$	$w[mm]$	$\frac{w}{adm}$
SW	0	6.200	6.200	3.900	>1	3.900	>1	3.900	>1	227.372	0.534	-105	0.442
hogging	4.492	6.394	5.819	5.952	>1	1.748	>1	6.527	>1	229.206	0.784	383	0.916
sagging	3.048	6.051	6.453	2.525	>1	5.372	>1	2.123	>1	274.177	0.939	-418	1.000
	3.471	6.031	6.487	2.334	>1	5.577	>1	1.877	>1	292.000	1.000	-463	1.108

Table 7.8. Minimum freeboard, von Mises equivalent stresses and maximum vertical deformations, for the case of docking at a maximum capacity of 27,000 t, with a sagging distribution of the mass, with requests from quasi-static hogging and sagging waves

Case	$h_w[m]$	$T_{Pp}[m]$	$T_{Pv}[m]$	$F_{Pp}[m]$	$\frac{F_{Pp}}{adm}$	$F_m[m]$	$\frac{F_m}{adm}$	$F_{Pv}[m]$	$\frac{F_{Pv}}{adm}$	$\sigma_{vM}[MPa]$	$\frac{\sigma_{vM}}{adm}$	$w[mm]$	$\frac{w}{adm}$
Sw	0	6.200	6.200	3.900	>1	3.900	>1	3.900	>1	255.514	0.534	-225	0.442
hogging	4.492	6.394	5.819	5.952	>1	1.748	>1	6.527	>1	253.706	0.869	245	0.586
sagging	1.008	6.152	6.284	3.444	>1	4.386	>1	3.312	>1	292.000	1.000	-357	0.854
	1.606	6.122	6.334	3.175	>1	4.675	>1	2.963	>1	317.237	1.086	-418	1.000
	2.501	6.078	6.408	2.771	>1	5.107	>1	2.441	>1	355.000	1.215	-511	1.222

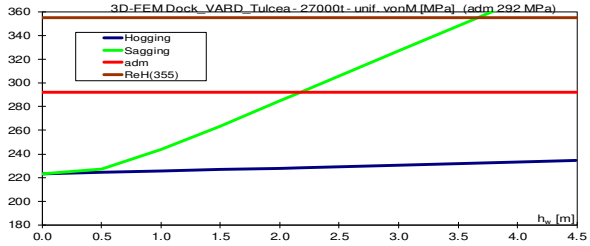

Figure 7.18. Maximum value for equivalent von Mises stress, for the case of docking at a maximum capacity of 27,000 t, with a uniform distribution of the mass

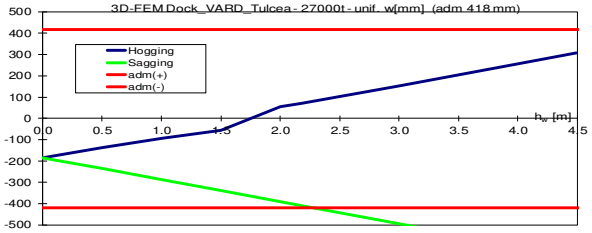

Figure 7.19. Maximum deflection values, for the case of docking at a maximum capacity of 27,000 t, with a uniform distribution of the mass

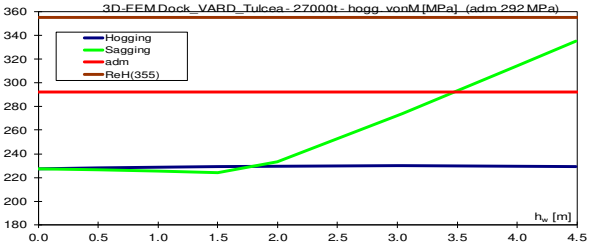

Figure 7.20. Maximum value for equivalent von Mises stress, for the case of docking at a maximum capacity of 27,000 t, with a hogging distribution of the mass

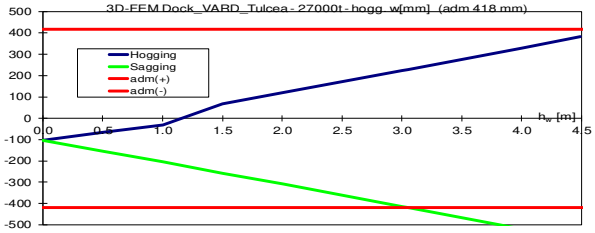

Figure 7.21 Maximum deflection values, for the case of docking at a maximum capacity of 27,000 t, with a hogging distribution of the mass

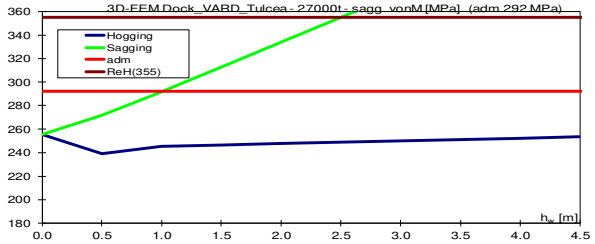

Figure 7.22. Maximum value for equivalent von Mises stress, for the case of docking at a maximum capacity of 27,000 t, with a sagging distribution of the mass

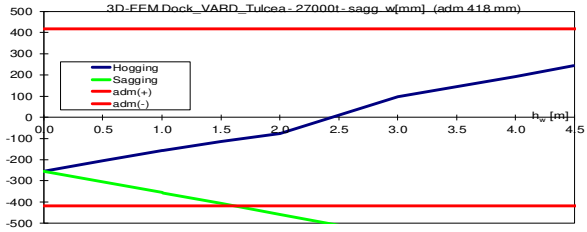

Figure 7.23. Maximum deflection values, for the case of docking at a maximum capacity of 27,000 t, with a sagging distribution of the mass

For all three cases analysed, in this subchapter, the criterion of the minimum freeboard is satisfied. *The docking case at the maximum capacity of 27000 t, with a sagging distribution of the mass, represents the extreme operating situation of the Dock_Vard_Tulcea floating dock*.

7.2.4. Conclusions on the structural analysis of the large floating dock Dock_VARD_Tulcea

The results of the analysis of the Dock_VARD_Tulcea floating dock [9], (subchapter 4.2.), in different operating cases (subchapters 7.2.1., .7.2.2., 7.2.3.) in quasi-static equivalent waves [1], they are summarized in table 7.9., as well as in the following conclusions:

- We made a 3D-FEM structural model, of the large floating dock [9], extended over its entire length, in a single board using FEMAP NX/Nastran software [42], with about 11 million degrees of freedom. To find out the balancing parameters dock - wave, an equivalent 1D beam model was made (table 4.9.), using their own codes and procedures for transferring data from 1D to 3D and vice versa [28], using the theoretical model in chapter 2.2 (Annexes 6 - 9).
- For the case without load, subchapter 3.2., corresponding to the case without docked ship, the dock is only ballasted for achieving of the 6.2 m draft, for any operating conditions in still water or wave. In this case, the vertical deformation criterion is not

satisfied, resulting in the wave height of 3.867 m, characteristic of a case of unrestricted operation for river navigation, and 40% restricted navigation on a coastal route.

- For the operating cases, made available by the VARD Shipyard in Tulcea [9], the mass of the docked ship is 19,747 t, with 7 different docking steps, in the case of still water, resulting in no operating restrictions. In case of analysis under wave conditions, when relocating the dock with the ship loaded on board, mainly the criterion of vertical deformation is not satisfied, resulting in the wave height of 3.851 m, characteristic of a case of unrestricted operation for river navigation, and with 40% restriction on a coastal route.
- For the extreme operating case, corresponding to the maximum docking capacity of 27,000 t, distributed according to the rules of the classification society [1], Significant restrictions appear in the case of sagging type waves, from the criteria of allowable stresses or vertical deformations. In the case of uniformly distributed mass or hogging type, the limit height of the wave is 2.173 – 3.048 m, in the case of coastal navigation resulting in a 20-30% restriction. In the case of the distribution of the docked mass of type sagging, the limit height of the wave is 1.008 m higher than 0.6 m, so without restrictions in case of use by the shipyard only in its water area.
- For all cases, high stress concentrators are identified at the level of the docking deck, at the airtight frames of the ballast towers above the level of the main deck, places where additional stiffening elements have been added.

Table 7.9. The operating conditions of the Dock-Vard Tulcea dock resulted from the structural analysis on 3D-FEM models, with requests from quasi-static equivalent meeting – following waves

Docking case	Light *T*6.2m	D19747t *T*6.2m	D27000t hogg. *T*6.2m	D27000t unif. *T*6.2m	D27000t sagg. *T6.*2m
$h_{w\ limit}$ [m]	3.867	3.851	3.048	2.173	1.008
Criterion	Vertical deformation w_{adm}, sagging EDW			Equivalent von Mises stress σ_{adm}, sagging EDW	
Inland	IN(2.0)	IN(2.0)	IN(2.0)	IN(2.0)	IN(1.0)
Costal	≈RE(40%)	≈RE(40%)	≈RE(30%)	≈RE(20%)	Sheltered operation

CHAPTER 8

EVALUATING OF THE OPERATING CAPACITY OF THE FLOATING DOCK DOCK_VARD_TULCEA, BASED ON THE CRITERIA FOR OSCILLATIONS IN EXTREME RANDOM WAVES AND TRANSVERSE STABILITY

This chapter first studies the condition of transit at the river and coastal navigation of the Dock_VARD_Tulcea floating dock, evaluated by the dynamics of the ship in real sea criteria - seakeeping. According to the random-wave navigation scenario, they are modelled in the short term using the power spectral density function with an ITTC parameter [58], [59], with the maximum significant wave height of 2 m for the river and 4.942 m for the coastal conditions, according to the norms of the ship classification companies at the length of 209.2 m of the dock [1], [3]. The maximum speed in transit of the dock, when relocating between two ports, is 12 km/h. The transit status of the floating dock is evaluated for several ballast cases, with a draft of 5.2 m; 6.2 m and 7.2 m, having the vertical position of the centre of gravity between 6 m and 16 m. Numerical analysis is performed using the DYN software [45], based on the hydrodynamic model presented in subchapter 2.4. The seakeeping criteria are interpreted in statistical terms of allowable values of the amplitude of movement and of acceleration. **The numerical results of this study evaluate the seakeeping criteria in different transit states of the floating dock and are published and presented in the reference article [60].**

In the second part of the chapter is carried out the evaluation of the safe operating capacity of the Dock_VARD_Tulcea floating dock, based on the criterion of intact transverse stability, according to the rules [1], using the *D_LDF* program *(Annex 4)*, based on the theoretical model presented in subchapter 2.1.5., for the same scenarios from analysis to seakeeping.

8.1. Short-term oscillation analysis of the floating dock Dock_VARD_Tulcea, in the river and coastal navigation area

In this subchapter we have analysed the safety of the floating dock Dock_VARD_Tulcea relocation operation, without docked mass, on river or coastal routes, from the point of view of the dynamic behaviour in random waves, based on the criteria for seakeeping (navigation) and of the theoretical model presented in subchapter 2.4.

The handling of the Dock_VARD_Tulcea floating dock, it is considered to be made with the help of a 4,000 H.P. river – sea tugboat [77]. The resistance of the tugboat - dock system is analysed by a theoretical model, with the tow cable long enough to allow the hypothesis of decoupled analysis of the dynamics of the dock and the tugboat.

Figure 8.1. presents the diagram of the drag of the tugboat and floating dock during navigation operations, under calm water conditions. From the analysis of the strength of the tugboat-dock system, a maximum towing speed of 12 km/h results, the analysis included the cases of 0 and 6 km / h. During the relocation operation, the floating dock is considered ballasted, in three cases, with the draft values of 5.2 m; 6.2 m; 7.2 m, according to table 8.1. According to the floating dock ballast scheme, the centre of gravity changes its vertical position between 6 m and 16 m, resulting in significant differences in terms of transverse stability characteristics, presented in table 8.2. and figures 8.9. - 8.11.a., which can be considered linear in any load case for the maximum roll angle of 6°. The numerical analysis of the floating dock during the relocation on the river and coastal route is performed with the DYN software [45].

Table 8.1. The characteristics of the floating dock Dock-VARD Tulcea, at the relocation operation

	Case 1	Case 2	Case 3
$L_{\max}[m]$	209.200		
$L_{CWL}[m]$	208.850	28.125	207.375
$T_m[m]$	7.2	6.2	5.2
$\nabla[m^3]$	7,587	66,338	55,162
$LCG[m]$	100.103	100.139	100.120
$z_G[m]$	6; 8; 10; 12; 14; 16		

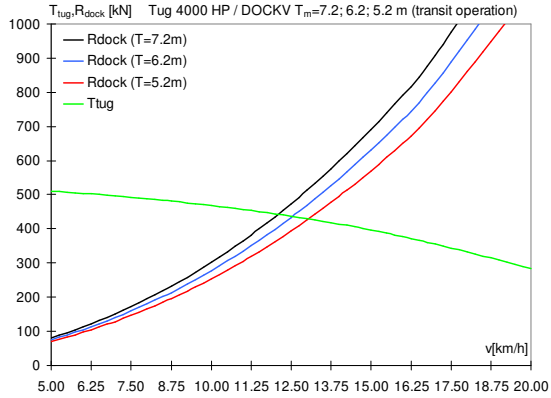

Figure 8.1. Drag resistance diagram for the tugboat - floating dock system, for the three relocation conditions

Table 8.2. Initial transverse metacentric height and roll angle corresponding to the maximum of the transverse static stability arm of the Dock_VARD_Tulcea floating dock

$z_G[m]$	$GM_{T_0}[m]$			$\varphi_{\max_{GZ}}[^\circ]$		
	Case 1	Case 2	Case 3	Case 1	Case 2	Case 3
	Figure 8.9.a.	Figure 8.10.a.	Figure 8.11.a.	Figure 8.9.a.	Figure 8.10.a.	Figure 8.11.a.
6	34.531	39.453	46.579	27.50	30.25	31.50
8	32.531	37.453	44.579	26.75	29.25	27.25
10	30.531	35.453	42.579	25.75	27.25	24.50
12	28.531	33.453	40.579	25.00	23.50	22.50
14	26.531	31.453	38.579	24.00	21.00	21.00
16	24.531	29.453	36.579	18.75	19.75	20.00

Random waves are modelled using the ITTC power spectral density function [58], [59], for a maximum significant wave height of 4.942 m, according to the norms of naval classification companies [1], [3].

Navigation safety for river and coastal transit operations, in the different relocation cases in tables 8.1. and 8.2., it is evaluated with respect to the limit of the significant height of the wave H_{slimit} *[m]* or the intensity limit of the sea in Beaufort degrees B_{limit}. The limit criteria are formulated in terms of the most probable RMS statistical values admissible for the amplitudes of the movements and accelerations at the vertical, pitch and roll oscillations of the floating dock (table 8.3.).

Table 8.3. The seakeeping limit criteria for the Dock_VARD_Tulcea floating dock, formulated for the components of heave, pitch and roll oscillations

Case	$RMS_{z\,max}$ [m]	$RMS_{\theta\,max}$ [rad]	$RMS_{\varphi\,max}$ [rad]	RMS_{axzmax} [m/s^2]	$RMS_{ac\theta\,max}$ [rad/s^2]	$RMS_{ac\varphi\,max}$ [rad/s^2]
1	2.6	0.03491	0.06981	0.981	0.00938	0.03212
2	3.6					
3	4.6					

8.1.1. Determining the response amplitude operators RAO to oscillations for the floating dock Dock_VARD_Tulcea

For the Dock_VARD_Tulcea floating dock, (figures 4.31. – 32., table 4.9.), based on the theoretical model, equations 2.18., using the DYN code [45], based on the significant wave height histogram, figure 2.7. – 8., the *RAO* response amplitude operators are obtained.

The floating dock is in transit on a river-maritime route, for three test speeds, v=0, 6, 12 km/h. The case with zero speed represents the tugboat damage situation during the towing of the dock. Three ballast conditions with six vertical positions of the centre of gravity are considered (tables 8.1.,8.2.). The heading angle of the dock - wave is considered in the range of $\mu = 0 - 180^0$ with the step $\delta\mu = 5^0$. For dynamic response in the field $\mu = 180 - 360^0$ the symmetry at the median plane of the floating dock is taken into account (figure 7.4.). The RAO response amplitude operators to heave, pitch and roll oscillations are calculated for the pulsation range of the wave ω = 0-3 rad / s and the step $\delta\omega$= 0.001 rad / s.

Figure 8.2.a., b., c. presents the RAO functions at vertical oscillations, for the dock - wave angle in the range from 0 to 180^0, and figure 8.5.b. presents the same function RAO at vertical oscillations for the 90^0 angle, a comparison for the three drafts. From the analysis of RAO functions to the heave oscillations (9 cases), it is found that the maximum value appears in the case of the transverse waves, figure 8.2.a. From figure 8.5.a. it turns out that due to the prismatic shape of the floating dock, the variation of the draft does not bring significant differences for the case of RAO functions at heave oscillations.

Figures 8.3.a., b., c. presents, like heave oscillations, the RAO response amplitude operators to pitch oscillations. From figure 8.5.b., it turns out that the maximum values for the pitch are in the case of the head waves, but significant values can also be observed in the case of following and oblique waves. Also, very low values are observed for the transverse wave case. In figure 8.5.b. you can see approximately identical values for the three different drafts, due to the prismatic shape of the dock.

Figures 8.4.a., b., c. presents the RAO response amplitude operator functions for roll oscillations, at the three 7.2 m, 6.2 m and 5.2 m drafts, at a speed of 12 km / h, for the entire range of angles dock - wave with vertical position of the centre of gravity z_G of 16 m. For all three drafts, the significant values of the roll oscillation are recorded for the transverse wave. Figure 8.4.1. presents RAO functions at roll oscillations for the full range of values of the vertical position of the centre of gravity z_G from 6 to 16 m. The maximum values for the roll oscillations are found in the case of the loading dock corresponding to the 5.2 m draft, and the minimum values in the case of loading for the 7.2 m draft.

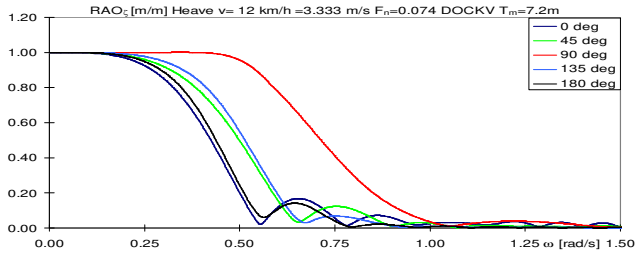

Figure 8.2.a RAO_ζ [m/m], heave, T_m=7.2m, v=12km/h, μ=0 - 180^0

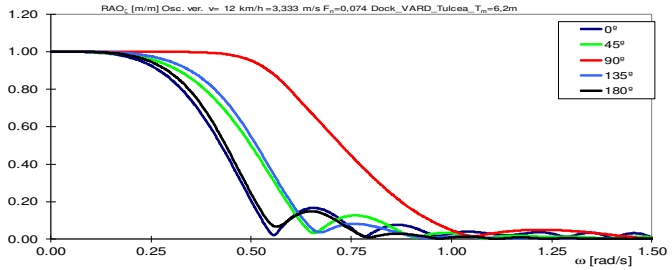

Figure 8.2.b. RAO_ζ [m/m], heave, T_m=6,2m, v=12km/h, μ=0 - 180^0

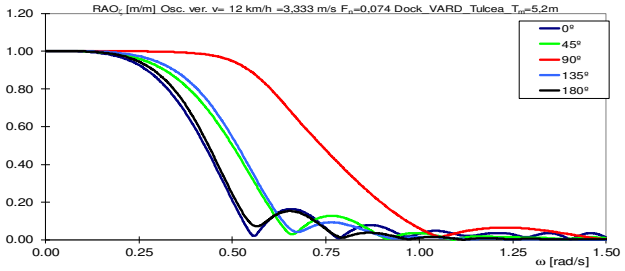

Figure 8.2.c. RAO_ζ [m/m], heave, T_m=5,2 m, v=12 km/h, μ=0 - 180^0

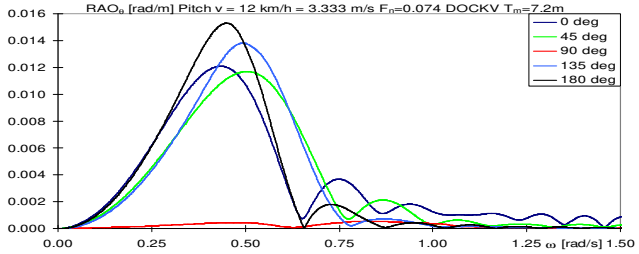

Figure 8.3.a. RAO_θ [rad/m], pitch, T_m=7.2m, v=12km/h, μ=0 - 180^0

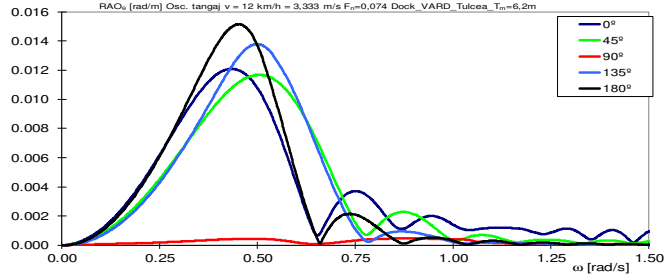

Figure 8.3.b. RAO_θ [rad/m], pitch, T_m=6,2m, v=12km/h, μ=0 - 180^0

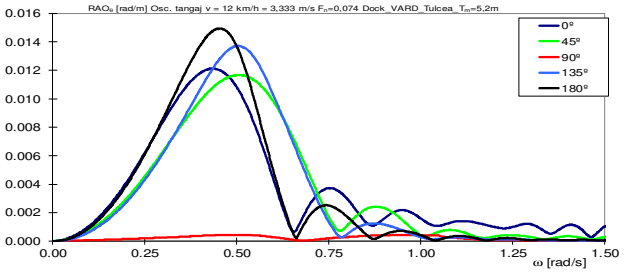

Figure 8.3.c. RAO_θ [rad/m], pitch, T_m=5,2m, v=12km/h, μ=0 - 180^0

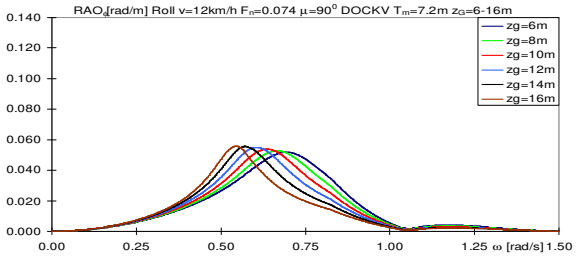

Figure 8.4.1.a. RAO_φ [rad/m], roll, T_m=7.2m, v=12km/h, z_G =6 - 16m

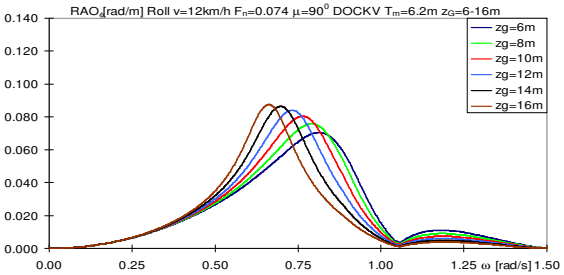

Figure 8.4.1.b RAO_φ [rad/m], roll, T_m=6.2m, v=12km/h, z_G =6 - 16m

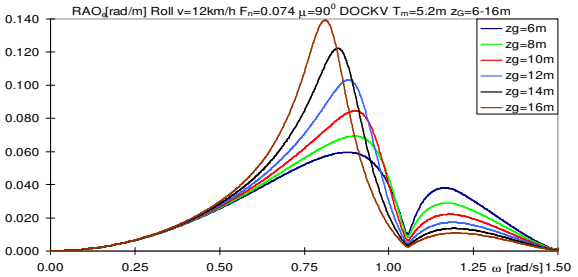

Figure 8.4.1.c. RAO_φ [rad/m], roll, T_m=5.2m, v=12km/h, z_G =6 - 16m

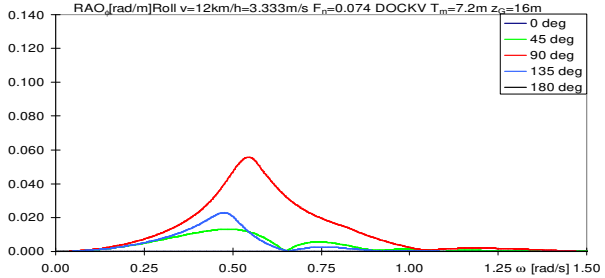

Figure 8.4.2.a. *RAO*$_{\varphi}$ [rad/m], roll, T_m=7.2m, v=12km/h, z_G =16m

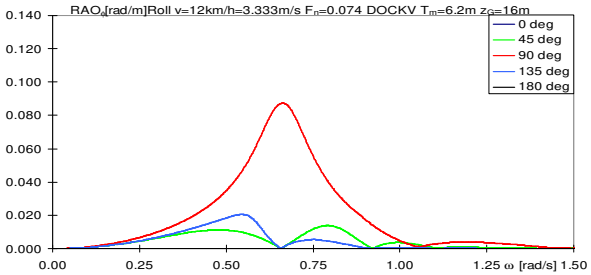

Figure 8.4.2.b. *RAO*$_{\varphi}$ [rad/m], roll, T_m=6.2m, v=12km/h, z_G =16m

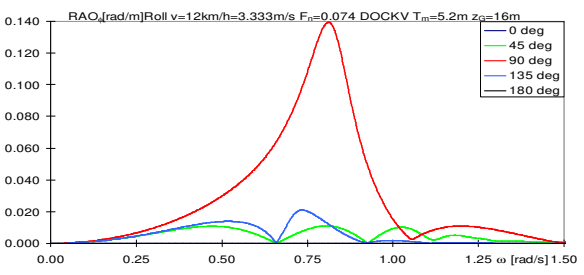

Figure 8.4.2.c. *RAO*$_{\varphi}$ [rad/m], roll, T_m=5.2m, v=12km/h, z_G =16m

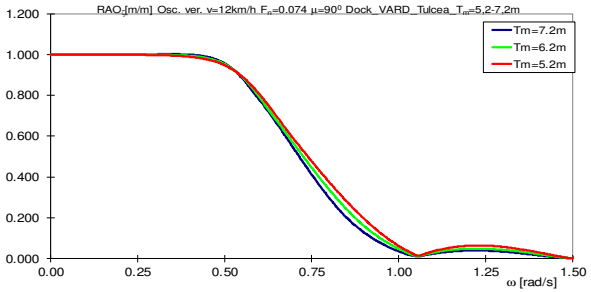

Figure 8.5.a RAO$_{\zeta}$ [m/m], heave, T_m=5.2 – 7.2m, v=12km/h, μ=90^0

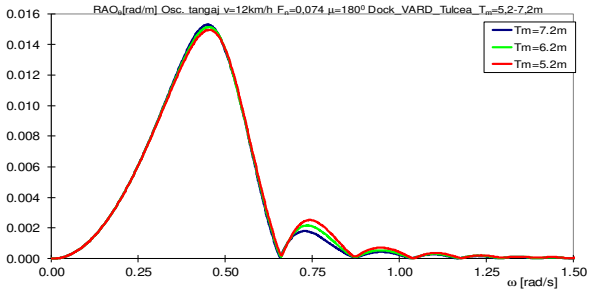

Figure 8.5.b. RAO$_{\theta}$ [rad/m], pitch, T_m=5.2 - 7,2m, v=12km/h, μ=90^0

8.1.2. Analysis of the short-term statistical response for the floating dock Dock_VARD_Tulcea

To evaluate the dynamics of the floating dock (Figure 7.4.) in random waves in the case of the river-maritime navigation scenario, based on the RAO response amplitude operator functions from the previous subchapter and the power spectral density function of the ITTC wave (equation 2.19., figures 2.7. - 8.), the values of the most likely RMS response to the oscillations of heave, pitch and roll oscillations, as well as their accelerations, are obtained (equation 2.20. - 22.). By imposing the limit criteria on the dynamics of the ship in the real sea - seakeeping (table 2.3., table 8.3., equation 2.23. – 25.), it results the operating restrictions of the floating dock expressed by the limit value of the significant height of the wave H_{slimit} *[m]* and the limit value of sea intensity in Beaufort degrees B_{limit}, for all loading and speed cases (table 8.1.).

Tables 8.4., 8.5. and 8.6. presents the most probable statistical values of the amplitudes of RMS oscillations and accelerations, for the three loading cases. For all loading cases and the values of the vertical position of the centre of gravity z_G, it turns out that the speed from 0 to 12 km/h has a hydrodynamic influence on the reduced roll oscillations. Considering the reference to the limit criteria for roll oscillations it can be concluded that the roll is maximum in case 3 of loading (-29.26% - +47.83%), average for case 2 of loading (-22.77% - -2.32%), and minimum for case 1 of loading (-58.04% - -31.53%).

Figures 8.6.a., b. and tables 8.4., 8.7. presents the seakeeping limits for the first ballast case associated with the 7.2 m draft, at all three values of the towing speed of the dock. In the case of the statistical response most likely the movements and accelerations of pitch and roll the limit criteria are satisfied.

Although the criterion of vertical acceleration is satisfied, because the freeboard is reduced ($RMS_{z\ max}$ =2.6 m), at the stern and at the bow of the dock, the criterion of the heave oscillations becomes a restriction in the case of the transverse and oblique wave, μ=30-150^0.

The influence of the vertical position of the centre of gravity on the navigation restrictions, are average in the case of the wave, small in the case of oblique waves and without influence in the case of meeting and following waves, at dock - wave angles of μ=155 - 180^0 and 0 - 25^0, when the roll oscillation becomes reduced or almost non-existent (figures 8.7.a., b.).

Figures 8.7.a., b. and tables 8.5., 8.8. presents the results of the second ballast case, at the three speeds. Similar to the previous ballast case, the criteria for pitch and roll movements, as well as all the criteria for acceleration, are met across the range of dock - wave heading angles.

The value of the freeboard is an intermediate one ($RMS_{z\ max}$ =3.6 m), such that, the only restrictions are generated by the criterion of heave oscillations, in the range of dock - wave heading angles from 60 to 120 degrees, transverse and oblique waves. Compared to the first ballast case, the significant height of the limit wave is higher, H_{slimit}[m]=4.204 > 3.620 m (tables 8.5, 8.8.), because the freeboard is larger by 1 m (table 8.3.), although the values of vertical and roll oscillations are much higher in this case (table 8.8.). From the point of view of the influence of the vertical position of the centre of gravity z_G, this is average in the cases of the transverse and oblique wave, without influences in the case of the head, following and oblique waves for the heading angle of μ=125 - 180^0 and 0 - 55^0.

Figures 8.8.a., b., and tables 8.6., 8.9. presents the limits of seakeeping criteria for the third ballast case. In this case, the freeboard is the largest, $RMS_{z\ max}$= 4.6 m, so that the criteria of vertical oscillations and accelerations are met under all conditions. Also, the same result can be observed in the case of oscillations and pitch accelerations. The only restrictions appear in the case of roll oscillations and accelerations (tables 8.8., 8.9.), at the oblique and transverse waves 75 - 105^0. The influence of the vertical position of the centre of gravity z_G appears for the cases of transverse waves, without influence in the case of the waves of encounter, following or oblique μ=110 – 180^0 or 0 – 70^0, with a limitation of the significant height of the wave H_{slimit}=2.713 m.

Table 8.4. Statistical values the most probable maximum RMS amplitudes for the movements and accelerations of the roll oscillations, at the draft of T_m=7.2m

v[km/h]	z_G[m]	ϕ_{RMS}[rad]	%	ϕ_{acRMS}[rad/s^2]	%
adm	-	0.06981	-	0.03212	-
0 (F_n=0)	6	0.039018	-44.11	0.013475	-58.04
	8	0.042231	-39.51	0.015616	-51.38
	10	0.044683	-36.00	0.017628	-45.11
	12	0.046299	-33.68	0.019383	-39.65
	14	0.047132	-32.49	0.020838	-35.12
	16	0.047321	-32.22	0.021977	-31.57
6 (Fn= 0.037)	6	0.039213	-43.83	0.013517	-57.91
	8	0.042431	-39.22	0.015670	-51.21
	10	0.044883	-35.71	0.017692	-44.91
	12	0.046489	-33.41	0.019453	-39.43
	14	0.047306	-32.24	0.020871	-35.01
	16	0.047475	-32.00	0.021916	-31.76
12 (F_n= 0.074)	6	0.039412	-43.55	0.013561	-57.78
	8	0.042636	-38.93	0.015726	-51.04
	10	0.045086	-35.42	0.017758	-44.71
	12	0.046682	-33.13	0.019525	-39.21
	14	0.047482	-31.99	0.020945	-34.78
	16	0.047631	-31.77	0.021989	-31.53

Table 8.5. Statistical values the most probable maximum RMS amplitudes for the movements and accelerations of the roll oscillations, at the draft of T_m=6.2m

v[km/h]	z_G[m]	ϕ_{RMS}[rad]	%	ϕ_{acRMS}[rad/s^2]	%
adm	-	0.06981	-	0.03212	-
0 (F_n=0)	6	0.053920	-22.77	0.028110	-12.48
	8	0.056936	-18.45	0.029900	-6.90
	10	0.059886	-14.22	0.030023	-6.52
	12	0.062410	-10.60	0.030829	-4.01
	14	0.064140	-8.13	0.031030	-3.38
	16	0.064711	-7.31	0.031267	-2.65
6 (Fn=0.037)	6	0.054013	-22.63	0.028235	-12.09
	8	0.057062	-18.26	0.029926	-6.82
	10	0.060051	-13.98	0.030147	-6.13
	12	0.062617	-10.31	0.030916	-3.74
	14	0.064389	-7.77	0.031047	-3.33
	16	0.064996	-6.90	0.031290	-2.57
12 (F_n=0.074)	6	0.054108	-22.50	0.028362	-11.69
	8	0.057190	-18.08	0.029995	-6.60
	10	0.060218	-13.74	0.030304	-5.64
	12	0.062826	-10.01	0.030915	-3.74
	14	0.064640	-7.41	0.031147	-3.02
	16	0.065286	-6.48	0.031370	-2.32

Table 8.6. Statistical values the most probable maximum RMS amplitudes for the movements and accelerations of the roll oscillations, at the draft of T_m=5.2m

v[km/h]	z_G[m]	ϕ_{RMS}[rad]	%	ϕ_{acRMS}[rad/s^2]	%
adm	-	0.06981	-	0.03212	-
0 (F_n=0)	6	0.049386	-29.26	0.031108	-3.14
	8	0.053044	-24.02	0.033109	3.09
	10	0.058344	-16.43	0.036480	13.59
	12	0.065212	-6.59	0.040557	26.28
	14	0.072999	4.56	0.044416	38.30
	16	0.081248	16.38	0.047316	47.33
6 (Fn= 0.037)	6	0.049402	-29.24	0.031129	-3.08
	8	0.053074	-23.98	0.033141	3.19
	10	0.058401	-16.35	0.036536	13.76
	12	0.065312	-6.45	0.040648	26.56
	14	0.073155	4.79	0.044544	38.69
	16	0.081472	16.70	0.047398	47.58
12 (F_n= 0.074)	6	0.049419	-29.21	0.031149	-3.01
	8	0.053110	-23.93	0.033798	5.23
	10	0.058597	-16.07	0.037525	16.84
	12	0.065367	-6.37	0.041504	29.23
	14	0.073312	5.01	0.044982	40.06
	16	0.081698	17.02	0.047479	47.83

Table 8.7. Limit values of significant wave height $H_{s\ limit}$[m] and sea state in Beaufort degrees B_{limit} to ensure the safety of the Dock_VARD_Tulcea floating dock, at the draft of T=7.2m

z_G[m]		*6*		*8*		*10*		*12*		*14*		*16*	
v[km/h]	*μ[°]*	*$H_{s\ limit}$*	*B_{limit}*	*$H_{s\ limit}$*	*B_{limit}*	*$H_{s\ limit}$*	*B_{limit}*	*$H_{s\ limit}$*	*B_{limit}*	*$H_{s\ limit}$*	*B_{limit}*	*$H_{s\ limit}$*	*B_{limit}*
0	*0*	*4.942*	*7.55*	*4.942*	*7.55*	*4.942*	*7.55*	*4.942*	*7.55*	*4.942*	*7.55*	*4.942*	*7.55*
	45	*4.624*	*7.33*	*4.634*	*7.34*	*4.640*	*7.34*	*4.646*	*7.35*	*4.768*	*7.43*	*4.660*	*7.36*
	70	*3.920*	*6.80*	*3.896*	*6.78*	*3.890*	*6.78*	*3.900*	*6.79*	*3.921*	*6.81*	*3.946*	*6.83*
	90	*4.152*	*7.01*	*4.034*	*6.91*	*3.935*	*6.82*	*3.859*	*6.75*	*3.808*	*6.71*	*3.779*	*6.68*
	110	*3.947*	*6.83*	*3.877*	*6.77*	*3.821*	*6.72*	*3.782*	*6.68*	*3.759*	*6.66*	*3.750*	*6.65*
	135	*4.467*	*7.22*	*4.452*	*7.21*	*4.447*	*7.21*	*4.451*	*7.21*	*4.459*	*7.22*	*4.467*	*7.22*
	180	*4.942*	*7.55*	*4.942*	*7.55*	*4.942*	*7.55*	*4.942*	*7.55*	*4.942*	*7.55*	*4.942*	*7.55*
6	*0*	*4.942*	*7.55*	*4.492*	*7.55*	*4.942*	*7.55*	*4.942*	*7.55*	*4.492*	*7.55*	*4.492*	*7.55*
	45	*4.601*	*7.32*	*4.618*	*7.33*	*4.629*	*7.34*	*4.634*	*7.34*	*4.637*	*7.34*	*4.641*	*7.34*
	70	*3.914*	*6.80*	*3.874*	*6.76*	*3.853*	*6.75*	*3.850*	*6.74*	*3.861*	*6.75*	*3.880*	*6.77*
	90	*4.165*	*7.02*	*4.064*	*6.92*	*3.946*	*6.83*	*3.870*	*6.76*	*3.819*	*6.72*	*3.790*	*6.69*
	110	*3.923*	*6.81*	*3.860*	*6.75*	*3.813*	*6.71*	*3.784*	*6.68*	*3.772*	*6.67*	*3.773*	*6.67*
	135	*4.461*	*7.22*	*4.459*	*7.22*	*4.466*	*7.22*	*4.476*	*7.23*	*4.485*	*7.24*	*4.490*	*7.24*
	180	*4.942*	*7.55*	*4.942*	*7.55*	*4.942*	*7.55*	*4.942*	*7.55*	*4.942*	*7.55*	*4.942*	*7.55*
12	*0*	*4.942*	*7.55*	*4.942*	*7.55*	*4.942*	*7.55*	*4.942*	*7.55*	*4.942*	*7.55*	*4.492*	*7.55*
	45	*4.606*	*7.32*	*4.618*	*7.33*	*4.633*	*7.34*	*4.644*	*7.35*	*4.650*	*7.35*	*4.652*	*7.35*
	70	*3.914*	*6.80*	*3.862*	*6.75*	*3.827*	*6.72*	*3.811*	*6.71*	*3.810*	*6.71*	*3.821*	*6.72*
	90	*4.161*	*7.01*	*4.041*	*6.91*	*3.942*	*6.82*	*3.866*	*6.76*	*3.815*	*6.71*	*3.787*	*6.69*
	110	*3.900*	*6.79*	*3.846*	*6.74*	*3.811*	*6.71*	*3.794*	*6.69*	*3.794*	*6.69*	*3.806*	*6.70*
	135	*4.478*	*7.23*	*4.489*	*7.24*	*4.503*	*7.25*	*4.513*	*7.26*	*4.518*	*7.26*	*4.519*	*7.26*
	180	*4.942*	*7.55*	*4.942*	*7.55*	*4.942*	*7.55*	*4.942*	*7.55*	*4.942*	*7.55*	*4.942*	*7.55*

Table 8.8. Limit values of significant wave height $H_{s\ limit}$[m] and sea state in Beaufort degrees B_{limit} to ensure the safety of the Dock_VARD_Tulcea floating dock, at the draft of T=6.2m, towed by fluvial – maritime tugboat

z_G[m]		6		8		10		12		14		16	
v[km/h]	μ[°]	$H_{s\ limit}$	B_{limit}	$H_{s\ limit}$	B_{limit}	$H_{s\ limit}$	B_{limit}	$H_{s\ limit}$	B_{limit}	$H_{s\ limit}$	B_{limit}	$H_{s\ limit}$	B_{limit}
0	0	4.942	7.55	4.942	7.55	4.942	7.55	4.942	7.55	4.942	7.55	4.942	7.55
	45	4.942	7.55	4.942	7.55	4.942	7.55	4.942	7.55	4.942	7.55	4.942	7.55
	70	4.942	7.55	4.942	7.55	4.910	7.53	4.829	7.47	4.730	7.41	4.627	7.33
	90	4.722	7.40	4.609	7.32	4.508	7.25	4.431	7.20	4.392	7.17	4.397	7.18
	110	4.673	7.37	4.602	7.32	4.530	7.27	4.466	7.22	4.421	7.19	4.404	7.18
	135	4.942	7.55	4.942	7.55	4.942	7.55	4.942	7.55	4.942	7.55	4.942	7.55
	180	4.942	7.55	4.942	7.55	4.942	7.55	4.942	7.55	4.942	7.55	4.942	7.55
6	0	4.942	7.55	4.942	7.55	4.942	7.55	4.942	7.55	4.942	7.55	4.942	7.55
	45	4.942	7.55	4.942	7.55	4.942	7.55	4.942	7.55	4.942	7.55	4.942	7.55
	70	4.932	7.54	4.874	7.51	4.574	7.30	4.711	7.39	4.614	7.33	4.527	7.27
	90	4.740	7.41	4.625	7.33	4.521	7.26	4.442	7.21	4.401	7.18	4.405	7.18
	110	4.757	7.43	4.686	7.38	4.606	7.32	4.528	7.27	4.463	7.22	4.422	7.19
	135	4.942	7.55	4.942	7.55	4.942	7.55	4.942	7.55	4.942	7.55	4.942	7.55
	180	4.942	7.55	4.942	7.55	4.942	7.55	4.942	7.55	4.942	7.55	4.942	7.55
12	0	4.942	7.55	4.942	7.55	4.942	7.55	4.942	7.55	4.942	7.55	4.942	7.55
	45	4.942	7.55	4.942	7.55	4.942	7.55	4.942	7.55	4.942	7.55	4.942	7.55
	70	4.838	7.48	4.771	7.43	4.690	7.38	4.601	7.32	4.516	7.26	4.451	7.21
	90	4.730	7.41	4.615	7.33	4.510	7.25	4.431	7.20	4.390	7.17	4.393	7.17
	110	4.843	7.48	4.776	7.44	4.695	7.38	4.607	7.32	4.523	7.26	4.458	7.22
	135	4.942	7.55	4.942	7.55	4.942	7.55	4.942	7.55	4.942	7.55	4.942	7.55
	180	4.942	7.55	4.942	7.55	4.942	7.55	4.942	7.55	4.942	7.55	4.942	7.55

Table 8.9. Limit values of significant wave height $H_{s\ limit}$[m] and sea state in Beaufort degrees B_{limit} to ensure the safety of the Dock_VARD_Tulceafloating dock, at the draft of T=5.2m, towed by fluvial – maritime tugboat

z_G[m]		6		8		10		12		14		16	
v[km/h]	μ[°]	$H_{s\ limit}$	B_{limit}	$H_{s\ limit}$	B_{limit}	$H_{s\ limit}$	B_{limit}	$H_{s\ limit}$	B_{limit}	$H_{s\ limit}$	B_{limit}	$H_{s\ limit}$	B_{limit}
0	0	4.492	7.55	4.492	7.55	4.492	7.55	4.492	7.55	4.492	7.55	4.492	7.55
	45												
	70												
	75												
	80											4.150	7.01
	85							3.817	6.71	3.226	6.19	2.992	5.98
	90			4.528	7.27	3.632	6.55	3.069	6.05	2.798	5.74	2.723	5.64
	95			4.492	7.55	3.850	6.74	3.215	6.18	2.920	5.89	2.835	5.78
	100					4.492	7.55	4.341	7.14	3.637	6.55	3.354	6.30
	105							4.492	7.55	4.492	7.55	4.904	7.53
	110											4.492	7.55
	135												
	180												
6	0	4.492	7.55	4.492	7.55	4.492	7.55	4.492	7.55	4.492	7.55	4.492	7.55
	45												
	70												
	80									4.190	7.03		
	85					4.324	7.13	3.449	6.39	3.036	6.02	3.125	6.10
	90			4.516	7.26	3.620	6.54	3.057	6.04	2.788	5.72	2.733	5.66
	95			4.492	7.55	4.346	7.14	3.463	6.40	3.044	6.03	2.787	5.72
	100					4.492	7.55	4.492	7.55	4.227	7.06	3.176	6.15
	105									4.492	7.55	4.166	7.02
	110											4.492	7.55
	135												
	180												
12	0	4.492	7.55	4.492	7.55	4.492	7.55	4.492	7.55	4.492	7.55	4.492	7.55
	45												
	70												
	80											3.618	6.54
	85							4.332	7.13	3.478	6.41	2.889	5.85
	90			4.540	7.28	3.644	6.56	3.080	6.06	2.808	5.75	2.713	5.63
	95			4.320	7.12	3.491	6.42	3.028	6.01	2.823	5.77	2.895	5.86
	100			4.492	7.55	4.445	7.21	3.657	6.57	3.295	6.25	3.640	6.56
	105					4.492	7.55	4.492	7.55	4.746	7.42	4.492	7.55
	110									4.492	7.55		
	135												
	180												

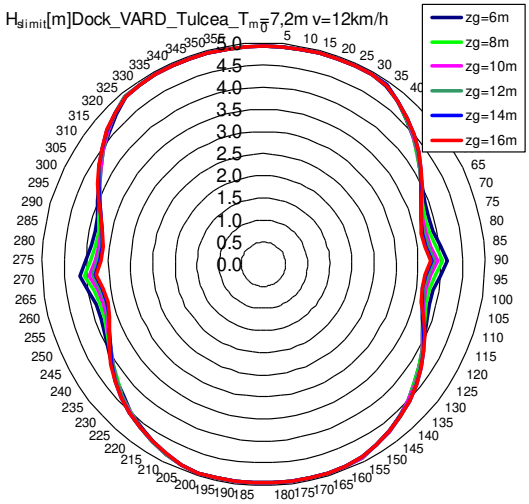

Figure 8.6.a. Polar diagram for the significant wave height limit H_S[m], T_m=7.2 m, v=12 km/h, z_G =6-16 m

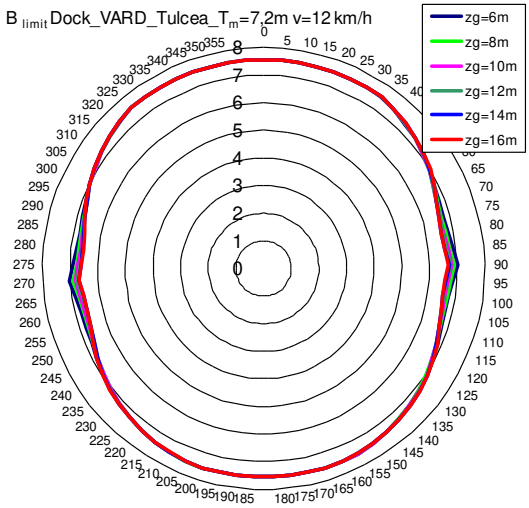

Figure 8.6.b. Polar diagram for the significant state in Beaufort degrees B limit, T_m=7.2 m, v=12 km/h, z_G =6-16 m

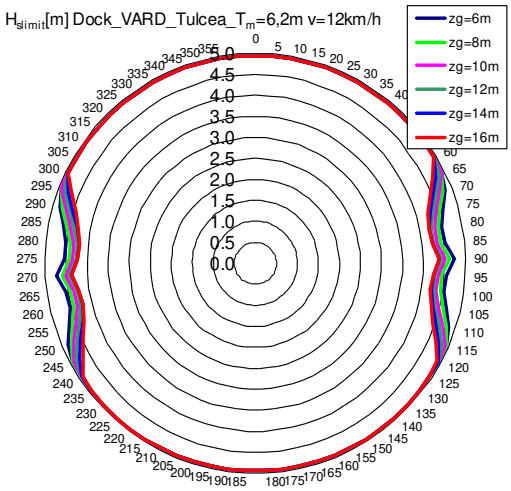

Figure 8.7.a. Polar diagram for the significant wave height limit H_S[m], T_m=6.2 m, v=12 km/h, z_G =6-16 m

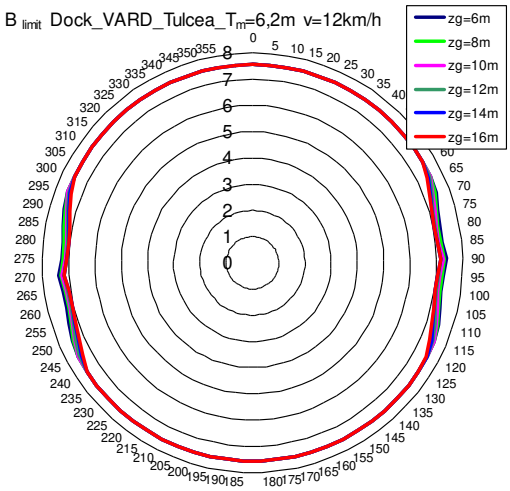

Figure 8.7.b. Polar diagram for the significant state in Beaufort degrees B limit, T_m=6.2 m, v=12km/h, z_G =6-16 m

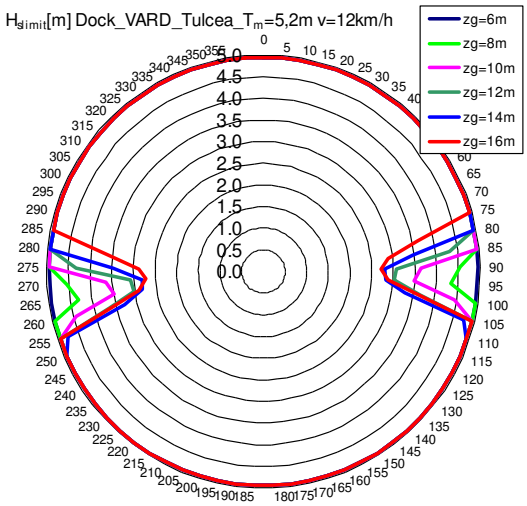

Figure 8.8.a. Polar diagram for the significant wave height limit H_S[m], T_m=5.2 m, v=12 km/h, z_G =6-16 m

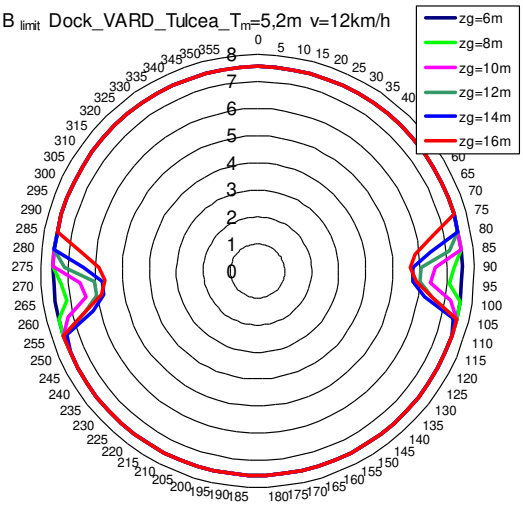

Figure 8.8.b. Polar diagram for the significant state in Beaufort degrees B limit, T_m=5.2 m, v=12 km/h,z_G=6-16 m

8.2. Analysis of the transversal stability of the floating dock Dock_VARD_Tulcea, taking into account the extreme weather conditions

In order to be able to evaluate the safe operating capacity of the Dock_VARD_Tulcea floating dock, with discontinuous side tanks, based on the criterion of intact transverse stability according to the rules of the ship classification companies [1], [3], we analysed the stability diagrams, from the figures:

- *Figures 8.9.a,b* - the curves of the static and dynamic stability arm, for case 1 of ballast / docking corresponding to the 7.2 m draft, with the variation of the vertical position of the centre of gravity z_G =6 – 16 m;
- *Figures 8.10.a,b* - the curves of the static and dynamic stability arm, for case 2 of ballast / docking corresponding to the 6.2 m draft, with the variation of the vertical position of the centre of gravity z_G =6 – 16 m;
- *Figures 8.11.a,b* - the curves of the static and dynamic stability arm, for the 3 ballast / docking case corresponding to the 5.2 m draft, with the variation of the vertical position of the centre of gravity z_G =6 - 16m.

The numerical results when evaluating the intact transverse stability criterion are:

- *Table 8.10.* - includes the evaluation of the general stability criterion and the dynamic - meteorological stability criterion (from wind and roll), for the case of the 7.2 m draft, with the variation of the position of the centre of gravity z_G =6 – 16 m ;
- *Table 8.11.* - includes the evaluation of the general stability criterion and the dynamic - meteorological stability criterion (from wind and roll), for the case of the 6.2 m draft, with the variation of the position of the centre of gravity z_G =6 – 16 m;
- *Table 8.12.* - includes the evaluation of the general stability criterion and the dynamic - meteorological stability criterion (from wind and roll), for the 5.2 m draft, with the variation of the position of the centre of gravity z_G =6 – 16 m;

The general criterion of stability is very well satisfied in all cases of variation of the draft, for the vertical position of the centre of gravity z_G from 6 to 16 m.

The dynamic - meteorological stability criterion (from wind and roll) leads to the following situations:

- For all draft cases, for the variation of the vertical position of the centre of gravity from 6 to 12 meters the criterion is satisfied, so the dock can be operated in an unprotected port or it can be relocated;
- For all draft cases, for the variation of the vertical position of the centre of gravity between 14 - 16 m, the meteorological criterion is not satisfied, so that the dock can only operate in protected ports, not allowing its relocation.

In *table 8.13.* a summary of the results obtained for the static and dynamic transverse stability criterion can be found.

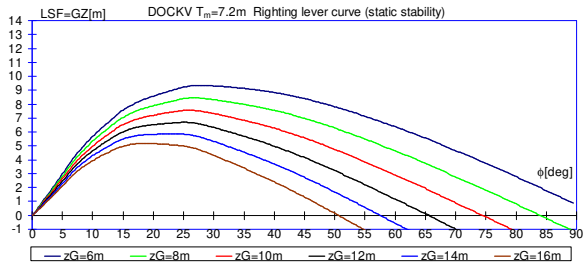

Figure 8.9.a. Righting lever curve for Dock_VARD_Tulcea, at draught de T_m=7.2m

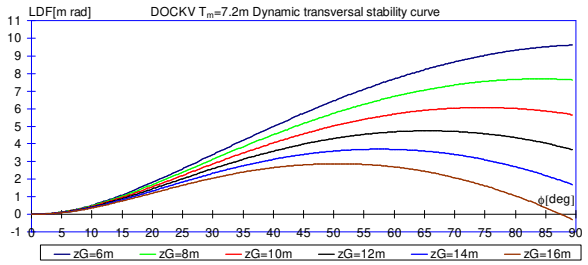

Figure 8.9.b. Dynamic transversal stability curve for Dock_VARD_Tulcea, at draught T_m=7.2m

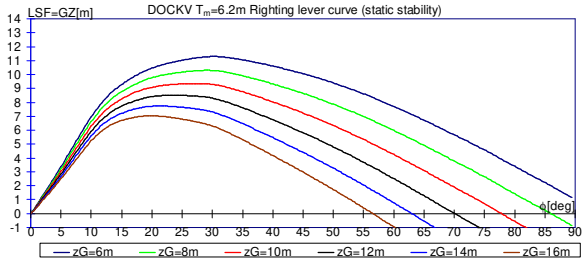

Figure 8.10.a. Righting lever curve for Dock_VARD_Tulcea, at draught de T_m=6.2m

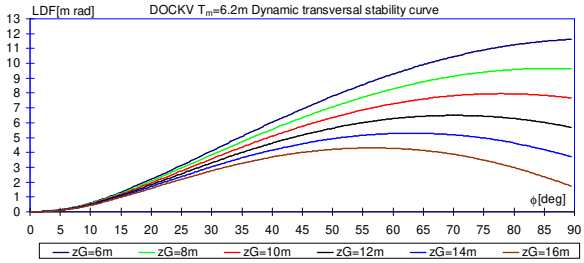

Figure 8.10.b. Dynamic transversal stability curve for Dock_VARD_Tulcea, at draught T_m=6.2m

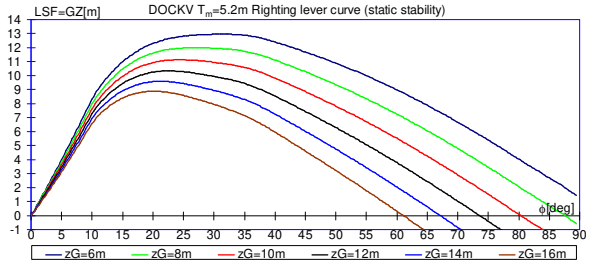

Figure 8.11.a. Righting lever curve for Dock_VARD_Tulcea, at draught de T_m=5.2m

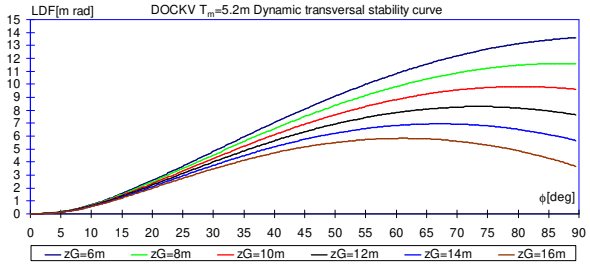

Figure 8.11.b. Dynamic transversal stability curve for Dock_VARD_Tulcea, at draught T_m=5.2m

Table 8.10. Verification of the intact transverse stability criterion, for the Dock_VARD_Tulcea floating dock, for case 1 at the draft of T_m=7.2 m

∇ [m³]	77587	77587	77587	77587	77587	77587
z_G[m]	6	8	10	12	14	16
h0=GM0[m]	34.531	32.531	30.531	28.531	26.531	24.531
>=1 m	YES	YES	YES	YES	YES	YES
LSF(30)= *GZ* (30)[m]	9.31716	8.31716	7.31716	6.31716	5.31716	4.31716
>=0.20 m	YES	YES	YES	YES	YES	YES
LDF(15deg)[mrad]	1.09760	1.02945	0.96130	0.89315	0.82500	0.75685
>=0.070 mrad	YES	YES	YES	YES	YES	YES
LDF(30deg)[mrad]	3.39827	3.13033	2.86238	2.59443	2.32648	2.05853
>=0.055 mrad	YES	YES	YES	YES	YES	YES
LDF(40deg)[mrad]	4.98943	4.52152	4.05361	3.58570	3.11779	2.64988
>=0.090 mrad	YES	YES	YES	YES	YES	YES
φ_st_max[º]	27.50	26.75	25.75	25.00	24.00	18.75
>=15 º	YES	YES	YES	YES	YES	YES
LSF(φ_max)= GZ (φ_max)[m]	9.356	8.442	7.554	6.693	5.859	5.162
>=0.25 m	YES	YES	YES	YES	YES	YES
LDF(φ_st_max) [mrad]	2.99069	2.65424	2.30842	2.02224	1.73267	1.09114
if *φ_st_max* < 30	0.0575	0.05825	0.05925	0.06	0.061	0.06625
	YES	YES	YES	YES	YES	YES
φ_steady (wind)	0.025105	0.026731	0.028585	0.030715	0.033185	0.036091
<=2 º	YES	YES	YES	YES	YES	YES
K_weather (wind and roll) (b/a)	1.28896	1.36525	1.18255	1.06089	0.97813	0.92272
>=1	YES	YES	YES	YES	**NO**	**NO**

Table 8.11. Verification of the intact transverse stability criterion, for the Dock_VARD_Tulcea floating dock, for case 2 at the draft of T_m=6.2 m

∇ [m^3]	66338	66338	66338	66338	66338	66338
z_G[m]	6	8	10	12	14	16
h0=GM0[m]	39.453	37.453	35.453	33.453	31.453	29.453
>=1 m	YES	YES	YES	YES	YES	YES
LSF(30)= *GZ* (30)[m]	11.30065	10.30065	9.30065	8.30065	7.30065	6.30065
>=0.20 m	YES	YES	YES	YES	YES	YES
LDF(15deg)[mrad]	1.32139	1.25324	1.18509	1.11694	1.04879	0.98065
>=0.070 mrad	YES	YES	YES	YES	YES	YES
LDF(30deg)[mrad]	4.10432	3.83637	3.56842	3.30047	3.03252	2.76457
>=0.055 mrad	YES	YES	YES	YES	YES	YES
LDF(40deg)[mrad]	6.02899	5.56108	5.09317	4.62526	4.15734	3.68943
>=0.090 mrad	YES	YES	YES	YES	YES	YES
φ_st_max[º]	30.25	29.25	27.25	24.00	21.25	20.00
>=15 º	YES	YES	YES	YES	YES	YES
LSF(φ_max)= GZ (φ_max)[m]	11.302	10.312	9.358	8.496	7.735	7.034
>=0.25 m	YES	YES	YES	YES	YES	YES
LDF(φ_st_max) [mrad]	4.15363	3.70144	3.11999	2.41727	1.87399	1.58474
if *φ_st_max* < 30 º	0.055	0.05575	0.05775	0.061	0.06375	0.065
	YES	YES	YES	YES	YES	YES
φ_steady (wind)	0.027821	0.029389	0.031146	0.033126	0.035373	0.037950
<=2 º	YES	YES	YES	YES	YES	YES
K_weather (wind and roll) (b/a)	1.58785	1.36341	1.17380	1.04706	0.95937	0.89827
>=1	YES	YES	YES	YES	**NO**	**NO**

Table 8.12. Verification of the intact transverse stability criterion, for the Dock_VARD_Tulcea floating dock, for case 3 at the draft of T_m=5,2 m

∇ [m^3]	55162	55162	55162	55162	55162	55162
z_G[m]	6	8	10	12	14	16
h0=GM0[m]	46.579	44.579	42.579	40.579	38.579	36.579
>=1 m	YES	YES	YES	YES	YES	YES
LSF(30)= *GZ* (30)[m]	12.94381	11.94381	10.94381	9.94381	8.94381	7.94381
>=0.20 m	YES	YES	YES	YES	YES	YES
LDF(15deg)[mrad]	1.56374	1.49559	1.42744	1.35929	1.29114	1.22299
>=0.070 mrad	YES	YES	YES	YES	YES	YES
LDF(30deg)[mrad]	4.81086	4.54291	4.27496	4.00702	3.73907	3.47112
>=0.055 mrad	YES	YES	YES	YES	YES	YES
LDF(40deg)[mrad]	7.04541	6.57750	6.10959	5.64168	5.17377	4.70586
>=0.090 mrad	YES	YES	YES	YES	YES	YES
φ_st_max[º]	31.50	27.25	24.50	22.50	21.00	20.00
>=15 º	YES	YES	YES	YES	YES	YES
LSF(φ_max)= GZ (φ_max)[m]	12.950	11.980	11.116	10.323	9.580	8.875
>=0.25 m	YES	YES	YES	YES	YES	YES
LDF(φ_st_max) [mrad]	5.14983	3.96858	3.21400	2.67406	2.27121	1.98354
if *φ_st_max* < 30 º	0.055	0.05775	0.0605	0.0625	0.064	0.065
	YES	YES	YES	YES	YES	YES
φ_steady (wind)	0.030484	0.031930	0.033518	0.035274	0.037224	0039400
<=2 º	DA	DA	DA	DA	DA	DA
K_weather (wind and roll) (b/a)	1.61169	1.31257	1.12711	1.00314	0.91669	0.85531
>=1	YES	YES	YES	YES	**NO**	**NO**

Table 8.13 Safe operating capacity of Dock_VARD_Tulcea floating dock evaluated based on intact transverse stability criterion

Case	T_m[m]	General stability	Weather criterion	Operation capabilities
1	7.2	satisfied	1.061 ÷ 1.365 >1	(z_G=6÷12 m) unsheltered harbour
		satisfied	not satisfied	sheltered harbour, no relocation
2	6.2	satisfied	1.047 ÷ 1.588 >1	(z_G=6÷12 m) unsheltered harbour
		satisfied	not satisfied	sheltered harbour, no relocation
3	5.2	satisfied	1.003 ÷ 1.612 >1	(z_G=6÷12 m) unsheltered harbour
		satisfied	not satisfied	sheltered harbour, no relocation

8.3. The conclusions of the dynamic analysis and the transverse stability of the large floating dock Dock_VARD_Tulcea

In order to evaluate the safety conditions when relocating the Dock_VARD_Tulcea floating dock we developed a numerical model with 280 sections and using the DYN software [45], with linear hydrodynamic formulation with the strip method (subchapter 2.4.) we have determined the functions of the RAO amplitude response operator for the main components of oscillation of the dock, heave, pitch and roll. For a transit scenario on a river-coastal route we modelled the irregular waves using the power spectral density function ITTC. Based on the criteria for seakeeping (table 8.3.), formulated in terms of the most probable admissible statistical values for the amplitudes of the heave, pitch and roll movements and accelerations, the operating limits of the short-term statistical floating dock are obtained, $H_{s\ limit}$ and B_{limit} , with a summary of the results in the tables 8.14. – 16.

The results of the short-term statistical analysis of Dock_VARD_Tulcea dock at the relocation operation, point out that the towing speed in the range 0 - 12 km/h has a reduced influence on the dynamic response in random waves (tables 8.14. – 16.). The influence of the vertical position of the centre of gravity of the dock, z_G = 6 - 16 m, on the dynamic response, it is significant at transverse waves, with a decrease in oblique waves and without effect at meeting or following waves.

Due to the lower freeboard, in the cases 1 and 2 of ballast the relocation restrictions of the dock are due to the vertical motions' criterion. In case 3 of ballast the movements and accelerations at the roll become maximum (tables 8.14. – 16.), so that the relocation restrictions of the dock are from the roll criteria. The limitations of the seakeeping criteria are always recorded in the case of transverse waves, as well as in oblique waves when the freeboard decreases (figures 8.6. – 8.). There are no restrictions when relocating on a river route (H_{slimit}>2 m). On the coastal route, transverse waves must be avoided. If, with the agreement of the naval classification companies, the requirements imposed by the roll criteria would be relaxed (RMS_{φ}≥5^0, $RMS_{ac\varphi}$≥0,15g/(B/2)), then in case 3 of ballast, no navigation restrictions on the coastal route would be obtained.

From the assessment of the floating dock according to the general stability criterion, subchapter 8.2., it turns out that it can be operated for all calculated displacement / draft cases and for the entire range of variations of the centre of gravity. The criterion of dynamic transverse stability is not met in cases where the vertical position of the centre of gravity of the dock exceeds 14 m, being possible to operate the dock only in a protected port.

Table 8.14. Limit values of significant wave height $H_{s\ limit}$ [m] and sea state in Beaufort degrees B_{limit}, for the case of the ballast of the dock at the draft of T_m=7,2 m

v[km/h]	z_G[m]	$H_{s\ limit}$[m]	B_{limit}	Seakeeping criteria
0 (F_n=0)	6	3.872÷4.942	6.76÷7.55	heave/ beam & quarter
	8	3.810÷4.942	6.71÷7.55	heave/ beam & quarter
	10	3.750÷4.942	6.65÷7.55	heave/ beam & quarter
	12	3.697÷4.942	6.61÷7.55	heave/ beam & quarter
	14	3.650÷4.942	6.57÷7.55	heave/ beam & quarter
	16	3.622÷4.942	6.54÷7.55	heave/ beam & quarter
6 (Fn=0.037)	6	3.869÷4.942	6.76÷7.55	heave/ beam & quarter
	8	3.809÷4.942	6.71÷7.55	heave/ beam & quarter
	10	3.743÷4.942	6.65÷7.55	heave/ beam & quarter
	12	3.683÷4.942	6.59÷7.55	heave/ beam & quarter
	14	3.642÷4.942	6.56÷7.55	heave/ beam & quarter
	16	3.621÷4.942	6.54÷7.55	heave/ beam & quarter
12 (F_n=0.074)	6	3.865÷4.942	6.76÷7.55	heave/ beam & quarter
	8	3.791÷4.942	6.69÷7.55	heave/ beam & quarter
	10	3.723÷4.942	6.63÷7.55	heave/ beam & quarter
	12	3.669÷4.942	6.58÷7.55	heave/ beam & quarter
	14	3.636÷4.942	6.55÷7.55	heave/ beam & quarter
	16	3.620÷4.942	6.54÷7.55	heave/ beam & quarter
limits	-	3.620	6.54	heave/ beam & quarter

Table 8.15. Limit values of significant wave height $H_{s\ limit}$ [m] and sea state in Beaufort degrees B_{limit}, for the case of the ballast of the dock at the draft of T_m=6,2 m

v[km/h]	z_G[m]	$H_{s\ limit}$[m]	B_{limit}	Seakeeping criteria
0 (F_n=0)	6	4.529÷4.942	7.27÷7.55	heave / beam-quarter
	8	4.435÷4.942	7.20÷7.55	heave / beam-quarter
	10	4.344÷4.942	7.14÷7.55	heave / beam-quarter
	12	4.267÷4.942	7.09÷7.55	heave / beam-quarter
	14	4.232÷4.942	7.06÷7.55	heave / beam-quarter
	16	4.219÷4.942	7.05÷7.55	heave / beam-quarter
6 (Fn=0.037)	6	4.486÷4.942	7.24÷7.55	heave / beam-quarter
	8	4.398÷4.942	7.18÷7.55	heave / beam-quarter
	10	4.316÷4.942	7.12÷7.55	heave / beam-quarter
	12	4.253÷4.942	7.08÷7.55	heave / beam-quarter
	14	4.222÷4.942	7.06÷7.55	heave / beam-quarter
	16	4.215÷4.942	7.05÷7.55	heave / beam-quarter
12 (F_n=0.074)	6	4.434÷4.942	7.20÷7.55	heave / beam-quarter
	8	4.354÷4.942	7.15÷7.55	heave / beam-quarter
	10	4.284÷4.942	7.10÷7.55	heave / beam-quarter
	12	4.235÷4.942	7.06÷7.55	heave / beam-quarter
	14	4.218÷4.942	7.05÷7.55	heave / beam-quarter
	16	4.204÷4.942	7.04÷7.55	heave / beam-quarter
limits	-	4.204	7.04	heave / beam-quarter

Table 8.16. Limit values of significant wave height $H_{s\ limit}$ [m] and sea state in Beaufort degrees B_{limit}, for the case of the ballast of the dock at the draft of T_m=5,2 m

v[km/h]	z_G[m]	$H_{s\ limit}$[m]	B_{limit}	Seakeeping criteria
0 (F_n=0)	6	4.942	7.55	no restrictions
	8	4.528÷4.942	7.27÷7.55	roll acc. / beam sea
	10	3.632÷4.942	6.55÷7.55	roll acc. / beam sea
	12	3.069÷4.942	6.05÷7.55	roll acc. / beam sea
	14	2.808÷4.942	5.75÷7.55	roll criteria / beam sea
	16	2.733 ÷4.942	5.65 ÷7.55	roll criteria / beam sea
6 (Fn=0.037)	6	4.942	7.55	no restrictions
	8	4.516÷4.942	7.26÷7.55	roll acc. / beam sea
	10	3.620÷4.942	6.54÷7.55	roll acc. / beam sea
	12	3.057÷4.942	6.04÷7.55	roll acc. / beam sea
	14	2.798÷4.942	5.74÷7.55	roll criteria / beam sea
	16	2.723÷4.942	5.64÷7.55	roll criteria / beam sea
12 (F_n=0.074)	6	4.942	7.55	no restrictions
	8	4.320÷4.942	7.12÷7.55	roll acc. / beam sea
	10	3.491÷4.942	6.42÷7.55	roll acc. / beam sea
	12	3.028÷4.942	6.01÷7.55	roll acc. / beam sea
	14	2.788÷4.942	5.72÷7.55	roll criteria / beam sea
	16	2.713÷4.942	5.63÷7.55	roll criteria / beam sea
limits	-	2.713	5.63	roll criteria / beam sea

CHAPTER 9

STUDY OF THE OSCILLATIONS OF THE RIVER – MARITIME TUGBOAT USED IN THE TRANSIT OPERATIONS OF THE FLOATING DOCKS

For the transport of goods and for special operations between ports and shipyards in the river and coastal area, a special type of tugboat was designed. One of the design criteria for evaluating the safety of the operation of such a ship is the analysis of its dynamics in the real sea - seakeeping. In the study we analysed the behaviour in the case of river and coastal navigation, of a tugboat with a total length of 48 m, in the case of loading according to the operating class. The operating scenario under this study includes navigation between the ports and the shipyards in Romania on the banks of the Danube River and on the Black Sea coast. (figure 2.7.). According to the random wave navigation scenario, the maximum levels of significant wave heights are 2 m in the case of river navigation and 4 m in the case of coastal navigation. For the presented cases, the extreme condition with 5 m significant height of the random wave is also taken into account. Numerical analysis is performed using the DYN software *[45]*, based on the hydrodynamic model presented in subchapter 2.4., and validated by the experimental test presented in chapter 3. The analysis is structured on the speed range from 0 to 20 km / h, for the range from 0 to 5 m of significant wave height, at tugboat - wave heading angles from 0 to 360 degrees.

The results of this chapter are published and presented in the article in the reference [62].

9.1. The numerical model of the tug for river – maritime navigation

For transport by waterways in Romania, one of the most used routes is between ports or shipyards on the Danube River and shipyards or ports on the Black Sea coast. In addition to transport using convoys, special operations for relocating floating docks or ships at different stages of manufacture from one shipyard to another are also required. For this purpose, several river-sea tugboats were designed, which can navigate even in irregular wave conditions. Among the numerous design criteria developed by the ship classification companies [1], safety of tugboats navigation must be evaluated on the basis of seakeeping. This study is focused on the real-world analysis of a tugboat on the river and coastal route in the Romanian sector, under several random wave conditions. [80]

For the numerical analysis of the behaviour in random waves, seakeeping, we used the DYN software [45], *the last version of it being validated by experimental tests from the hull basin, chapter 3, for the cases of head, following and transverse waves [78].*

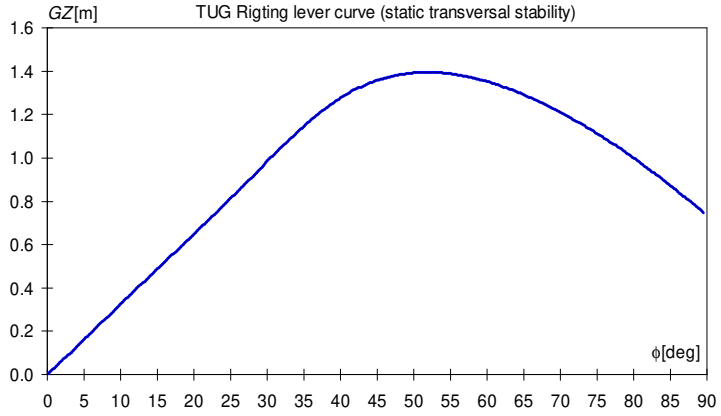

Figure 9.1. *GZ[m] the transversal stability diagram of the river - maritime tugboat*

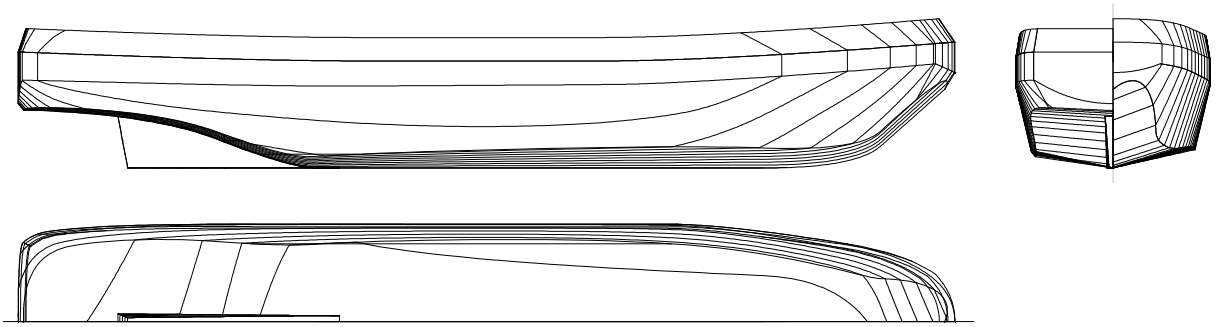

Figure 9.2. Lines plan of the 4000 H.P. river-maritime tugboat *[77], [79]*

The numerical analysis of the oscillations of the ship in the real sea is developed for a Romanian tugboat, with the installed power of 4000 H.P., on a river and sea navigation route, having the main characteristics shown in *table 9.1.* and the lines plan presented in *figure 9.2*. The numerical model of the tugboat body has 83 cross sections, with a finer division at both ends. The tugboat has significant transverse stability, *figure 9.1.*, making it possible to linearize the roll recovery term for angles greater than 15 degrees. The following limits for significant wave height are taken into account for the assessment of the navigational capabilities of the river-sea tug boat: on the river route IN (0.6); IN(1.2); IN(2.0) and along the coastal route C (2.5); C(3.0); C(4.0).

Table 9.1. *The main features of the model for the 4000 H.P. tugboat [79]*

Symbol and unit of measure	Value	Symbol and unit of measure	Value	Symbol and unit of measure	Value
$L_{\max}[m]$	48	$MP[CP]$	4,000	$J_x[tm^2]$	11,102
$L_{CWL}[m]$	47	$BP[kN]$	539	$GMT_o[m]$	1.8385
$B_{\max_{WL}}[m]$	10	$v[km/h]$	20	$\varphi_{GZ_{\max}}[^\circ]$	51
$B_{WL}[m]$	9.604	$\nabla[m^3]$	919.45	$T_\zeta[s]$	4.525
$H_{Pupa}[m]$	7.15	$x_G[m]$	1.1079	$T_\theta[s]$	4.657
$H_{mijloc}[m]$	6.35	$z_{GS}[m]$	3,35	$T_\varphi[s]$	6.032
$H_{\text{Pr}ova}[m]$	7.75	$LCF[m]$	-1.447	$\rho[kg/m^3]$	1.000 – 1.025
$F_s[m]$	0.3	$KB[m]$	2.1371	N_S	83
$T[m], T_{pp}[m], T_{pv}[m]$	3.5	C_B	0.582	$d_x[m]$	0.5875

9.2. Determining the response amplitude operators RAO to the oscillations of the 4000 H.P. river – maritime tug

For the river - sea tugboat (*figure 9.2., table 9.1.*), the functions of the RAO response amplitude operators at the oscillations for vertical displacements, pitch and roll angles, are obtained using the DYN software [45]. *Figures 9.3.a, b.* and figures *9.4.a, b.* presents RAO functions at vertical and pitch oscillations, for speeds of 0 and 20 km/h, for the ship - wave heading angle of 0, 45, 90, 135, 180°. *Figures 9.3.c., d.* and figures *9.4.c., d.* presents RAO functions at vertical and pitch oscillations for the ship heading angle - 90 and 180 degrees, considering the full range of towing speeds from 0 to 20 km/h.

For transverse waves (90 degrees), the influence of the tugboat speed for RAO functions at vertical and pitch oscillations is very low. For head waves (180 degrees), the influence of the tugboat speed for RAO functions at vertical and pitch oscillations is significant.

Figures 9.5.a., b. presents RAO functions at roll oscillations, for speeds of 0 and 20 km/h, for the range of ship – wave heading angles of 70, 80, 90, 100 and 110 degrees. *Figures 9.5. c., d.* presents RAO functions at roll oscillations for ship - wave angles of 80 and 100 degrees, for all tugboat operating speeds. Although for the transverse wave (90 degrees), speed has no influence on the RAO function at the roll oscillation, between 70 and 110 degrees the influence of speed is recorded.

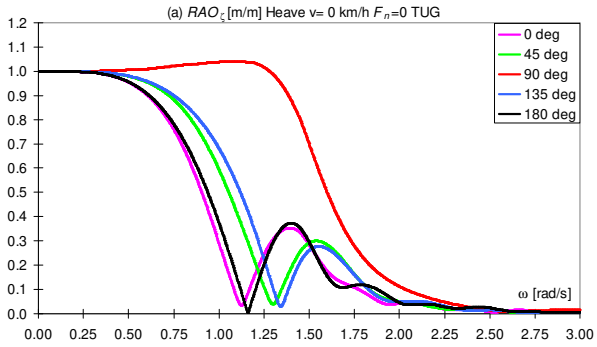

Figure 9.3.a. *RAO_ζ [m/m] heave, v=0 km/h, μ=0˚ – 180˚*

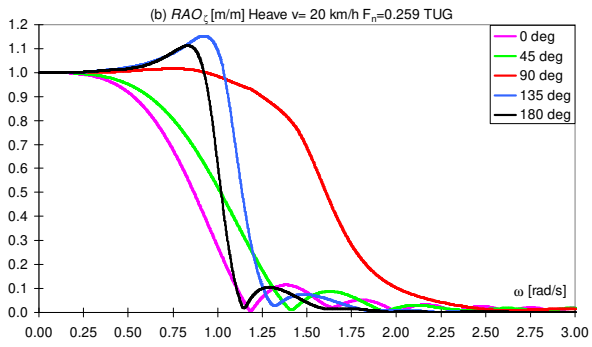

Figure 9.3.b. *RAO_ζ [m/m] heave, v=20 km/h, μ=0˚ - 180˚*

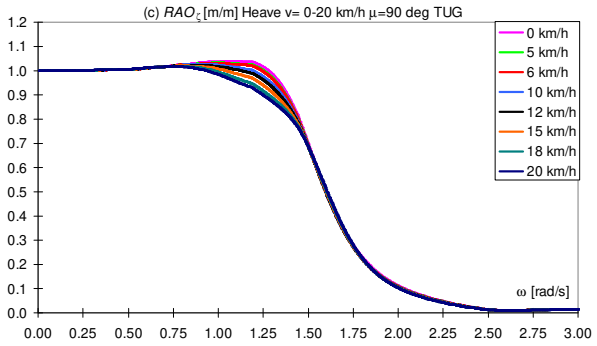

Figure 9.3.c. *RAO_ζ [m/m] heave, v=0-20 km/h μ=90 º*

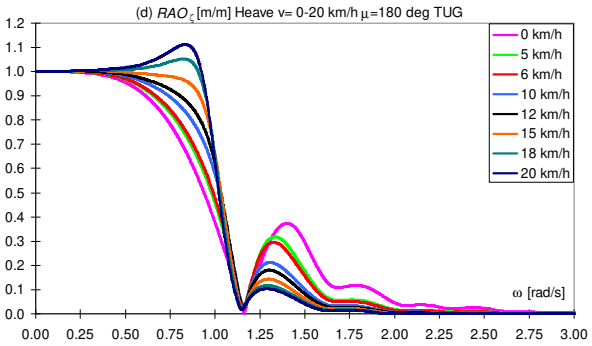

Figure 9.3.d. *RAO_ζ [m/m] heave, v=0-20 km/h μ=180 º*

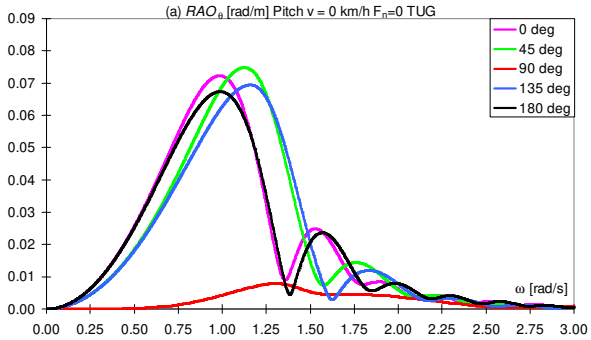

Figure 9.4.a. *RAO_θ [rad/m] pitch, v=0 km/h, μ=0˚ – 180˚*

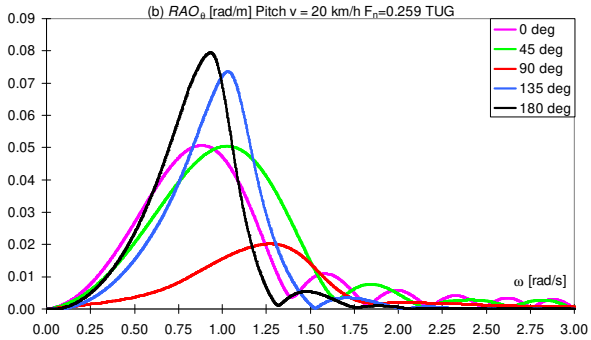

Figure 9.4.b. *RAO_θ [rad/m] pitch, v=20 km/h, μ=0˚ – 180˚*

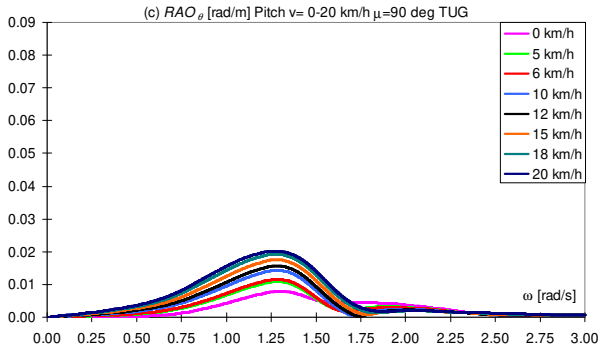

Figure 9.4.c. *RAO_θ [rad/m] pitch, v=0-20 km/h μ=90 º*

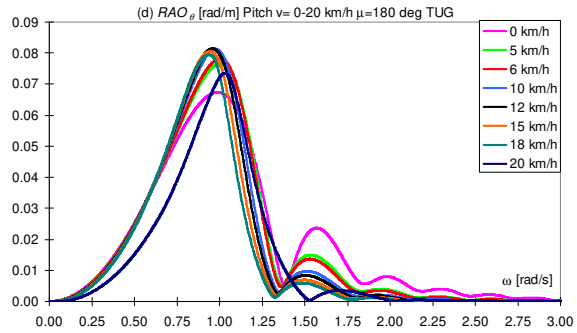

Figure 9.4.d. *RAO_θ [rad/m] pitch, v=0-20 km/h μ=180 º*

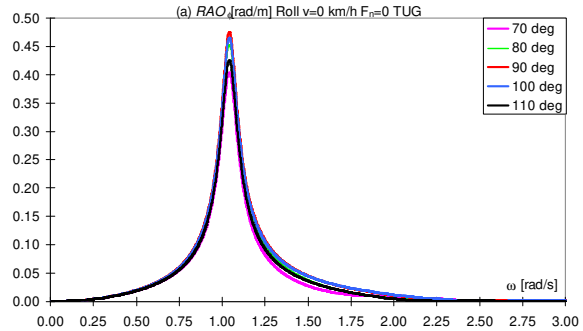

Figure 9.5.a. *RAO_φ [rad/m] roll, v=0 km/h, μ=70˚ – 110˚*

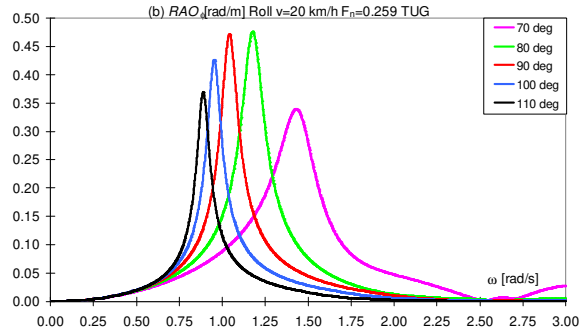

Figure 9.5.b. *RAO_φ [rad/m] roll, v=20 km/h, μ=70˚ – 110˚*

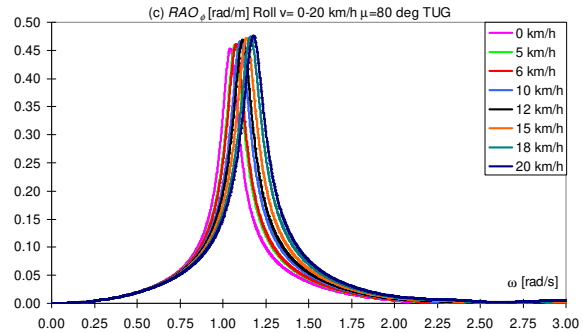

Figure 9.5.c. *RAO_φ [rad/m] roll, v=0 - 20 km/h, μ=80˚*

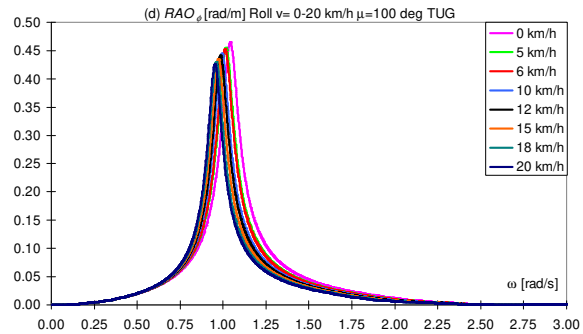

Figure 9.5.d. *RAO_φ [rad/m] roll, v=0 - 20 km/h, μ=100˚*

9.3. Analysis of the short-term statistical response for the river – maritime tug

For the river - sea tugboat (*figure 9.2., table 4.1.*), the most probable statistical response (RMS) to movements of vertical oscillations, pitch and roll, as well as of the associated accelerations, is obtained using the DYN software [45], for the spectrally intended power function of the random waves in *figures 2.8. – 9.* Based on the significant histogram of the wave height (*figure 2.10.*), the probability of occurrence and surpassing of waves is estimated. For the vertical movement, three reference points are considered, positioned at the stern, middle and bow, where a combined criterion of vertical oscillation, roll and pitch is applied (equations 2.51. – 53.). Since the ship is not symmetrical with respect to the midship, we considered the maximum between the pitch-induced accelerations at the stern and the tugboat bow.

Figures 9.6.a., b., c. shows the most likely static response for combined vertical movements.

Figure 9.7.a. and figure *9.8.a.* presents the most probable statistical answer for the angles of oscillation at pitch and roll.

Figure 9.6.d., Figure 9.7.b. and Figure *9.8.b.* presents the most probable statistical answer for the accelerations of heave, pitch and roll oscillations.

Considering the speed in the range 0 to 20 km/h and the extreme condition of navigation H_s=5 m, with probability of occurrence of 0,1% (*figure 2.10.*), *table 9.2.* presents the maximum statistical response most likely for the movements and accelerations of the tugboats. Also, in *table* 9.2. the permissible values for the seakeeping criteria of the river-sea tugboat are also presented. The greatest influence of speed is recorded for accelerations at vertical and pitch oscillations, averages for vertical and pitch movements and very low for roll movements and accelerations. The combined vertical movements of the stern and the bow, the vertical accelerations, the movement and the acceleration of pitching have the maximum values in the case of the meeting waves. The combined vertical movements of the central area, as well as the movements, the roll accelerations, have maximum values in transverse waves. The highest exceedance is recorded for the criterion of acceleration at pitch, with 39,.9%.

Figures 9.9.a., b. and figures 9.10.a., b. presents polar navigation safety diagrams according to seakeeping criteria, expressed in terms as the limit value of the significant wave height $H_{s_{\lim it}}(v,\mu)$ and the sea state limit value in Beaufort degrees $B_{\lim it}(v,\mu)$ for the river - maritime tugboat. Considering the reference to the main ship-wave angles, following and oblique - stern (0-45 degrees), transverse and oblique (70-110 degrees), meeting and oblique - bow (135-180 degrees), *table 9.3.* presents the limits of the sea state to ensure the safety of the tugboat's navigation, and in *table 9.4.* criteria for seakeeping are presented which induce restrictions. There are no restrictions for river routes, IN (2.0). For coastal routes, for speed range 0 - 6 km/h, the main restrictions appear from cross waves C (3.80), and in the range of speeds 10 - 20 km / h the main restrictions appear at meeting waves and oblique - bow C (3,67) - C (2,41).

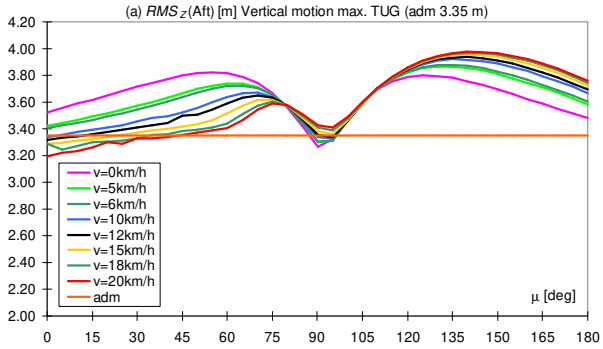

Figure 9.6.a. The most likely statistical answer *RMS_z [m] maximum, combined oscillations at the stern*

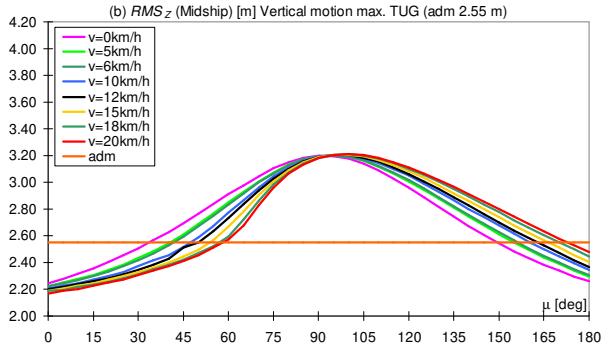

Figure 9.6.b. The most likely statistical answer *RMS_z [m] maximum, oscillations combined in the middle*

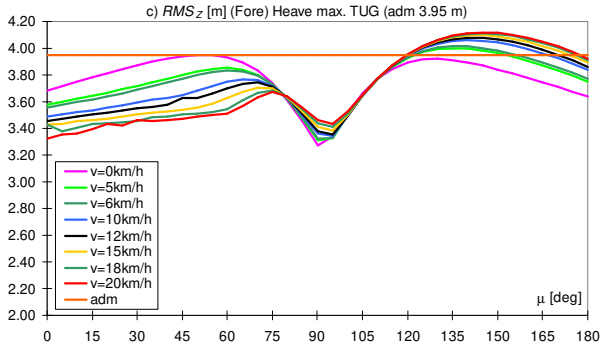

Figure 9.6.c The most likely statistical answer *RMS_z [m] maximum, oscillations combined at the bow*

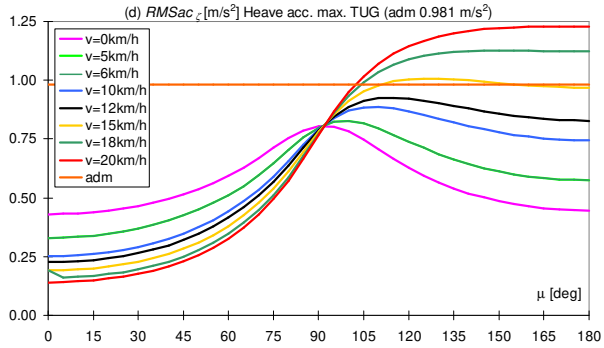

Figure 9.6.d The most likely statistical answer *$RMSac_\zeta$ [m/s²] maximum, vertical accelerations*

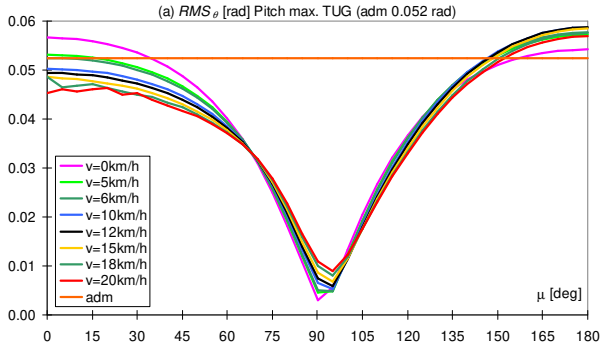

Figure 9.7.a. The most likely statistical answer maximum, at the pitch oscillation *RMS_θ [rad]*

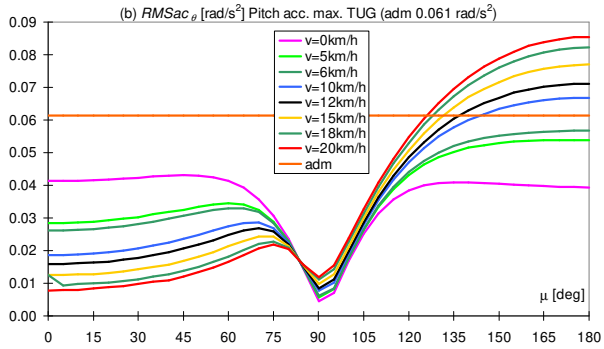

Figure 9.7.b. The most likely statistical answer maximum, at the pitch acceleration *$RMSac_\theta$ [rad/s²]*

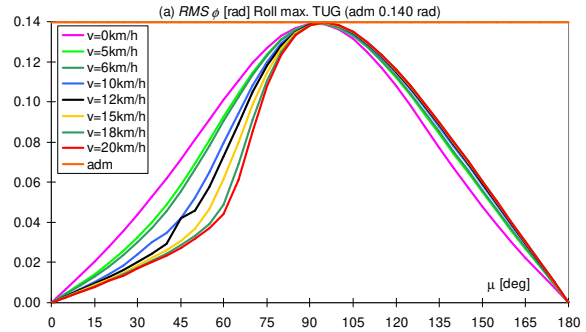

Figure 9.8.a. The most likely statistical answer maximum, at the roll oscillation *RMS_φ [rad]*

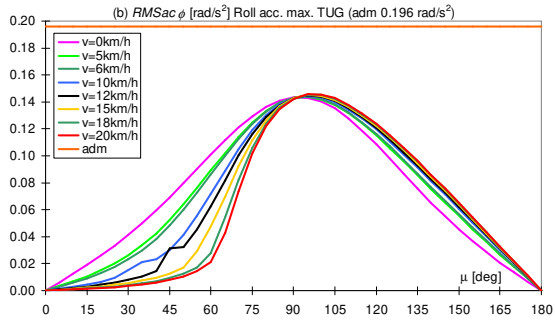

Figure 9.8.b. The most likely statistical answer maximum, at the roll acceleration *$RMSac_\varphi$ [rad/s²]*

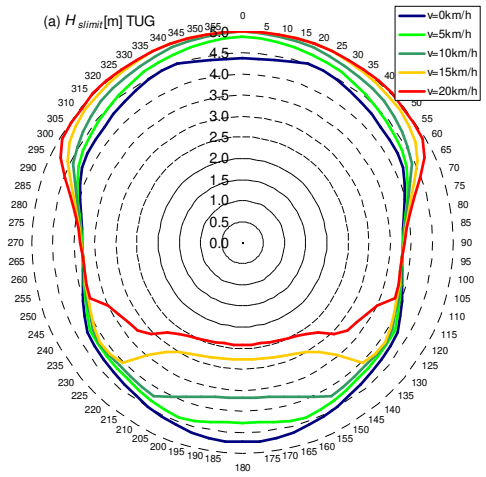

Figure 9.9.a. Polar diagram for significant wave height $H_{s\,limit}(v,\mu)$ [m], μ=0-360 º, v=0,5,10,15,20 km/h

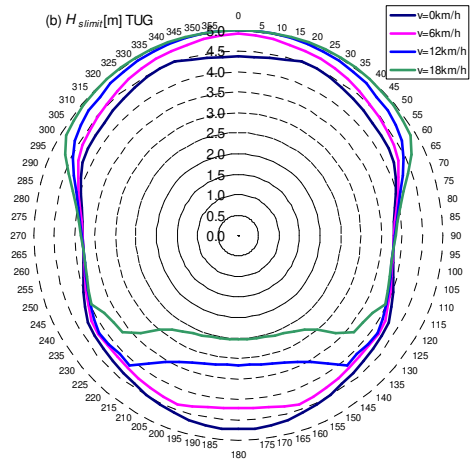

Figure 9.9.b. Polar diagram for significant wave height $H_{s\,limit}(v,\mu)$ [m], μ=0-360 º, v=0,6,12,18 km/h

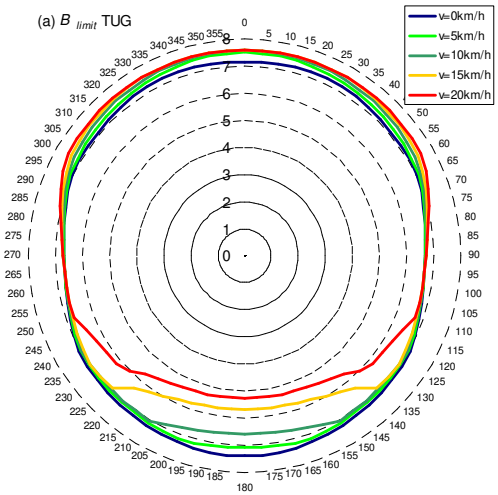

Figure 9.10.a. Polar diagram in sea state in Beaufort degrees $B_{limit}(v,\mu)$, μ=0-360 º, v=0,5,10,15,20 km/h

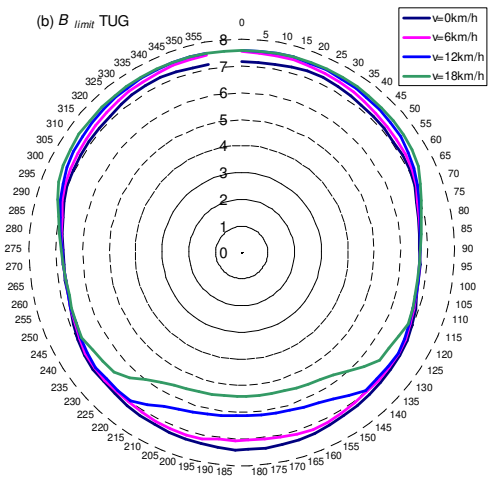

Figure 9.10.b. Polar diagram in sea state in Beaufort degrees $B_{limit}(v,\mu)$, μ=0-360 º, v=0,6,12,18 km/h

Table 9.2 The most probable maximum statistical values for the movements and accelerations of the oscillations of the tugboat, with reference to the extreme wave height of H_s=5 m

v[km/h]	$RMS_{z\,aft}$[m]	$RMS_{z\,mid}$[m]	$RMS_{z\,fore}$[m]	RMS_{θ} [rad]	RMS_{φ} [rad]	$RMSac_{\zeta}$ [m/s^2]	$RMSac_{\theta}$ [rad/s^2]	$RMSac_{\varphi}$ [rad/s^2]
Adm	*3.350*	2.550	3.950	0.052	0.140	0.981	0.061	0.196
0	3.822	3.199	3.949	0.0566	0.1388	0.804	0.043	0.143
	14.08%	25.44%	-0.03%	8.12%	-0.58%	-18.00%	-29.65%	-26.95%
5	3.867	3.201	4.002	0.0572	0.1389	0.827	0.054	0.144
	15.43%	25.55%	1.32%	9.25%	32.63%	-15.6%	-11.98%	-26.64%
6	3.880	3.202	4.015	0.0577	0.1390	0.836	0.057	0.144
	15.81%	25.58%	1.66%	10.11%	32.69%	-14.76%	-7.43%	-26.57%
10	3.920	3.205	4.062	0.0587	0.1392	0.887	0.067	0.15
	17.01%	25.69%	2.84%	12.11%	32.92%	-9.61%	8.99%	-26.29%
12	3.936	3.206	4.079	0.0588	0.1393	0.926	0.071	0.145
	17.50%	25.73%	3.26%	12.26%	33.03%	-5.60%	16.09%	-26.16%
15	3.956	3.208	4.099	0.0584	0.1395	1.008	0.077	0.145
	18.08%	25.81%	3.76%	11.58%	33.17%	2.76%	25.58%	-25.97%
18	3.969	3.212	4.112	0.0576	0.1396	1.127	0.082	0.146
	18.48%	25.95%	4.11%	10.08%	33.30%	14.89%	34.10%	-25.79%
20	3.976	3.214	4.118	0.0570	0.1397	1.229	0.086	0.146
	18.69%	26.03%	4.26%	8.79%	-0.002%	25.32%	39.49%	-25.68%

Table 9.3. Limit values of significant wave height $H_{s\ limit}$[m] and sea state in Beaufort degrees B_{limit} for ensuring the safety at sea from the criteria for seakeeping of the river-sea tugboat

$v[km/h]$		0		5		6		10		12		15		18		20	
$\mu[°]$		$H_{s\ limit}$	B_{limit}	$H_{s\ limit}$	B_{limit}	$H_{s\ limit}$	B_{limit}	$H_{s\ limit}$	B_{limit}	$H_{s\ limit}$	B_{limit}	$H_{s\ limit}$	B_{limit}	$H_{s\ limit}$	B_{limit}	$H_{s\ limit}$	B_{limit}
0		4.356	7.15	4.878	7.51	4.916	7.53	5.000	7.59	5.000	7.59	5.000	7.59	5.000	7.59	5.000	7.59
45		4.296	7.11	4.497	7.25	4.542	7.28	4.725	7.40	4.760	7.43	4.897	7.52	4.951	7.56	4.995	7.59
70		4.079	6.95	4.145	7.00	4.159	7.01	4.225	7.06	4.263	7.08	4.329	7.13	4.410	7.19	4.473	7.23
90		3.789	6.69	3.799	6.70	3.800	6.70	3.807	6.70	3.811	6.71	3.817	6.71	3.825	6.72	3.830	6.73
110		3.994	6.87	3.948	6.83	3.940	6.82	3.910	6.80	3.897	6.78	3.881	6.77	3.867	6.76	3.838	6.73
135		4.317	7.12	4.188	7.03	4.170	7.02	4.113	6.98	4.095	6.96	4.031	6.90	3.343	6.29	3.049	6.03
180		4.705	7.39	4.257	7.08	4.196	7.04	3.675	6.59	3.159	6.13	2.752	5.68	2.521	5.39	2.413	5.26
Navigation limit	River	IN(2.0)		IN(2.0)		IN(2.0)		IN(2.0)		IN(2.0)		IN(2.0)		IN(2.0)		IN(2.0)	
	Coastal 0-45^0	C(4.29)		C(4.49)		C(4.54)		C(4.72)		C(4.76)		C(4.89)		C(4.95)		C(4.99)	
	Coastal 70-110^0	**C(3.79)**		**C(3.80)**		**C(3.80)**		C(3.81)		C(3.81)		C(3.82)		C(3.82)		C(3.83)	
	Coastal 135-180^0	C(4.32)		C(4.18)		C(4.17)		**C(3.67)**		**C(3.15)**		**C(2.75)**		**C(2.52)**		**C(2.41)**	

Table 9.4. *The seakeeping criteria leading to navigation restrictions for the river-costal tug F-Q follow and quarter-stern sea; B-Q beam and quarter sea; H-Q head and quarter-bow sea v.a,m,f.m – vertical aft, midhsip, fore motion; p.m –pitch motion; h.a – heave acceleration; p.a – pitch acceleration*,

$v[km/h]$	**F-Q**	**B-Q**	**H-Q**
0	v.a.m ; p.m	v.a.m ; v.m.m	v.a.m ; p.m
5	v.a.m ; p.m	v.a.m ; v.m.m	v.a.m ; p.m
6	v.a.m ; p.m	v.a.m ; v.m.m	v.a.m ; p.m
10	v.a.m	v.a.m ; v.m.m	v.a.m ; p.m; p.a
12	v.a.m	v.a.m ; v.m.m	v.a.m; v.m.m; v.f.m; p.m; p.a
15	v.a.m	v.a.m ; v.m.m	v.a.m; v.m.m;v.f.m; h.a; p.m; p.a
18	v.a.m	v.a.m ; v.m.m	v.a.m; v.m.m;v.f.m; h.a; p.m; p.a
20	v.a.m	v.a.m ; v.m.m	v.a.m; v.m.m;v.f.m; h.a; p.m; p.a

9.4. Conclusions of the analysis of the dynamics of the river – maritime tug in random waves

Operating safety of the 4000 H.P. river-maritime tugboat (figure 9.2. and table 9.1.) was analysed using the DYN software [45], based on the seakeeping criteria formulated for the main components of oscillations and accelerations, heave, pitch and roll, in irregular waves specific to the navigation route (figure 2.7.), on the Danube River (Hs≤2m), as well as in the coastal area of the Romanian Black Sea coast (Hs≤5m). RAO response amplitude operators' analysis (figures 9.3. – 5.a, b, c, d) shows that with the variation of the marching speed in the range of 0 - 20 km / h, the amplitude of the dynamic response to the vertical and pitch oscillations increases in the case of the meeting waves. At beam waves, the influence of speed is very low on the main components of oscillation of the tugboat.

Taking into account the extreme state of irregular waves with maximum significant height Hs=5 m, on the Black Sea coast (figures 2.9.-10.), for the variation of the speed of the tug in the range 0 - 20 km / h, the statistical values those of the probable maximum RMS (figures 9.6.-8.) exceed the allowable values of the seakeeping criteria (table 4.2) as follows:

- vertical oscillations combined at the stern, 14.08 – 18.69%,
- vertical oscillations combined in the middle 25.44 – 26.03%,
- vertical oscillations combined in the front 4.26%;
- pitch oscillation 8.12 – 8.79%;
- acceleration at vertical oscillations 25.32%;
- acceleration at pitch oscillations 39.49%.

The movement and acceleration at pitch falls within the limits of the seakeeping criteria due to the significant transverse stability of the tugboat (figure 9.1.)

Based on the influence of the speed on the RAO response amplitude functions and the most likely maximum RMS statistical response values, the criteria for seakeeping are identified which lead to navigation restrictions for the river-maritime tugboat (table 9.4.).

Considering the polar diagrams H_{slimit}, B_{limit} (figure 9.9. and figure 9.10., table 9.3) for the river route on the Danube, the tugboat has no navigation restrictions, H_{slimit} = 2m. For the route on the Black Sea coast, for speeds between 0 -10 km/h the navigation restriction is H_{slimit} = 3.67 – 3.80 m, close to the limit H_{slimit} = 4 m, B_{limit} = 6.70, with probability of overcoming $P[H_s>3.80\ m] \approx 0.9\%$, and for the speed range of 12 - 20 km/h the navigation restriction is H_{slimit} = 2.41 – 3.15 m, B_{limit} = 5.26 – 6.13, with probability of overcoming $P[H_s>2.41\ m] \approx 4.8\%$.

It turns out that in order to ensure the navigational safety of the 4000 H.P. tugboat on the coastal routes, the speed of the ship must be reduced below 10 km / h, depending on the state of the sea.

CHAPTER 10

FINAL CONCLUSIONS AND PERSONAL CONTRIBUTIONS

10.1. Final conclusions

In order to optimize and increase the launching or docking capacities of the floating structures within the shipyards, the use of floating docks has now been extended (chapter 1), which needs to be evaluated on a wide range of operating conditions, which in many cases lead to extreme demands. The study within the thesis is focused on developing its own integrated methodology used for the comparative analysis of the operating capacity of three types of floating docks (Chapter 4), based on several safety criteria for buoyancy, transverse stability, local and global resistance, as well as seakeeping (navigation). Each floating dock is analysed for several docking scenarios, according to the norms of the ship classification companies [1], [3], including the case of relocation between shipyards on river and coastal routes. Thus, based on the conclusions of this study, the limitations imposed to ensure the operational safety of three types of floating docks selected, subject to extreme demands in quasi-static and random waves, are highlighted.

The study within the thesis is structured according to the formulated objectives (introduction) and leads to the following final conclusions:

1. To analyse the dynamic behaviour in waves of floating docks, we validated the theoretical model for oscillations in subchapter 2.4 and the associated program code DYN (OSC) [45], using the experimental model at scale 1:16 of a river-maritime research vessel (figures 3.1 - 3.2, table 3.1), with full shapes similar to the floating docks, within the towing tank of the Naval Architecture University in Galați (chapter 3). From the comparative analysis between the numerical and the experimental model, a good correlation between them is obtained, the following average differences being recorded for the amplitude operator functions: for vertical oscillations 16.79%, for pitch oscillations 12.32% and for roll oscillations 16.79% (figures 3.14 - 3.27, tables 3.3 - 3.6). The numerical model leads to higher values of the dynamic response, based on a linear hydrodynamic theoretical model, while the nonlinearities in the experimental model lead to an attenuation of the response on the main spectral component. From a practical point of view (ITTC [58], [59]) it can be considered that the numerical model provides a dynamic response that allows the conservative assessment of the operational safety of the docks based on the criteria for seakeeping (navigation).

2. Analysis of the operational capacity at extreme demands of the first constructive version, for the small floating dock with continuous lateral ballast tanks, Dock60_CWT (subchapter 4.1, figure 4.2, figures 4.9-4.11, table 4.1), with a length of 60 m and a maximum docking capacity of 828 t, combining the safety limit criteria (chapter 2), leads to the following conclusions:

- Based on the 1D equivalent beam model (subchapters 5.1, 5.2), subject to requests from quasi-static equivalent head – following and oblique waves, with the theoretical models in the subchapters 2.1.3, 2.1.4, 2.3.1, the preliminary buoyancy and global strength criteria can be evaluated (tables 4.3, 4.4, 4.5), for five operating cases imposed by the constructive norms [1], of the floating docks (table 4.7, figures 4.9.). In the case of light operation case, the only restriction is from the minimum freeboard criterion H_{wlimit}=1.934m, at the head-follow waves (tables 5.2.a, b, figures 5.1.-3.1.-2.a., b.), as well as at the oblique waves (table 5.6.a, figures 5.9.-13.b., figures 5.14.b), regardless of the heading angle dock-wave (μ=0-360^0). In the case of maximum ballast, restrictions result only from the minimum freeboard criterion H_{wlimit}=0.600m (tables 5.2.a,b, figures 5.1.-3.1.-2.a., b.). For the three cases of docking at the maximum capacity of 828t, the restrictions also result from the freeboard criterion H_{wlimit}=0.550m, at the head-follow waves (tables 5.2.a, b, figures 5.1.-3.1.-2.a., b.), as well as at the oblique waves (table 5.6.b, c, d, figures 5.4.-8.2 .a.-d., figures 5.9.-13.b, Fig. 5.14.b).
- Based on the 3D-FEM structural model (figs. 4.12-14) extended in a board, completely along the length of the floating dock, (subchapter 5.3.1), subject to requests from quasi-static equivalent head-follow waves, with the theoretical model in subchapter 2.2, as well as the extended 3D-FEM model on both edges (subchapter 5.3.2), subject to requests from quasi-static oblique equivalent waves, with the theoretical model from subchapter 2.3.2, the criteria of local and global stress is evaluated (table 4.3), for the five operating cases (table 4.7). From the analysis of the results of the stress criteria on 3D-FEM models, at the head and follow waves (table 5.9., figures 5.15.1.a-e) and oblique (table 5.13., figures 5.17.a-c, figures 5.18.a-b, figures 5.23-36.1.a-b.), do not lead to additional restrictions compared to the analysis on 1D models, respectively the only restrictions are from the minimum freeboard criterion, resulting in the limits for the height of quasi-static equivalent waves: 1.934 m in the light case, 0.600 m in the maximum ballast, 0.550 m in the three docking cases at the maximum capacity of the floating dock Dock60_CWT.
- Based on the hydrodynamic model (subchapter 6.1), with the theoretical model in subchapter 2.4, the safety of the floating dock relocation operation Dock60_CWT is evaluated, in the case without docked mass, on river routes and on the Black Sea coast routes (figure 2.8), in random waves, based on the seakeeping limit criteria (table 2.3, table 6.1). From the analysis of the dynamic response to the vertical oscillations, pitch and roll, in random waves (tables 6.3 and 6.5, figures 6.3-8.a, figures 6.9-14.b), restrictions on the relocation of the floating dock Dock60_CWT are registered predominantly in the case of the transverse and oblique random waves (μ=70^o-110^o, μ=250^o-290^0), from the criteria for the most statistical amplitude probable at the combined vertical oscillations and the accelerations at the roller oscillation. From the analysis of the drag resistance curves of the tug - floating dock convoy (figure 6.1), it results that the towing speed can be maximum 18 km/h. As the towing speed of the floating dock Dock60_CWT increases, the restrictions become extreme, resulting in the following limit values of significant wave height (H_{slimit}) and Beaufort intensity (BI_{limit}): 1.456 m (3.09) at v=0 km/h; 1.418 m (2.93) at v=5 km/h; 1.382 m (2.75) at v=10 km/h; 0.990 m (0.89) at v=15 km/h and 0.652 m (0.59) at v=18 km/h.
- Based on the theoretical model in subchapter 2.1.5, we analysed for the floating dock Dock60_CWT the general and meteorological criteria of intact transverse stability [2], [16], [17] (subchapter 6.2), at all five docking cases (table 4.7). For all docking cases, the general stability criteria do not impose restrictions. The dynamic (meteorological) stability criterion leads to restrictions in the case of maximum ballast, as well as in cases of docking at a maximum capacity of 828 t for the extreme position of the centre of gravity of the docked mass z_G≥8.5m, when the floating dock can only be operated in calm water conditions (tables 6.7).
- Cumulating the results obtained in the multicriteria analysis of the floating dock Dock60_CTW, the following operating conditions result:
  - In the light case, the floating dock can be operated stationary in unprotected water IN(1.4) (H_{limit}=1.456 m) and protected SW (H_{limit}=0 - calm water), respectively it can

be relocated on river routes with the middle class navigation IN(1.4) (H_{limit}=1.382-1.418 m) up to the towing speed of 10 km / h and restricted to the middle class IN(0.6) (H_{limit}=0.652-0.990 m), if the towing speed increases above 15 km/h. The floating dock Dock60_CWT can be relocated on the waterways of the coastal area only with special approval from the navigation authorities, in favourable weather conditions and low towing speed (maximum 10 km/h).

- In the case of maximum ballast, without docked mass, the floating dock can be operated in unprotected water IN(0.6) (H_{limit}=0.600 m) and protected SW (H_{limit}=0 - calm water), but it is not designed for relocation under this condition.
- In the three cases of docking at a maximum capacity of 828 t, the floating dock can be operated stationary in unprotected water ≈IN(0.6) (H_{limit}=0.550 m) and protected SW (H_{limit}=0 - calm water), with the maximum upright position of the docked vessel z_{GS}≤7.5m, respectively, they are not designed for the condition of relocation with docked mass on board.

3. Analysis of the operational capacity at extreme demands of the second constructive version, the small floating dock with discontinuous ballast superior lateral tanks, Dock60_NWT (subchapter 4.1, figure 4.1, figures 4.12-4.14, table 4.1), with a length of 60 m and a maximum docking capacity of 828 t, with the initial structure ($a_{Fr}=2a_0$) and reinforced ($a_{Fr}=a_0$), combining the safety limit criteria (chapter 2), leads to the following conclusions:

- Based on the 1D equivalent beam model (subchapters 5.1, 5.2) with stresses from quasi-static head, following and oblique waves, using the theoretical models of subchapters 2.1.3, 2.1.4, 2.3.1, the preliminary buoyancy and global strength criteria are evaluated (tables 4.3, 4.4, 4.5), in five operating cases according to the constructive norms [1], of the floating docks (table 4.6, figures 4.12.). From the analysis of the initial structure of the dock ($a_{Fr}=2a_0$), carried out only in the case of head - following waves, the following conclusions are drawn: in the case of light operation case, the major restrictions are imposed by the criterion of the global resistance at the permissible vertical bending moment, in the condition of hogging, H_{wlimit}=0.378 m (tables 5.1.a,b); in the case of maximum ballast, restrictions result only from the minimum freeboard criterion H_{wlimit}=0.326m (tables 5.1.a,b, figures 5.1-3.1.a,b) similar for the reinforced structure; for the case of docking at the maximum capacity with uniformly distributed mass, the main restrictions are from the criterion of global resistance, at the allowable vertical bending moment, in the condition of hogging, H_{wlimit}=0.252 m (tables 5.1.a,b); for the case of docking at the maximum capacity with sagging distributed mass the restrictions are from the minimum freeboard criterion H_{wlimit}=0.420 m (tables 5.1.a,b); for the case of docking at the maximum capacity with hogging distributed significant restrictions are from the criterion of the global resistance permissible vertical bending moment, in the condition of hogging, H_{wlimit}=0 m calm water (tables 5.1.a,b), being the extremely demanding case. From the analysis of the reinforced structure ($a_{Fr}=a_0$), which is considered as a reference for the floating dock Dock60_NWT, with requests from head, follow and oblique waves, the following conclusions are drawn: in the case without docked mass (table 5.5.a, figures 5.9.-13.a) for heading dock-wave system μ=0-45^0 the restrictions are from the criterion of overall strength at the allowable vertical bending moment, in the condition of hogging, H_{wlimit}=0.640-1.278 m, and for μ=60-90^0 the restrictions are from the minimum freeboard criterion H_{wlimit}=1.800 m; in the cases of docking at the maximum capacity with uniformly distributed mass and sagging type mass distribution (tables 5.5.b,c figures 5.9.-13.a) the main restrictions are imposed by the minimum freeboard criterion H_{wlimit}=0.420 m, regardless of the meeting angle dock-wave; in the cases of docking to the maximum capacity with distributed hogging mass (table 5.5.d, figures 5.9.-13.a) for μ=0-30^0 the restrictions are from the criterion of overall strength at the allowable vertical bending moment, in the condition of hogging, H_{wlimit}=0.261-0.318 m, and for μ=45-90^0 the restrictions are from the minimum freeboard criterion H_{wlimit}=0.420 m.
- Based on the 3D-FEM structural mode (Figs. 4.12-14) extended in a board, completely along the length of the floating dock (subchapter 5.3.1), subject to requests from quasi-static

equivalent head and follow waves, with the theoretical model in subchapter 2.2, as well as the extended 3D-FEM model on both sides (subchapter 5.3.2), subject to requests from quasi-static oblique equivalent waves, with the theoretical model of subchapter 2.3.2, the local and global resistance criteria are evaluated (table 4.3), for the five operating cases (table 4.6). From the analysis of the results of the resistance criteria on the 3D-FEM models, at the head-follow waves (tables 5.10-11, figures 5.15.2.a-e) and oblique (table 5.14, figures 5.20.a-f), the following conclusions are drawn: in the case without docked table, for μ=0-60^0 the restrictions are from the criterion of resistance to structural stability, in the condition of hogging wave, H_{wlimit}=0.582-1.041 m, and for μ=75-90^0 the restrictions are from the minimum free board criterion H_{wlimit}=1.800 m; in the cases of docking to the maximum capacity with uniformly distributed mass and type sagging the restrictions are imposed by the minimum free board criterion H_{wlimit}=0.420 m, regardless of the heading angle dock-wave; in the case of docking to the maximum capacity with hogging distributed mass, for μ=0-60^0 the restrictions are from the criterion of resistance to structural stability, in the condition of hogging wave, H_{wlimit}=0.186-0.350 m, and for μ=75-90^0 the restrictions are from the minimum freeboard criterion H_{wlimit}=0.420 m.

- Using the hydrodynamic model (subchapter 6.1), with the theoretical model in subchapter 2.4, the safety assessment of the floating dock Dock60_NWT relocation operation is performed, in the case without docked mass, on river routes and on the Black Sea coast routes, in random waves, based on the seakeeping limit criteria (table 2.3, table 6.1). From the analysis of the dynamic response to the vertical oscillations, pitch and roll, in random waves (tables 6.4, 6.5, figures 6.3-8.b), restrictions on relocation of the floating dock Dock60_NWT they are mostly recorded in the case of random and oblique waves (μ=70^o-110^o, μ=250^o-290^0), from the criteria for the most statistically probable amplitude at the vertical combined oscillations, coupled with the minimum freeboard criterion. Analogous to the dock with continuous lateral tanks, based on the resistance curves at the forwarding of the tug - floating dock convoy (figure 6.1), the maximum towing speed is 18 km/h. As the towing speed of the floating dock increases Dock60_NWT the restrictions are accentuated, resulting in the following limit values other than the significant wave height (H_{slimit}) and Beaufort intensity (B_{limit}): 1.071m (0.97) at v=0 km/h; 0.988 m (0.89) at v=5 km/h; 0.938 m (0.85) at v=10 km/h; 0.708 m (0.64) at v=15 km/h and 0.626 m (0.56) at v=18 km/h.
- Based on the theoretical model in subchapter 2.1.5, we analysed for the floating dock Dock60_NWT general and meteorological criteria of intact transverse stability [2], [16], [17] (subchapter 6.2), to all five docking cases (table 4.6). For all docking cases, the general stability criteria do not impose restrictions. Analogous to the floating dock with continuous lateral tanks, the dynamic (meteorological) stability criterion leads to restrictions in the case of maximum ballast, as well as in cases of docking at a maximum capacity of 828 t for the extreme position of the centre of gravity of the docked mass z_{GS}≥8.5m, when the floating dock can only be operated under calm water conditions (table 6.6.).
- From the combined multicriteria analysis of the floating dock Dock60_NTW, considering as a reference the reinforced structure (a_{Fr}=a_0), the following extreme operating conditions result:
  - In the case without a docking mass, the floating dock can be operated stationary in unprotected water ≈IN(0.6) (H_{limit}=0.582 m) and protected SW (H_{limit}=0 – still water), respectively it can be relocated on inland river routes with the middle class navigation IN(0.6) (H_{limit}=0.582 m) up to the maximum towing speed of 18 km/h. It is not recommended to relocate the floating dock Dock60_NWT on waterways in the coastal area.
  - In the case of maximum ballast, without docked mass, the floating dock can only be operated in protected water area SW (H_{limit}=0 – still water) and it cannot be relocated under this condition.
  - In the three cases of docking at a maximum capacity of 828 t, the floating dock can only be operated stationary in the protected water areas SW (H_{limit}=0.186-0.420 m),

with the maximum upright position of the docked vessel z_{GS}≤7.5m, with no possibility of relocation.

4. Analysis of the operational capacity at extreme demands of the third constructive version, the large floating dock with discontinuous superior lateral ballast tanks, Dock_VARD_Tulcea [9] (subchapter 4.2, table 4.9, figure 4.24, figure 4.27., figures 4.30-32, figure 4.36.), with a length of 209.2 m and a maximum docking capacity of 27,000 t, combining the safety limit criteria (chapter 2), leads to the following conclusions:

- Based on the results obtained in the analysis of small docks with requests from quasi-static equivalent waves, we considered in the case of the large floating dock only the conditions of quasi-static of head-following waves, which lead to the extreme structural response.
- Based on the 1D equivalent beam model (subchapter 7.1), with requests from quasi-static head-following waves, with the theoretical model in subchapter 2.1.4, the preliminary buoyancy and overall resistance criteria are evaluated (table 4.10.), for five operating cases. The following conclusions are drawn from the analysis of the floating dock structure: the minimum freeboard criterion does not impose restrictions in any docking case (table 7.1.a); in the case without docked mass and ballast for the reference draft T = 6.2m (table 7.1.b) the criteria of global stress do not impose restrictions, so that H_{limit}=4.492m; in the case of the transition of the docked ship of 19,747 t from the dock along the entire length of the rails on the main deck of the floating dock, in calm water with assisted ballast for the reference draft T = 6.2 m (tables 7.1.c,d, figures 7.1.a,b, figures 7.2.a-d), the criteria of preliminary global resistance do not impose restrictions; for the case of docking at the maximum capacity with uniformly distributed mass, the main restriction is from the criterion of the global resistance for vertical shear force, in the sagging condition, H_{wlimit}=3.231 m (table 7.1.e); for the case of docking at maximum capacity with distributed hogging mass type, the main restriction is from the criterion of the global resistance vertical shear force, in the sagging condition, H_{wlimit}=3.769 m (table 7.1.f); for the case of docking at maximum capacity with distributed sagging mass type the main restriction is from the criterion of the global resistance permissible vertical shear force, in the condition of sagging, H_{wlimit}=2.197m (table 7.1.g).
- Based on the 3D-FEM structural model (figure 7.45) extended in a board, completely along the length of the floating dock, (subchapter 7.2), subject to requests from quasi-static equivalent head-following waves, with the theoretical model in subchapter 2.2, the criteria of local and global resistance are evaluated (table 4.9.), for the five operating cases. From the analysis of the results of the resistance criteria on 3D-FEM models, at quasi-static head-following waves, the following conclusions are drawn: in the case without docked mass and ballast for the reference draft T = 6.2m (subchapter 7.2.1, table 7.3., figures 7.5-9), the main constraint is from the allowable vertical deflection criterion, so that H_{limit}=3.867 m; in the case of the transition of the docked ship of 19,747 t, with assisted ballast for the reference draft T = 6.2m (subchapter 7.2.2, tables 7.4 - 7.5., figures 7.11-15), in the condition of calm water there are no restrictions, and with the 19,747 t ship completely docked the restrictions are imposed by the criterion of permissible vertical deformation, at sagging wave H_{wlimit}=3.851 m; in the case of docking at a maximum capacity of 27,000 t (subchapter 7.2.3) the restrictions for the uniform distributed mass (table 7.6., figures 7.18 - 19) according to the admissible stresses criterion in sagging type wave, H_{limit}=2.173 m; for distributed hogging mass (table 7.7., figures 7.20 – 21) according to the allowable vertical deformation criterion, sagging wave, H_{limit}=3.048 m, and for distributed sagging mass type (table 7.8., figures 7.22-23) according to the admissible stresses criterion at sagging wave, H_{limit}=1.008 m.
- Based on the hydrodynamic model (subchapter 8.1), with the theoretical model in subchapter 2.4, the safety assessment of the relocation operation of the large floating dock Dock_VARD_Tulcea is performed, for three ballast drafts (T=5.2, 6.2, 7.2 m) and six values of the position of the centre of gravity (z_{GS}=6-16 m), along river and coastal routes, in random waves, based on the seakeeping limit criteria (table 2.3, table 8.3.) applied to the dynamic response to heave, pitch and roll oscillations. From the analysis of the forward resistance curves of the floating tug-dock convoy, for the three relocation

ballast drafts (figure 8.1), it turns out that the maximum towing speed is 12 km/h. From the analysis of the dynamic response in random waves for the ballast draft T = 7.2m (tables 8.4,8.7, figures 8.2-4.a, 8.5.a.-b.) the following ensue: the variation of the vertical position of the centre of gravity of the dock has an average influence on the amplitude of the oscillations at the cross wave, small or even negligible for the rest of the meeting angles dock-wave; the influence of the towing speed on the navigation restrictions is average and is recorded for μ=30-150^0 (210-330^0), mainly from the limit criterion to the combined vertical oscillations, with the limit values of the significant wave height (H_{slimit}) and Beaufort intensity (BI_{limit}): 3.622–3.872m (6.54-6.76) at v=0 km/h; 3.621-3.869 m (6.54-6.76) at v=6 km/h; 3.620-3.865 m (6.54-6.76) at v=12 km/h. From the analysis of the dynamic response in random waves for the ballast draft T=6.2m (tables 8.5,8.8, figures 8.2.-4.b) the following ensue: the influence of the vertical position of the centre of gravity of the dock on the amplitude of the oscillations is average at transverse and oblique waves, respectively negligible at head-following waves; an average influence of the towing speed on the navigation restrictions for μ=60-120^0 (240-300^0), from the limit criterion to the vertical oscillations, with the limit values of the significant height of the waves (H_{slimit}) and Beaufort intensity (B_{limit}): 4.219–4.529m (7.05-7.27) at v=0 km/h; 4.215-4.486 m (7.05-7.24) at v=6 km/h; 4.204-4.434 m (7.04-7.20) at v=12 km/h. From the analysis of the dynamic response in random waves for the ballast draft T=5.2m (tables 8.6,8.9, figures 8.2-4.c.) the following ensue: a significant influence of the vertical position of the centre of gravity and of the document on the oscillating amplitude for the transverse values; an average influence of the towing speed on the navigation restrictions for μ=75-105^0 (255-285^0), from the limit criterion to the roll oscillations, with the limit values other significant wave heights (H_{slimit}) and Beaufort intensity (B_{limit}): 2.733–4.942m (5.65-7.55) at v=0 km/h; 2.723-4.492 m (5.64-7.55) at v=6 km/h; 2.713-4.492 m (5.63-7.55) at v=12 km/h.

- I have analysed for the floating dock Dock_VARD_Tulcea general and meteorological criteria for intact transverse stability [2], [16], [17] (subchapter 8.2), with the theoretical model from subchapter 2.1.5, for three docking drafts T=5.2 m, 6.2 m, 7.2 m and the vertical position of the centre of gravity of the dock z_{GS}=6-16m. For all the analysed cases, the general stability criteria do not impose restrictions. The dynamic (meteorological) stability criterion imposes restrictions on all docking cases analysed for the vertical position of the centre of gravity of the dock z_G≥14m, when it can be operated only in calm water (tables 8.10-12).
- Based on the combined multicriteria analysis of the large floating dock Dock_Vard_Tulcea, considering the draft as a reference T=6.2 m, ensured by assisted ballast in all cases, the following extreme operating conditions result:
  - In the case without a docking mass, the floating dock can be operated stationary in unprotected water IN(2.0) and RE(40%) (H_{limit}=3.867 m) and protected SW (H_{limit}=0), respectively it can be relocated on inland river routes with the navigation class IN(2.0) and coastal with the middle class RE(40%), C(3.8), (H_{limit}=3.867 m), having the maximum towing speed of 12 km/h. It does not require special approval for navigation on the Black Sea coastal area.
  - In the case of the dock of the 19,747 t in calm water conditions there are no restrictions. The operation of the dock in waves having boarded mass of 19,747 t can be carried out without restrictions in the river area IN(2.0) and coastal for the class RE(40%), C(3.8), (H_{limit}=3.851 m), being able to be relocated under this condition.
  - In case of docking to the maximum capacity of 27,000 t with uniformly distributed mass, the floating dock can be operated without restrictions in the river area IN(2,0) and coastal with class restrictions RE(20%), (H_{limit}=2.173 m), being allowed to relocate the dock only with special approval.
  - In case of docking to the maximum capacity of 27,000 t with the distributed mass type hogging, the floating dock can be operated without restrictions in the river area IN(2.0) and coastal with class restrictions RE(30%), C(3.0), (H_{limit}=3.048 m), being allowed to relocate the dock.

- In case of docking to the maximum capacity of 27,000 t with distributed mass sagging type, the floating dock can be operated with restrictions in the river area IN(1.0) and can be operated in the coastal area only with special approval. It is recommended to relocate the dock only in the case of inland river routes, but also in this case with the restriction IN(1.0).
- For all operating cases the vertical position of the centre of gravity of the floating dock must be z_{GS}≤14m, to meet the dynamic stability criterion (meteorological).

5. Analysis of the navigational capabilities of the 4,000 HP river-sea tug [77], [79] (table 9.1, figure 9.2), used to relocate the three types of floating docks included in the study, based on the hydrodynamic model (chapter 9), with the theoretical formulation of subchapter 2.4, on river and coastal routes, in random waves, with the criteria for seakeeping for vertical, pitch and roll oscillations (table 2.3), it leads to restrictions for all tug-wave heading angles from the boundary criteria on the combined heave and pitch oscillations, being more significant at the head waves, oblique bow and crossbeams. Considering the full range of towing speeds (v_{max}=18 km/h), of the three floating docks, according to the advancement resistance curves (Figures 6.1, 8.1), the navigation restrictions are accentuated as the speed increases and the following limit values of the significant wave heights result (H_{slimit}) and Beaufort intensity (B_{limit}): 3.789m (6.69) at v=0 km/h; 3.791m (6.69) at v=5 km/h; 3.790 m (6.69) at v=6 km/h; 3.675 m (6.59) at v=10 km/h; 3.159 m (6.13) at v=12 km/h, 2.752 m (5.68) at v=15 km/h; 2.521m (5.39) at v=18 km/h. From the comparative analysis of the operating limits when relocating floating docks and tugs, the following conclusions are drawn:

- Small docks Dock60_CWT and Dock60_NWT, in the case without docked mass, they can be relocated on river routes IN(0.6) or IN(1.4), up to a maximum speed of 18 km / h, without any additional restrictions imposed by the operation of the tug (IN(2.0)).
- Large dock Dock_VARD_Tulcea can be relocated on river routes IN(1.0) or IN(2.0), in all cases of docking, up to a maximum speed of 12 km/h, without any additional restrictions imposed by the operation of the tug (IN(2.0)). Also, in the cases of relocation on the coastal routes, without docked mass or at the dock of the ship of 19,747 t the operation of the floating tug-boat convoy can be done for v_{max}=10 km/h restricted to the class RE(40%), C(3.6)-C(3.8), and for v_{max}=12 km/h restricted to the class RE(30%), C(3.0). In the case of docked mass at the maximum capacity of 27,000 t, with hogging distribution, the operation of the convoy can be done up to the maximum speed of 12 km / h in the average navigation class RE(30%), C(3.0). In cases of docking at a maximum capacity of 27,000 t, with uniform distribution or sagging type, although the tug allows the maximum towing speed of 12 km / h, this operation is limited by the criteria of local and global structural strength of the floating dock (H_{limit}=1.008-2.713m), relocation is possible only with special approval from the navigation authorities and under favourable weather conditions.

6. Based on the integrated methodology of multicriteria analysis of the operating capacity of the three floating docks at extreme demands, developed within the thesis, with the synthesis results presented in table 10.1 (figure 10.1.), the following conclusions are drawn:

- From the comparative analysis of the small docks, with continuous upper ballast tanks Dock60_CWT and discontinuous Dock60_NWT (chapters 5, 6), it turns out that most operating restrictions are registered in the case of the second constructive variant (NWT), being caused by the criteria of local and global structural resistance.
- Floating docks with discontinuous lateral ballast tanks (NWT) have their own steel body mass smaller than the variant with continuous side ballast tanks (CWT) (subchapter 4.1) and in addition it is suitable for the conversion of existing barges into floating docks, with lower costs than for a completely new construction (subchapter 4.2).
- In the case of large docks Dock_Vard_Tulcea, with the reinforced structure and significant free board, less restrictive operating conditions are provided for the constructive variant with discontinuous upper side ballast tanks (chapters 7, 8).

Table 10.1. Summary of the analysis of the operating conditions of floating docks at extreme demands

Docking case	Operating conditions	Dock60_CWT [a] (828 t)	Dock60_NWT [a] (828 t)	Dock_Vard_Tulcea [b] (27000 t)
(1) without docking mass	Harbour	unprotected IN(1.4) and protected SW	unprotected IN(0.6) and protected SW	unprotected IN(2.0), C(3.8)& unprotected SW
	River relocation	IN(1.4) - 10km/h IN(0.6) - 18km/h	IN(0.6) - 18km/h	IN(2.0) - 12 km/h
	Costal relocation	only with special approval (10km/h)	no	C(3.6) - 10 km/h C(3.0) - 12 km/h
(2)[a] maxim ballast (2)[b] docking OSV with mass 19747t	Harbour	unprotected IN(0.6) and protected SW	protected SW	unprotected IN(2.0), C(3.8) & protected SW
	River relocation	no	no	IN(2.0) - 12 km/h
	Costal relocation	no	no	C(3.6) - 10 km/h C(3.0) - 12 km/h
(3) maximum capacity, with uniform mass	Harbour	unprotected IN(0.6) and protected SW	protected SW	unprotected IN(2.0) and protected SW
	River relocation	no	no	IN(2.0) - 12 km/h
	Costal relocation	no	no	only with special approval (12 km/h)
(4) maximum capacity, with mass type sagging	Harbour	unprotected IN(0.6) and protected SW	protected SW	unprotected IN(1.0) and protected SW
	River relocation	no	no	IN(1.0) - 12km/h
	Costal relocation	no	no	only with special approval (12 km/h)
(5) maximum capacity, with mass type hogging	Harbour	unprotected IN(0.6) and protected SW	protected SW	unprotected IN(2.0), C(3.0) & protected SW
	River relocation	no	no	IN(2.0) - 12 km/h
	Costal relocation	no	no	C(3.0) - 12 km/h

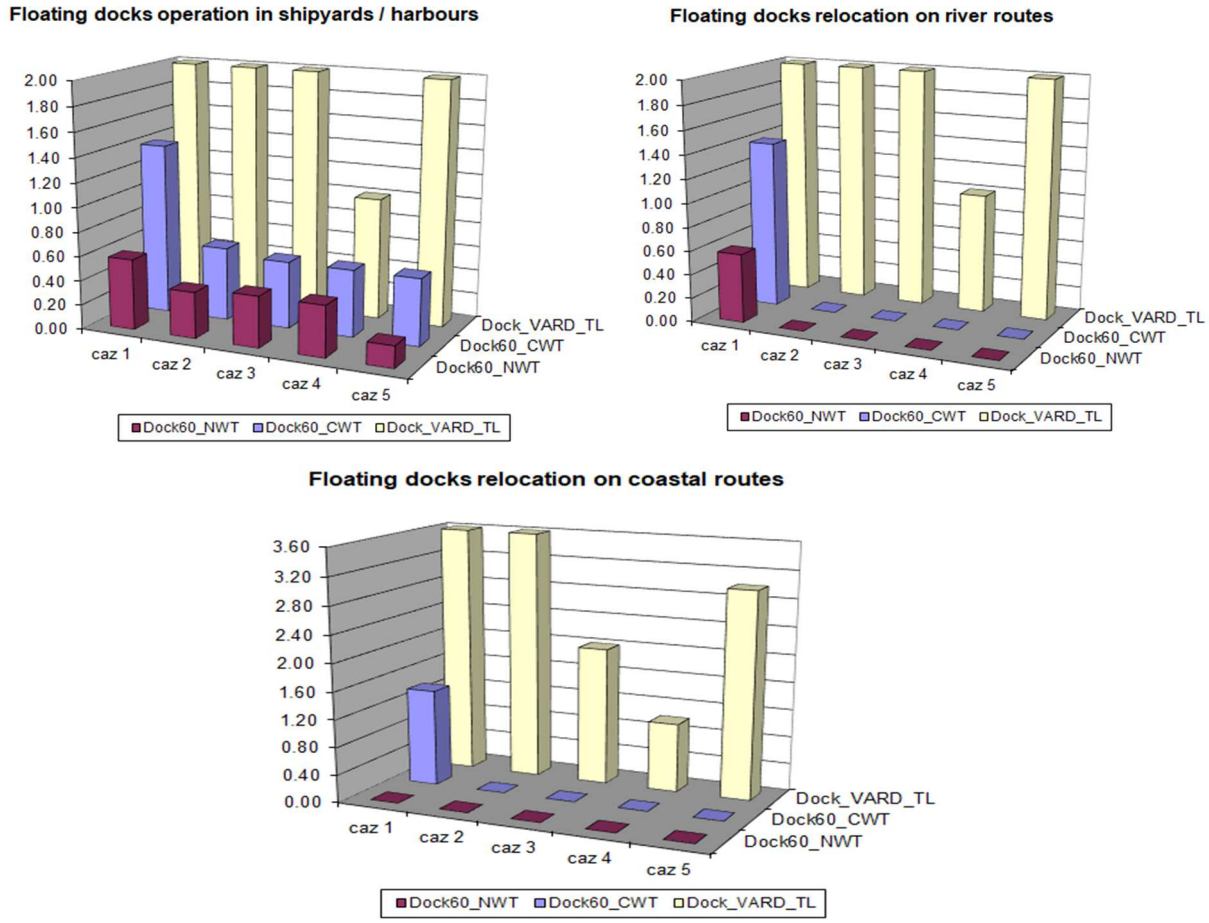

Figure 10.1. The operating limits of the three floating docks subjected to extreme demands

10.2. Personal contributions

In this thesis I have elaborated the following personal contributions:

1. On the basis of the specialized literature we have realized the documentation regarding the current state of the docking techniques of the ships in the shipyards, as well as the constructive versions applied to the development of the floating docks (chapter 1).

2. We have made a synthesis of the theoretical models underlying the methods of analysing the operating capacity of floating docks at requests from quasi-static and random waves, defining the safety limit criteria (chapter 2), including the following:

- Methods for preliminary analysis of floating docks based on 1D equivalent beam models, in calm water demands and quasi-static head-following waves, (subchapter 2.1), for evaluating minimum freeboard criteria, overall strength, bending moments and vertical shear forces, intact transverse stability (general and dynamic);
- Methods for structural analysis of floating docks based on fully extended 3D-FEM models, along a dock, in calm water requests and quasi-static equivalent head-following waves (subchapter 2.2), for the evaluation of the criteria of local and global resistance, allowable stresses with respect to the material flow limit, structural stability and permissible vertical deflection;
- Methods for structural analysis of floating docks based on 1D and 3D-FEM equivalent beam models, fully extended along the length and width of the dock, at requests from quasi-static oblique equivalent waves, (subchapter 2.3), for evaluating the criteria of local and global resistance formulated in terms: bending moments and allowable vertical and horizontal bending forces, permissible torsional moments, allowable stresses at the material flow limit, structural stability (buckling) and allowable deformations;
- Methods for analysing the dynamic behaviour of floating docks in random waves, at vertical, pitch and roll oscillations, linear, with the determination of the short-term statistical response in navigation conditions on river and coastal routes, depending on the towing speed of the dock, (subchapter 2.4), for the evaluation of the navigation criteria (seakeeping) formulated in terms of the statistical values the most probable amplitudes of the movements and accelerations on the significant components from the fluctuations of the floating docks.

3. Based on the theoretical models in subchapter 2.1 we have developed the FDOCK software package with the logic scheme of figure 2.1, which includes the following modules:

- Program module D_CDB (Annex 1), developed for calculating the hydrostatic curves of floating docks (with outer and inner shell between side ballast tanks), straight and Bonjean fairing curves (subchapter 2.1.2);
- Program module D_AC (Annex 2), developed for the preliminary calculation of the equilibrium position in calm water of floating docks (with outer and inner shell between the lateral ballast tanks), based on a non-linear iterative procedure for buoyancy and longitudinal axis conditions (subchapter 2.1.3).
- Program module D_ACAVD (Annex 3), developed for balancing floating docks (with outer and inner lining between side tanks) in quasi-static waves of encounter-tracking, calculating VBM bending moments and VSF vertical cutting forces, using an iterative non-iterative procedure. with two parameters (subchapter 2.1.4);
- Program module D_LDF (Annex 4), developed for the calculation of the transverse stability diagram, including the influence of the free surface of the on-board tanks (partially filled) and the longitudinal trim of the dock, using a non-linear iterative procedure at wide angles of transverse inclination, for floating docks (with outer and inner casing between the lateral ballast tanks) (subchapter 2.1.5);
- Program module D_DRSU (Annex 5), developed for processing the data recorded in the floating docks (with double casing), in nature, taking into account the longitudinal trim and the vertical deformation of the dock (subchapter 2.1.1).

4. For the transposition of the mass distribution from the 3D-FEM structural models into the 1D equivalent beam models, used to determine the floating dock balancing parameters in quasi-static equivalent waves (subchapters 2.2, 2.3), we developed the following codes directly implemented in the program Femap / NX Nastran [42]: module mass_prop_edit.bas (annex 6) for mass editing, module totalmass_to_data_table.bas (Annex 7) for mass reading, the macro-command file group_selection.prg (Annex 8) for generating mass groups for 3D-FEM models, the macro-command file mass_selection.prg (Annex 9) for mass extraction from mass groups for 3D-FEM models. We also implemented user-type functions in the Femap / NX Nastran program [42] for applying quasi-static wave pressures to the double outer shell of floating docks, 3D-FEM models, with expressions (2.9), (2.14.).

5. Based on an experimental model at 1:16 scale of a fluvial-maritime research vessel, with full shapes, similar to the floating docks resulting from the conversion of barges, within the hull basin at the “Dunărea de Jos” University in Galați, The University of Naval Architecture, we validated the linear analysis program for vertical oscillations, pitch and roll, the modulus of amplitude response functions in regular waves (chapter 3, sub-chapter 2.4), from the DYN program (OSC) [45]. The program of experimental and numerical analysis includes a set of 8 regular waves, with frequency in the range f=0,427-1,008 Hz, which are obtained with the wave generator within the basin, with the model in head ($\mu=180^0$), follow ($\mu=0^0$) and beam ($\mu=90^0$) waves, with model speeds of 0 and 1.28 m / s (table 3.2). The comparative analysis of the experimental and numerical results allows to highlight the sensitivity of the numerical model used to obtain the dynamic response in waves of floating docks.

6. For the comparative study of floating docks with continuous upper (CWT) and discontinuous (NWT) side tanks, we developed the numerical model for two small docks (Dock60), having a length of 60 m and a maximum docking capacity of 828 t (subchapter 4.1). The two docks have double symmetry at the centreline and midship section. The structural dimensioning of the floating docks is realized with the Poseidon program [39], according to the constructive norms of the DNV-GL docks [1]. For the study we considered 5 cases of loading, without docked mass, maximum ballast, with docked mass at maximum capacity of 828 t, having uniform distributions, type sagging and hogging, as well as two schemes for the location of the keel blocks (short and long). For the two floating docks we developed 1D equivalent beam numerical models, 300 elastic Timoshenko beam type elements and 301 nodes, and the 3D-FEM model with 472,830 (237,928) or 378,210 (162,065) of thick plate finite elements (Mindlin) and the membrane, including also concentrated mass elements, with 398,995 (201,153) or 320,771 (190,618) nodes, depending on the extension of the 3D-FEM model, on both edges or on one board, with continuous or discontinuous upper ballast tanks, having the average discretization degree of 200 mm, corresponding to a local and global structural analysis (subchapter 4.1).
7. For the two floating docks, Dock60_CWT and Dock60_NWT, we performed in the first phase the preliminary structural analysis, based on the 1D equivalent beam models, subjected to requests from quasi-static equivalent head-following waves, with the height of h_w=0-2.568 m (step 0.1-0.25 m), the conditions of calm water, sagging and hogging (empty and ridge of wave) (subchapter 5.1). In the second stage, also based on the 1D equivalent beam model, the requests from the quasi-static oblique equivalent waves are considered ($\mu=0\text{-}90^0$, step 15^0, taking into account the symmetry of the bodies), with a maximum height of 2.568 m (subchapter 5.2). Based on the analyses with 1D models, we evaluated the criteria of minimum free board, general resistance permissible sectional stresses, the ultimate bending moment, allowable deformations, which led to the need to strengthen the initial structure. We also determined the parameters for balancing the system of small floating docks – quasi-static head-following waves, oblique and calm water, use to apply the external pressures from the quasi-static waves on the double bottom of floating docks, for 3D-FEM models. In order to ensure the correspondence between the 1D and 3D structural models, using our own procedures (annexes 6-9) we imported into the 1D model the mass diagram of the 3D-FEM model, and the interior and exterior shapes in the two structural

models are based on the same 3D-CAD model. Based on the structural analysis of the two small floating docks on 3D-FEM models (subchapter 5.3), with the same characteristics of quasi-static waves as in the case of 1D models, areas with tension concentrators were highlighted, respectively the docks were evaluated on the basis of local and global resistance criteria, allowable von Mises stresses relative to the flow limit of the material and the structural stability. We performed the comparative structural analyses of the two floating docks, on 1D and 3D models, using the program codes and the theoretical models presented in subchapters 2.1.3, 2.1.4, 2.2, 2.3.1, 2.3.2 (the logic schemes in the figures 2.2 & 2.5).

8. For the comparative study of the relocation operation of the two small floating docks, Dock60_CWT, Dock60_NWT (subchapter 4.1), in the case of no boarded mass, in terms of seakeeping criteria (navigation), we performed the oscillation analysis of the docks in random waves (subchapter 6), using the DYN program (OSC) [45], experimentally validated at the hull basin (chapter 3), with a linear hydrodynamic theoretical model and short-term statistical formulation (subchapter 2.4, the logic scheme in figure 2.9). Dynamic response includes the main components of floating docks, vertical, pitch, roll, and I considered the full range of random dock-wave meeting angles μ=0-180^0(360^0), step 5^0, function of the power spectrum density of the order type ITTC [58], [59] for random waves with the maximum significant height H_s=2.568m, step 0.05m, and with the speed range 0, 5, 10, 15, 18 km / h, where the maximum speed results from the analysis of the curves of the resistance to the advancement of the small tug-dock convoy (figure 6.1). The results of this comparative analysis for the two small docks allowed to highlight the navigation restrictions under extreme conditions when relocating the docks on river and coastal routes in the Romanian Black Sea area. Also, using the D_LDF module (annex 4, subchapter 2.1.5), we evaluated for both small docks the general and dynamic (meteorological) transverse stability criteria, depending on the loading cases and the vertical position of the centre of gravity of the docked mass in relation to the pontoon bridge of the floating dock (0.5-8.5 m).

9. Based on the technical data made available by VARD Tulcea Shipyard, we developed the model of a large floating dock, with a length of 209.2m and a maximum docking capacity of 27,000 t, Dock_VARD_Tulcea [9] (subchapter 4.2), to study what operating capabilities at extreme demands are ensured in the case of the docks made by converting existing barges, in the most economical option, the addition of additional discontinuous ballast tanks (NWT) and the extension of the width of the pontoon with other ballast tanks on both sides. For structural analysis of large dock and discontinuous upper ballast tanks (chapter 7), we developed two numerical models, one of 1D equivalent beam, with 280 Timoshenko elastic beam elements and 281 nodes, as well as a 3D-FEM model, with 1,353,139 thick plate finite elements (Mindlin) and membrane, plus concentrated mass elements, with 1,834,221 nodes, with the average discretization degree of 187.5 mm, corresponding to a local and global structural analysis. The dock is analysed in 5 cases of docking, without docked mass, with docked ship of 19,747 t, where were considered the 7 intermediate stages of transfer from the quay on the dock deck, with docked mass to the maximum capacity of 27,000 t, having uniform, type sagging and hogging distributions, being ensured in all cases the same draft reference of T=6.2m through assisted ballast. Structural analysis in quasi-static head-following waves, under the conditions of sagging-hogging wave and calm water, which lead to the extreme demands of the docks according to the results of chapter 5, is realized for the height of hw=0-4.492 m (step 0.50 m), using the program codes and theoretical models presented in subchapters 2.1.3, 2.1.4, 2.2, 2.3.1, 2.3.2 (the logic schemes in figures 2.2 & 2.5). Based on the 1D equivalent beam model (subchapter 7.1), with the mass distribution and the shapes of the double bottom imported from the 3D-FEM model, the preliminary criteria of minimum freeboard and of general resistance, the bending moment and the permissible vertical shear force, the ultimate bending moment, allowable deformations, are evaluated and the balancing parameters of the large floating dock - quasi-static head-following wave are obtained. Based on the structural analysis of the large floating dock with 3D-FEM model fully extended in length, in a board, (subchapter 7.2), areas with stress concentrators are highlighted, which are the cases of operation with extreme demands, respectively the dock is evaluated based on the criteria of local and global resistance, allowable von Mises stresses with respect to the material flow limit and structural stability.

10. For the analysis of the dynamic behaviour in random waves of the large floating dock Dock_Vard_Tulcea [9] (chapter 8), for the relocation operation, which is currently carried out without docked mass, but under special conditions and for the 4 studied docking cases, with the evaluation of the seakeeping criteria (navigation), we used the DYN program (OSC) [45], with the theoretical model from subchapter 2.4 (the logic scheme in figure 2.9.). The analysis at the vertical oscillations, pitch and roll, of the large floating dock is performed for the speeds v = 0, 6, 12 km/h, according to the forward resistance curves of the tug-dock convoy, for three drafts T = 5.2, 6.2, 7.2 m assisted ballast (including the reference draft in chapter 7), for six values of the vertical position of the centre of gravity of the dock z_G = 6-16 m, heading angle dock-wave μ=0-180^0(360^0), step 5^0, random waves with the density function of the power spectrum of type ITTC [58], [59] and the maximum significant height H_s=4.492m, step 0.05m. The analysis led to obtaining the navigation restrictions in the current and special cases of relocation of the large floating dock, on the Danube river route (H_s=0.6-2 m) and the Black Sea coast. Due to the increase of the free board compared to the small docks (chapter 6), the large dock has smaller restrictions on the seakeeping criteria (navigation). Based on the D_LDF module (annex 4, subchapter 2.1.5) we evaluated for the large dock the criteria of general and dynamic (meteorological) transverse stability, depending on the docking cases and the vertical position of the centre of gravity of the large floating dock.
11. In order to carry out the relocation operations of the three floating docks, we considered in the study a 4,000 HP river-maritime tug [77], capable of providing maximum towing speeds of 18 km / h for small docks (figure 6.1, Dock60_CWT/NWT) and 12 km/h (figure 8.1, Dock_Vard_Tulcea) for the large floating dock. To analyse how the navigational characteristics of the tugboat interfere with those of the floating docks, we performed the analysis of the tugboat oscillations using the DYN (OSC) program [45], with the theoretical model in subchapter 2.4 (figure 2.9), for the entire speed range v = 0, 5, 6, 10, 12, 15, 18 km/h, random waves with ITTC spectrum [58], [59] and significant height H_s=0 - 5 m, step 0.05 m, heading angle of the tug-wave system μ=0-180^0(360^0), step 5^0. We considered that the tug-dock convoy linking system allows independent dynamic analysis of oscillations of constituent floating bodies. The navigational restrictions of the floating dock affect the performance of the convoy only in the case of the large dock on the coastal route, in the river case the restrictions are generated only by the two small docks.
12. The research developed within the thesis allowed the development of an integrated methodology for analysing the structure of floating docks at extreme demands, with the development of program code tools (annexes 1-9) and 1D and 3D numerical models for the evaluation of the limiting criteria for the operation of the docks, with the dissemination of the results by making a total of 14 articles published in the conference volumes and to national and international journals, of which 4 are indexed WOS- Web of Science and Scopus, 3 are being indexed WOS and Scopus and 7 are indexed in other international databases.

10.3. Future research perspectives

Future directions for extending scientific research within the thesis will include the following items:

- extending the studies of floating docks to extreme demands, for other constructive variants, other operating areas with or without docked mass, for several docking scenarios requested by shipping companies;
- development of theoretical models and optimization of structural analysis programs of floating docks in quasi-static head-following waves and oblique waves;
- development of nonlinear hydrodynamic theoretical models and programs for obtaining the dynamic response of floating docks to oscillations in oblique waves;
- achieving the technological transfer to the design companies and the shipyards of the integrated multicriteria methodology and software tools developed within the thesis for the analysis of floating docks at extreme demands.

SELECTIVE BIBLIOGRAPHY

1. D.N.V. 2017, *Rules and Classification of Floating Docks*, Det Norske Veritas, Hovik, Norway, https://www.dnvgl.com/
2. D.N.V. 2018, *Rules and Classification of Floating Docks*, Det Norske Veritas, Hovik, Norway, https://www.dnvgl.com/
3. R.I.N.A. 2010, *Rules for the Classification of Floating Docks*, https://www.rina.org/en
4. Burlacu E., *Raport de documentare ”Studiul actual privind analiza structurală a docurilor plutitoare”*, Universitatea Dunărea de Jos din Galați, 2017, Galați.
5. Pintilie Alexandru – *Note de curs Tehnologia montării și probării instalațiilor navale* – anul universitar 2013-2014, Universitatea Ovidius din Constanța
6. Bidoaie I., Iosifescu C., Valsan E., *Tehnologia fabricării navei și montării mecanismelor*, Editura Didactică și Pedagogică, 1977, București
7. Harison B. Andrews, Archer M Nickerson, *Some Practical Aspects of ship launching*, paper presented before the October 1945 meeting of the New England Section of The Society of Naval Architects and Marine Engineers
8. Heger R. E., *Floating dry dock accidents involving transerve bending failure of the pontoon*, Royal Institution of Naval Architects, 2003, USA
9. Technical drawings of floating dock ATLANTE II, S.N. VARD Tulcea
10. ***, https://www.google.com/search?biw=1366&bih=635&tbm=isch&sxsrf=ACYBGNTsNY0kiGlUCIMPHgi8QlvkseE0NQ%3A1567955709979&sa=1&ei=_Rp1XZqzO6LgkgX605D4Bg&q=Plecarea+celui+mai+mare+vapor+de+la+Santierul+Naval+Tulcea+la+Constanta+pentru+a+i+se+monta+pupa&oq=Plecarea+celui+mai+mare+vapor+de+la+Santierul+Naval+Tulcea+la+Constanta+pentru+a+i+se+monta+pupa&gs_l=img.3...180997.180997..181793...0.0..0.92.92.1.....0....2j1..gws-wiz-img.O2F1tgSVUjA&ved=0ahUKEwjapfeYwsHkAhUisKQKHfopBG8Q4dUDCAY&uact=5#imgrc=WbhHo33RdPkWMM:
11. ATLANTE II – CONVERSION FESABILITY STUDY, S:N. VARD Tulcea, 2016
12. ***, https://www.vard.com/SiteCollectionImages/Locations/Images/Floating%20dock%20-%20Atlante%20II_5.jpg
13. ***, https://www.facebook.com/photo.php?fbid=1428441637314771&set=pcb.1428441807314754&type=3&theater
14. ***, https://www.facebook.com/photo.php?fbid=1428441580648110&set=pcb.1428441807314754&type=3&theater
15. ***, https://www.revocean.org/wp-content/uploads/2019/08/REV-24082019_11_web.jpg
16. Bidoae R., Ionas O., *Arhitectura navei. Statica navei*, Editura Didactica si Pedagogica, 2004, Bucuresti.
17. Eyres D.J, *Ship construction*, Butterworth-Heinemann, 2007, Oxford, ISBN 13:9-78-0-75-06-8070-7, ISBN 10: 0-75-068070-9
18. ***, www.shipyards.gr
19. Manea E., Zăgan R., Manea M.-G., Militaru C., *Îmbunătățirea activităților de mentenanță și a performanțelor șantierelor navale, Vol. 1 - Managementul calității, aplicații pentru îmbunătățirea activităților de mentenanță și a performanțelor Șantierelor Navale*, Ed. Dobrogea, C-ța, 2018, ISBN 978-1006-565-138-8,
20. Volney E., *General discusion of floating drydocks*, presented at the Annual Meeting, New York, N.Y. November 14-15, 1957, of The Society of Naval Architects and Marine Engineers, 289-306
21. ***, https://en.wikipedia.org/wiki/USS_ARD-1#/media/File:USSARD1undertowUSSBridgeAF1PanamaCanal28October1934.jpg
22. ***, https://www.cruiseindustrynews.com/images/stories/wire/2018/dec/IMG_7196c.jpg
23. ***, Norden Ship Design House – 180m Floating Dock http://www.nordenshipdesign.com/icerik.php?id=79&ustid=23

24. ***, Norden Ship Design House – 50m Floating Dock http://www.nordenshipdesign.com/icerik.php?id=81&ustid=23
25. ***, http://www.gz-salvage.com.cn/en/index.php?ac=article&at=read&did=355
26. Hughes O.F., *Ship structural design. A rationally-based, computer-aided optimization approach*, SNAME, Wiley & Sons, 1995, New York., ISBN: 13 978-0939773473, ISBN 10: 0939773473
27. Domnişoru, L., Găvan, E., Popovici, O., *Analiza structurilor navale prin metoda elementului finit*, Editura Didactică şi Pedagogică, 2005, Bucureşti, ISBN 973-30-1075-8
28. Domnișoru Leonard, *Structural Analysis and hydroelasticity of ships*, The university foundation ”Dunărea de Jos” Publishing House,2006, Galați, ISBN(10): 973-627-338-5, ISBN(13): 978-973-627-338-4
29. Bertram, V., *Practical Ship Hydrodynamics*, Butterworth Heinemann, 2000, Oxford, ISBN: 13-978-0-08-097150-6
30. Domnişoru, L., *Dinamica navei. Oscilaţii şi vibraţii ale corpului navei*, Editura Tehnică 2001, Bucureşti, ISBN 973-31-2026-X
31. Faltinsen, O. M., *Sea loads on ships and offshore structures*, Cambridge University Press, 1993, ISBN 0521 45870 6
32. Voitkunski, Y.I. *Ship theory handbook. Statics of ships. Ship motions. (Vol.2)* Sudostroenie, 1985, Sankt Petersburg
33. IACS, 2018, *Standard wave*, Recommendation no. 34., www.iacs.org.uk
34. ISSC 2018, *International Ships and Offshore Structures Congress. Environemen. Loads. Quasi-static response. Ultimate strenght. Dynamic response. Design principels and criteria*, Schiffbautechnische Gesellschaft, Hamburg, www.issc2018.org
35. **Burlacu, E.**, Pacuraru, F., Domnișoru, L., *On the Development of Design Software for Floating Dock Units Operating Capabilites Analysis*, Galați 8-9 Iunie 2017, Mechanical Testing and Diagnosis, Galati University Press, ISSN 2247-9635, Vol.1, Issue 7, pp. 5-17,
36. PLL 2017, *Users' guide*. *Pascal language programming,* Free Pascal IDE for Win32, Compiler Version 3.0.0, Open Source Software, www.freepascal.org
37. **Burlacu, E.**, Domnișoru, L., *On the Global Strength Analysis of Preliminary Design for Several Floating Dock Types*, , Mechanical Testing and Diagnosis, Galați University Press, 2019, Vol.1, Issue 9, pp. 5-16, ISSN 2247-9635
38. ISO 2005, *Ship and marine technology. Ship structures. Requirements for their ultimate limit state assessment*, ISO/CD 18072-2, International Standard Organization, www.iso.org
39. D.N.V.-G.L. 2017, *Rules for classification. Ships. Inland navigation vessels. Floating docks. Poseidon Program,* Det Norske Veritas, Hovik, Germanischer Lloyd, Hamburg, https://www.dnvgl.com/
40. Burlacu E., *Raport ştiințific nr. 2 „Analiza structurii unui doc plutitor în cazul solicitărilor extreme. Soluții pentru extinderea capabilității de operare”*, Universitatea Dunărea de Jos din Galați, 2019, Galați.
41. **Burlacu, E.**, Domnișoru, L., *Strength Investigation of a Small Size Floating Dock Unit by 3D-FEM Models in Head Design Waves*, ModTech 6th International Conference Modern Technologies in Industrial Engineering, Maritime Engineering and Navigation, Romania, IOP Conference Series: Materials Science and Engineering, Vol. 400, 2018, Issue 8, ISSN 1757-899X, ISSN: 1757-8981
42. FNN 2018, *Femap/NX Nastran user's guide*, Siemens PLM Software Inc., http://www.plm.automation.siemens.com
43. Burlacu E., *Raport ştiințific nr. 1 „Metode de analiză structurală 3D-FEM pentru docurile plutitoare. Siguranța structurală în cazurile standard de operare”,* Universitatea Dunărea de Jos din Galați, 2018, Galați.
44. Domnișoru L., *Special shapters on ships structures analyss applications*, 2017, Editura Fundației Universitare Dunărea de Jos, ISBN 978-973-627-589-0
45. Domnişoru, L., Rubanenco, I., Mirciu, I., *Pachetul de programe DYN, softuri pentru analiza răspunsului corpului navei la oscilaţii şi vibraţii globale induse de valuri regulate şi aleatoare*, Facultatea de Arhitectură Navală, Universitatea „Dunărea de Jos”, 2009-2019, Galaţi
46. Domnisoru, L. *Program SH_GECH pentru calculul caracteristicilor grinzii echivalente a corpului navei*, Facultatea de Arhitectură Navală, Universitatea „Dunărea de Jos”, 2017, Galaţi
47. Năstăsescu, V., *Metoda elementului finit*, Editura Academiei Tehnice Militară, 1995, Bucureşti.
48. Zienkiewicz, O.C., Taylor, R.L., *The Finite Element Method.*, 2000, Butterwoth Heinemann.
49. Bathe, K.J., *Finite Elemente Methoden*, Springer Verlag, Berlin, 1990
50. Hadăr, A., Marin, C., Petre, C., Voicu, A., *Metode numerice în inginerie*, Editura Politehnica Press, 2005, Bucureşti, ISBN 973-8449-34-0

51. **Burlacu, E.**, Domnișoru, L., *On a Small Size Floating Dock Structural Analysis in Oblique Design Waves by 3D-FEM Approach*, ModTech 7th International Conference Modern Technologies in Industrial Engineering, Maritime Engineering and Navigation, Romania, IOP Conference Series: Materials Science and Engineering, Vol. 591, 2019, Issue 1, ISSN 1757-899X, ISSN 2286-4369
52. Domnişoru, L., Modiga, A., Gasparotti, C., *Global Strength Assessment in Oblique Waves of a Large Gas Carrier Ship, Based on a Non-linear Iterative Method*, IOP Conference Series: Materials Science and Engineering, Section G. Maritime Engineering and Navigation, ModTech 2016 4th International Conference - Modern Technologies in Industrial Engineering, Vol. 145 / 8 - August 2016, IOP Publishing, Bristol, UK,15-18 June, Iasi, ModTech Publishing House, Universitatea Tehnică “Gheorghe Asachi” Iaşi, ISSN 1757-899X, doi:10.1088/1757-899X/145/8/082009
53. Domnişoru, L., *Metoda elementului finit în construcţii navale*, Editura Tehnică Bucureşti, 2001, București, ISBN 9733120235
54. Mansour, A, Lin, D. *Strength of ship and ocean structures*, The Society of Naval rchitecture and Marine Engineering, 2008, New Jersey, ISBN 9781615836673 1615836675 9780939773664 093977366X
55. Obreja D., *Teoria navei. Concepte si metode metode pentru analiza performantelor de navigație*, Editura Didactica si Pedagogica, 2005, București, ISBN 973-30-1401-X
56. Tupper E.C., *Introduction to the naval architecture*, Butterworth – Heinemann, 2002, Oxford, ISBN 0 7506 6554 8
57. D.N.V. 2012, *Modelling and analysis of marine operations, Recommended practice*, DNV-RP-H103. Hovik: Det Norske Veritas, www.dnv-gl.org
58. ITTC 2005, *Testing and Extrapolation Methods, Loads and Responses on Seakeeping Experiments*, Recommended Procedures and Guidelines 7.5-02-07-02.1, International Towing Tank Conference, http://ittc.sname.org/.
59. ITTC 2011, *Ship Models, Recommended Procedures and Guidelines 7.5-01.01.01*, International Towing Tank Conference, http://ittc.sname.org/.
60. **Burlacu, E.**, Domnișoru, L., *The Transit State Evaluation of a Large Floating Dock by Seakeeping Criteria*, MARTECH 2018, Progress in Maritime Engineering and Technology (Editors Carlos Guedes Soares & T.A.Santos), CRC Press / A.A. Balkema Publishers a member of Taylor & Francis Group London, 4th International Conference on Maritime Technology and Engineering, 2018, pp.611-620, ISBN 978-1-138-58539-3
61. Gasparotti C., *Creșterea siguranței navigației în bazinul Mării Negre, Teză de doctorat,* 2015, Editura Fundației Universitare Dunărea de Jos, ISBN 978-973-827-560-0
62. **Burlacu, E.**, Păcuraru F., Domnișoru, L., *On a River – Costal Tug Operation Safety Assessment in Irregular Waves*, ICTTE International Conference on Traffic and Transport Engineering, Inland Waterways Traffic and Transport Research, 2018, Belgrade, Serbia, pp.187-194, ISBN 978-86-916153-4-5
63. **Burlacu, E.**, Domnișoru, L., *Dynamic Response Investigation of a Small Size Floating Dock Unit in Irregular Oblique Waves*, ModTech 6th International Conference Modern Technologies in Industrial Engineering, Constanta, România, Maritime Engineering and Navigation, IOP Conference Series: Materials Science and Engineering, Vol. 400, 2018, Issue 8, ISSN 1757-899X, ISSN: 1757-8981
64. Bertram, V., Veelo, B., Söding, H., Graf, K., *Development of a freely available strip method for Seakeeping*. Proc. 5th International Conference on Computer and IT Applications in the Maritime Industries, May 2006, Leiden.
65. Solas, *International convention for the safety of life at sea. Safety of navigation*, IMO, 2017, www.imo.org
66. Price, W.G., Bishop, R.E.D. *Probabilistic theory of ship dynamics*. London: Chapman and Hall,1974, ISBN 0412124300
67. Obreja, D., *Survey Vessel Caspica. Model Resistance Tests, Report No. 617*, Facultatea de Arhitectură Navală, Universitatea „Dunărea de Jos” și SDG Ship Design Group, 2013, Galați.
68. **Burlacu, E.**, Domnișoru, L., Obreja, D., *Seakeeping Prediction of a Survey Vessel Operating in the Caspian Sea*, OMAE The 37th International Conference on Offshore Mechanics and Arctic Engineering, 2018, Madrid, Spain, ASME The American Society of Mechanical Engineers, Paper No. OMAE2018-77126, ISBN: 978-079185132-6, DOI: 10.1115/OMAE2018-77126
69. Cussons 2010, *Marine Research. Towing Tanks Modernization*, Cusson Marine Technology Ltd., Manchester, http://www.cussons.co.uk
70 Mocanu C.I., *Rezistența materialelor*, ediția a II-a, Editura Fundației Universitare Dunărea de Jos din Galați, 2005, Galați, ISBN 973-87793-2-4

71 Buzdugan G., *Rezistența Materialelor*, Ed. Academiei R.S.R., 1986, București
72. Rawson K.J., Tupper E.C., *Basic Ship Theory*, (Ed.V) Butterworth Heinemann, Oxford, 2001, ISBN 0-7506-5396-5, ISBN 0-7506-5397-3
73 **Burlacu, E.**, Domnișoru, L., *The Structural Evaluation of a Large Floating Dock in Head Design Waves by Strength Criteria*, ModTech 7th International Conference Modern Technologies in Industrial Engineering, Maritime Engineering and Navigation, Romania, IOP Conference Series: Materials Science and Engineering, Vol. 591, 2019, Issue 1, ISSN 1757-899X, ISSN 2286-4369,
74. ***, https://www.facebook.com/VardTulceaSA/photos/a.677032898993908/1702018959828625/?type=3&theater
75. ***, https://www.facebook.com/VardTulceaSA/photos/a.677032898993908/1702018939828627/?type=3&theater
76. ***, https://www.facebook.com/VardTulceaSA/photos/a.677032898993908/1702018943161960/?type=3&theater
77. Dragomir, D. *Compendiu de forme navale*. Editura Fundației Universitare Dunărea de Jos, 2014, Galați. ISBN 978-973-627-517-3
78 Biran A. B., *Ship hydrostatics and stability*, Butterworth-Heinemann, 2003, Oxford, ISBN 13: 978-0-08-098287-8
79 ANR 2006, *Album of ship types. Maritime tug 4000HP*., Constanța, Romanian Naval Autority
80. DNV-GL 2018, *Rules for classification. Tugs and escort vessels*. Det Norske Veritas, Hovik. Available from internet: https://rules.dnvgl.com